A PRESSURIZED THERMAL SHOCK EVALUATION OF THE CALVERT CLIFFS UNIT 1 NUCLEAR POWER PLANT

List of Chapters

Chapter 1 Introduction

Chapter 2 Calvert Cliffs Unit 1 Nuclear Power Plant System Description

Chapter 3 Development of Overcooling Sequences for Calvert Cliffs Unit 1 Nuclear Power Plant

Chapter 4 Thermal-Hydraulic Analysis of Potential Overcooling Transients Occurring at Calvert Cliffs Unit 1 Nuclear Power Plant

Chapter 5 Probabilistic Fracture-Mechanics Analysis of Calvert Cliffs Unit 1 Sequences

Chapter 6 Risk Integration of Potential Calvert Cliffs Unit 1 Overcooling Sequences

Chapter 7 Sensitivity and Uncertainty Analysis

Chapter 8 Summary and Conclusions

5.0. PROBABILISTIC FRACTURE-MECHANICS ANALYSIS OF CALVERT CLIFFS UNIT 1 SEQUENCES

5.1. Introduction
5.2. Description of Basic Problem
5.3. Calculational Models

- 5.3.1. Fracture-Mechanics Model
- 5.3.2. Stress-Analysis Model
- 5.3.3. Thermal Analysis Model
- 5.3.4. Probabilistic Analysis Model

5.4. Flaw-Related Data for the Calvert Cliffs-1 Reactor Pressure Vessel

5.5. Results of Analysis

- 5.5.1. Types of Analyses Conducted
- 5.5.2. Conditional Probability of Vessel Failure
- 5.5.3. Sensitivity Analysis
- 5.5.4. Effect of Including WPS
- 5.5.5. Effect of Proposed Remedial Measures on P(F E)
  - 5.5.5.1. Reduction in fluence rate
  - 5.5.5.2. Annealing
  - 5.5.5.3. Increasing temperature of HPI coolant

Chapter 5 Appendices

K. Contribution to P(F|E) of Flaws in the Circumferential Welds and in the Plate Segments

L. Compilation of Results of Calvert Cliffs-1 Probabilistic Fracture-Mechanics Analysis

LIST OF FIGURES

5.1. Cross section and developed view of plate-type PWR pressure vessel

5.2. Cross sections of Calvert Cliffs-1 pressure vessel and core showing locations of vessel welds in beltline region

5.3. Developed view of inner surface of beltline region of Calvert Cliffs-1 pressure vessel, showing locations of welds

5.4. Illustration of a method of selecting $(K_{Ia})_{max}$

5.5. Critical-crack-depth curves for a typical postulated PTS transient

5.6. OCA-P program logic

5.7. Graphic illustration of the error in P_J, consistent with the criteria used for establishing the number of vessels simulated (N_{vJ})

5.8. P(F|E) vs EFPY for Calvert Cliffs-1 postulated PTS transients

5.9. Histogram of percent of initiations vs crack depth for first initiation event (Calvert Cliffs-1 postulated transient No. 8.3; 32 EFPY)

5.10. Histogram of percent of failures vs time of failure (Calvert Cliffs-1 postulated transient No. 8.3; 32 EFPY)

5.11. Histogram of percent of total initiations vs relative temperature at which initiations take place (Calvert Cliffs-1 postulated transient No. 8.3; 32 EFPY)

5.12. Histogram of percent of total arrest events vs relative temperature at which arrest events take place (Calvert Cliffs-1 postulated transient No. 8.3; 32 EFPY)

5.13. P, T and h vs t for Calvert Cliffs-1 postulated transient No. 8.3

5.14. Wall temperature vs a/w, t for Calvert Cliffs-1 postulated transient No. 8.3

5.15. Wall temperature vs t, a/w for Calvert Cliffs-1 postulated

transient No. 8.3

5.16. Critical-crack-depth curves for Calvert Cliffs-1 postulated transient No. 8.3; 32 EFPY, weld 2-203A

5.17. Effect on P(F|E) for transient No. 8.2 of reducing fluence rate at 7 EFPY by factors of 2, 4 and 8

5.18. Effect on P(F|E) for transient No. 8.3 of reducing fluence rate at 7 EFPY by factors of 2, 4 and 8

LIST OF TABLES

5.1. Parameters simulated in OCA-P

5.2. Material properties, fluences and volumes used in the LEFM analysis of the Calvert Cliffs-1 reactor vessel

5.3. Summary of calculated values of P(F|E) for the Calvert Cliffs-1 postulated transients

5.4(A) Summary sheet of OCA-P output for Calvert Cliffs-1 postulated transient No. 2.1

5.4(B) Summary sheet of OCA-P output for Calvert Cliffs-1 postulated transient No. 2.4

5.4(C) Summary sheet of OCA-P output for Calvert Cliffs-1 postulated transient No. 8.2

5.4(D) Summary sheet of OCA-P output for Calvert Cliffs-1 postulated transient No. 8.3

5.5. Sensitivity of P(F|E) at 41 EFPY to 1σ changes in the mean values of several of the simulated parameters

5.6. Effect of including WPS in calculation of P(F|E) at 32 EFPY

5.7. Benefit of remedial measures, $P(F|E)_{wRM}/P(F|E)_{w/oRM}$,[a] at 42 EFPY for dominant transients

5.0 PROBABILISTIC FRACTURE-MECHANICS ANALYSIS OF CALVERT CLIFFS UNIT 1 SEQUENCES

R. D. Cheverton
Oak Ridge National Laboratory

D. G. Ball
Martin Marietta Energy Systems, Inc.
Computer Sciences Division

5.1 Introduction

This chapter provides detailed information regarding the probabilistic fracture-mechanics analysis of the Calvert Cliffs-1 reactor vessel and discusses (1) the conditions necessary for failure (through-wall cracking) of a PWR pressure vessel as a result of a PTS transient, (2) the fracture-mechanics models used for evaluating vessel integrity, and (3) the results of a probabilistic fracture-mechanics analysis of the Calvert Cliffs-1 reactor vessel for PTS loading conditions. Supplementary information is included in Appendices K and L, as noted in this chapter.

5.2 Description of Basic Problem

During a PTS transient in a pressurized-water reactor (PWR), the reactor pressure vessel is subjected to thermal shock in the sense that thermal stresses are created in the vessel wall as a result of rapid removal of heat from its inner surface. The thermal stresses are superimposed on the pressure stresses with the result that the net stresses are positive (tensile) at and near the inner surface of the wall and are substantially lower and perhaps negative elsewhere, depending on the magnitude of the pressure stress. The concern over the high tensile stresses near the inner surface is that they result in high stress intensity factors (K_I) for inner-surface flaws that may be present. To compound the matter, the reduced temperature associated with the thermal shock and radiation damage result in relatively low fracture-toughness values for the vessel

material, particularly near the inner surface. Thus, there is a possibility of propagation of initially very shallow as well as deeper flaws, and the probability increases with time because of the time dependence of radiation damage.

The positive gradient in temperature and the negative gradients in stress and fluence through the wall tend to provide a mechanism for crack arrest. Even so, if the crack is very long on the surface and propagates deep enough, the remaining vessel ligament will become plastic, and the vessel internal pressure will ultimately result in rupture of the vessel. Thus, for each thermal transient there will be a maximum permissible pressure that is a function of the time that the vessel has been in operation.

Crack propagation may also be limited by a phenomenon referred to as warm prestressing (WPS), which has been demonstrated to some extent in the laboratory with small specimens[1] and also in a rather large, thick-walled cylinder during a thermal-shock experiment.[2] In such cases, WPS simply refers to the inability of a crack to initiate while K_I is decreasing with time, that is, while the crack is closing. While this special situation is encountered during some specific overcooling accidents, caution must be exercised in taking credit for WPS because changes in the pressure that affect little else can delay or eliminate the requisite conditions for WPS.

The area of the vessel of particular concern in the event of a PTS transient is the so-called beltline region, that is, the area directly across from the core where (1) the radiation damage is the greatest, (2) the thermal shock could be severe, and (3) a rupture of the vessel could preclude flooding of the core. Whether or not a particular degree of rupture associated with a particular transient could in fact preclude flooding of the core has not been determined but is under investigation. For the purpose of this report, it is sufficient to predict whether a flaw will propagate completely through the wall of the vessel.

The radiation-induced reduction in fracture toughness of the vessel material is a function of the fast-neutron fluence and the concentrations of copper (a contaminant) and nickel (an alloying element). Furthermore, for the same values of fluence, copper and nickel, radiation damage tends to be greater in the welds that join the segments of the vessel than in the segments (base material). In most PWR vessels the highest concentrations of copper are found in the welds, and many of these welds have high concentrations of nickel as well. Thus, for some PWR vessels the welds are of primary concern. However, the much larger surface area of the segments may offset the difference in radiation damage between segments and welds, if the density of surface flaws in the segments is about the same as, or greater than, that for the welds.

The beltline region of reactor pressure vessels is fabricated using either forged-ring segments or rolled-plate segments. Vessels made with forgings have only circumferential welds, while plate-type vessels have both circumferential and axial welds, as shown in Fig. 5.1. For plate-type vessels with staggered axial welds and for which radiation damage is much more severe in the welds than in the base material, the final surface length of a propagating inner-surface axial flaw tends to be limited to the length of the axial weld in which it resides, that is, the height of the shell course. Furthermore, only that portion of a weld that is within the axial bounds of the core need be considered because of the steep attenuation of the fast-neutron flux, and thus radiation damage, beyond the fuel region. F5.

If the chemistry in adjacent plate segments is about the same, the extended surface length of an axially oriented flaw in a plate segment is also limited by the height of the core but not by the height of a shell course.

Because of an azimuthal variation in the fast-neutron flux (see Fig. 5.1) and possibly in chemistry, the extended length of an initially short, circumferentially oriented flaw located in a circumferential weld or in a plate segment also tends to be limited.

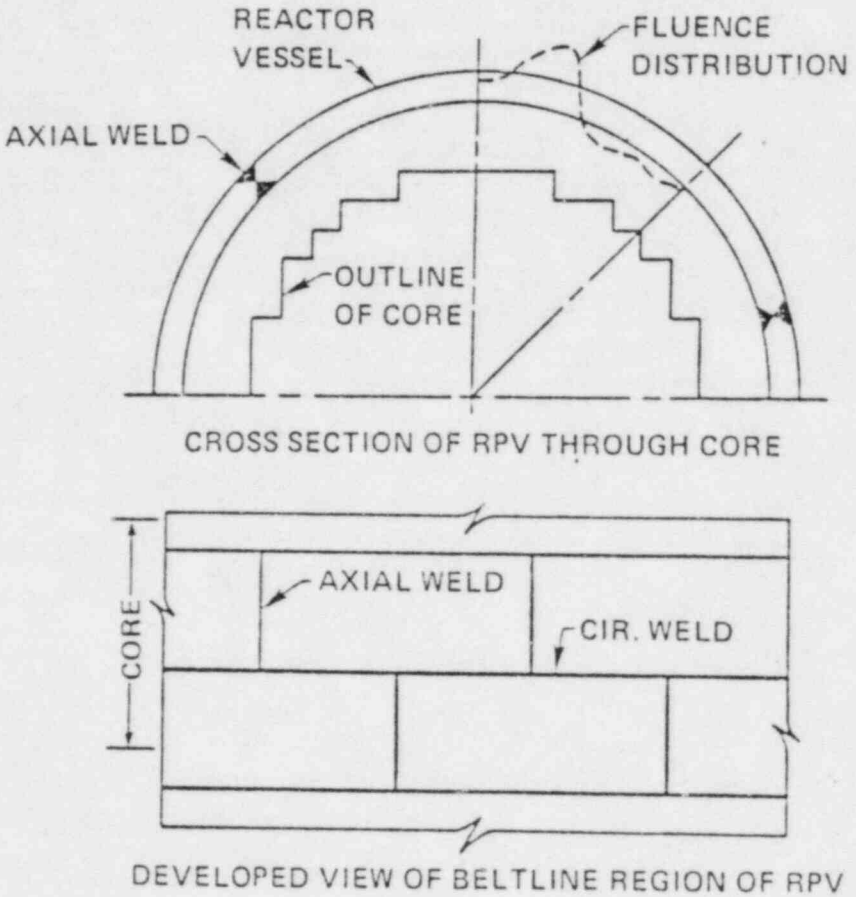

Fig. 5.1. Cross section and developed view of plate-type PWR pressure vessel.

The behavior of an assumed flaw can be predicted for a given transient using fracture-mechanics methods of analysis. In such an analysis the parameters and considerations involved are the size, shape, and orientation of the flaw; the thermal and pressure stresses resulting from a specific transient; the temperature and fast-neutron fluence distributions throughout the vessel wall; the effect of fluence and material chemistry on radiation damage; a variety of material properties; and a comparison of the stress intensity factor (K_I) associated with the tip of the flaw with the material's static crack-initiation and crack-arrest fracture-toughness values (K_{Ic} and K_{Ia}). Each of these factors must be considered in the development of an appropriate analytical model for evaluating the integrity of a PWR vessel when subjected to PTS loading conditions. The necessary models for performing a probabilistic fracture-mechanics analysis for the Calvert Cliffs-1 reactor pressure vessel and the results of the analysis are discussed in the remainder of this chapter.

5.3 Calculational Models

The conditional probability of vessel failure (through-wall cracking) was calculated for the Calvert Cliffs-1 reactor pressure vessel using the OCA-P code.[3] OCA-P accepts as input the primary system pressure, the temperature of the coolant in the reactor-vessel downcomer, and the fluid-film heat transfer coefficient adjacent to the vessel wall, all as a function of time in a specified PTS transient. The code then performs one-dimensional thermal and stress analyses for the vessel wall and finally a probabilistic fracture-mechanics analysis. Details of OCA-P necessary for an understanding of the Calvert Cliffs-1 vessel analysis are discussed below.

5.3.1 Fracture-Mechanics Model

The fracture-mechanics (FM) model in OCA-P is based on linear elastic fracture mechanics (LEFM) and uses a specified maximum value of K_{Ia} to account for upper-shelf behavior. The stress intensity factor (K_I) is calculated using superposition techniques in conjunction with influence coefficients that were calculated using finite-element techniques. The application of this procedure makes it possible to perform a large number of deterministic FM calculations at reasonable cost, a necessary condition for performing the probabilistic analysis.

The Calvert Cliffs-1 vessel was fabricated from sections of plate and has both axial and circumferential welds in the beltline region, as shown in Figs. 5.2 and 5.3. The length of flaws in the axial welds with depths greater than ~40 mm was assumed to be approximately the height of a shell course, and the shape was assumed to be semielliptical (this flaw is referred to as the 2-m flaw). Since the ends of this flaw are fixed, propagation was judged on the basis of the K ratios (K_I/K_{Ic}, K_I/K_{Ia}) at the deepest point of the flaw. Deep axial flaws in the plate region were assumed to be two-dimensional (infinite length) since their surface length could extend the full length of the core.

F5.2
F5.3

Shallower flaws were assumed to be two-dimensional, because long shallow flaws are essentially two-dimensional, and short flaws tend to grow on the surface to become long flaws,[4] at least in the absence of cladding. Because the effect of cladding on the surface extension of short flaws is not known at this time, any possible beneficial effect has been discounted.

Cladding on the inner surface of PWR pressure vessels was included in the OCA-P analysis as a discrete region to the extent that the thermal and stress effects were account for. As mentioned above, the effect of cladding on the surface extension of finite-length flaws was not considered.

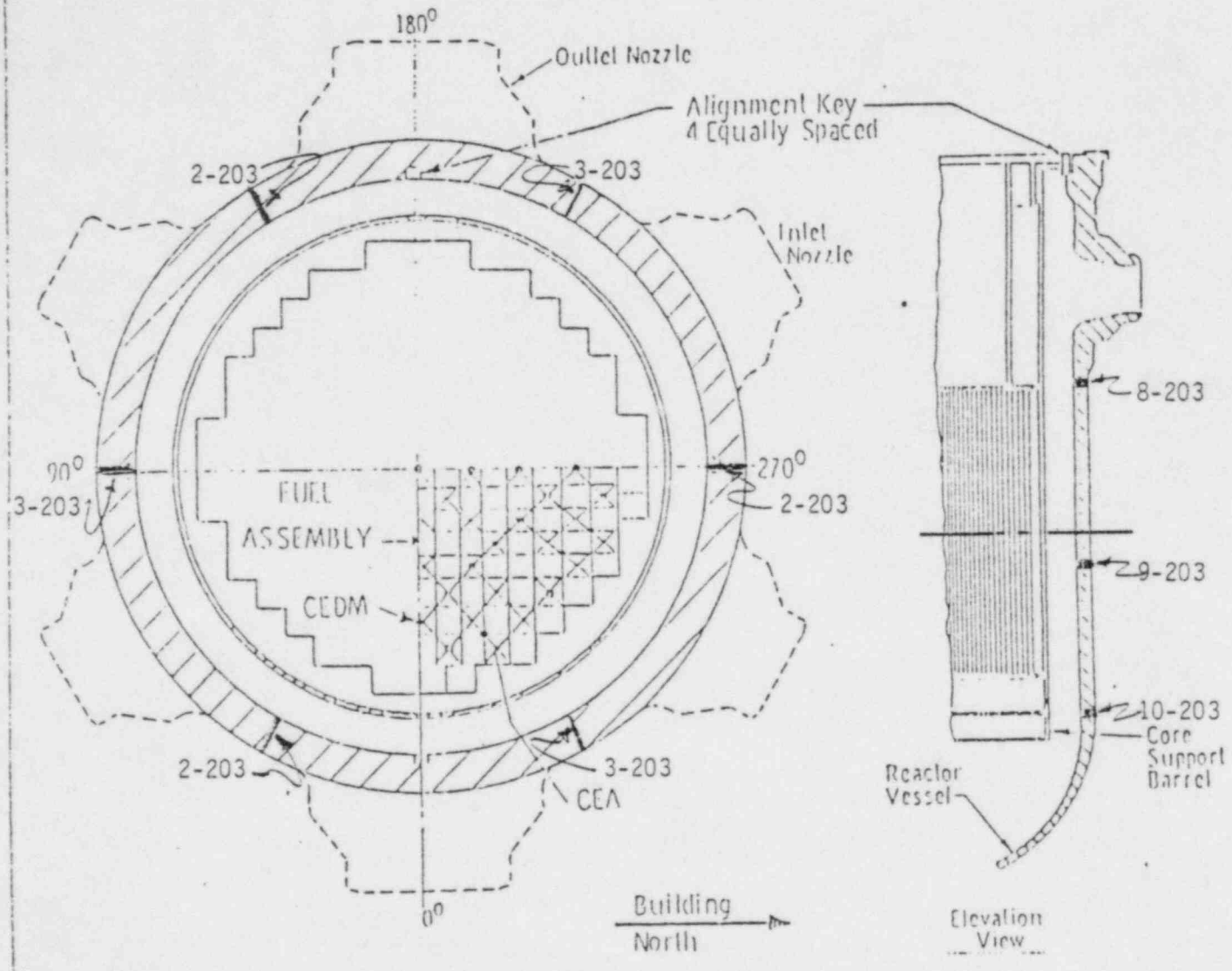

Fig. 5.2. Cross sections of Calvert Cliffs-1 pressure vessel and core showing locations of vessel welds in beltline region.

BALTIMORE GAS & ELECTRIC CO. Calvert Cliffs Nuclear Power Plant	CORE ORIENTATION	Figure 3.3-11

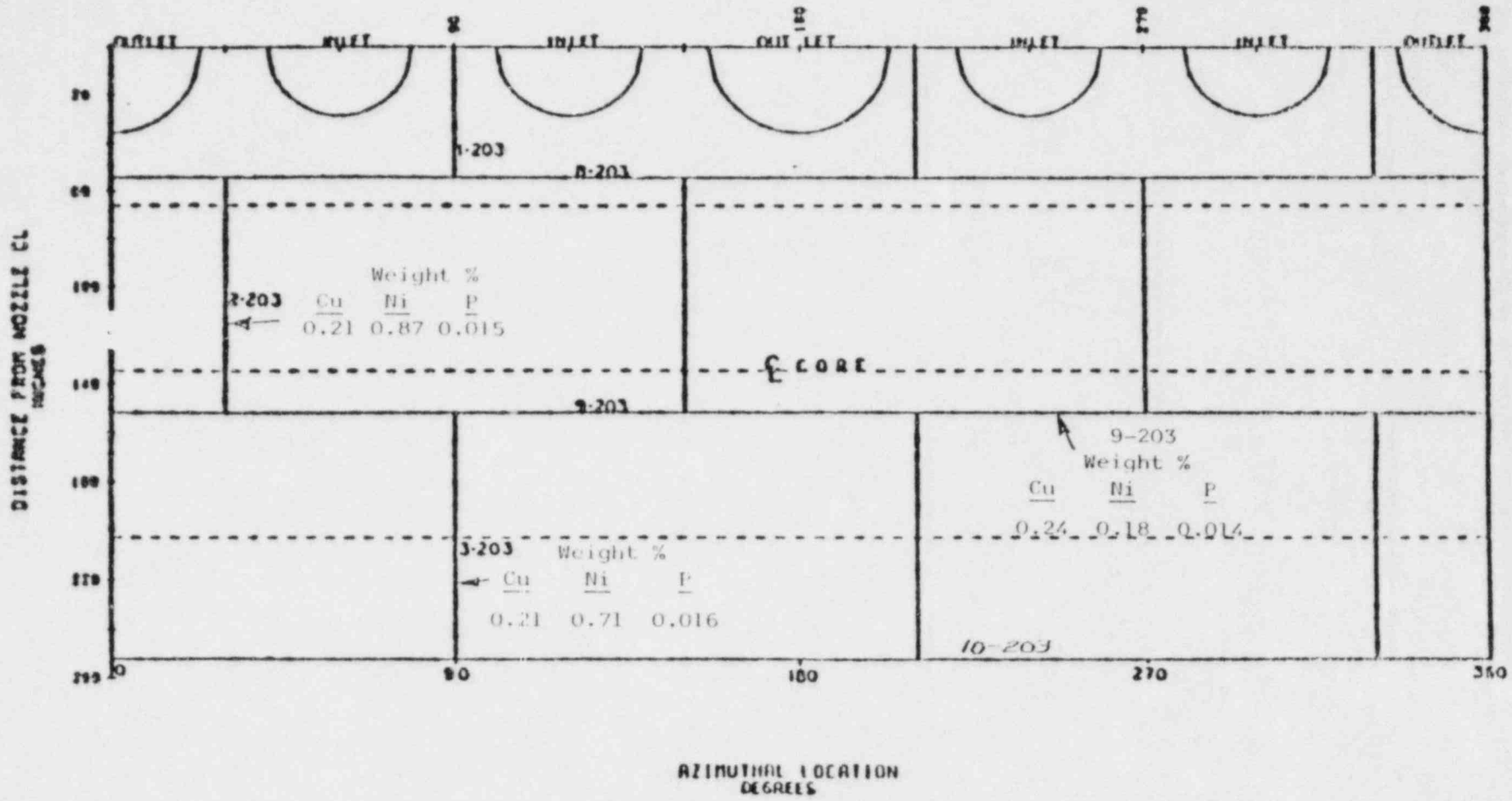

Fig. 5.3. Developed view of inner surface of beltline region of Calvert Cliffs-1 pressure vessel, showing locations of welds.

Because of the difference in the coefficient of thermal expansion between the cladding and base material, the calculated stresses in the cladding exceed the yield strength of the cladding by an appreciable amount, and this results in an overestimation of the K_I values for the flaws, which were assumed to terminate in the cladding or extend through the cladding into the base material. An alternative approach would be to limit the stress in the cladding to the yield stress, but this underestimates K_I because K_I is sensitive to the strain, which is not limited by the yielding phenomenon. The difference in K_I between these two extremes is not large; thus the conservative extreme was selected.

Material properties required for the fracture-mechanics analysis include the static crack initiation and arrest toughness values (K_{Ic} and K_{Ia}) and the nil-ductility reference temperature (RTNDT). For the probabilistic fracture-mechanics analysis, mean values of these parameters are required, and they were obtained for the vessel material as follows:

$$\overline{K}_{Ic} = 1.43 \{36.5 + 3.084 \exp [0.036 (T - RTNDT + 56)]\}, \text{ MPa } \sqrt{m} \qquad (5.1)$$

$$\overline{K}_{Ia} = 1.25 \{29.5 + 1.344 \exp [0.0261 (T - RTNDT + 89)]\}, \text{ MPa } \sqrt{m} \qquad (5.2)$$

where the quantity in braces represents the ASME Section XI[5] lower-bound toughness value and T is the temperature at the tip of the flaw in °C. These expressions were obtained by letting the ASME lower bound curves represent the mean values minus two standard deviations (2σ) and by letting $\sigma_{(K_{Ic})} = 0.15\ \overline{K}_{Ic}$ and $\sigma_{(K_{Ia})} = 0.10\ K_{Ia}$.

In many cases, if crack arrest takes place, it must do so at upper-shelf temperatures, that is, at temperatures that, under static loading conditions, result in ductile rather than brittle behavior of the material. Crack arrest under these conditions is not well understood but has been included in an

approximate manner by specifying a maximum value of K_{Ia} that corresponds to the upper portion of an upper-shelf tearing-resistance curve. As illustrated in Fig. 5.4, which is a plot of K vs crack depth (a) and temperature (T) at a specific time in a transient, if the load line (K_I vs a, T) intersects the K_{Ia} curve at $K_{Ia} < (K_{Ia})_{max}$, upper-shelf temperatures are not encountered. If, on the other hand, the load line misses the rising portion of the K_{Ia} curve and then decreases, as it does for some transients, there is, according to the model, a possibility of crack arrest at upper-shelf temperatures.

The tearing resistance curve selected for this study represents a specific high copper, low-upper-shelf weld material that had been irradiated to a fluence of $\sim 1.2 \times 10^{19}$ neutrons/cm^2 at a temperature of ~300°C and tested at 200°C.[6] The upper, nearly flat portion of this curve corresponds to a K_J value of ~220 MPa $\sqrt{m}$, and this value was used for $(K_{Ia})_{max}$; K_J was obtained using the relation

$$K_J = \sqrt{JE} \tag{5.3}$$

where

J = strain energy release rate

E = Young's modulus

The tearing resistance of PWR vessel materials tends to decrease with increasing temperature and fluence, and thus the effects of temperature and fluence tend to compensate for each other through the wall of the vessel. Because of this and the very approximate nature of the treatment of arrest on the upper shelf, no attempt was made to account more accurately for the effects of temperature and fluence on $(K_{Ia})_{max}$.

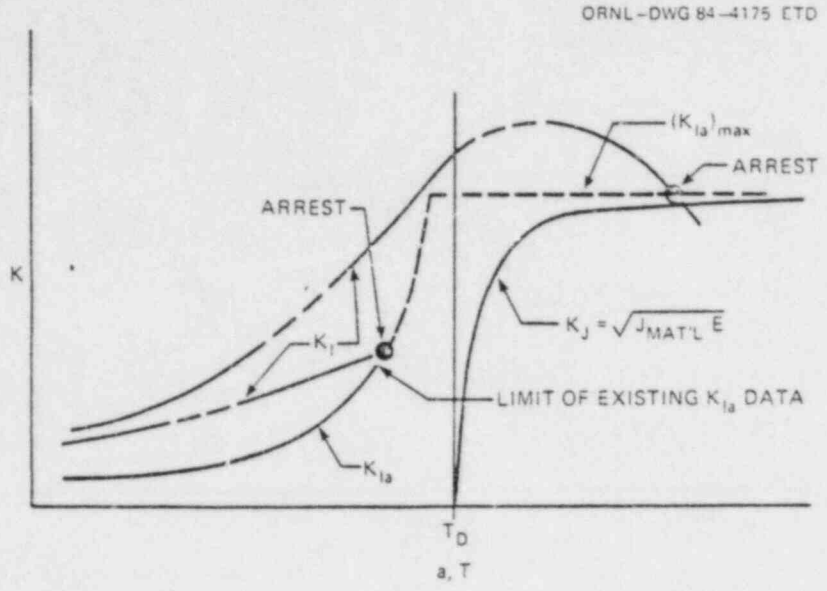

Fig. 5.4. Illustration of a method of selecting $(K_{Ia})_{max}$.

The nil-ductility reference temperature (RTNDT) is equal to the sum of an initial (zero fluence) value ($RTNDT_o$) and an increase due to radiation damage ($\Delta RTNDT$); that is,

$$RTNDT = RTNDT_o + \Delta RTNDT \tag{5.4}$$

The correlation for $\overline{\Delta RTNDT}$ used in these studies was recently proposed by Randall[7] and is

$$\overline{\Delta RTNDT} = 0.56\ [-10 + 470\ Cu + 350\ CU\ Ni]\ (F \times 10^{-19})^{0.27},\ °C \tag{5.5}$$

or

$$\overline{\Delta RTNDT} = 0.56\ [283\ (F \times 10^{-19})^{0.194} - 48],\ °C \tag{5.6}$$

whichever is smaller, where

Cu, Ni = concentrations of copper and nickel, wt %,

F = fast-neutron fluence (neutron energy > 1 MeV), neutrons/cm^2.

Equations (5.5) and (5.6) were derived without distinguishing between weld and base material. A more recent attempt to correlate the data does differentiate between the two materials, and the results indicate (1) substantially less damage for the base material than for welds and (2) greater damage for the welds than indicated by Eq. (5.5).[7] For this study, Eqs. (5.5) and (5.6) were used for the weld material, and a differential between weld and plate material was obtained from the most recent correlations[7] and was applied in the evaluation of flaw behavior in the base material.

The attenuation of the fluence through the wall of the vessel is approximated with

$$F = F_o \, e^{-0.0094 \, a} \tag{5.7}$$

where F_o is the fluence at the inner surface of the vessel and a is the crack depth in millimeters. The specific value of the coefficient in the exponent accounts to some extent for the effect of space-wise spectral changes in radiation damage.[7]

If the assumption is made that a short and shallow surface flaw can extend on the surface through the cladding to become a long flaw (and this assumption is made for these studies), then it must be assumed that under the

proper circumstances a very shallow flaw that initially resides entirely within the cladding can propagate radially. Unfortunately, the fracture-toughness properties of the cladding material are very uncertain, and the few experimental data that are available indicate a radiation-induced reduction in fracture toughness similar to that for the base material. As an expediency, which may or may not be conservative, it was assumed that the cladding has the same fracture-toughness properties as the base material [Eqs. (5.1), (5.2), (5.5) and (5.6)]. In the OCA-P analysis, assumptions regarding the fracture behavior of the cladding influence only the initiation of very shallow flaws that initially terminate in the cladding. Under some circumstances, including the above assumption regarding the fracture toughness of the cladding, these shallow flaws will initiate and result in vessel failure. Therefore, it was necessary to include the fracture properties of the cladding.

The deterministic fracture-mechanics model described above is used in OCA-P to predict the behavior of a flaw during a specified PTS transient at a specified time in the life of the vessel, and the calculated behavior can be illustrated with a set of critical-crack-depth curves similar to those shown in Fig. 5.5. The figure consists of a plot of crack depths corresponding to various events and conditions as a function of the time in the transient at which the events or conditions take place or exist. Figure 5.5 includes (for 2-D, axially oriented flaws only) the locus of points for $K_I = K_{Ic}$ (crack-initiation curve), $K_I = K_{Ia}$ (crack-arrest curve), $K_I = (K_I)_{max}$ (warm prestress curve with $\dot{K}_I = 0$), and K_I = constant (iso K_I curves). For times less than those indicated by the WPS curve, crack initiation will take place, but for greater times initiation will not take place unless perhaps there is a perturbation in K_I that negates the requisite conditions for WPS.

F5.5

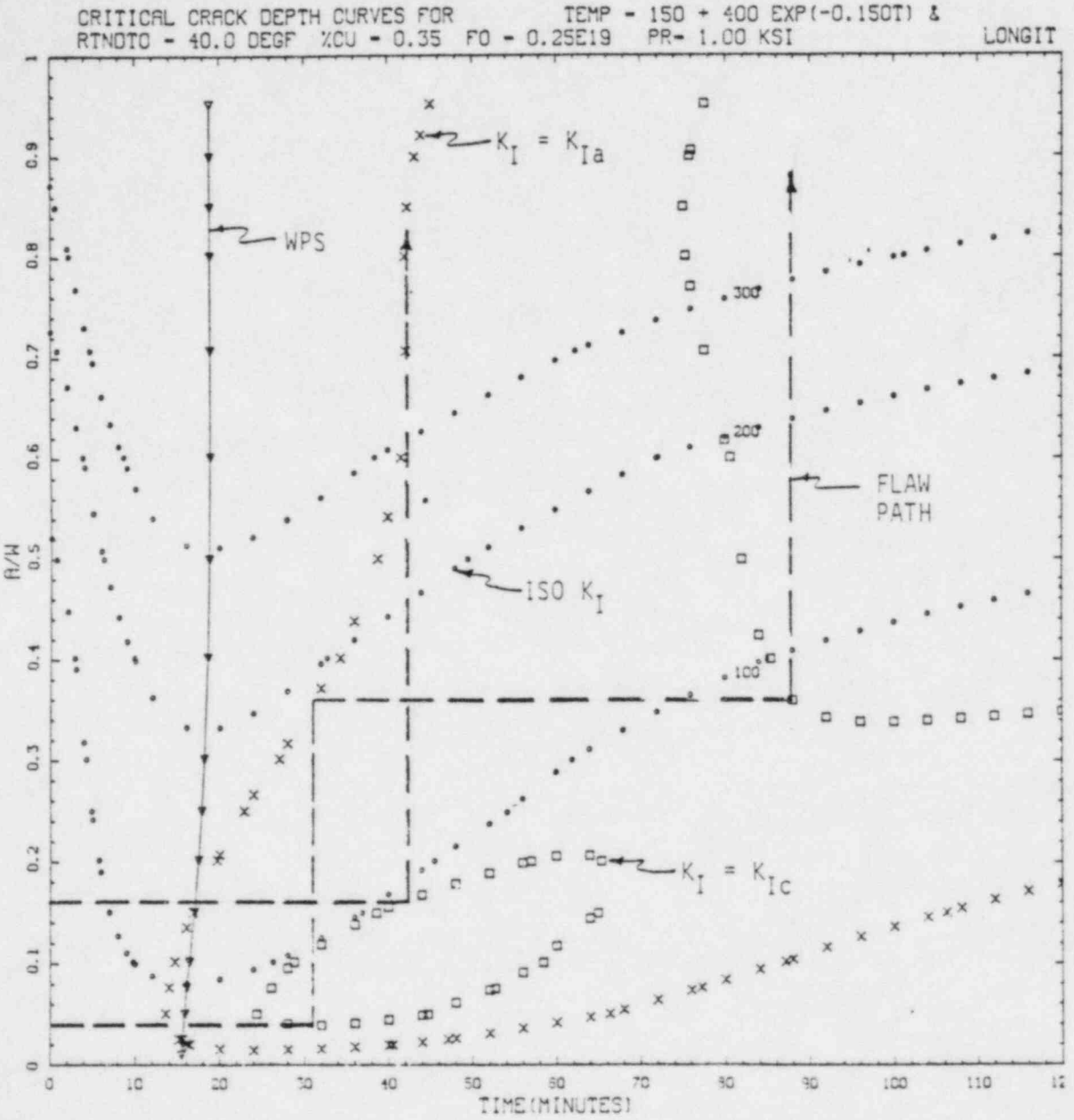

Fig. 5.5. Critical-crack-depth curves for a typical postulated PTS transient.

The dashed lines in Fig. 5.5 indicate the behavior of two initially shallow flaws, ignoring the effects of WPS. The deeper flaw would initiate at a time of 42 min into the transient and would extend through the wall without arresting. The other flaw would initiate at an earlier time, would arrest at a point 36% of the way through the wall, and then would reinitiate at a time of ~88 min and penetrate the wall. Earlier in the life of the vessel the tendency for complete penetration of the wall is less.

5.3.2 Stress-Analysis Model

When using the superposition technique in combination with influence coefficients to calculate K_I, the stresses required are those at the crack plane in the absence of the crack and with no variation in the direction of the length of the crack. For the Calvert Cliffs-1 analysis, it was assumed that there was no azimuthal variation as well, and thus the one-dimensional stress analysis model incorporated in OCA-P was adequate.

Material properties required for the stress analysis included the coefficient of thermal expansion (α), Young's modulus (E), and Poisson's ratio (ν). Although these properties have some temperature dependence, it was determined[8] that the use of appropriate average values results in an error in the calculated value of K_I of less than 10%. Thus, average values were used based on the data in Ref. 9. The values used for the Calvert Cliffs-1 analysis are as follows:

Property	Base Material	Cladding
$\bar{\alpha}$, $°C^{-1}$	1.45×10^{-5}	1.79×10^{-5}
$\bar{E}$, MPa	1.93×10^{5}	1.86×10^{5}
$\bar{\nu}$	0.30	0.30

5.3.3 Thermal Analysis Model

Temperatures in the wall of the vessel are required for two purposes: to calculate the thermal stresses and to calculate the fracture toughness. The temperatures required for determining the fracture toughness are those in the plane of the flaw, while those used in the one-dimensional analysis of the thermal stresses must represent some type of average distribution through the wall. The thermal stresses in the vicinity of the crack plane are more sensitive to the radial temperature distribution at the crack plane than elsewhere. Since these temperatures are the same as those needed for the fracture-toughness determinations, and since only one set of temperatures was to be used for both the stress and toughness calculations, the local temperatures would be the choice. These particular temperatures were not available, but fortunately the results of the thermal-hydraulic analysis indicated that for the transients of interest there was not much azimuthal variation in the downcomer coolant temperature. Thus, the time-dependent temperature distributions in the wall of the vessel were calculated with the one-dimensional thermal-analysis model in OCA-P, using average downcomer coolant temperatures and heat transfer coefficients.

Material properties required for the thermal analysis include the thermal conductivity (k), specific heat (c_p), and density (ρ) of the vessel material. The values used are as follows:

Property	Base Material	Cladding
k, W/m·°C	41.5	17.3
c_p, J/kg·°C	502	502
ρ, Kg/m^3	7830	7830

5.3.4 Probabilistic Analysis Model

The OCA-P probabilistic model, which is similar to that developed by Gamble and Strosnider,[10] is based on Monte Carlo techniques; that is, a large number of vessels is generated, and each vessel is then subjected to a fracture-mechanics analysis to determine whether the vessel will fail. Each vessel is defined by randomly selected values of several parameters that are judged to have significant uncertainties associated with them. The calculated probability of vessel failure is simply the number of vessels that fail divided by the total number of vessels generated. It constitutes a conditional probability of failure, $P(F|E)$, because the assumption is made that the PTS transient (event) takes place. A logic diagram summarizing the various steps in the OCA-P probabilistic analysis is shown in Fig. 5.6. F5.6

The parameters simulated for the Calvert Cliffs-1 analysis are crack depth f(a), F_o, RTNDT, Cu, Ni, K_{Ic}, and K_{Ia}. Normal distributions were assumed for all of these parameters except the crack depth; the standard deviations and truncation values used in the analysis are included in Table 5.1. T5.1

The probability of having a flaw in a specific weld with a depth in a specific range of crack depths Δa_i is given by

$$P(\Delta a_i) = NV \int_{\Delta a_i} f(a)B(a)da \qquad (5.8)$$

where

N = flaws of all depths per unit volume of the specific weld

V = volume of the specific weld

f(a) = flaw-depth density function

B(a) = probability of nondetection

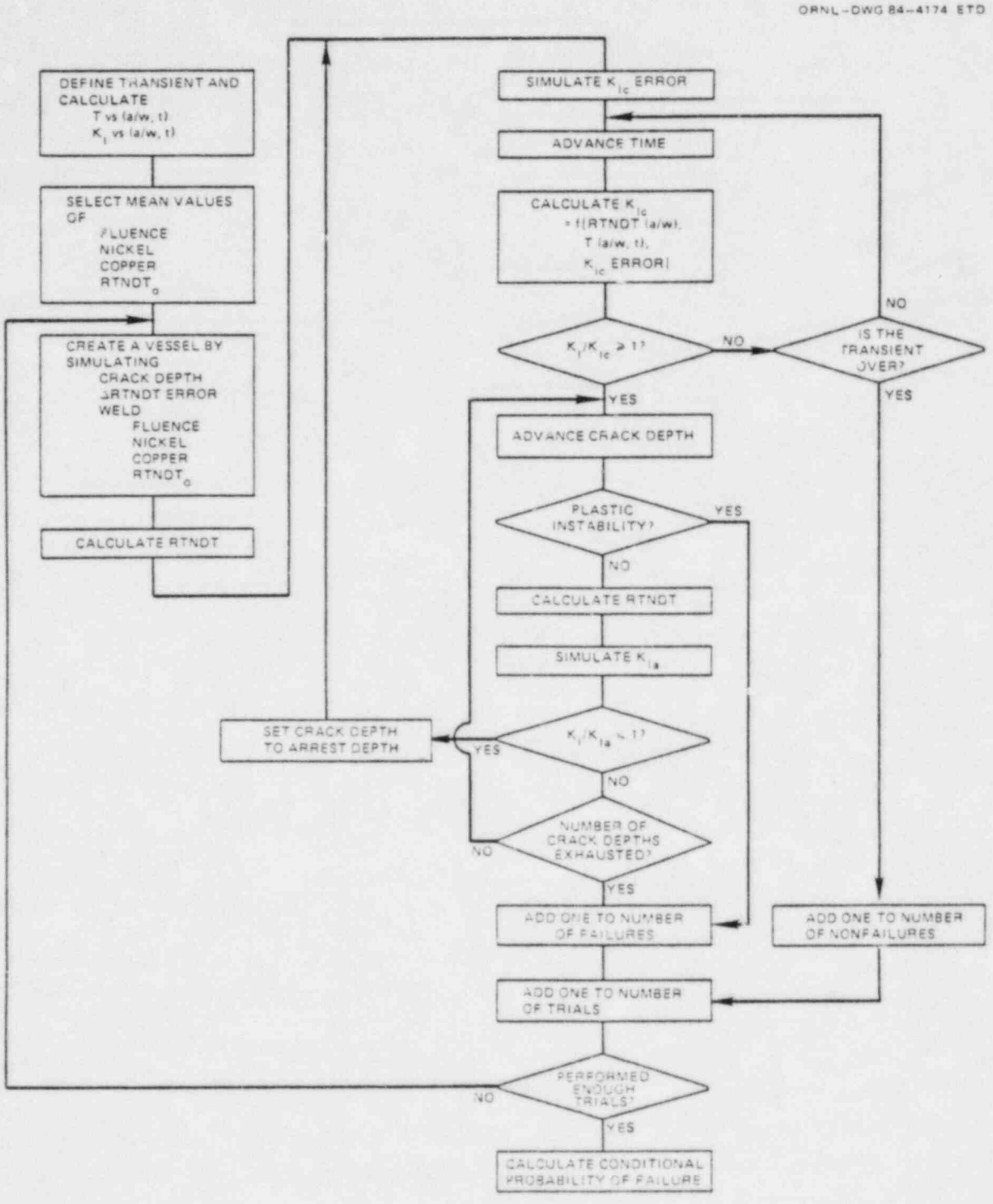

Fig. 5.6. OCA-P program logic.

Table 5.1. Parameters simulated in OCA-P

Parameter	Standard[a] deviation (σ)	Truncation
Fluence (F)	0.3 μ(F)	F = 0
Copper	0.025%	--
Nickel	0.0	--
$RTNDT_o$	9°C[b]	b
ΔRTNDT	13°C[b]	b
K_{Ic}	0.15 $\mu(K_{Ic})$	$\pm 3\sigma$
K_{Ia}	0.10 $\mu(K_{Ia})$	$\pm 3\sigma$

[a] Normal distribution used for each parameter.

[b] $\sigma_{(RTNDT)} = \left[\sigma^2(RTNDT_o) + \sigma^2(\Delta RTNDT)\right]^{1/2}$, truncated at $\pm 3\sigma$.

The parameters N and f(a) pertain to vessel conditions prior to preservice inspection and repair, and B(a) is derived on the basis of repairing or otherwise disposing of all detected flaws.

The value of N and the functions f(a) and B(a) are not well known because most of the available inspection data do not pertain to surface flaws that extend into and through the cladding of a PWR pressure vessel. For the Calvert Cliffs-1 analysis, the functions f(a) and B(a) were those suggested in the Marshall Report[11] and are as follows:

$$f(a) = 0.16\, e^{-0.16\, a} \tag{5.9}$$

$$B(a) = 0.005 + 0.995\, e^{-0.113\, a} \tag{5.10}$$

where

a = crack depth, mm

$$\int_0^\infty f(a)da = 1$$

For the Calvert Cliffs-1 vessel the probability of nondetection, B(a), should probably be set equal to unity, independent of a, because it is not likely that a reliable inspection was made for flaws in and extending a short distance beyond the cladding. Furthermore, it is not likely that any detected flaws of this type were repaired. Even so, Eq. (5.1) was used in the Calvert Cliffs-1 analysis. If B(a) = 1 were used instead, P(F|E) would be about twice as much. Thus the results of this study can be interpreted accordingly.

The value of N used in the Calvert Cliffs-1 analysis was 1 flaw/m^3 of weld and base material, and it was assumed that all flaws were inner-surface flaws normal to the surface. Flaws in welds were oriented in the length-direction of the weld, while those in the plate segments were oriented axially. The assumed value of the flaw density (1 flaw/m^3) agrees with that suggested in the Marshall Report,

but the uncertainty is considered to be very large (values of N corresponding to 1σ variations are estimated to be 10^{-2} and 10^{2} flaws/m^3).

The volume (V) of a weld or plate segment used for calculating the number of surface flaws was the total volume of that portion of the weld or segment that was nearly within the axial confines corresponding to the active length of the core.

As mentioned above, the calculated probability of vessel failure for this study is the number of simulated vessels calculated to fail divided by the total number of vessels simulated or otherwise accounted for. Thus,

$$P(F|E) = \sum_j \frac{N'_{fj}}{N'_{vj}} V_j N \int_0^W f(a)B(a)da \,, \qquad (5.11)$$

where

N'_{fj} = number of vessels with a flaw in the jth region that fail

N'_{vj} = number of vessels simulated with a flaw in the jth region

V_j = volume of jth region

The integral in Eq. (5.11) accounts for the vessels that have no flaws whatsoever, and each term in Eq. (5.11) represents the contribution to P(F|E) of each specified region of the vessel.

For very small values of P(F|E), the value of N'_{vj} required to achieve reasonable accuracy becomes quite large. Under some circumstances the value of N'_{vj} can be reduced by using stratified sampling of one or more of the parameters simulated. This was done for the flaw depth, assuming a uniform distribution of depths. This procedure allows a more frequent sampling of the less probable deep flaws, which, for low-probability transients that are characterized by high pressure and a mild thermal shock, are responsible for most of the initiation events that lead to failure. The results are then

weighted by the actual flaw-depth density to obtain

$$P(F|E) = \sum_j \sum_i \frac{N'_{fij}}{N'_{vij}} \left[\frac{\int_{\Delta a_i} f(a)B(a)da}{\int_0^W f(a)B(a)da} \right] NV_j \int_0^W f(a)B(a)da \ , \qquad (5.12)$$

where

N'_{fij} = number of vessels that fail with a flaw in the jth region with depth in Δa_i

N'_{vij} = number of vessels simulated with a flaw in the jth region with depth in Δa_i

A deterministic analysis is made for each of the simulated vessels to determine if failure will occur during a particular transient at a specified time in the life of the plant. The criterion by which failure is judged is as follows: if, following an initiation event, K_I remains greater than K_{Ia} up to or beyond the point at which plastic instability occurs in the remaining ligament, failure is assumed. The onset of plastic instability is evaluated on the basis of achieving an average pressure stress in the remaining ligament equal to the flow stress. The flow stress is assumed to be independent of temperature and fluence and is specified as 550 MPa.

The number of vessels that must be simulated depends upon the accuracy required for the calculated value of P(F|E), and as small a number as practical is used to minimize computer costs. The minimum number of simulated vessels required to satisfy a specified accuracy is estimated by applying the central

limit theorem.[12] Using this approach and specifying a 95% confidence level yields

$$P(F|E)_j = \hat{P}_j \, NV_j \int_0^W f(a)B(a)da \pm 1.96 \, \sigma_j \tag{5.13}$$

where

$P(F|E)_j$ = true value of the conditional probability of vessel failure for those vessels having flaws in the jth region only

σ_j = one standard deviation,

$\hat{P}_j = \frac{N'_{fj}}{N'_{vj}}$.

For the direct approach (not using stratified sampling)

$$\sigma_j = \left[\frac{\hat{P}_j(1 - \hat{P}_j)}{N'_{vj}}\right]^{1/2} NV_j \int_0^W f(a)B(a)da \, . \tag{5.14}$$

When stratified sampling is used,

$$\sigma_j = \left\{\sum_i \left[\frac{\int_{\Delta a_i} f(a)B(a)da}{\int_0^W f(a)B(a)da}\right]^2 \left[\frac{\hat{P}_{ij}(1 - \hat{P}_{ij})}{N'_{vij}}\right]\right\}^{1/2} NV_j \int_0^W f(a)B(a)da \, , \tag{5.15}$$

where $\hat{P}_{ij} = \frac{N'_{fij}}{N'_{vij}}$.

The value of σ corresponding to all of the vessels simulated is

$$\sigma_{P(F|E)} = \sqrt{\Sigma \sigma_j^{\,2}} \, , \tag{5.16}$$

and the error, ε_j, associated with the jth region is

$$\varepsilon_j = \frac{1.96\ \sigma_j}{\hat{P}_j\ NV_j \int_0^W f(a)B(a)da} . \qquad (5.17)$$

The total error, ε, considering all regions of interest is

$$\varepsilon = \frac{1.96\ \sigma_{P(F|E)}}{\sum_j \hat{P}_j\ NV_j \int_0^W f(a)B(a)da} . \qquad (5.18)$$

Three specific criteria were used in selecting the number of vessels to be simulated:

(1) $(N'_{vj})_{max} = 500{,}000$

(2) $(N'_{vj})_{min} = 10{,}000$

(3) $\varepsilon_j = 10\%$

The application of these criteria in terms of ε_j vs $\hat{P}_j$ is shown in Fig. 5.7 for the direct (nonstratified) sampling method. F5.7

For the purpose of estimating the absolute frequency of vessel failure or identifying dominant transients, the magnitude of the errors indicated in Fig. 5.7 was acceptable for most transients. However, for some transients and for the sensitivity studies, larger values of N'_{vj} and/or the stratified-sampling technique were used where appropriate to reduce the error.

5.4 Flaw-Related Data for the Calvert Cliffs-1 Reactor Pressure Vessel

As already mentioned, the areas of the vessel of particular concern with regard to flaw propagation are the ones that are most likely to have flaws and

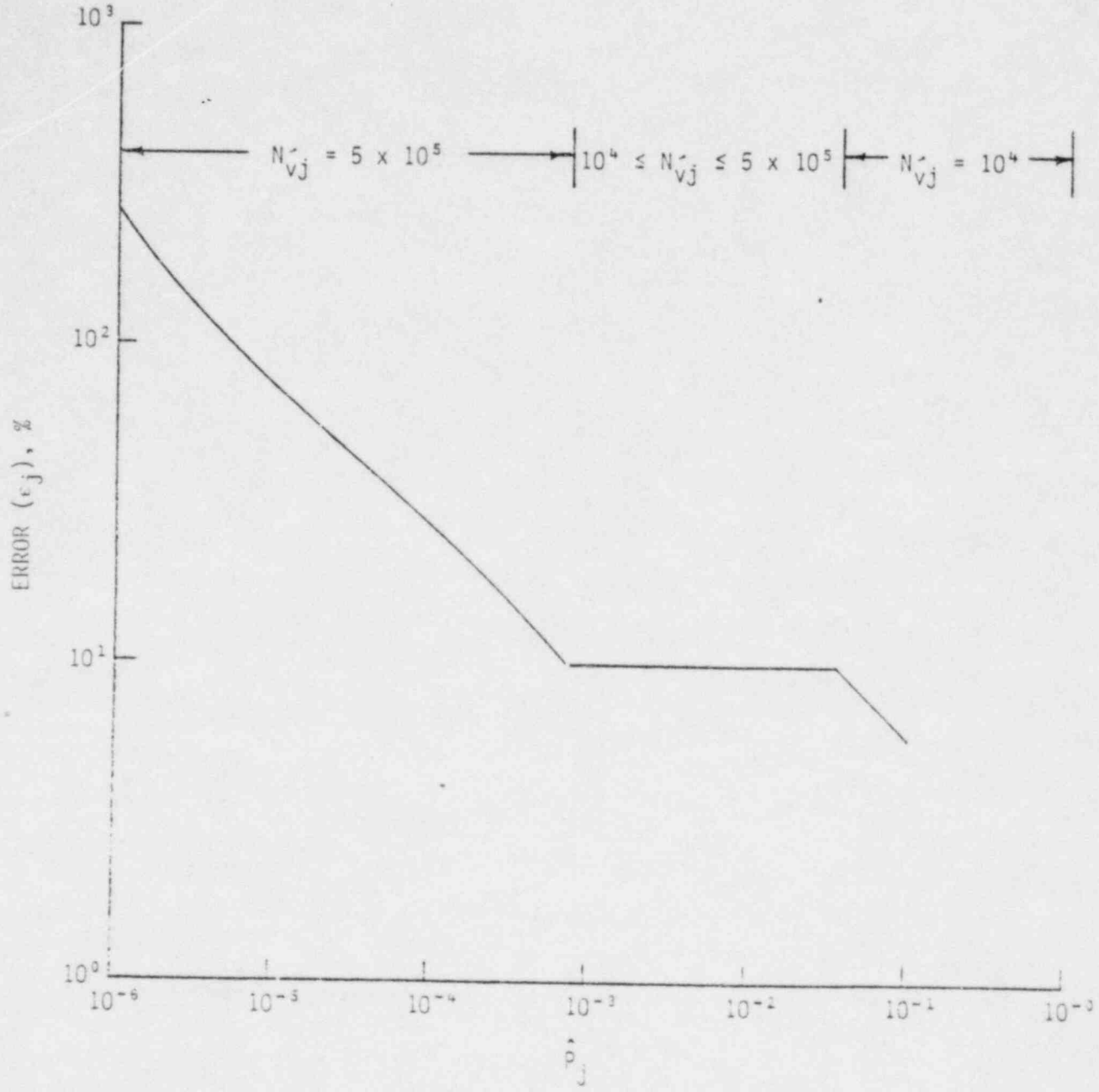

Fig. 5.7. Graphic illustration of the error in $\hat{P}_j$ consistent with the criteria used for establishing the number of vessels simulated (N'_{vj}).

relatively high values of F_o, $RTNDT_o$, Cu and Ni. The region directly opposite the active portion of the core is exposed to the highest neutron fluxes, and the attenuation beyond the active length of the core is very steep. Thus, only this beltline region of the vessel was considered.

Within the beltline region the concentration of copper is significantly less in the base material than in the welds, as indicated by the data in Table 5.2 and Figs. 5.2 and 5.3. However, preliminary OCA-P calculations (see Appendix K) indicated that because of their much larger surface area the plate segments would contribute significantly to vessel failure, assuming the same flaw density in both the plate segments and welds. These preliminary calculations also indicated that welds 2-203A,B,C and 3-203A, each of which is oriented in an axial direction, contributed far more than all the other welds. Thus, the regions of the vessel to be considered were these four axial welds and the plate segments. However, the contribution to P(F|E) of axial flaws in the plate segments was calculated for only a few of the transients and was not included in any of the reported values of P(F|E) except as discussed in Sect. 5.5.2 and Appendix K. This was done to maintain consistency between all tabulated values.

As discussed in Appendix K, the contribution of the one circumferential weld in the beltline region was relatively small because of the low concentration of nickel and a much smaller value of K_I for deep circumferential flaws as compared to axial flaws of the same depth.

The information in Table 5.2 was taken from Refs. 13, 14 and 15; values listed for chemistry, fluence and RTNDT were considered to be mean values.

Table 5.2.
Material properties, fluences and volumes used in the LEFM analysis of the Calvert Cliffs-1 reactor vessel

Material identification		Chemistry		Neutron fluence[a] at inner surface, 32 EFPY (10^{19} n/cm^2)	Initial RTNDT (°C)	Material[b] volume (m^3)
Form	Number	Cu (wt %)	Ni (wt %)			
Plate	D-7205-1	0.12	0.57	0.33	−12	0
	D-7205-2	0.12	0.50	0.33	−12	0
	D-7205-3	0.12	0.54	0.33	−12	0
	D-7206-1	0.11	0.55	6.06	−7	2.43
	D-7206-2	0.12	0.64	6.06	−34	2.43
	D-7206-3	0.12	0.64	6.06	−12	2.43
	D-7207-1	0.13	0.54	6.06	−12	2.08
	D-7207-2	0.11	0.56	6.06	−12	2.08
	D-7207-3	0.11	0.53	6.06	−7	2.08
Axial Weld	1-203A	0.21	0.85	0.33	−49	0
	1-203B,C	0.21	0.85	0.17	−49	0
	2-203A	0.21	0.87	6.06	−49	0.025
	2-203B,C	0.21	0.87	3.03	−49	0.050
	3-203A	0.20	0.71	6.06	−49	0.021
	3-203B,C	0.20	0.71	3.03	−49	0.042
Cir Weld	8-203	0.35	0.74	0.33	−51	0
	9-203	0.24	0.18	6.06	−62	0.139

[a]Maximum value in region.

[b]Volume within high-fluence region.

5.5 Results of Analysis

5.5.1 Types of Analyses Conducted

Probabilistic fracture-mechanics calculations were performed to determine (1) the conditional probability of vessel failure [P(F|E)] for a number of postulated Calvert Cliffs-1 transients, (2) the sensitivity of P(F|E) to small changes in the mean values of certain parameters, (3) the effect of including WPS, and (4) the effect on P(F|E) of certain proposed remedial measures. The results of these efforts are presented below.

5.5.2 Conditional Probability of Vessel Failure

The specific transients considered for a detailed OCA-P analysis are described in Chapter 3, and those actually calculated with values of $P(F|E) \geq 10^{-7}$ are indicated in Table 5.3. For these transients the actual systems-analysis output (primary-system pressure, reactor-vessel downcomer coolant temperature, and fluid-film heat-transfer coefficient) was used as input to the OCA-P analysis, and stratified sampling techniques were not used. Values of P(F|E) for less severe transients [$P(F|E) < 10^{-7}$] were estimated in a conservative manner by using bounding transients and stratified sampling techniques. These transients were characterized by a step change in coolant temperature and a constant maximum pressure. None of the transients evaluated in this manner were dominant, and thus the possibly excessive degree of conservatism was of no consequence. Those transients not calculated were judged not to be dominant and to have values of P(F|E) at 32 EFPY less than 10^{-7}.

For all of the calculated transients with $P(F|E) \geq 10^{-7}$, values of P(F|E) were obtained for 32 and 41 EFPY. The latter time corresponds to $RTNDT_s$ (2σ) = 132°C (270°F) for weld 2-203A, while 32 EFPY is the normal design end of life. Five of these transients were eventually tentatively defined as dominant, and

Table 5.3. Summary of calculated values of P(F|E) for the Calvert Cliffs-1 postulated transients

EFPY	9.2	16.8	24.4	32.0	41.2	53.0
F_o,[a] 10^{19} n/cm^2	1.52	3.03	4.55	6.06	7.88	10.24
$\overline{RTNDT}_s$,[a] °C	46	66	79	89	99	110
Transient	Conditional Probability of Failure, P(F|E)					
1.3				6E-7	4.9E-6	
1.4				3.3E-6	1.7E-5	
1.5				3.0E-5	1.2E-4	
1.6				5.1E-5		
1.7				1.9E-4	4.8E-4	
1.8				2.5E-4	6.2E-4	
2.1				2E-7	1.4E-6	6.0E-6
2.4		2E-7	2.8E-6	1.7E-5	6.8E-5	2.4E-4
2.5				7.6E-6	3.2E-5	
2.6				8.2E-6	3.4E-5	
2.7				1.8E-4	4.5E-4	
2.8				2.3E-6	1.1E-5	
3.6				7.2E-6	3.6E-5	
3.10				6.7E-5		
4.6				2E-7	1.0E-6	
4.13				6.0E-6		
8.1			6E-8	4E-7	2.2E-6	8.8E-6
8.2	5E-7	1.2E-5	5.9E-5	1.5E-4	2.9E-4	5.9E-4
8.3	3.6E-4	1.9E-3	3.9E-3	5.9E-3	8.0E-3	1.0E-2

[a]Mean values at inner surface for weld 2-203A; add 33°C to obtain 2σ value [NRC 2σ screening value is 132°C (270°F)].

for these, P(F|E) was calculated for additional values of EFPY. The corresponding plots of P(F|E) vs EFPY, F_o and $\overline{RTNDT_s}$ are shown in Fig. 5.8. F5.8

Values of P(F|E) in Table 5.3 and Fig. 5.8 do not include the contribution of the plate segments. This contribution was calculated for transients No. 8.2 and 8.3 (dominant transients) and was found to be <5% for No. 8.2 and ~50% for No. 8.3. Thus, for these two transients, factors of 1.05 and 1.5 can be applied to the values of P(F|E) in Table 5.3 and Fig. 5.8.

A summary of more detailed results for each of the four* dominant sequences at 41.2 EFPY (270°F RT_{NDT}) is presented in Tables 5.4A, 5.4B, 5.4C, and 5.4D. Additional summaries are presented in Appendix L at 32 EFPY for each analyzed transient. These summary sheets provide data for a variety of histograms. T5.4
Four examples of histogram plots that can be produced from the summary sheets are provided for transient 8.3 in Figures 5.9-5.12. F5.9 –5.12

Appendix L also includes for each transient calculated a definition of the transient input to OCA-P (downcomer coolant temperature vs time, primary-system pressure vs time, and fluid-film heat transfer coefficient at the vessel inner surface vs time), temperature distributions in the wall, and a set of critical-crack-depth curves for weld 2-203A based on mean values of all parameters except K_{Ic} and K_{Ia}, which are -2σ values, and 32 EFPY. Examples of these graphical outputs are shown in Figs. 5.13–5.16 for transient No. 8.3. F5.13 –5.16

5.5.3 Sensitivity Analysis

The sensitivity analysis was conducted by determining the change in P(F|E) corresponding to a change in the mean value of each of several parameters. The mean value of only one parameter was changed at a time while all other parameters retained their original mean values. The parameters changed were K_{Ic}, K_{Ia}, RTNDT, Cu, F, fluid-film heat transfer coefficient, downcomer coolant temperature, primary-system pressure, and flaw density. The amount of the change for each parameter was one standard deviation, and the sign of the change was such that an increase in P(F|E) occurred.

The values of σ used in the sensitivity analysis for K_{Ic}, K_{Ia}, RTNDT, Cu, and F are listed in Table 5.1, and the values of the flaw density, N, corresponding to the application of $\pm 1\sigma$ were 10^2 and 10^{-2} times the original mean

---

*There are actually five dominant sequences identified in Chapter 6.0. However since sequences 2.3 and 2.4 are assumed to be identical, data are provided in this chapter only for sequence 2.4.

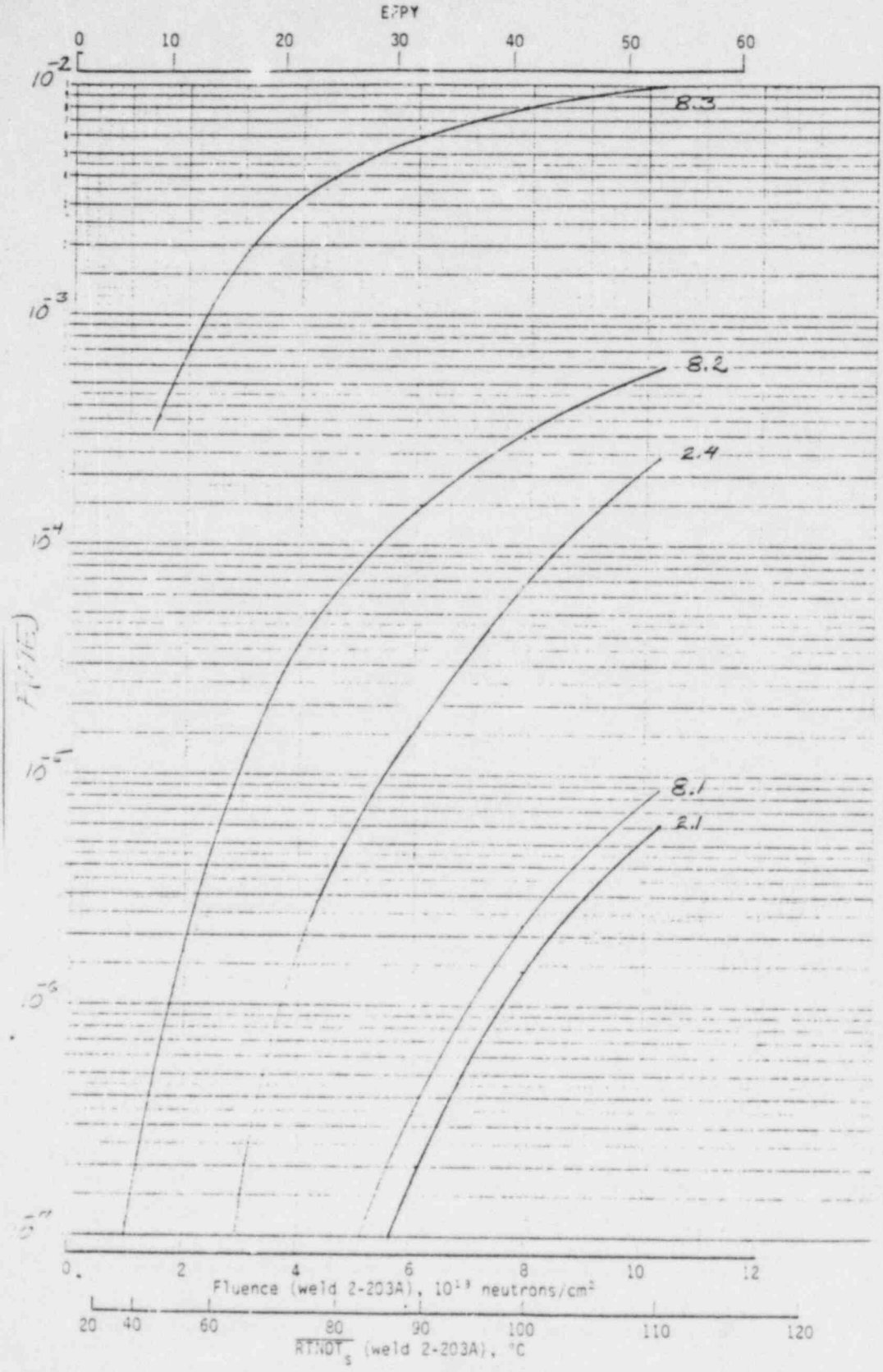

Fig. 5.8. P(F|E) vs EFPY for Calvert Cliffs-1 postulated PTS transients.

PTS C CLIFFS CLAD 2.1 1. FLAWS/M**3 FO = 7.88CD+15

WELD	UNADJUSTED P(F/E)	UNADJUSTED %STD	UNADJUSTED %ERR	P(INITIA)	N*V	ADJUSTED P(F/E)	ADJUSTED %ERR	TRIALS
1	5.52D-05	1.58E-05	28.59	1.05E-03	0.025	1.3ED-06		500000
2	0.000+00	0.00E+00	0.00	1.17D-05	0.050	0.000+00		500000
3	1.17D-06	2.30E-06	196.00	1.95D-04	0.021	2.47D-08		500000
				VESSEL		1.40D-06	28.30	

DEPTHS FOR INITIAL INITIATION (MM)

	2.16	6.66	11.62	17.03	22.95	29.42	36.51	44.25	52.72
NUMBER	19	656	245	91	14	4	1	0	0
PERCENT	1.8	65.0	22.9	8.5	1.3	0.4	0.1	0.0	0.0

TIMES OF FAILURE(MINUTES)

	0.0	10.0	20.0	30.0	40.0	50.0	60.0	70.0	80.0	90.0	100.0	110.0	120.0
NUMBER	0	0	0	0	0	6	7	13	8	11	1	0	
PERCENT	0.0	0.0	0.0	0.0	0.0	16.7	14.6	27.1	16.7	22.9	2.1	0.0	

INITIATION T-RINDT(DEG.C)

	-55.6	-41.7	-27.8	-13.9	0.0	13.9	27.8	41.7	55.6	69.4	83.3	97.2	111.1
NUMBER	0	2	74	302	513	194	65	22	0	0	0	0	
PERCENT	0.0	0.2	6.2	25.3	42.9	16.2	7.4	1.8	0.0	0.0	0.0	0.0	

ARREST T-RINDT(DEG.C)

	-27.8	-13.9	0.0	13.9	27.8	41.7	55.6	69.4	83.3	97.2	111.1	125.0	138.9
NUMBER	0	0	1	9	4	8	42	391	581	112	0	0	
PERCENT	0.0	0.0	0.1	0.8	0.3	0.7	3.7	34.1	50.6	9.8	0.0	0.0	

Table 5.4(A). Summary sheet of OCA-P output for Calvert Cliffs-1 postulated transient No. 2.1

IPTS C CLIFFS CLAD 2.4 1. FLAWS/M**3 FO = 7.EECD+1S

WELD	P(F/E) UNADJUSTED	95%CI	%ERR	P(INITIA)	N*V	P(F/E) ADJUSTED	%ERR	NTRIALS
1	2.25D-03	1.7ED-C4	7.91	3.15D-C3	0.025	5.62D-C5		160000
2	4.11D-05	1.3EC-C5	33.13	7.2ED-C5	C.C5C	2.CEC-C6		500000
3	4.73D-04	4.62C-C5	9.76	7.44C-C4	0.021	9.94D-C6		500000
				VESSEL		6.62C-C5	6.74	

DEPTHS FOR INITIAL INITIATION (MM)

	2.16	6.6E	11.62	17.03	22.95	29.42	36.51	44.25	52.72
NUMBER	22	582	366	135	36	10	1	1	0
PERCENT	1.4	63.2	23.6	8.7	2.3	C.6	0.1	C.1	0.0

TIMES OF FAILURE(MINUTES)

	0.0	10.0	20.0	30.0	40.0	50.0	60.0	70.0	80.0	90.0	100.0	110.0	120.0
NUMBER	C	C	0	32	121	54	150	172	170	122	107	82	
PERCENT	0.0	C.C	C.0	3.0	11.5	5.0	14.3	16.4	16.2	11.6	10.2	7.8	

INITIATION T-KINDT(DEG.C)

	-55.6	-41.7	-27.8	-13.9	0.0	13.9	27.8	41.7	55.6	69.4	83.3	97.2	111.1
NUMBER	2	14	103	506	665	311	622	426	13	0	0	0	
PERCENT	C.1	C.5	3.9	19.0	25.1	11.7	23.3	16.0	0.5	C.0	0.C	C.0	

ARREST T-KINDT(DEG.C)

	-27.8	-13.9	0.C	13.9	27.8	41.7	55.6	69.4	83.3	97.2	111.1	125.0	138.9
NUMBER	C	C	0	11	3	1	18	273	1155	155	C	0	
PERCENT	C.C	C.C	C.0	0.7	C.2	C.1	1.1	16.9	71.5	9.6	0.C	0.0	

Table 5.4(B). Summary sheet of OCA-P output for Calvert Cliffs-1 postulated transient No. 2.4

IPTS C CLIFFS CLAD ~~STGHP/T8~~ 4/84 . 1. FLAWS/M**3 FO = 7.880D+19 (8.2)

WELD	UNADJUSTED P(F/E)	95%CI	%ERR	P(INITIA)	N*V	ADJUSTED P(F/E)	%ERR	NTRIALS
1	7.640-03	5.66D-04	7.96	1.65D-02	0.025	1.76D-04		50000
2	5.84D-04	7.25D-05	7.98	4.63D-03	0.050	4.52D-05		360000
3	3.25D-03	2.57D-04	7.93	9.55D-03	0.021	6.82D-05		110000
					VESSEL	2.93D-04	5.29	

DEPTHS FOR INITIAL INITIATION (MM)

	2.16	6.86	11.62	17.03	22.95	29.42	36.51	44.25	52.72
NUMBER	7	5045	565	314	123	38	7	4	0
PERCENT	0.1	82.7	9.3	5.1	2.0	0.6	0.1	0.1	0.0

TIMES OF FAILURE(MINUTES)

	0.0	10.0	20.0	30.0	40.0	50.0	60.0	70.0	80.0	90.0	100.0	110.0	120.0
NUMBER	0	0	0	0	0	0	0	5	69	212	480	1040	
PERCENT	0.0	0.0	0.0	0.0	0.0	0.0	0.0	0.5	3.8	11.7	26.5	57.5	

INITIATION T-RTNDT(DEG.C)

	-55.6	-41.7	-27.8	-13.9	0.0	13.9	27.8	41.7	55.6	69.4	83.3	97.2	111.1
NUMBER	569	1457	2335	1588	611	775	189	10	0	0	0	0	
PERCENT	7.6	19.3	31.0	21.1	8.1	10.3	2.5	0.1	0.0	0.0	0.0	0.0	

ARREST T-RTNDT(DEG.C)

	-27.8	-13.9	0.0	13.9	27.8	41.7	55.6	69.4	83.3	97.2	111.1	125.0	138.9
NUMBER	540	1114	408	26	3	479	2161	228	0	0	0	0	
PERCENT	17.5	20.8	7.6	0.5	0.1	8.9	40.3	4.3	0.0	0.0	0.0	0.0	

CC-5.34

Table 5.4(C). Summary sheet of OCA-P output for Calvert Cliffs-1 postulated transient No. 8.2

IPTS C CLIFFS CLAD 8.3 1. FLAWS/M**3 FO = 7.EEC0+15

WELL	ADJUSTED P(F/L)	ADJUSTED SCALE	ADJUSTED ALPHA	P(INITIA)	MAV	ADJUSTED P(F/L)	ADJUSTED ALPHA	MINIALS
1	1.190D-01	4.226-03	3.89	1.150-01	0.025	2.570-03		10000
2	8.670-02	3.836-03	3.77	8.050-02	0.030	3.030-03		10000
3	5.540-02	4.256-03	4.45	5.000-02	0.021	2.000-03		10000
				WELL		8.010-03	2.85	

DEPTHS FOR INITIAL INITIATION (MM)

	2.10	6.28	11.02	17.03	22.55	29.42	36.51	44.25	52.72
NUMBER	230	3136	940	254	60	17	5	2	0
PERCENT	4.5	60.5	20.1	6.3	1.7	0.4	0.1	0.0	0.0

TIMES TO FAILURE(MINUTES)

	0.0	10.0	20.0	30.0	40.0	50.0	60.0	70.0	80.0	90.0	100.0	110.0	120.0
NUMBER	0	0	0	0	0	0	0	1	7	2822	802	1044	
PERCENT	0.0	0.0	0.0	0.0	0.0	0.0	0.0	0.0	0.1	60.4	17.1	22.3	

INITIATION T-MIN(DEG.C)

	-55.6	-41.7	-27.8	-13.9	0.0	13.9	27.8	41.7	55.6	69.4	83.3	97.2	111.1
NUMBER	545	565	1528	1235	362	73	96	72	14	1	0	0	
PERCENT	11.6	19.4	32.6	26.3	7.7	1.6	2.0	1.4	0.3	0.0	0.0	0.0	

ARREST T-MIN.(DEG.C)

	-27.8	-13.9	0.0	13.9	27.8	41.7	55.6	69.4	83.3	97.2	111.1	125.0	138.9
NUMBER	4	27	36	5	2	17	173	62	1	0	0	0	
PERCENT	1.2	8.4	5.3	1.6	0.6	5.3	53.9	19.3	0.3	0.0	0.0	0.0	

CC-5.35

Table 5.4(D). Summary sheet of OCA-P output for Calvert Cliffs-1 postulated transient No. 8.3

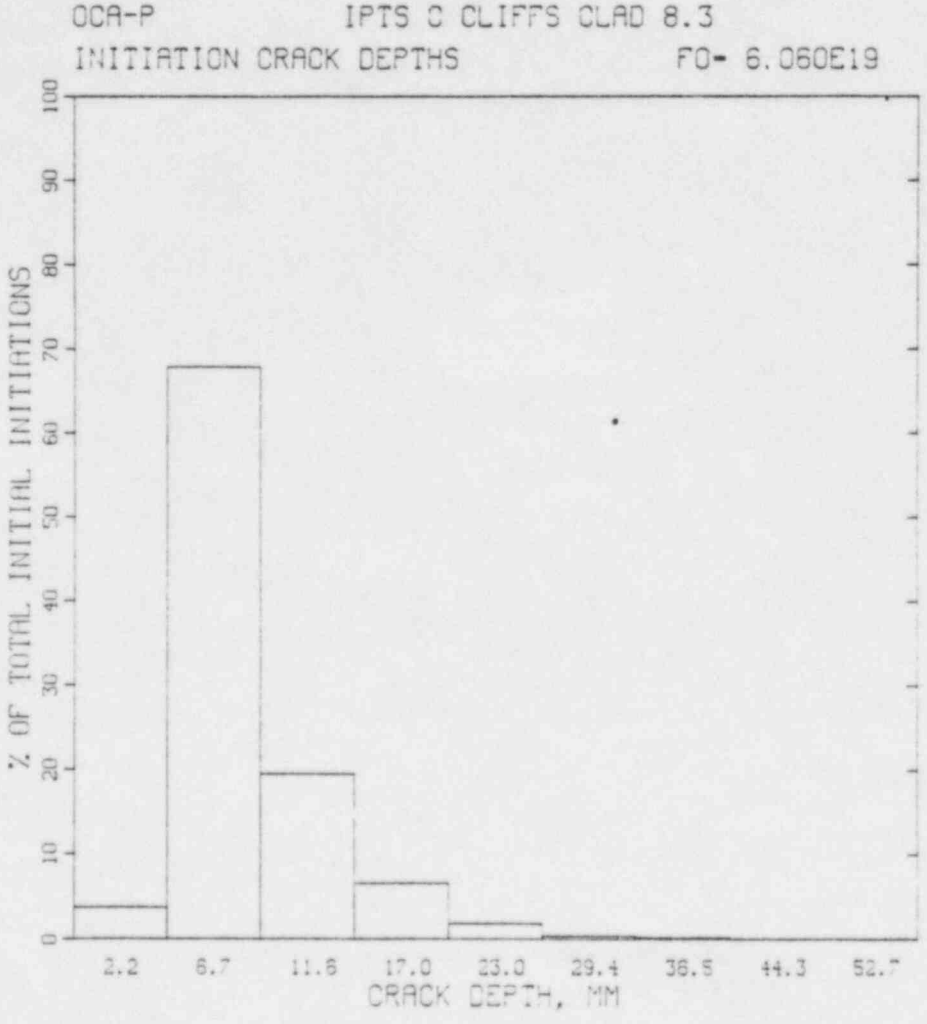

Fig. 5.9. Histogram of percent of initiations vs crack depth for first initiation event (Calvert Cliffs-1 postulated transient No. 8.3; 32 EFPY).

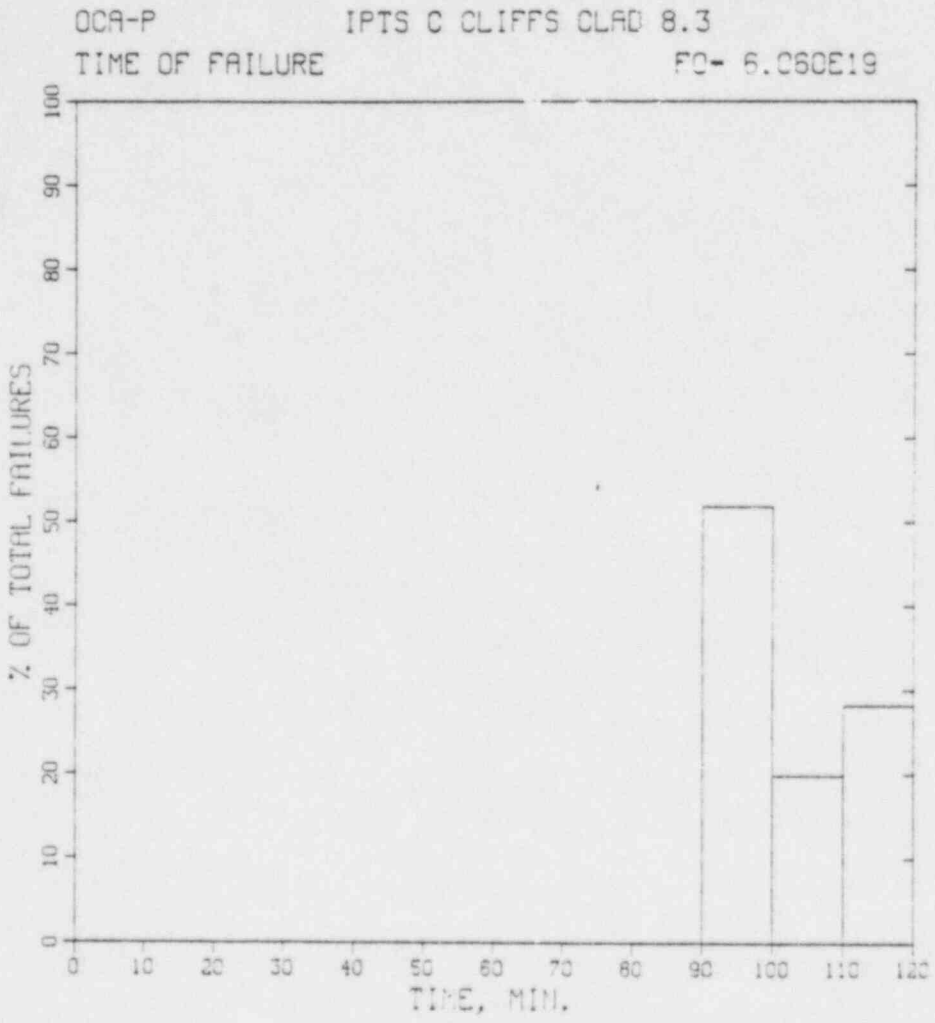

Fig. 5.10. Histogram of percent of failures vs time of failure (Calvert Cliffs-1 postulated transient No. 8.3; 32 EFPY).

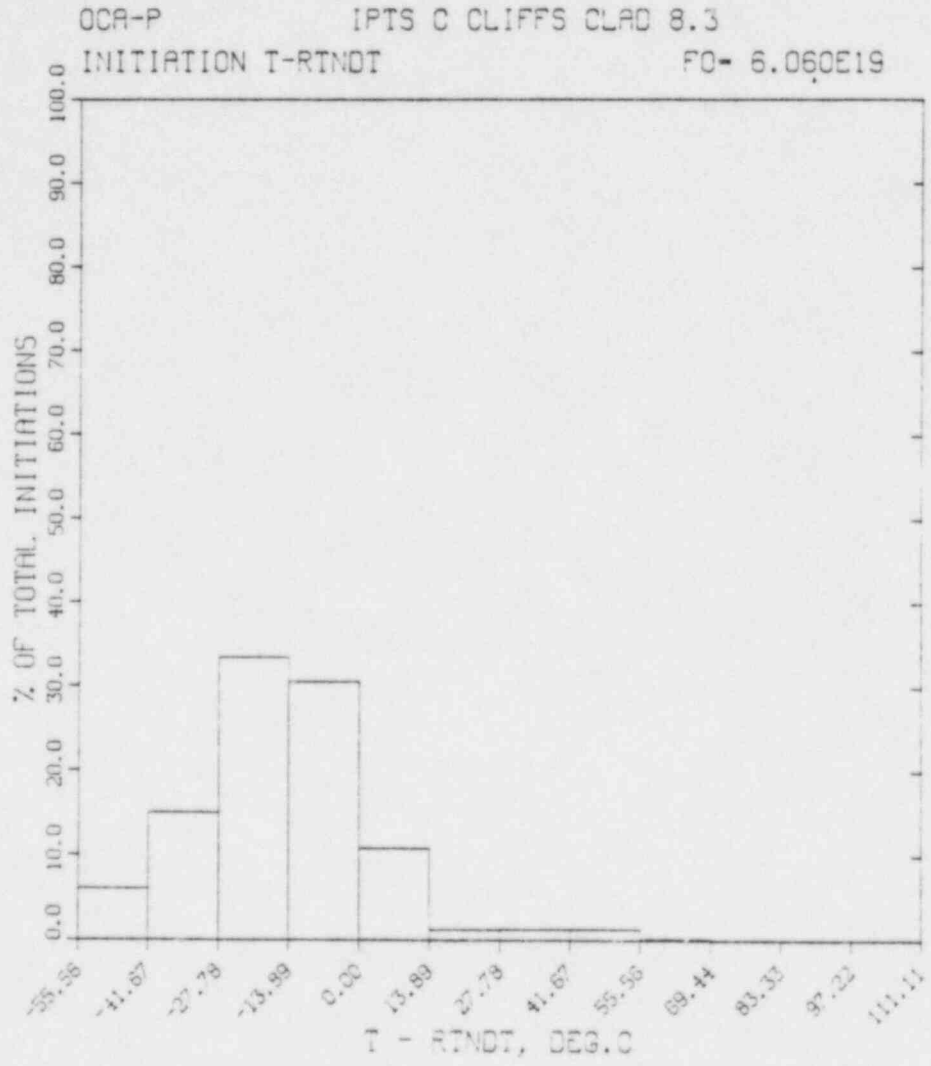

Fig. 5.11. Histogram of percent of total initiations vs relative temperature at which initiations take place (Calvert Cliffs-1 postulated transient No. 8.3; 32 EFPY).

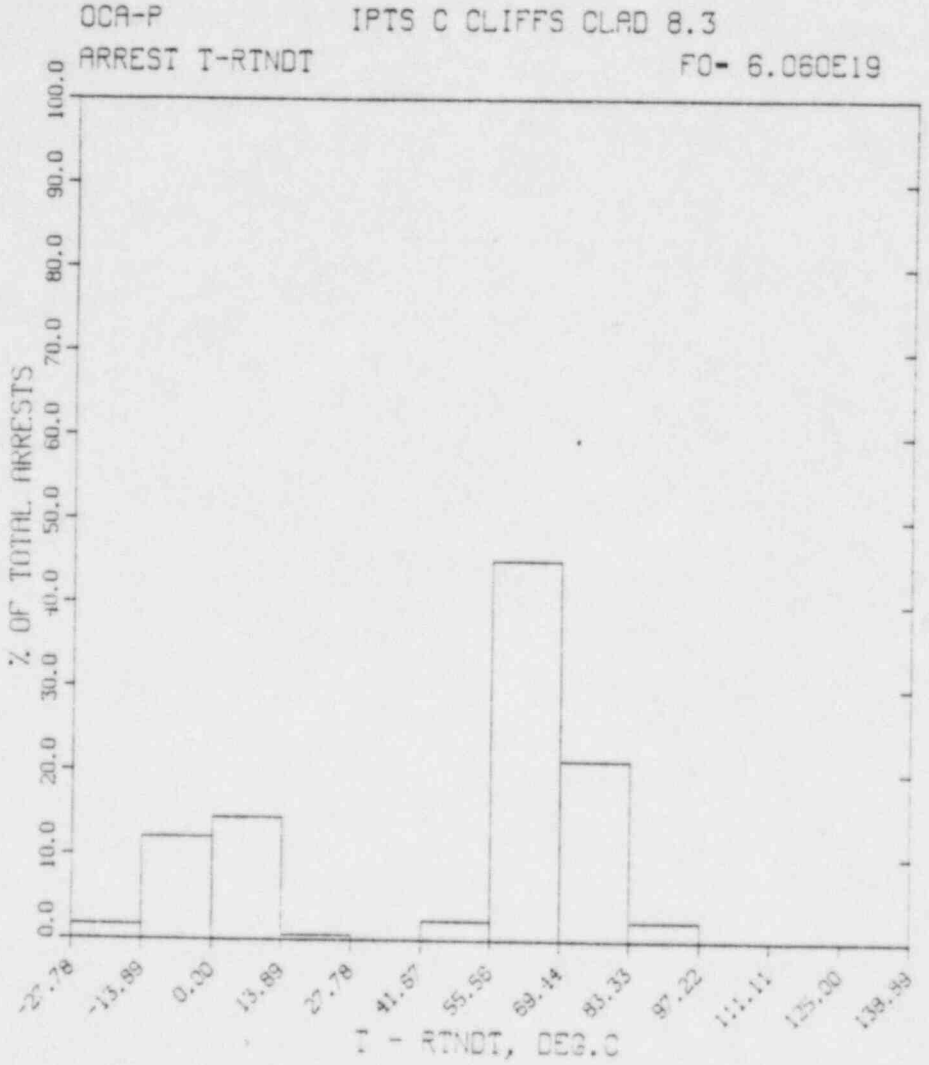

Fig. 5.12. Histogram of percent of total arrest events vs relative temperature at which arrest events take place (Calvert Cliffs-1 postulated transient No. 8.3; 32 EFPY).

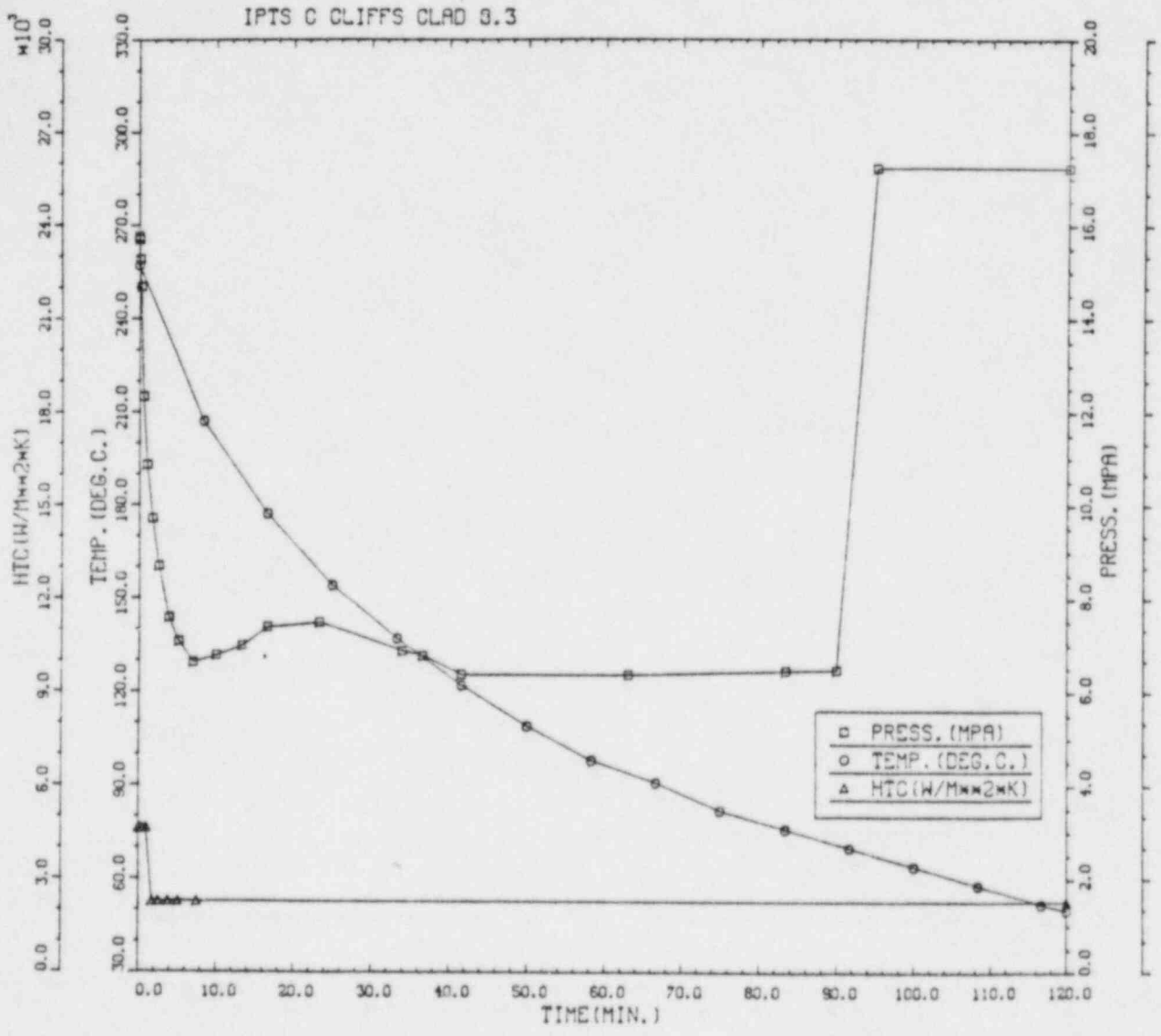

Fig. 5.13. P, T and h vs t for Calvert Cliffs-1 postulated transient No. 8.3.

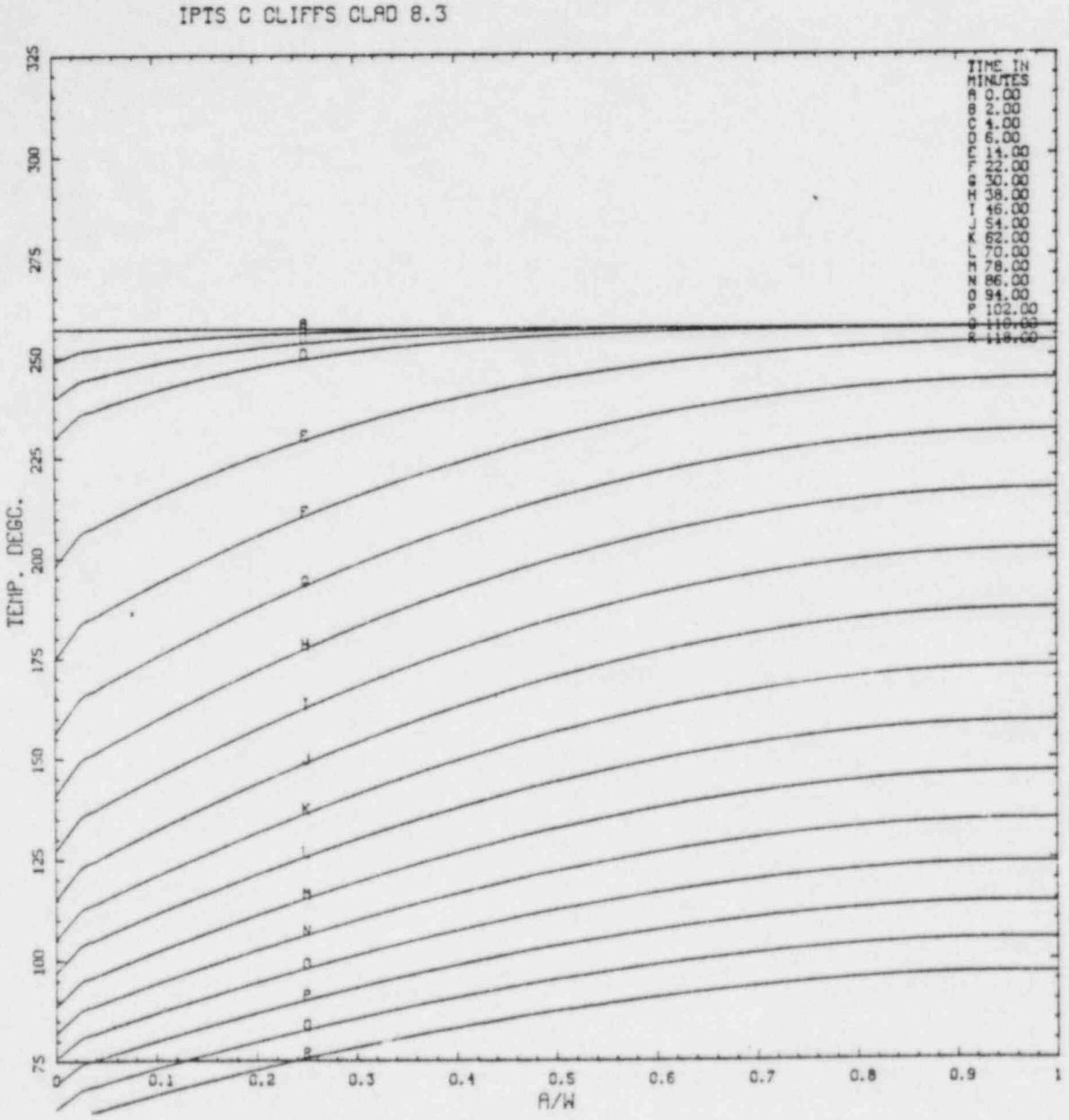

Fig. 5.14. Wall temperature vs a/w, t for Calvert Cliffs-1 postulated transient No. 8.3.

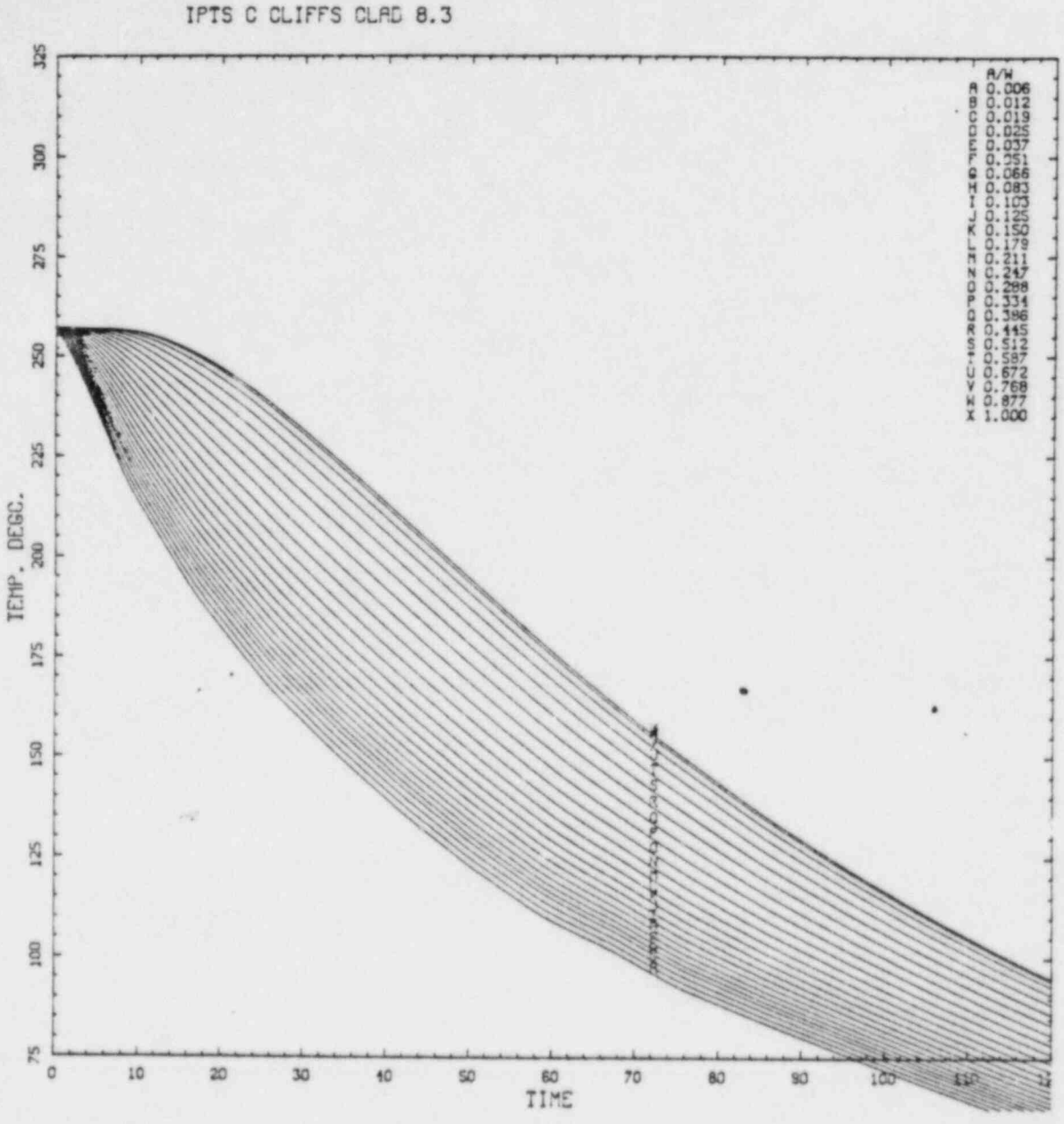

Fig. 5.15. Wall temperature vs t, a/w for Calvert Cliffs-1 postulated transient No. 8.3.

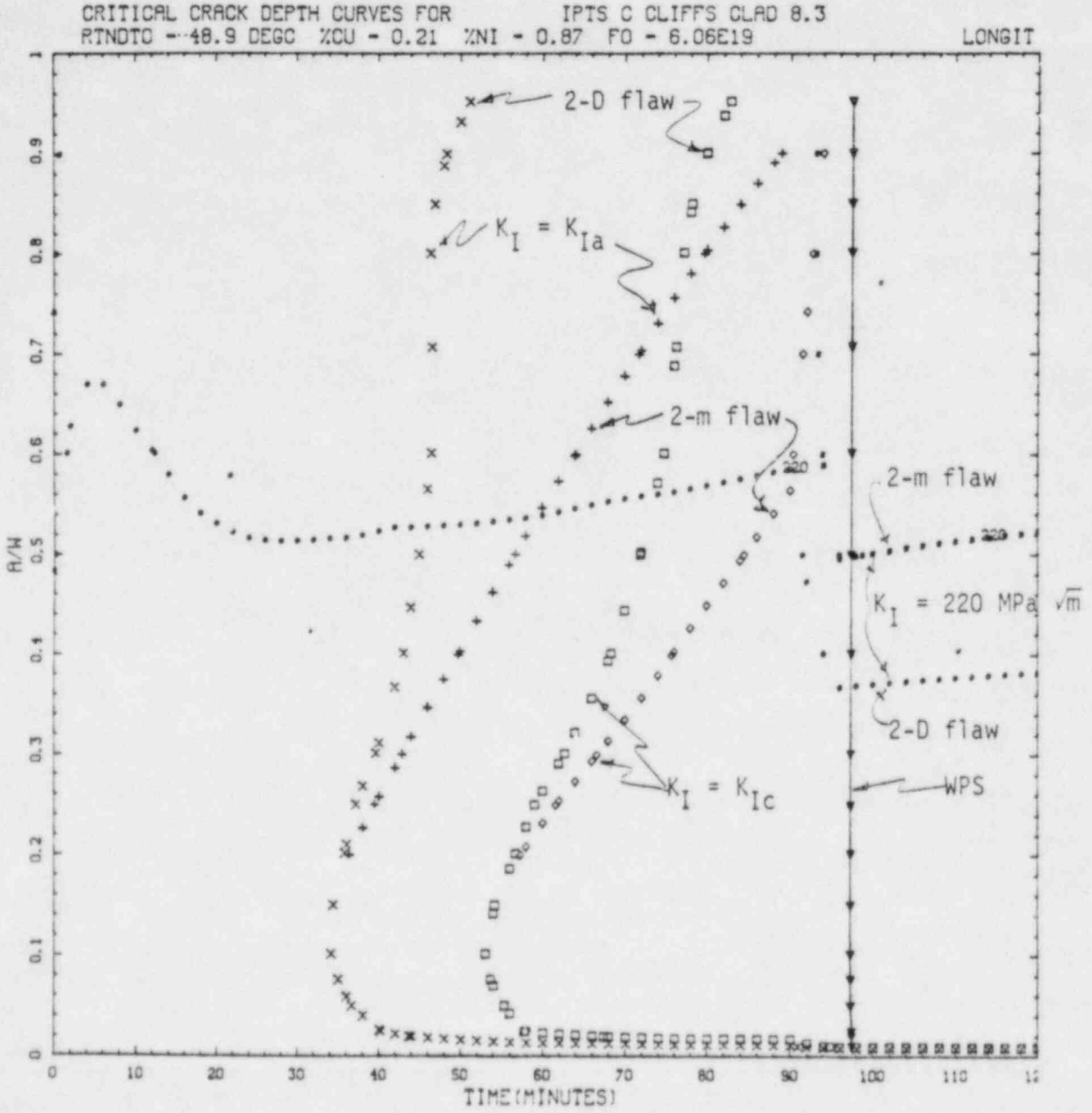

Fig. 5.16. Critical-crack-depth curves for Calvert Cliffs-1 postulated transient No. 8.3; 32 EFPY, weld 2-203A.

value. For the sensitivity analysis the change in the downcomer coolant temperature considered was a linear change in temperature from zero at time zero to 28°C (50°F) at a time corresponding to the minimum point in the temperature vs time curve. From then on, the change in temperature was a constant value of 28°C. The change in the heat transfer coefficient, h, was 0.25 h, and for the pressure it was 0.34 MPa (50 psi).

The results of the sensitivity study are presented in Table 5.5 for 41 EFPY. Table 5.5 includes (1) the values of P(F|E) at both 32 and 41 EFPY corresponding to the original mean values of the parameters and (2) the ratio $P(F|E)_{\sigma}/P(F|E)_{41}$ corresponding to each of the changes. T5.5

It is of interest to note that aside from the sensitivity to N, P(F|E) is most sensitive to the reduction in downcomer coolant temperature and is least sensitive to variations in the arrest toughness, the heat transfer coefficient and the primary system pressure. It is also of interest to note that the sensitivities are dependent on the transients.

5.5.4 Effect of Including WPS

During many of the postulated PTS transients, the stress intensity factor K_I, for all crack depths first increases with time, reaches a maximum, and then decreases. For the shallow flaws that are generally responsible for the initial crack initiation event, once K_I begins to decrease it does so throughout the remainder of the transient. This time-dependent behavior of K_I may prevent failure of a vessel because a flaw cannot initiate while K_I is decreasing, even though $K_I/K_{Ic} \geq 1$. As mentioned earlier, this phenomenon is referred to as warm prestressing (WPS), and the time of incipient WPS is the time at which $\dot{K}_I$ becomes equal to zero.

Table 5.5. Sensitivity of P(F|E) at 41 EFPY to 1σ changes in the mean values of several of the simulated parameters

	P(F|E)		$P(F\|E)_\sigma / P(F\|E)_{41}$[a] Simulated Parameter[b]								
Transient	At 32 EFPY	At 41 EFPY	F_o $+\sigma$	K_{Ic} $-\sigma$	K_{Ia} $-\sigma$	RTNDT $+\sigma$	Cu $+\sigma$	h	T_c	P	N $+\sigma$
1.6	5.1E-5	1.8E-4	3.1	3.1	1.1	4.8	4.6	1.3	15.0	1.2	100
1.7	1.9E-4	4.8E-4	2.3	2.5	1.0	3.1	3.3	1.0	8.3	1.0	100
1.8	2.5E-4	6.2E-4	2.3	2.6	1.0	3.1	3.2	1.2	8.1	1.1	100
2.1	2E-7	1.4E-6	4.3	2.6	1.0	7.9	6.0	1.0	4.4	1.0	100
2.4	1.7E-5	6.8E-5	3.5	3.4	1.0	5.1	5.4	1.3	16.2	1.1	100
2.5	7.6E-6	3.2E-5									100
2.6	8.2E-6	3.4E-5	3.5	4.1	1.1	5.6	5.9	1.2	8.8	1.2	100
2.7	1.8E-4	4.5E-4	2.1	2.4	1.0	2.9	3.1	1.1	5.1	1.0	100
2.8	2.3E-6	1.1E-5									100
3.6	7.2E-6	3.6E-5									100
4.6	2E-7	1.0E-6									100
8.1	4E-7	2.2E-6	4.0	4.0	2.8	10.0	6.8	1.2	30.0	2.3	100
8.2	1.5E-4	2.9E-4	2.0	3.8	1.4	3.1	2.7	1.1	11.0	1.3	100
8.3	5.9E-3	8.0E-3	1.3	1.8	1.0	1.5	1.5	1.0	2.3	1.0	100

[a] $P(F|E)_{41}$ is value at 41 EFPY, which corresponds to $\overline{RTNDT}_s + 2\sigma = 132°C$ (270°F) for weld 2-203A; $P(F|E)_\sigma$ is increased value of P(F|E) due to 1σ change in each simulated parameter, one at a time.

[b] Parameter adjusted by 1σ so as to achieve an increase in P(F|E) relative to P(F|E) at 41 EFPY.

For most of the Calvert Cliffs-1 postulated transients, WPS could be a factor because the calculations indicate that for these transients K_I does not become equal to K_{Ic} until after the time of incipient WPS. A typical case is illustrated in Fig. 5.5. The reason for not including WPS in most of the calculations is that the K_I vs t curves for the shallow flaws are very flat, making it difficult to determine where the maximum is. Furthermore, unforeseen perturbations in pressure and coolant temperature might exist and defeat WPS. Even so, it is of interest to see what the effect is for the idealized transients, and the results of such a study are presented in Table 5.6.

For some transients, such as No. 8.3 (see Fig.5.16) there can be more than one time during the transient at which $\dot{K}_I = 0$. For these transients, the time selected for incipient WPS was that corresponding to the maximum value of K_I.

Table 5.6 shows, for each of the transients considered, the time of incipient WPS, the calculated values of P(F|E) without WPS included in the analysis, and the ratio of P(F|E) with and without WPS included. It is apparent that for these idealized transients the benefit of WPS can be large but is dependent on the transient. T5.6

5.5.5 Effect of Proposed Remedial Measures on P(F|E).

The proposed remedial measures considered in the fracture-mechanics studies were (1) reduction in the fluence rate, (2) annealing of the vessel, and (3) an increase in the initial temperature of the HPI coolant.

5.5.5.1 Reduction in fluence rate

The reduction in fluence rate was assumed to take place on January 1, 1985, and it was assumed to be the same at all critical locations in the vessel wall. The effect was simply to change the proportionality constant between F_0 and EFPY beyond January 1, 1985. At this time the vessel will have been in service for ~7 EFPY, and the fluence for weld 2-203A will be 1.1×10^{19} neutrons/cm^2.

Table 5.6. Effect of Including WPS in calculation of P(F|E) at 32 EFPY

Transient	P(F|E) w/o WPS	Time of WPS (min)	$P(F\|E)_{w/WPS}$ [a] / $P(F\|E)_{w/oWPS}$
1.3	6E-7	18	<5E-2
1.4	3.3E-6	18	<1E-2
1.5	3.0E-5	18	<2E-3
1.6	5.1E-5	20	<2E-3
1.7	1.9E-4	18	<2E-3
1.8	2.5E-4	40	1E-1
2.1	2E-7	18	<1E-1
2.4	1.7E-5	50	1E-1
2.5	7.6E-6	15	<4E-3
2.6	8.2E-6	20	<4E-3
2.7	1.8E-4	50	2E-1
2.8	2.3E-6	18	<1E-2
3.6	7.2E-5	15	<4E-3
3.10	6.7E-5		
4.6	2E-7	20	<1E-1
4.13	6.0E-6		
8.1	4E-7	50	<E-1
8.2	1.5E-4	57	<2E-3
8.3	5.9E-3	100	5E-1

[a] $P(F|E)_{w/WPS}$ is the value of P(F|E) with WPS included in the analysis, and $P(F|E)_{w/oWPS}$ is the value without WPS included.

The fluence rate beyond 7 EFPY for weld 2-203A was assumed to be constant and equal to $0.199 \times 10^{19}/f$, where f is a factor by which the fluence rate can be changed. Thus,

$$F_o \times 10^{-19} = 1.1 + \frac{0.199\ (t - 7)}{f}\ , \qquad (5.19)$$

where

t = time of service, EFPY.

The effectiveness of reducing the fluence rate at 7 EFPY was evaluated at 10, 20, 32 and 50 EFPY for those transients included in Fig. 5.8, using f = 2, 4 and 8. The results for 32 EFPY are presented in Table 5.7, and for all values of t in Figs. 5.17 and 5.18.

5.5.5.2 Annealing

Annealing of the pressure vessel will increase the fracture toughness of the vessel material, and the amount of the increase will depend on the annealing temperature and time, the chemistry of the material, and the number of times the vessel is annealed. Test results from small specimens indicate that essentially full recovery of the initial fracture toughness might be achieved by annealing in the temperature range 400-450°C for ~200 h.[16] Although preliminary studies indicate that such a process would probably be feasible in

Table 5.7. Benefit of remedial measures, $P(F|E)_{wRM}/P(F|E)_{w/oRM}$,[a] at 42 EFPY for dominant transients

Transient	P(F|E) Original Mean Value at 32 EFPY	Reduction in Fluence Rate on Jan. 1, 1985 — Rate Reduction Factor 2	4	8	Annealing at 9 EFPY	Increase HPI Injection Temperature by 22°C
2.1	2E-7	b	b	b	b	
2.4	1.7E-5	5E-2	b	b	2E-1	
8.1	4E-7	b	b	b	b	
8.2	1.5E-4	2E-1	3E-2	5E-3	5E-1	1E-1
8.3	5.9E-3	5E-1	2E-1	8E-2	8E-1	4E-1

[a] $P(F|E)_{wRM}$: P(F|E) with remedial measure.
$P(F|E)_{w/oRM}$: P(F|E) without remedial measure.
[b] $P(F|E)_{wRM} < 10^{-7}$.

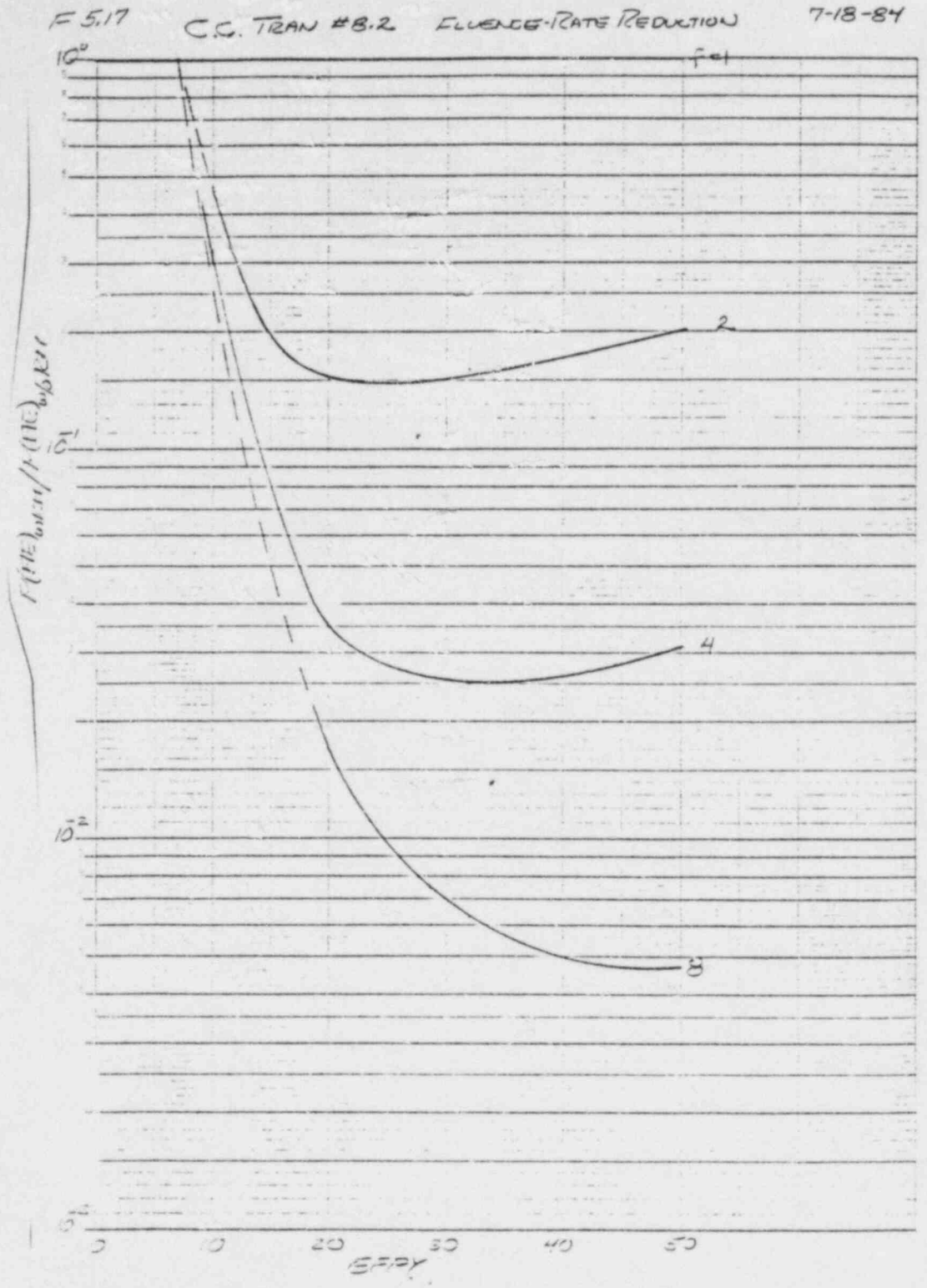

Fig. 5.17. Effect on P(F|E) for transient No. 8.2 of reducing fluence rate at 7 EFPY by factors of 2, 4 and 8.

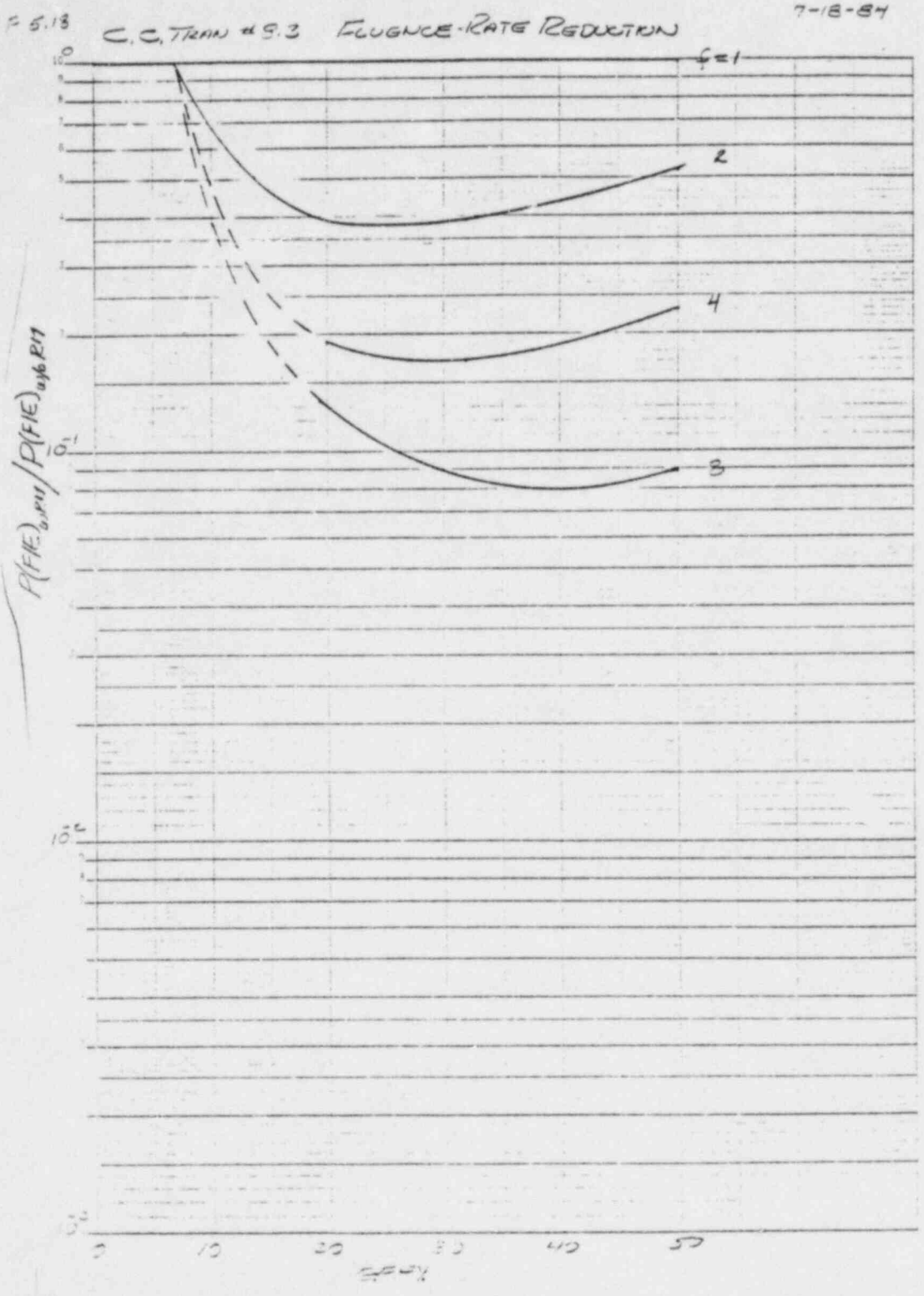

Fig. 5.18. Effect on P(F|E) for transient No. 8.3 of reducing fluence rate at 7 EFPY by factors of 2, 4 and 8.

some PWR plants, the feasibility of annealing the Calvert Cliffs-1 reactor vessel under these conditions has not been established. Nevertheless, for the purpose of this study it was assumed that the Calvert Cliffs-1 vessel would be annealed when the plant achieved ~9 EFPY (~January 1987), and that there would be complete recovery of fracture toughness. In effect, after annealing at 9 y, the fluence at 9 y would be zero. Thus, after 9 y,

$$F_o \times 10^{-19} \text{ (weld 2-203A)} = 0.199\ (t - 9)\ , \qquad (5.21)$$

where

t = total time of service, EFPY.

This fluence can be entered in Fig. 5.8 to obtain values of P(F|E) after annealing. The benefit at 32 EFPY of this assumed annealing situation is indicated in Table 5.7.

5.5.5.3 Increasing temperature of HPI coolant

The effect of increasing the HPI coolant temperature was evaluated for transients No. 8.2 and 8.3. The injection temperature of the HPI coolant was increased by ~~20~~ 22°C, and this resulted in a 17°C higher temperature for the downcomer coolant by the end of the 2-h transients (the rate of increase was assumed to be linear with time in the transient). The benefit of this remedial measure at 32 EFPY is indicated in Table 5.7.

REFERENCES

1. F. J. Loss, R. A. Gray, Jr., and J. R. Hawthorne, Significance of Warm Prestress to Crack Initiation During Thermal Shock, Report NRL/NUREG-8165, Naval Research Laboratory, NTIS, Sept. 29, 1977.

2. R. D. Cheverton and S. K. Iskander, "Thermal-Shock Investigations," in Heavy-Section Steel Technology Program Quarterly Progress Report October-December 1980, NUREG/CR-1941 (ORNL/NUREG/TM-437), pp. 37–54, Union Carbide Corporation-Nuclear Division, Oak Ridge National Laboratory.

3. R. D. Cheverton and D. G. Ball, OCA-P, A Deterministic and Probabilistic Fracture-Mechanics Code for Application to Pressure Vessels, NUREG/CR-3618 (ORNL-5991), Union Carbide Corporation-Nuclear Division, Oak Ridge National Laboratory (May 1984).

4. R. D. Cheverton, D. G. Ball and S. E. Bolt, "Thermal-Shock Investigations," in Heavy-Section Steel Technology Program Quarterly Progress Report April–June 1983, NUREG/CR-3334, Vol. 2 (ORNL/TM-8787/V2), pp. 57–74, Union Carbide Corporation-Nuclear Division, Oak Ridge National Laboratory.

5. T. U. Marston (Ed.), Flaw Evaluation Procedures, ASME Section XI, Background and Application of ASME Section XI, Appendix A, Special Report, EPRI NP-719-SR, American Society of Mechanical Engineers, Electric Power Research Institute, August 1978.

6. Letter from F. J. Loss (NRL) to R. H. Bryan (ORNL), March 31, 1981.

7. P. N. Randall, U.S. Nuclear Regulatory Commission, personal communication to R. D. Cheverton, Oak Ridge National Laboratory.

8. R. D. Cheverton and D. G. Ball, "Thermal-Shock Investigations," in Heavy-Section Steel Technology Program Quarterly Progress Report October–December 1982, NUREG/CR-2751, Vol. 4 (ORNL/TM-8369/V4), p. 68, Union Carbide Corporation-Nuclear Division, Oak Ridge National Laboratory.

9. ASME Boiler and Pressure Vessel Code, Section III, Division I, Subsection NA, Appendix I, American Society of Mechanical Engineers, New York, 1974.

10. R. M. Gamble and J. Strosnider, Jr., An Assessment of the Failure Rate for the Beltline Region of PWR Pressure Vessels During Normal Operation and Certain Transient Conditions, NUREG-0778, June 1981.

11. W. Marshall, An Assessment of the Integrity of PWR Pressure Vessels, United Kingdom Atomic Energy Authority, Second Report, March 1982.

12. R. Y. Rubinstein, Simulation and the Monte Carlo Method, Israel Institute of Technology, John Wiley & Sons, New York, 1981, pp. 115–117.

13. R. B. Pond, Jr., letter to J. D. White, Re: Weld Data for PTS Studies - Calvert Cliffs Unit No. 1, Oct. 27, 1983.

14. M. E. Bowman, letter to J. D. White, Oct. 28, 1983.

15. D. E. Peck, letter to S. E. Titland, Re: Materials Data for A-49 Project, Oct. 21, 1983.

16. J. R. Hawthorne, Naval Research Laboratory, personal communication to R. D. Cheverton, Oak Ridge National Laboratory.

APPENDIX K

CONTRIBUTION TO P(F|E) OF FLAWS IN THE CIRCUMFERENTIAL WELDS AND IN THE PLATE SEGMENTS

Flaws anywhere in the beltline region of the reactor vessel will contribute to the probability of vessel failure. However, aside from the effect of flaw depth, some contribute more than others because of differences in orientation, length, local chemistry of the material, and local fluence. Axial flaws have the highest values of K_I, and in Calvert Cliffs-1 the axial welds have higher concentrations of nickel than the circumferential weld of concern and higher concentrations of both copper and nickel than the base material.

The difference in radiation damage between the axial welds and base material is rather large, and thus the extended surface length of an axial flaw in a weld tends to be limited to the height of a shell course, and for deep flaws this limit on surface length results in significantly lower K_I values than for much longer flaws. The extended surface length of axially oriented flaws in the plate segments is not limited to the height of a shell course, if the fracture-toughness properties in adjacent segments are similar. However, the extended length does tend to be limited to about the active height of the core by the steep attenuation of the neutron flux beyond the ends of the core. Flaws in circumferential welds may be limited in surface-length extension by azimuthal gradients in temperature, fluence and material properties, but not by the length of the weld since it is continuous.

Thus far, the OCA-P fracture-mechanics model does not account for gradients in fluence and coolant temperature along the specified surface flaw path. In lieu of considering this sort of detail, all flaws in the circumferential welds were assumed to be two dimensional. Axial flaws in the plate segments were also

assumed to be two dimensional for the additional reason that the maximum length-to-depth ratio nearly corresponds to two-dimensional conditions.

The use of a two-dimensional model for flaws in the circumferential weld is probably quite conservative relative to the treatment of the other flaws. However, as indicated below, even under these conditions the contribution of these flaws to P(F|E) is negligible, and thus the excessive conservatism is of no practical concern.

The contributions of flaws in the circumferential welds and of axial flaws in plate segments were calculated for the two most dominant transients (Nos. 8.2 and 8.3), and the time in the life of the vessel considered was 32 EFPY. The flaw density was assumed to be the same for all categories of flaws considered, and since the total volume of the plate segments is much greater than that of the welds, the plate segments contributed many more flaws than the welds.

The chemistry, fluence, volume and initial value of RTNDT for each distinct region of the vessel considered for the three categories of flaws (axial weld, axial plate and circumferential weld) are given in Table K-1 for the plate regions and in Table 5.2 for the weld regions. In an attempt to account for the azimuthal variation in fluence in the plate regions, each plate segment was divided into a one-third-volume region with high fluence and a two-thirds-volume region with lower fluence. Also, the initial values of RTNDT given in Table 5.2 for the plate segments were reduced by 33°C to account for a lower radiation damage rate in the plate segments than in the welds (see Sect. 5.3.1).

The results of the analysis indicate that for transient No. 8.3 the circumferential flaws add ~5% to P(F|E) and the plate segments ~50%. For transient No. 8.2, which is a less severe transient, the contributions were much less, being only 5% for the plate segments.

The dominant transients for Calvert Cliffs-1 (8.2 and 8.3) not only have the highest frequencies of failure associated with them, but they also have the highest values of P(F|E). Thus, because of the trends observed in the above study it is expected that the contributions of circumferential-weld and plate-segment flaws to P(F|E) would be no greater for the other transients. Thus, the inclusion of these contributions does not result in different transients being dominant.

Table K-1. Material properties, fluences and volumes used in evaluation of plate-segment contribution to P(F|E)

Region	Cu (wt %)	Ni (wt %)	F_o (10^{19}n/cm^2)	$RTNDT_o$[a] (°C)	V (m^3)
1	0.11	0.55	6.06	–40	0.81
2	0.12	0.64	6.06	–67	0.81
3	0.12	0.64	6.06	–45	0.81
4	0.13	0.54	6.06	–45	0.67
5	0.11	0.56	6.06	–45	0.67
6	0.11	0.53	6.06	–40	0.67
7	0.11	0.55	3.03	–40	1.62
8	0.12	0.64	3.03	–67	1.62
9	0.12	0.64	3.03	–45	1.62
10	0.13	0.54	3.03	–45	1.34
11	0.11	0.56	3.03	–45	1.34
12	0.11	0.53	3.03	–40	1.34

[a]These values are 33°C lower than the actual values given in Table 5.2 to account for lower radiation-damage rate in base material relative to weld material.

APPENDIX L

COMPILATION OF RESULTS OF CALVERT CLIFFS-1 PROBABILISTIC FRACTURE-MECHANICS ANALYSIS

Detailed results of the Calvert Cliffs-1 probabilistic fracture-mechanics analysis are included in this appendix so that a more thorough understanding of the effect of the various assumptions used in the fracture-mechanics model and the different inputs to the fracture-mechanics analysis can be obtained. For instance, the duration of all postulated transients for this study was specified as two hours. In many cases most of the failures do not occur until late in the transient. If the duration of the transient were one instead of two hours, $P(F|E)$ would be reduced substantially.

Sets of data are included in this appendix for each of the transients for which $P(F|E) > 10^{-7}$. A set of data includes, in this order, (1) a figure of primary-system pressure, downcomer coolant temperature, and fluid-film heat-transfer coefficient vs time in the transient; (2) a summary of digital output that includes $P(F|E)$ for each axial weld in the vessel, the estimated error in $P(F|E)$, and histogram data for crack depths, times and values of T − RTNDT at the crack tip corresponding to initiation, arrest and failure events; (3) a plot of vessel wall temperature vs a/w, t; (4) a plot of vessel wall temperature vs t, a/w; and (5) a set of critical-crack-depth curves obtained using -2σ values of K_{Ic} and K_{Ia}, mean values of all other parameters, and fluences corresponding to 32 EFPY. The various curves in the set of critical-crack-depth curves are identified in Fig. 5.16 (see Chapter 5).

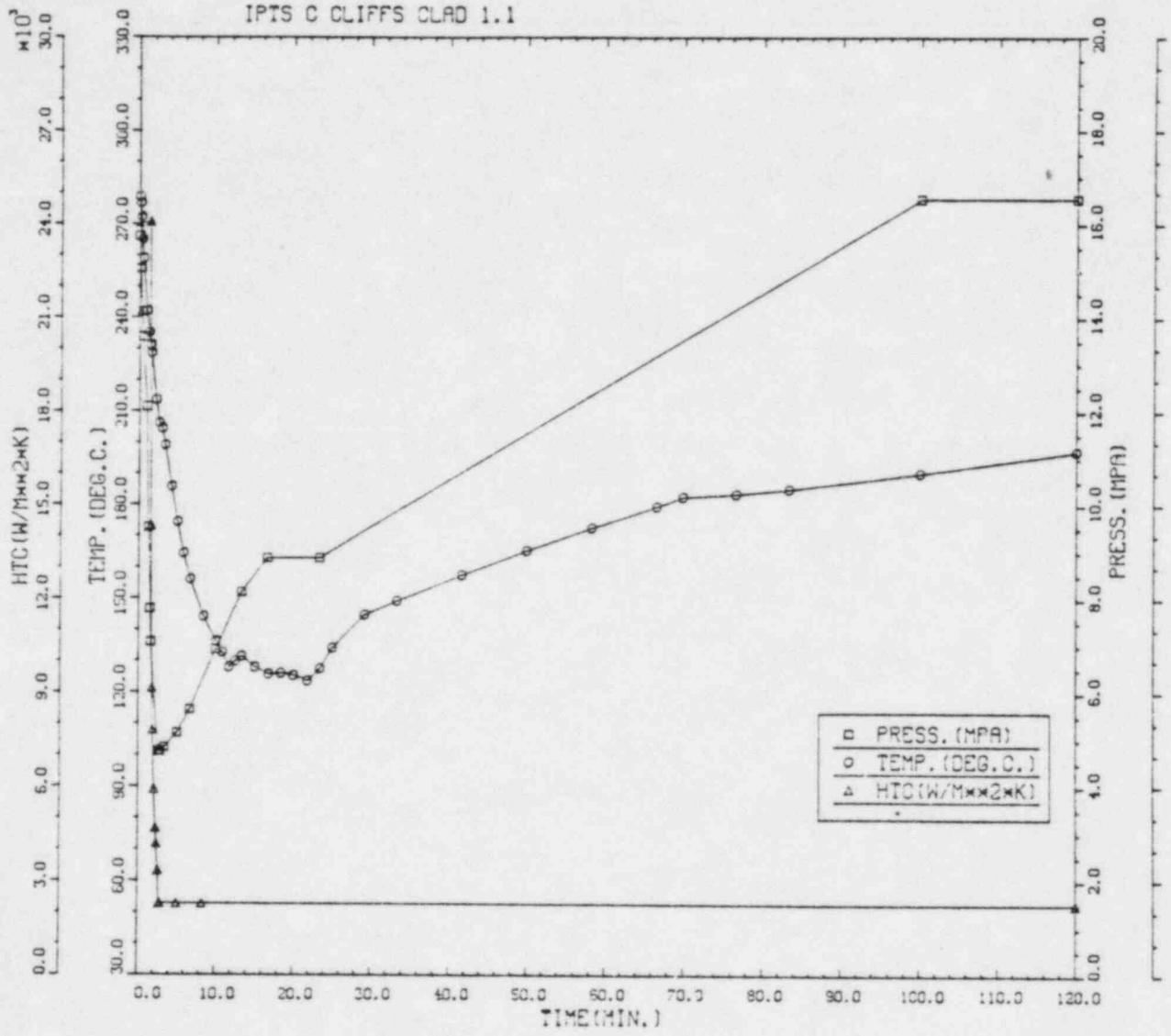
IPTS C CLIFFS CLAD 1.1
HTC(W/M**2*K)
*10³
TEMP.(DEG.C.)
PRESS.(MPA)
TIME(MIN.)
PRESS.(MPA)
TEMP.(DEG.C.)
HTC(W/M**2*K)

IPTS C CLIFFS CLAD 1.1 1. FLAWS/M**3 FO = 6.060D+19

WELD	UNADJUSTED P(F/E)	95%CI	%ERR	P(INITIA)	N*V	ADJUSTED P(F/E)	%ERR	NTRIALS
1	1.17D-06	2.30D-06	196.00	2.33D-04	0.025	2.94D-08		500000
2	0.00D+00	0.00D+00	0.00	2.35D-06	0.050	0.00D+00		500000
3	0.00D+00	0.00D+00	0.00	3.17D-05	0.021	0.00D+00		500000
					VESSEL	2.94D-08	196.00	

DEPTHS FOR INITIAL INITIATION (MM)

	2.16	6.68	11.52	17.03	22.95	29.42	36.51	44.25	52.72
NUMBER	4	145	60	13	4	1	0	0	0
PERCENT	1.8	63.9	26.4	5.7	1.8	0.4	0.0	0.0	0.0

TIMES OF FAILURE(MINUTES)

	0.0	10.0	20.0	30.0	40.0	50.0	60.0	70.0	80.0	90.0	100.0	110.0	120.0
NUMBER	0	0	0	0	1	0	0	0	0	0	0	0	0
PERCENT	0.0	0.0	0.0	0.0	100.0	0.0	0.0	0.0	0.0	0.0	0.0	0.0	

INITIATION T-RTNDT(DEG.C)

	-55.6	-41.7	-27.8	-13.9	0.0	13.9	27.8	41.7	55.6	69.4	83.3	97.2	111.1
NUMBER	0	0	5	51	120	50	5	2	0	0	0	0	
PERCENT	0.0	0.0	2.1	21.9	51.5	21.5	2.1	0.9	0.0	0.0	0.0	0.0	

ARREST T-RTNDT(DEG.C)

	-27.8	-13.9	0.0	13.9	27.8	41.7	55.6	69.4	83.3	97.2	111.1	125.0	138.9
NUMBER	0	0	0	1	0	2	14	88	90	35	1	0	
PERCENT	0.0	0.0	0.0	0.4	0.0	0.9	6.0	37.9	38.8	15.5	0.4	0.0	

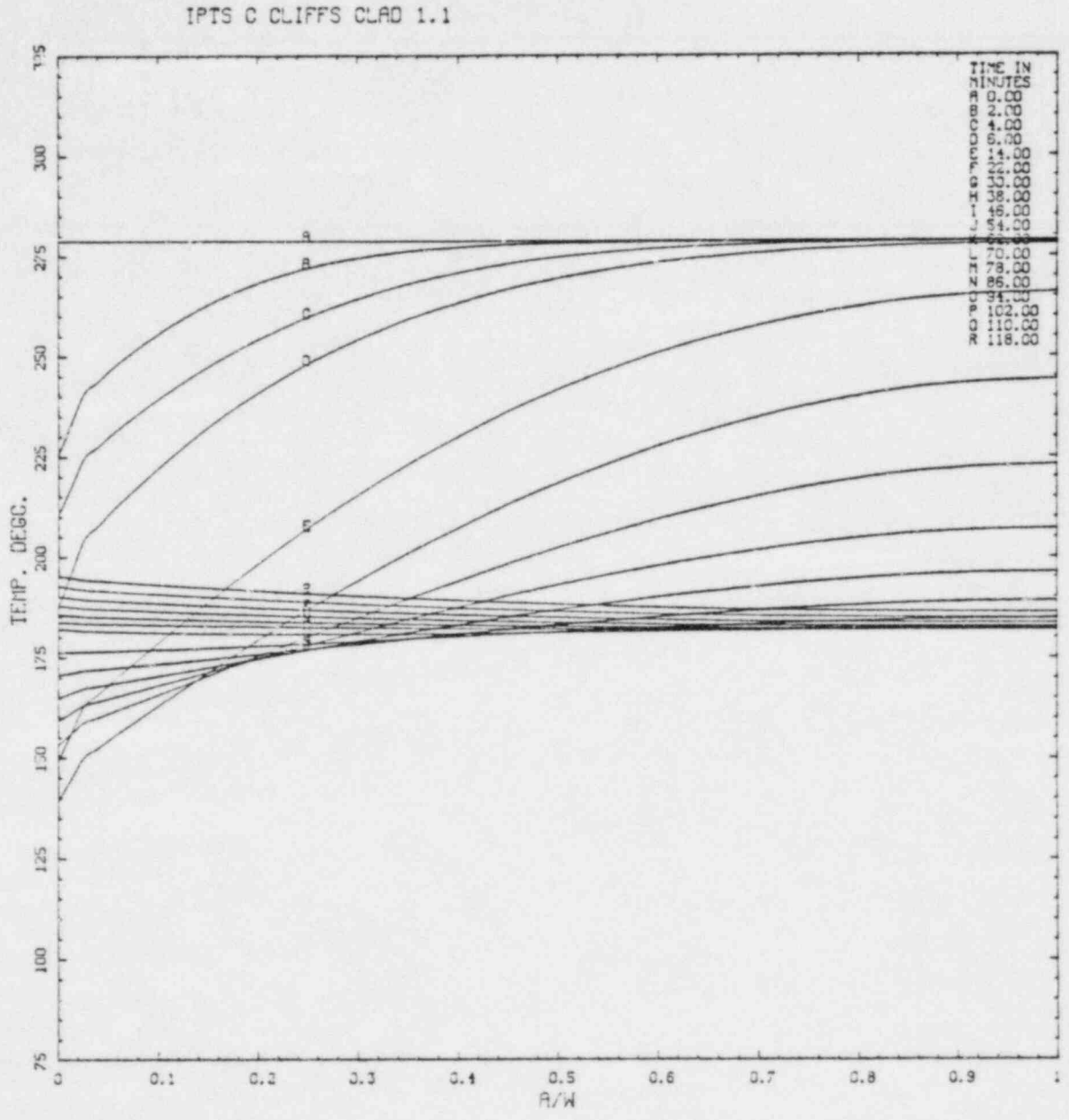
IPTS C CLIFFS CLAD 1.1
TIME IN MINUTES
A 0.00
B 2.00
C 4.00
D 6.00
E 14.00
F 22.00
G 30.00
H 38.00
I 46.00
J 54.00
K 62.00
L 70.00
M 78.00
N 86.00
O 94.00
P 102.00
Q 110.00
R 118.00
TEMP. DEGC.
R/W
75
100
125
150
175
200
225
250
275
300
325
0
0.1
0.2
0.3
0.4
0.5
0.6
0.7
0.8
0.9
1

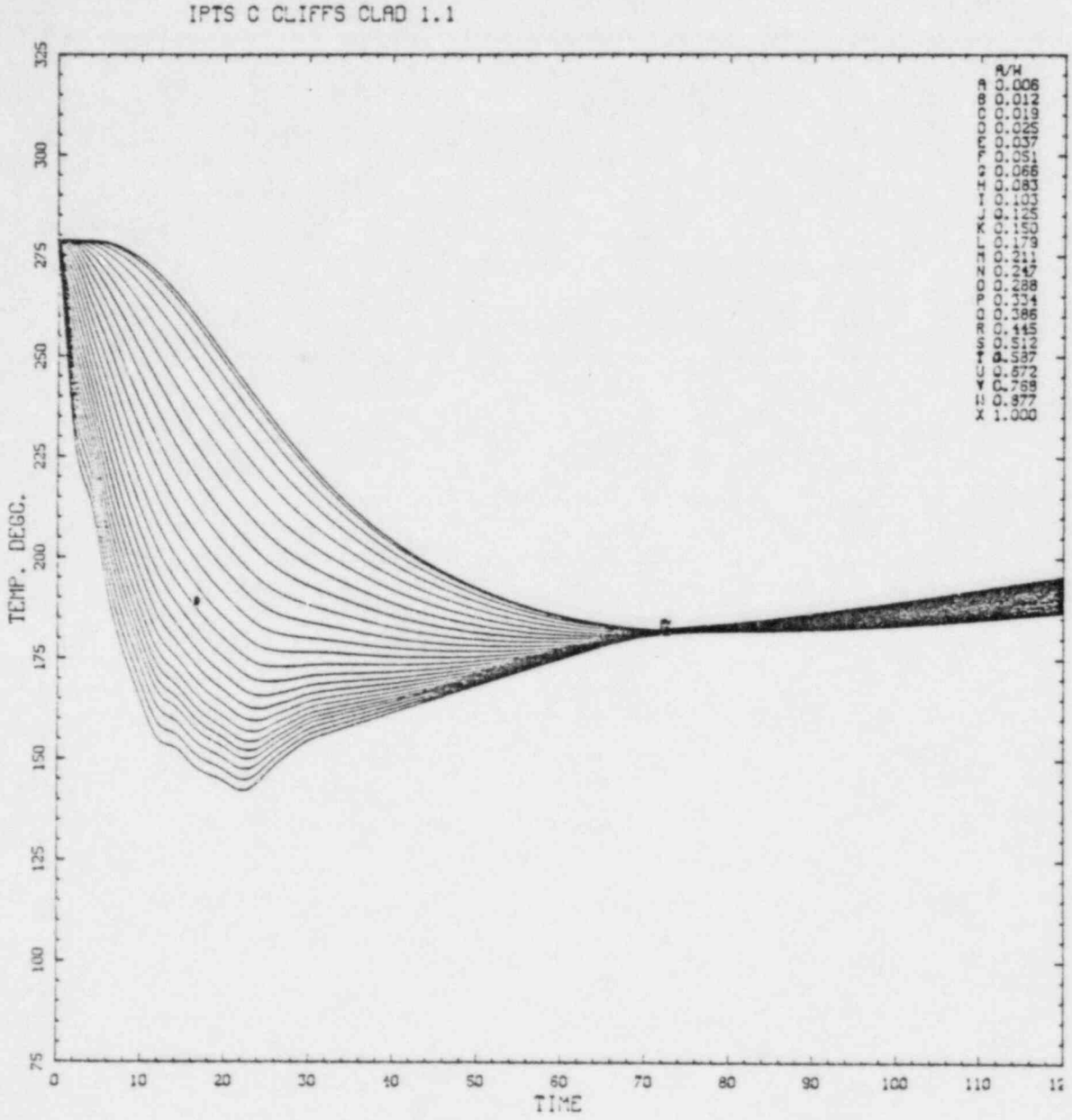
IPTS C CLIFFS CLAD 1.1
TEMP. DEGC.
TIME
A/W
A 0.006
B 0.012
C 0.019
D 0.025
E 0.037
F 0.051
G 0.066
H 0.083
I 0.103
J 0.125
K 0.150
L 0.179
M 0.211
N 0.247
O 0.288
P 0.334
Q 0.386
R 0.445
S 0.512
T 0.587
U 0.672
V 0.768
W 0.877
X 1.000

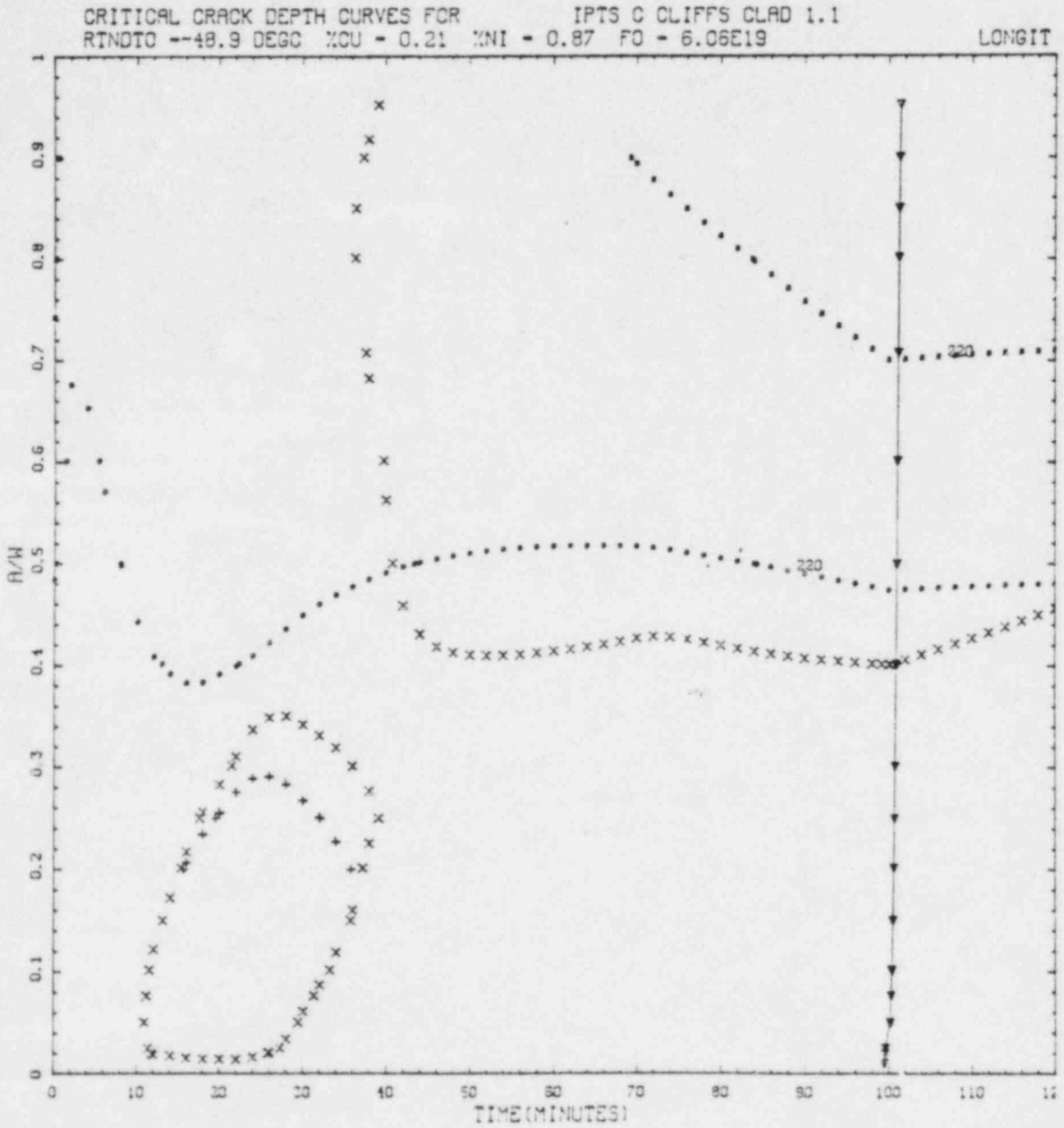
CRITICAL CRACK DEPTH CURVES FOR IPTS C CLIFFS CLAD 1.1
RTNDTO --48.9 DEGC %CU - 0.21 %NI - 0.87 FO - 6.06E19
LONGIT
A/W
TIME(MINUTES)
320
320

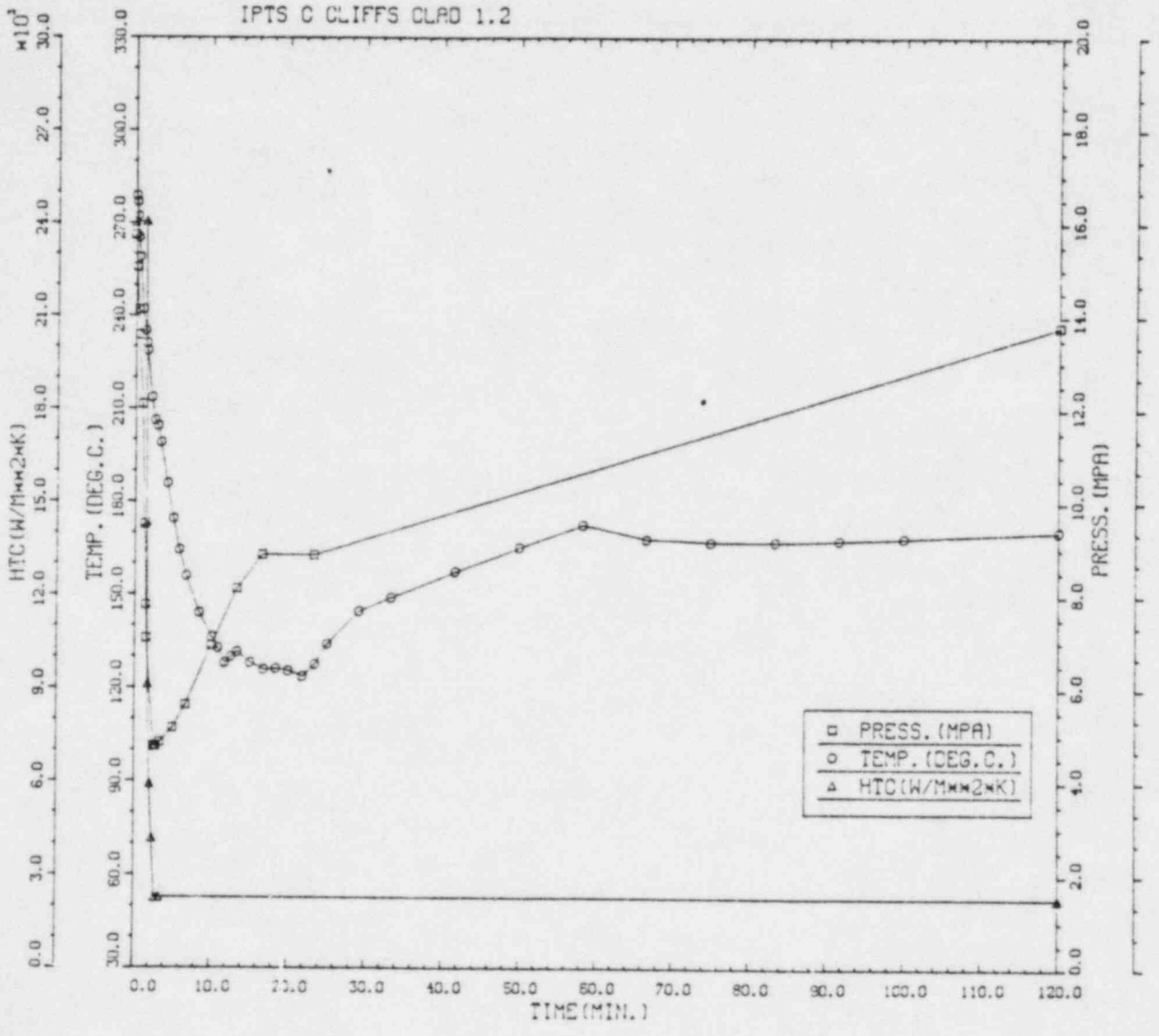
IPTS C CLIFFS CLAD 1.2
HTC(W/M**2K)
*10**3
TEMP.(DEG.C.)
PRESS.(MPA)
TIME(MIN.)
PRESS.(MPA)
TEMP.(DEG.C.)
HTC(W/M**2K)

IPTS C CLIFFS CLAD 1.2 1. FLAWS/M**3 FO = 6.060D+19

WELD	UNADJUSTED P(F/E)	95%CI	%ERR	P(INITIA)	N*V	ADJUSTED P(F/E)	%ERR	NTRIALS
1	3.52D-06	3.99D-06	113.16	2.34D-04	0.025	8.81D-08		500000
2	0.00D+00	0.00D+00	0.00	2.35D-06	0.050	0.00D+00		500000
3	0.00D+00	0.00D+00	0.00	3.17D-05	0.021	0.00D+00		500000
					VESSEL	8.81D-08	113.16	

DEPTHS FOR INITIAL INITIATION (MM)

	2.16	5.68	11.52	17.03	22.35	29.42	35.51	44.25	52.72
NUMBER	4	145	61	13	4	1	0	0	0
PERCENT	1.8	63.6	26.8	5.7	1.8	0.4	0.0	0.0	0.0

TIMES OF FAILURE(MINUTES)

	0.0	10.0	20.0	30.0	40.0	50.0	60.0	70.0	80.0	90.0	100.0	110.0	120.0
NUMBER	0	0	0	0	0	0	1	0	1	0	0	1	
PERCENT	0.0	0.0	0.0	0.0	0.0	0.0	33.3	0.0	33.3	0.0	0.0	33.3	

INITIATION T-RTNDT(DEG.C)

	-55.6	-41.7	-27.8	-13.9	0.0	13.9	27.8	41.7	55.6	69.4	83.3	97.2	111.1
NUMBER	0	0	5	51	120	52	6	2	0	0	0	0	
PERCENT	0.0	0.0	2.1	21.6	50.8	22.0	2.5	0.8	0.0	0.0	0.0	0.0	

ARREST T-RTNDT(DEG.C)

	-27.8	-13.9	0.0	13.9	27.8	41.7	55.6	69.4	83.3	97.2	111.1	125.0	138.9
NUMBER	0	0	0	1	0	2	14	88	91	35	1	0	
PERCENT	0.0	0.0	0.0	0.4	0.0	0.9	6.0	37.8	39.1	15.5	0.4	0.0	

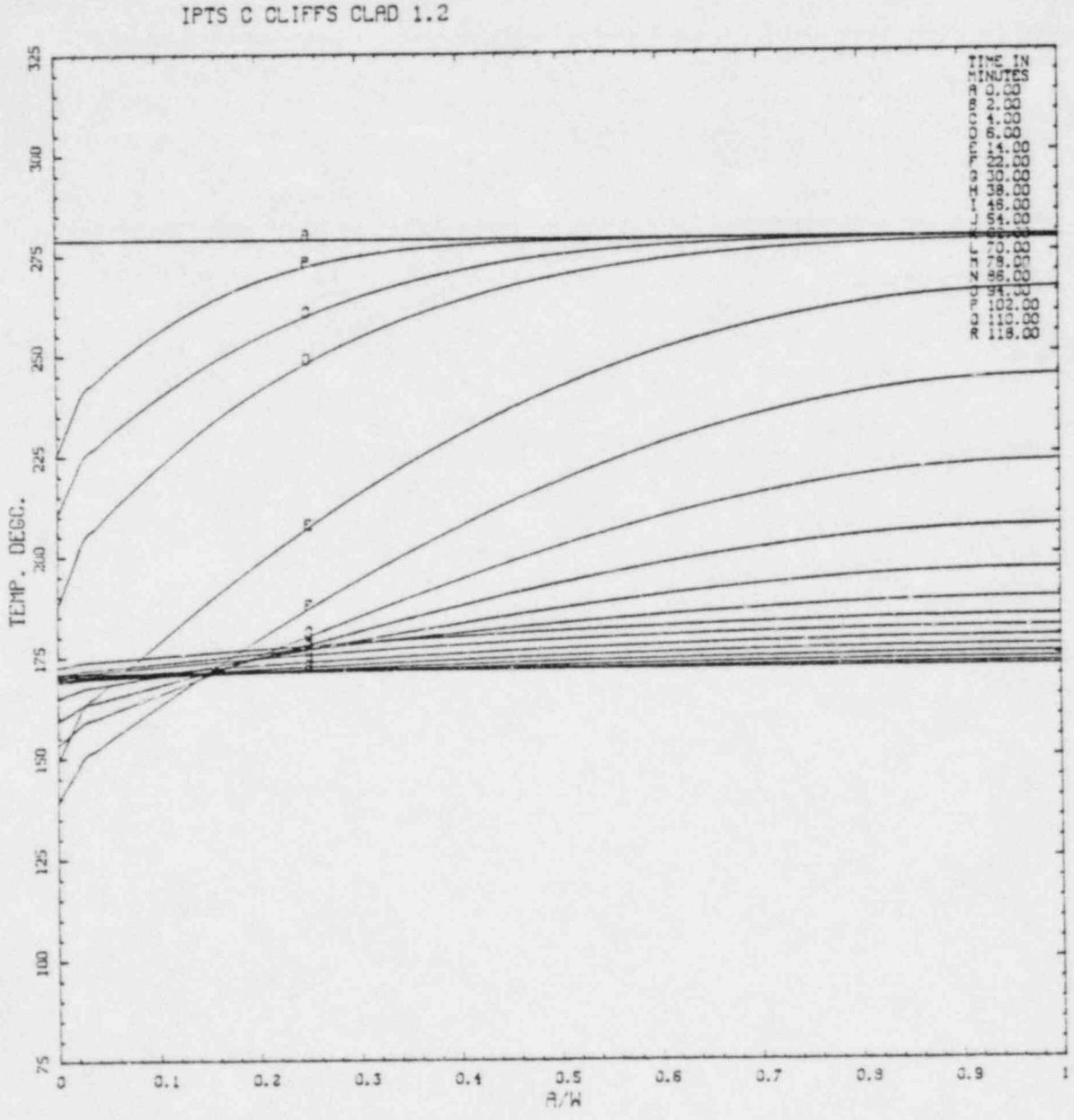
IPTS C CLIFFS CLAD 1.2
TEMP. DEGC.
R/W
TIME IN MINUTES
A 0.000
B 2.000
C 4.000
D 6.000
E 14.000
F 22.000
G 30.000
H 38.000
I 46.000
J 54.000
K 62.000
L 70.000
M 78.000
N 86.000
O 94.000
P 102.000
Q 110.000
R 118.000

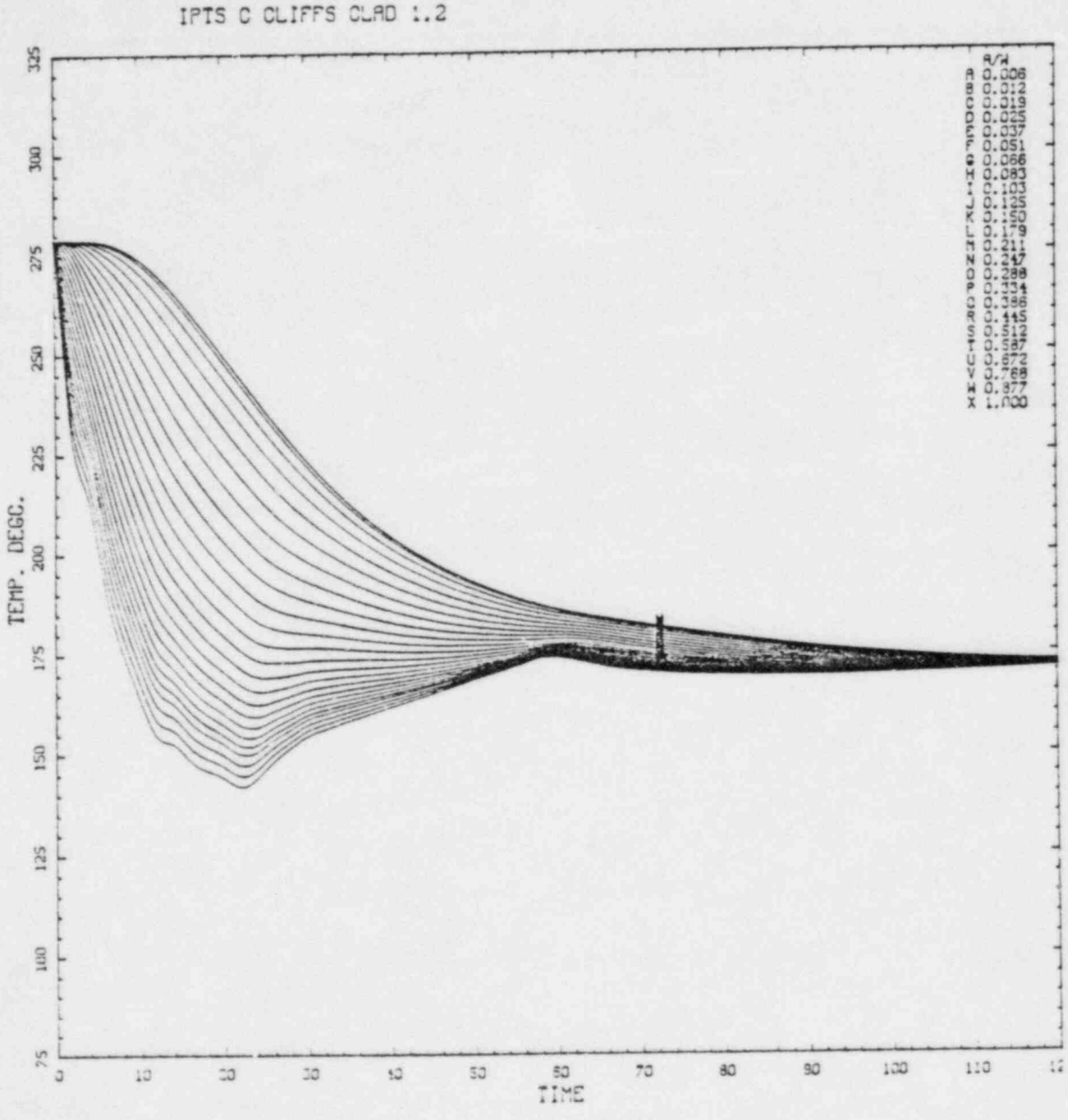
IPTS C CLIFFS CLAD 1.2
TEMP. DEGC.
TIME
325
300
275
250
225
200
175
150
125
100
75
0
10
20
30
40
50
60
70
80
90
100
110

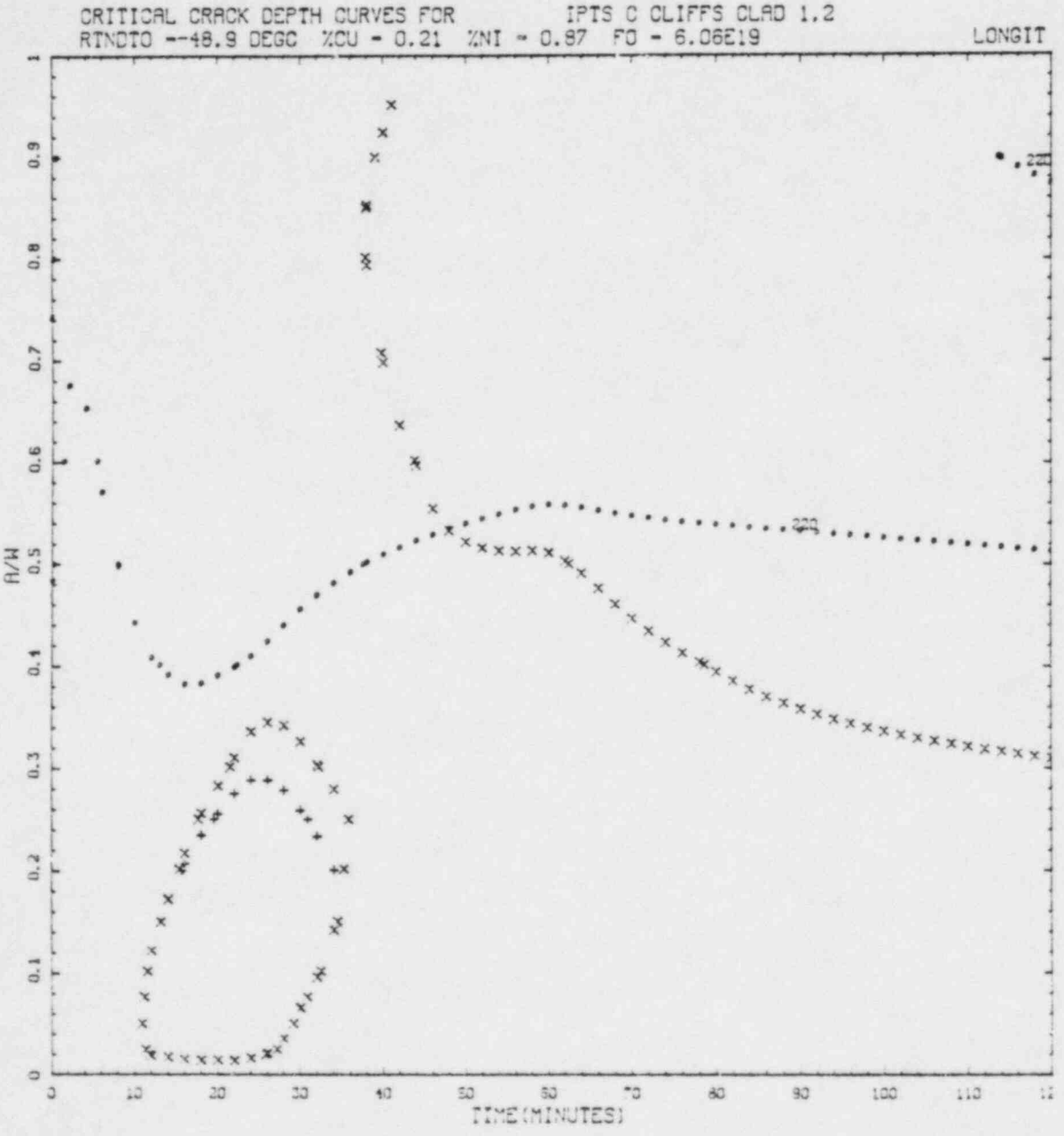
CRITICAL CRACK DEPTH CURVES FOR IPTS C CLIFFS CLAD 1.2
RTNDTO --48.9 DEGC %CU - 0.21 %NI - 0.87 FO - 6.06E19
LONGIT
A/W
TIME(MINUTES)

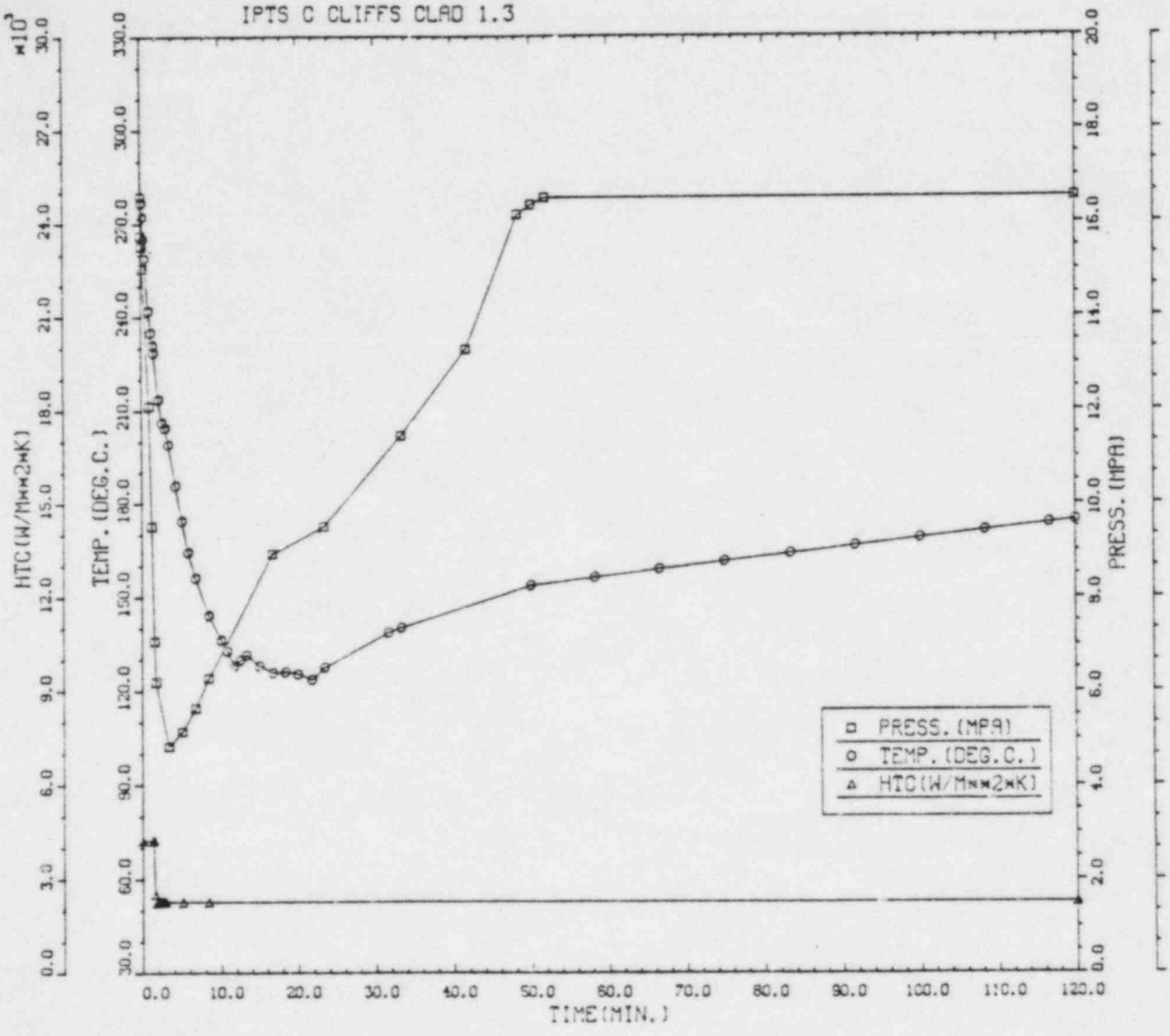
IPTS C CLIFFS CLAD 1.3
HTC(W/M**2*K)
*10³
TEMP.(DEG.C.)
PRESS.(MPA)
TIME(MIN.)
PRESS.(MPA)
TEMP.(DEG.C.)
HTC(W/M**2*K)

IPTS C CLIFFS CLAD 1.3 1. FLAWS/M**3 FO = 6.060D+19

WELD	P(F/E)	95%CI	%ERR	P(INITIA)	N*V	P(F/E)	%ERR	NTRIALS
	UNADJUSTED					ADJUSTED		
1	2.35D-05	1.03D-05	43.83	2.60D-04	0.025	5.87D-07		500000
2	0.00D+00	0.00D+00	0.00	2.35D-06	0.050	0.00D+00		500000
3	0.00D+00	0.00D+00	0.00	3.52D-05	0.021	0.00D+00		500000
					VESSEL	5.87D-07	43.83	

DEPTHS FOR INITIAL INITIATION (MM)

	2.16	6.68	11.52	17.03	22.95	29.42	36.51	44.25	52.72
NUMBER	5	165	65	13	4	1	0	0	0
PERCENT	2.0	65.2	25.7	5.1	1.6	0.4	0.0	0.0	0.0

TIMES OF FAILURE(MINUTES)

	0.0	10.0	20.0	30.0	40.0	50.0	60.0	70.0	80.0	90.0	100.0	110.0	120.0
NUMBER	0	0	0	1	9	2	5	1	1	1	0	0	
PERCENT	0.0	0.0	0.0	5.0	45.0	10.0	25.0	5.0	5.0	5.0	0.0	0.0	

INITIATION T-RTNDT(DEG.C)

	-55.6	-41.7	-27.8	-13.9	0.0	13.9	27.8	41.7	55.6	69.4	83.3	97.2	111.1
NUMBER	0	0	7	54	135	55	25	12	1	0	0	0	
PERCENT	0.0	0.0	2.4	18.7	46.7	19.0	8.7	4.2	0.3	0.0	0.0	0.0	

ARREST T-RTNDT(DEG.C)

	-27.8	-13.9	0.0	13.9	27.8	41.7	55.6	69.4	83.3	97.2	111.1	125.0	138.9
NUMBER	0	0	0	1	0	3	19	84	104	57	1	0	
PERCENT	0.0	0.0	0.0	0.4	0.0	1.1	7.1	31.2	38.7	21.2	0.4	0.0	

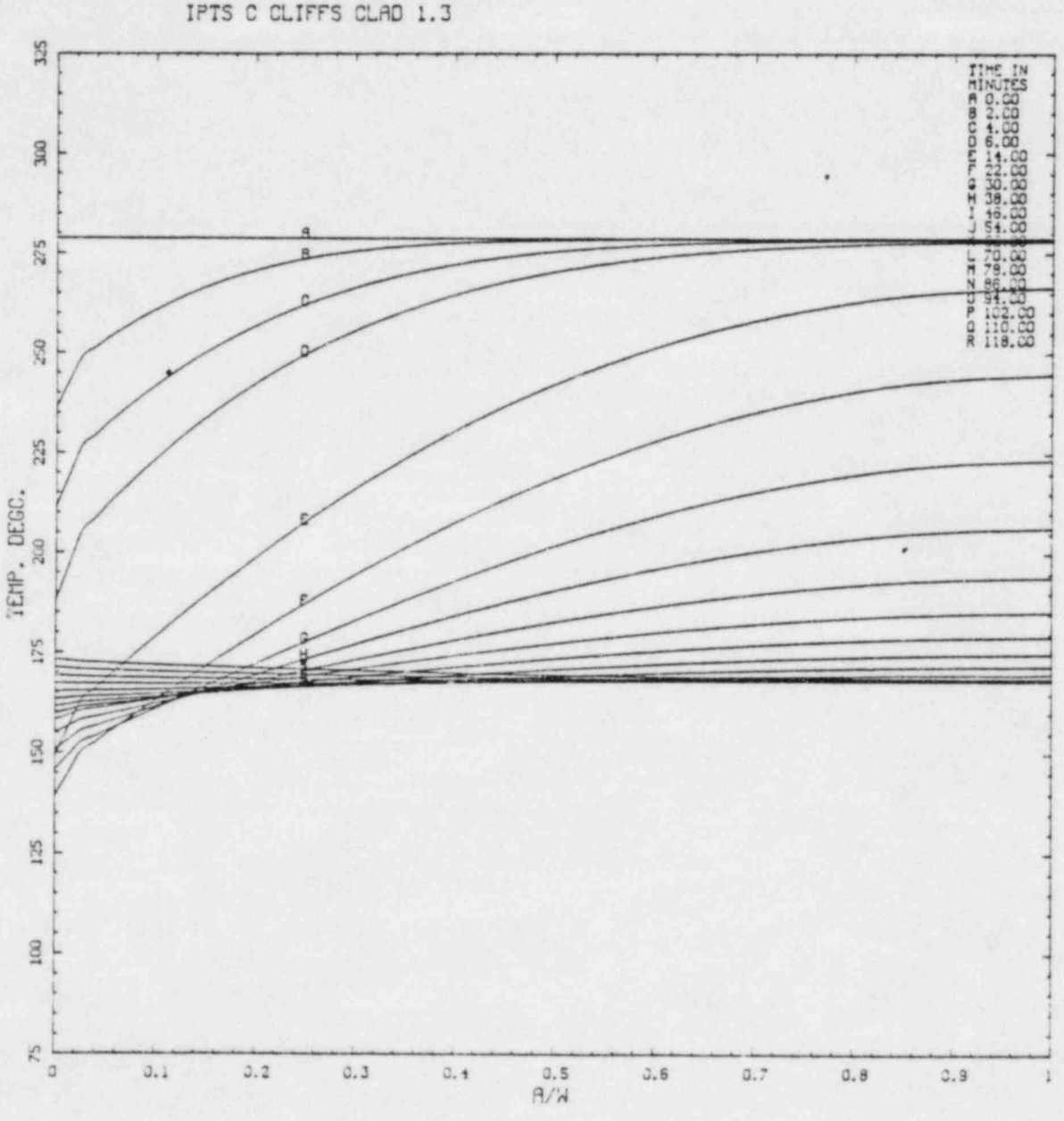
IPTS C CLIFFS CLAD 1.3
TEMP. DEGC.
R/W
TIME IN MINUTES
A 0.00
B 2.00
C 4.00
D 6.00
E 14.00
F 22.00
G 30.00
H 38.00
I 46.00
J 54.00
K 62.00
L 70.00
M 78.00
N 86.00
O 94.00
P 102.00
Q 110.00
R 118.00

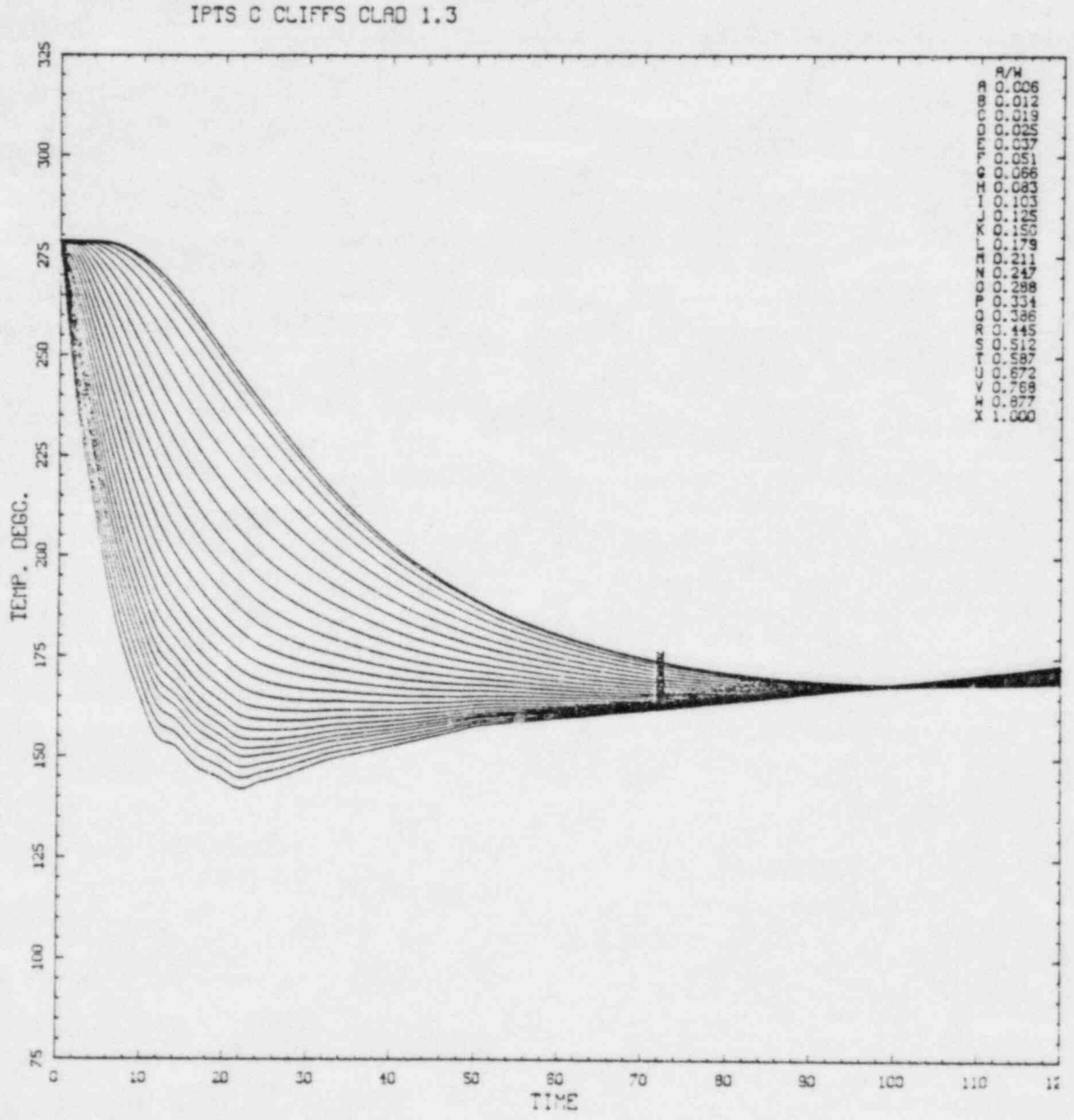
IPTS C CLIFFS CLAD 1.3
TEMP. DEGC.
TIME
R/W
A 0.006
B 0.012
C 0.019
D 0.025
E 0.037
F 0.051
G 0.066
H 0.083
I 0.103
J 0.125
K 0.150
L 0.179
M 0.211
N 0.247
O 0.288
P 0.334
Q 0.386
R 0.445
S 0.512
T 0.587
U 0.672
V 0.768
W 0.877
X 1.000

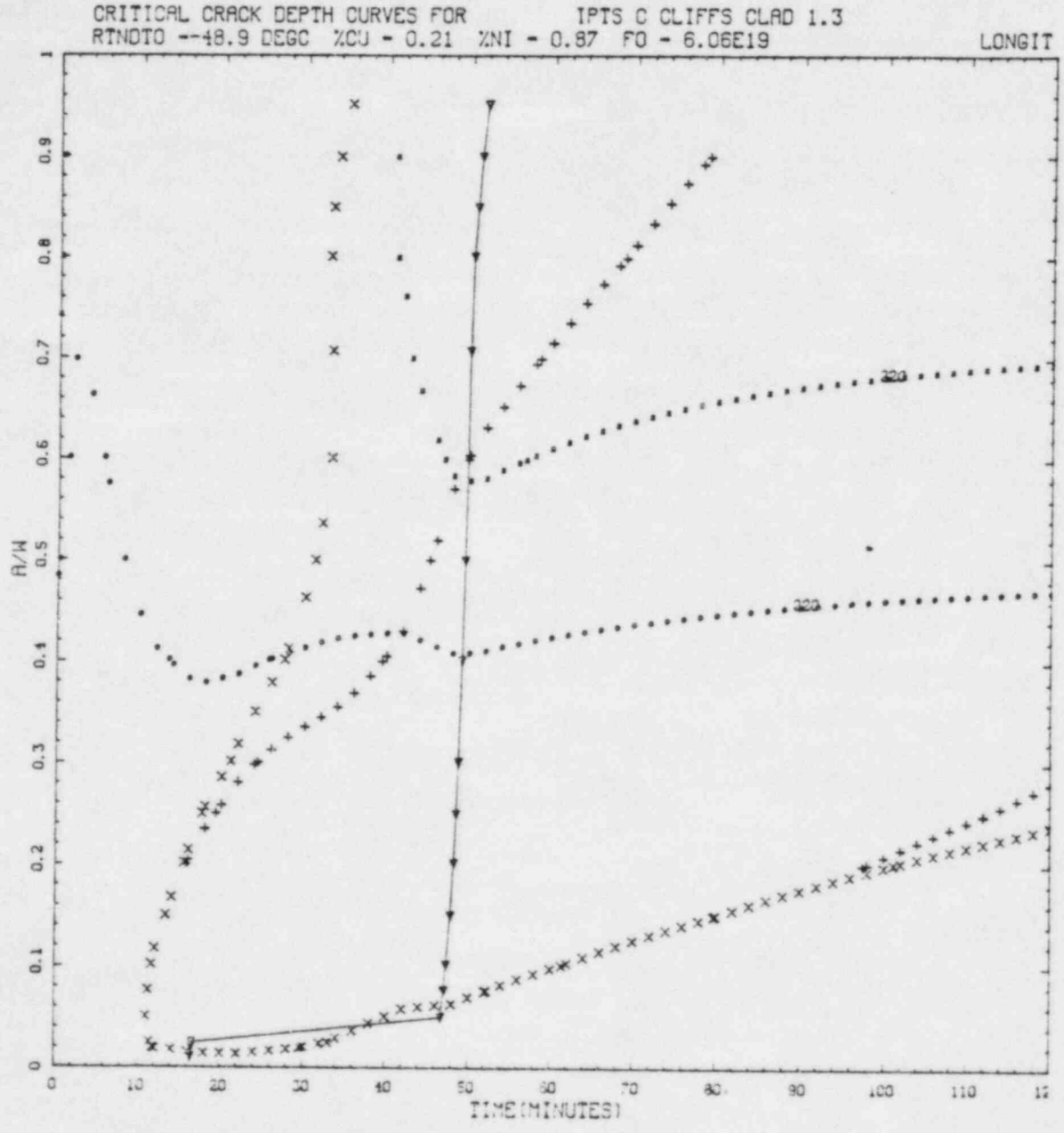
CRITICAL CRACK DEPTH CURVES FOR IPTS C CLIFFS CLAD 1.3
RTNDTO --48.9 DEGC %CU - 0.21 %NI - 0.87 FO - 6.06E19
LONGIT
A/W
TIME(MINUTES)
0
0.1
0.2
0.3
0.4
0.5
0.6
0.7
0.8
0.9
1
10
20
30
40
50
60
70
80
90
100
110
320
320

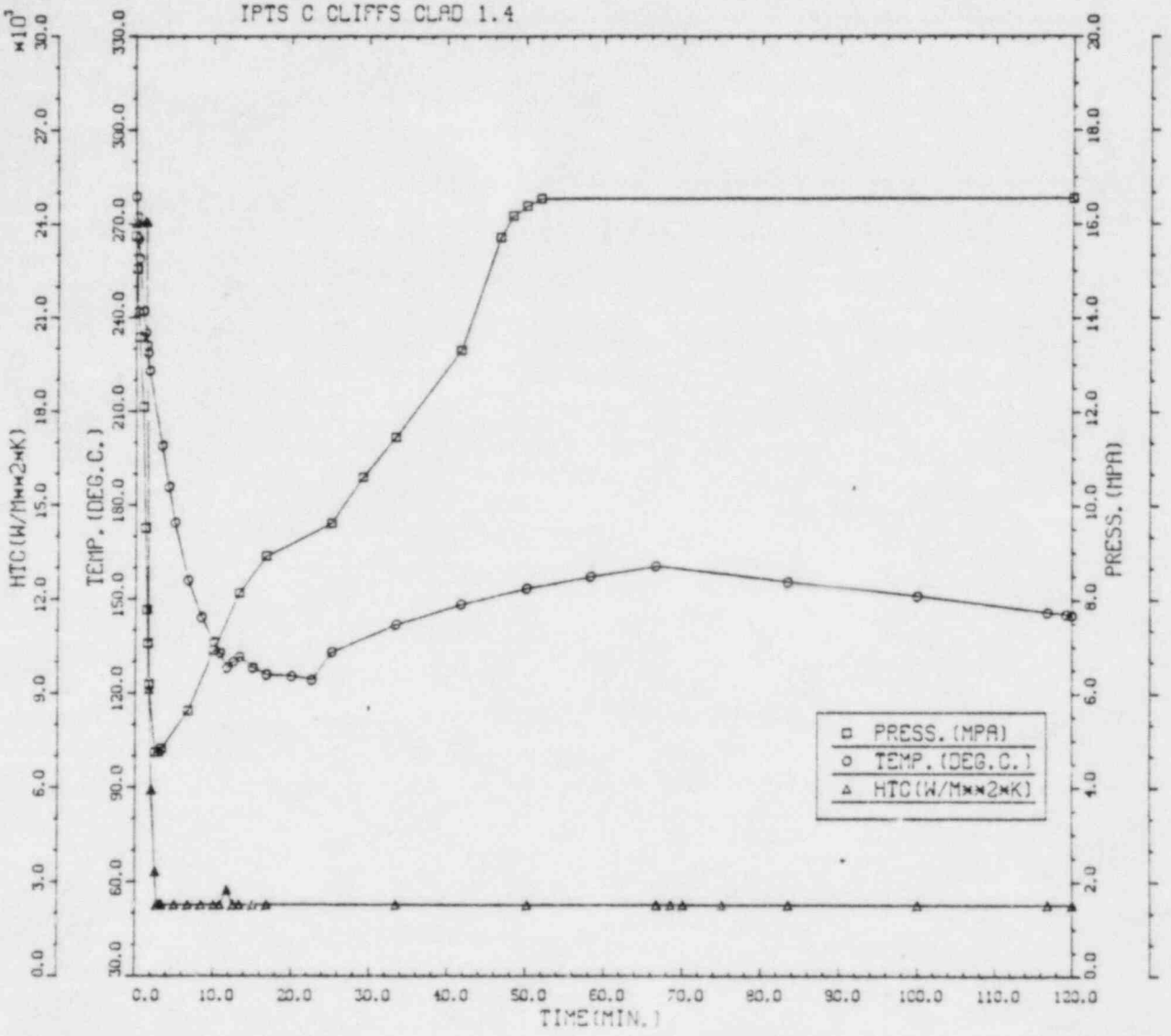
IPTS C CLIFFS CLAD 1.4
HTC(W/M**2*K)
*10³
TEMP.(DEG.C.)
PRESS.(MPA)
TIME(MIN.)
PRESS.(MPA)
TEMP.(DEG.C.)
HTC(W/M**2*K)

IPTS C CLIFFS CLAD 1.4 1. FLAWS/M**3 FO = 6.060D+19

WELD	UNADJUSTED P(F/E)	95%CI	%ERR	P(INITIA)	N*V	ADJUSTED P(F/E)	%ERR	NTRIALS
1	1.22D-04	2.35D-05	19.22	2.37D-04	0.025	3.05D-06		500000
2	1.17D-05	2.30D-06	196.00	2.35D-05	0.050	5.87D-08		500000
3	1.06D-05	6.91D-06	65.33	3.41D-05	0.021	2.22D-07		500000
					VESSEL	3.33D-06	18.45	

DEPTHS FOR INITIAL INITIATION (MM)

	2.16	6.68	11.62	17.03	22.95	29.42	36.51	44.25	52.72
NUMBER	5	149	61	13	4	1	0	0	0
PERCENT	2.1	63.9	26.2	5.6	1.7	0.4	0.0	0.0	0.0

TIMES OF FAILURE(MINUTES)

	0.0	10.0	20.0	30.0	40.0	50.0	60.0	70.0	80.0	90.0	100.0	110.0	120.0
NUMBER	0	0	0	2	10	4	2	6	14	25	22	29	
PERCENT	0.0	0.0	0.0	1.8	8.8	3.5	1.8	5.3	12.3	21.9	19.3	25.4	

INITIATION T-RTNDT(DEG.C)

	-55.6	-41.7	-27.8	-13.9	0.0	13.9	27.8	41.7	55.6	69.4	83.3	97.2	111.1
NUMBER	0	0	7	47	126	70	77	31	0	0	0	0	
PERCENT	0.0	0.0	2.0	13.1	35.2	19.6	21.5	8.7	0.0	0.0	0.0	0.0	

ARREST T-RTNDT(DEG.C)

	-27.8	-13.9	0.0	13.9	27.8	41.7	55.6	69.4	83.3	97.2	111.1	125.0	138.9
NUMBER	0	0	0	1	0	3	10	96	93	49	2	0	
PERCENT	0.0	0.0	0.0	0.4	0.0	1.2	4.1	35.2	38.1	20.1	0.8	0.0	

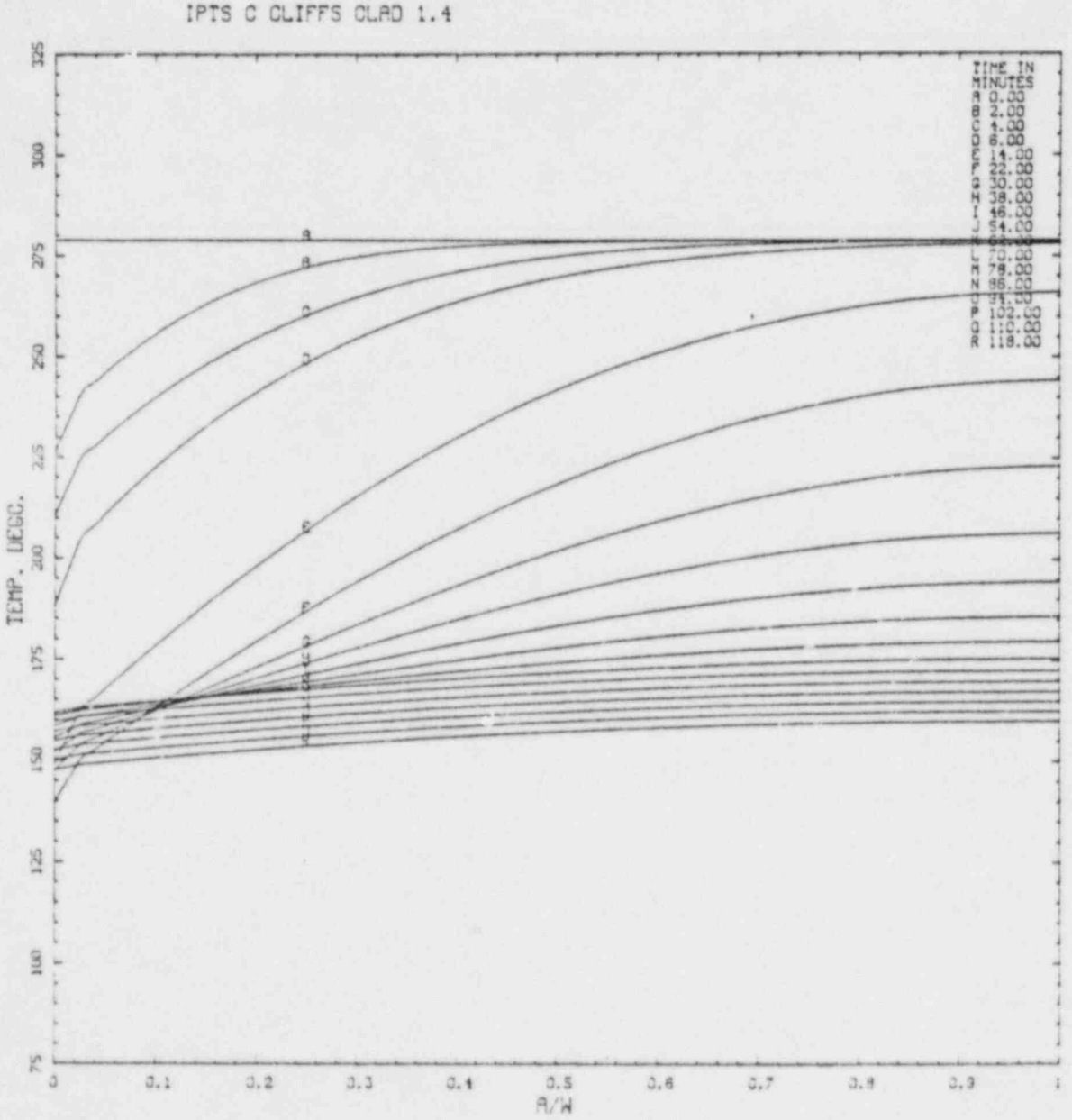
IPTS C CLIFFS CLAD 1.4
TEMP. DEGC.
R/W
TIME IN MINUTES
A 0.00
B 2.00
C 4.00
D 6.00
E 14.00
F 22.00
G 30.00
H 38.00
I 46.00
J 54.00
K 62.00
L 70.00
M 78.00
N 86.00
O 94.00
P 102.00
Q 110.00
R 118.00

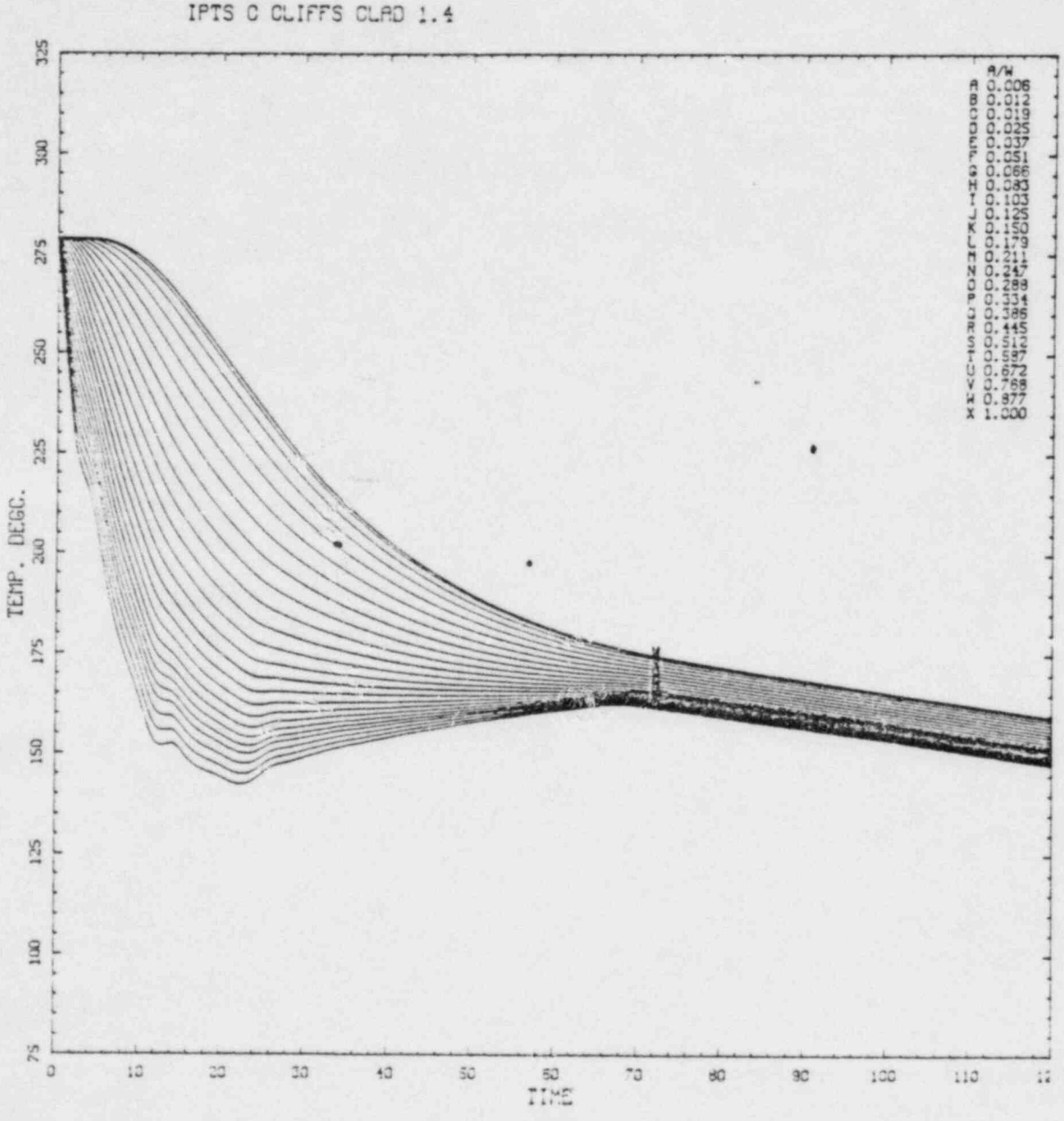
IPTS C CLIFFS CLAD 1.4
TEMP. DEGC.
TIME
A/W
A 0.006
B 0.012
C 0.019
D 0.025
E 0.037
F 0.051
G 0.066
H 0.083
I 0.103
J 0.125
K 0.150
L 0.179
M 0.211
N 0.247
O 0.288
P 0.334
Q 0.386
R 0.445
S 0.513
T 0.587
U 0.672
V 0.768
W 0.877
X 1.000

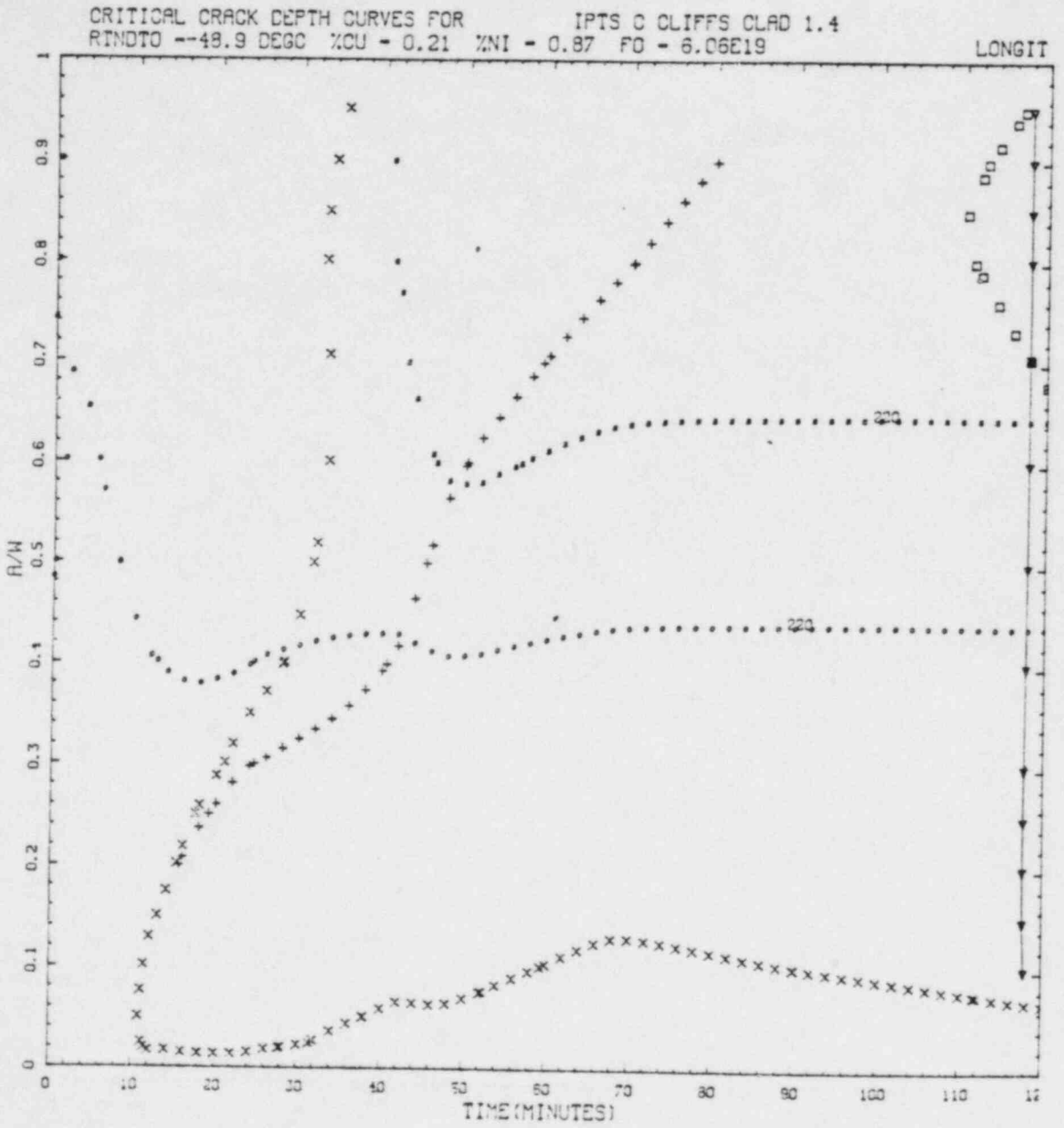
CRITICAL CRACK DEPTH CURVES FOR IPTS C CLIFFS CLAD 1.4
RTNDTO --48.9 DEGC %CU - 0.21 %NI - 0.87 FO - 6.06E19
LONGIT
A/W
TIME(MINUTES)
220
220

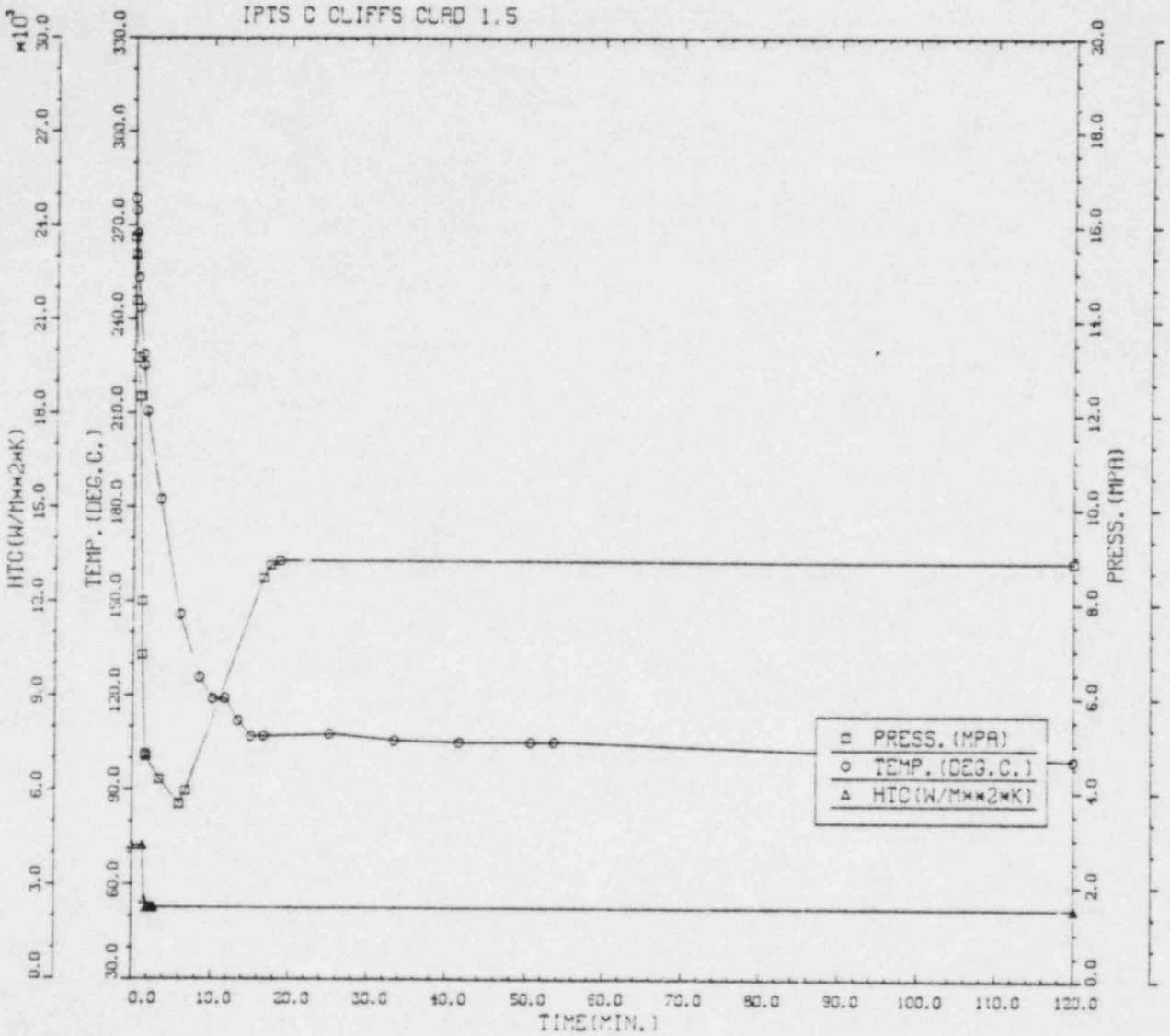
IPTS C CLIFFS CLAD 1.5
HTC(W/M**2*K)
TEMP.(DEG.C.)
PRESS.(MPA)
TIME(MIN.)
PRESS.(MPA)
TEMP.(DEG.C.)
HTC(W/M**2*K)

IPTS C CLIFFS CLAD 1.5 1. FLAWS/M**3 FO = 6.060D+19

WELD	UNADJUSTED P(F/E)	95%CI	%ERR	P(INITIA)	N*V	ADJUSTED P(F/E)	%ERR	NTRIALS
1	1.03D-03	1.02D-04	9.99	2.24D-03	0.025	2.56D-05		220000
2	1.17D-05	7.28D-06	61.98	4.11D-05	0.050	5.87D-07		500000
3	1.93D-04	2.95D-05	15.30	5.20D-04	0.021	4.05D-06		500000
					VESSEL	3.03D-05	8.79	

DEPTHS FOR INITIAL INITIATION (MM)

	2.16	6.68	11.62	17.03	22.95	29.42	36.51	44.25	52.72
NUMBER	65	854	272	95	22	7	1	1	0
PERCENT	4.9	64.3	20.7	7.2	1.7	0.5	0.1	0.1	0.0

TIMES OF FAILURE(MINUTES)

	0.0	10.0	20.0	30.0	40.0	50.0	60.0	70.0	80.0	90.0	100.0	110.0	120.0
NUMBER	0	0	0	0	4	36	70	94	110	88	82	74	
PERCENT	0.0	0.0	0.0	0.0	0.7	6.5	12.5	16.8	19.7	15.8	14.7	13.3	

INITIATION T-RTNDT(DEG.C)

	-55.6	-41.7	-27.8	-13.9	0.0	13.9	27.8	41.7	55.6	69.4	83.3	97.2	111.1
NUMBER	0	5	44	242	790	806	460	66	0	0	0	0	
PERCENT	0.0	0.2	1.8	10.0	32.7	33.4	19.1	2.7	0.0	0.0	0.0	0.0	

ARREST T-RTNDT(DEG.C)

	-27.8	-13.9	0.0	13.9	27.8	41.7	55.6	69.4	83.3	97.2	111.1	125.0	138.9
NUMBER	0	0	0	2	4	6	105	825	583	178	51	0	
PERCENT	0.0	0.0	0.0	0.1	0.2	0.3	5.7	44.5	36.8	9.6	2.7	0.0	

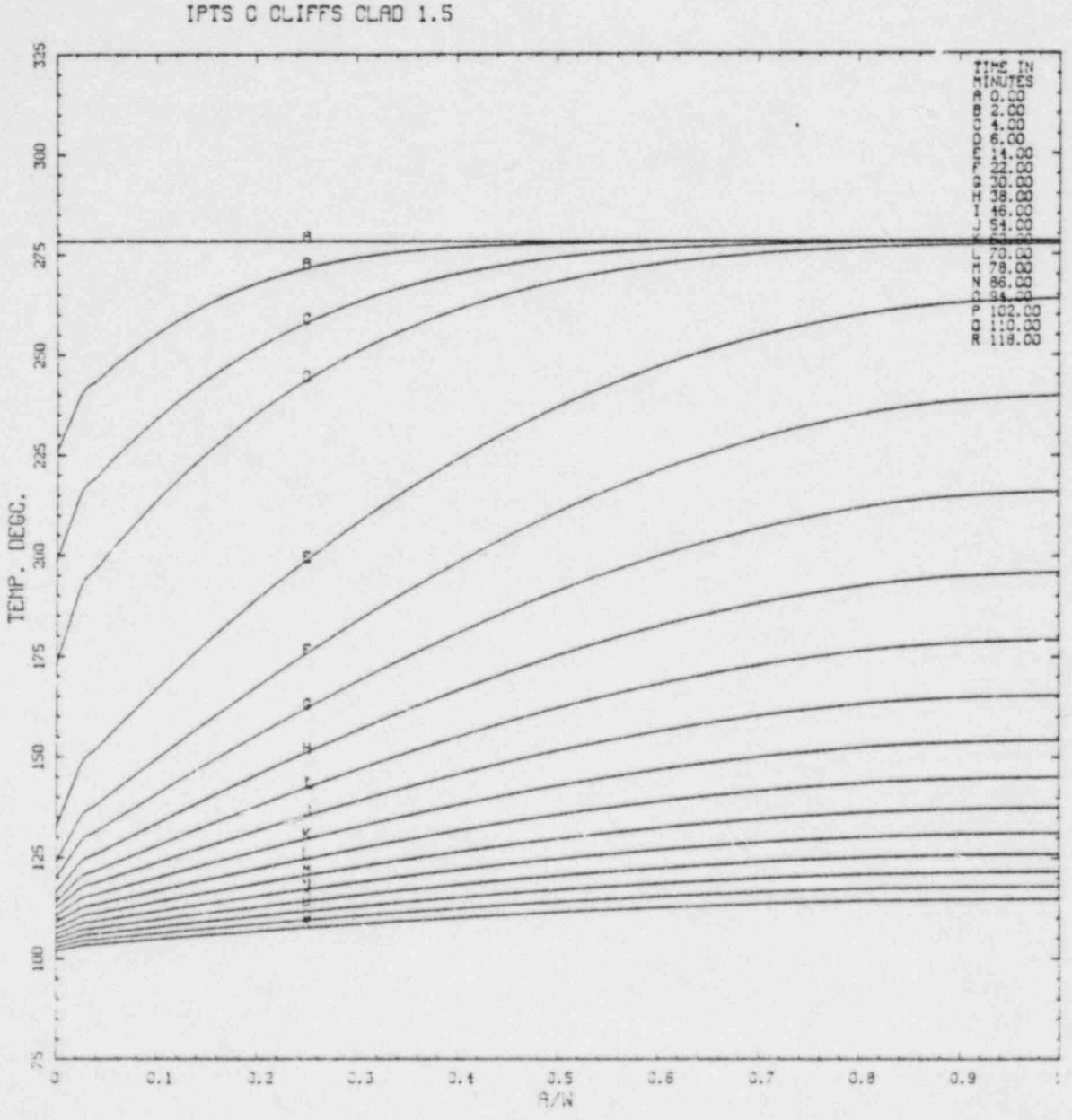
IPTS C CLIFFS CLAD 1.5
TEMP. DEGC.
R/W
TIME IN MINUTES
A 0.00
B 2.00
C 4.00
D 6.00
E 14.00
F 22.00
G 30.00
H 38.00
I 46.00
J 54.00
K 62.00
L 70.00
M 78.00
N 86.00
O 94.00
P 102.00
Q 110.00
R 118.00

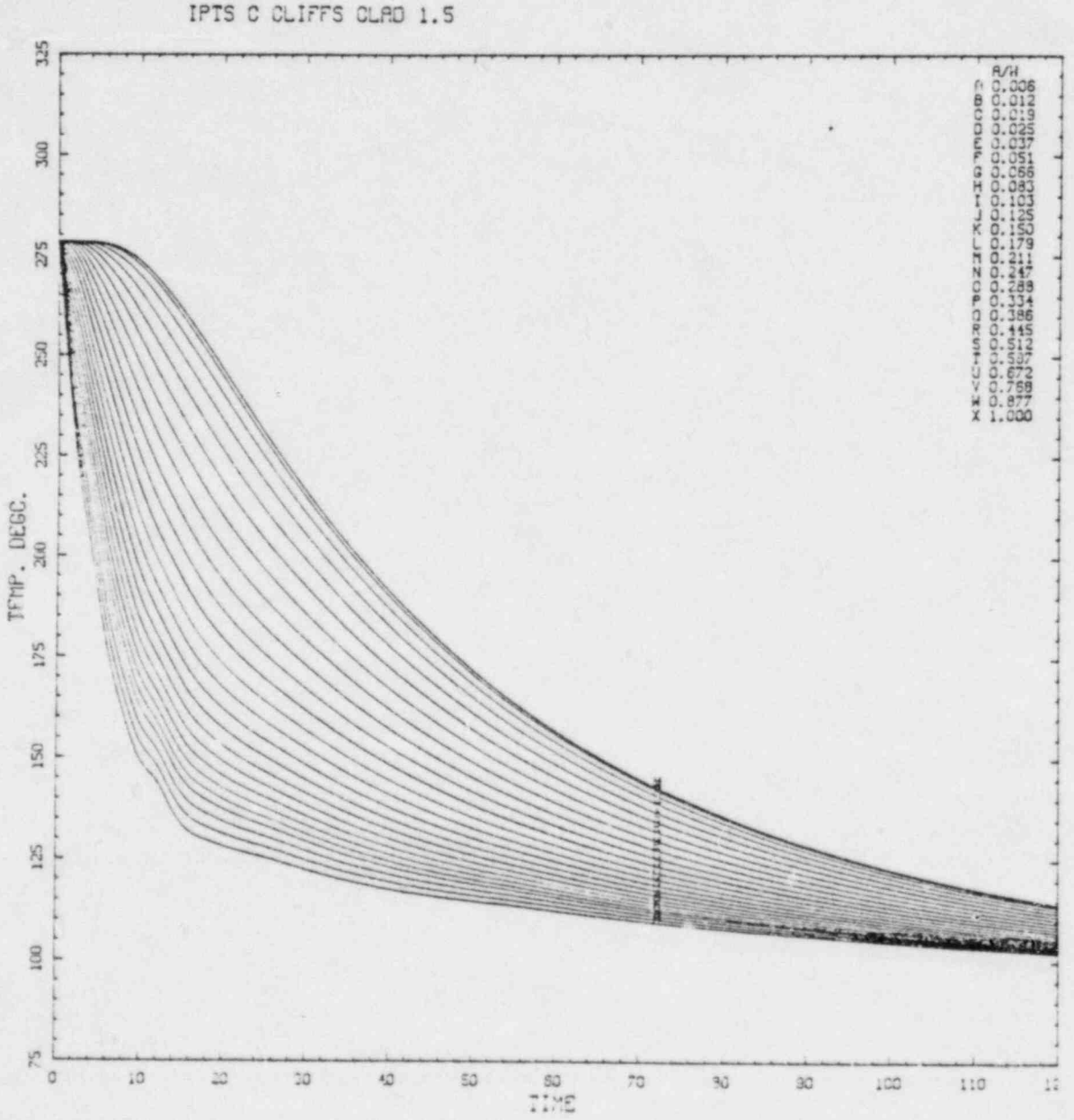
IPTS C CLIFFS CLAD 1.5
TEMP. DEGC.
TIME
R/W
A 0.006
B 0.012
C 0.019
D 0.026
E 0.037
F 0.051
G 0.066
H 0.083
I 0.103
J 0.126
K 0.150
L 0.179
M 0.211
N 0.247
O 0.288
P 0.334
Q 0.386
R 0.445
S 0.512
T 0.587
U 0.672
V 0.768
W 0.877
X 1.000

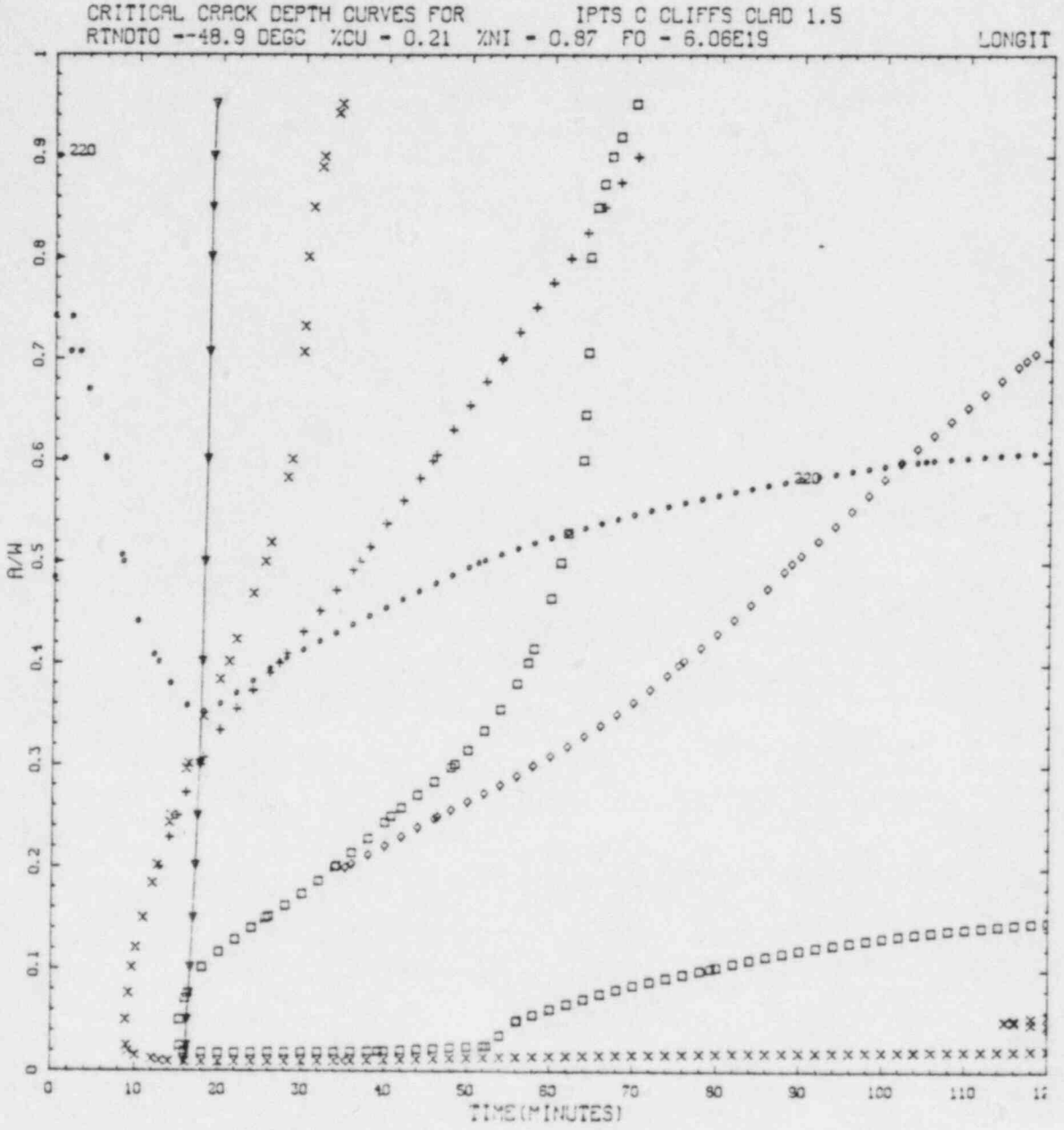
CRITICAL CRACK DEPTH CURVES FOR IPTS C CLIFFS CLAD 1.5
RTNDTO --48.9 DEGC %CU - 0.21 %NI - 0.87 FO - 6.06E19
LONGIT
220
220
A/W
TIME(MINUTES)
0
0.1
0.2
0.3
0.4
0.5
0.6
0.7
0.8
0.9
1
10
20
30
40
50
60
70
80
90
100
110

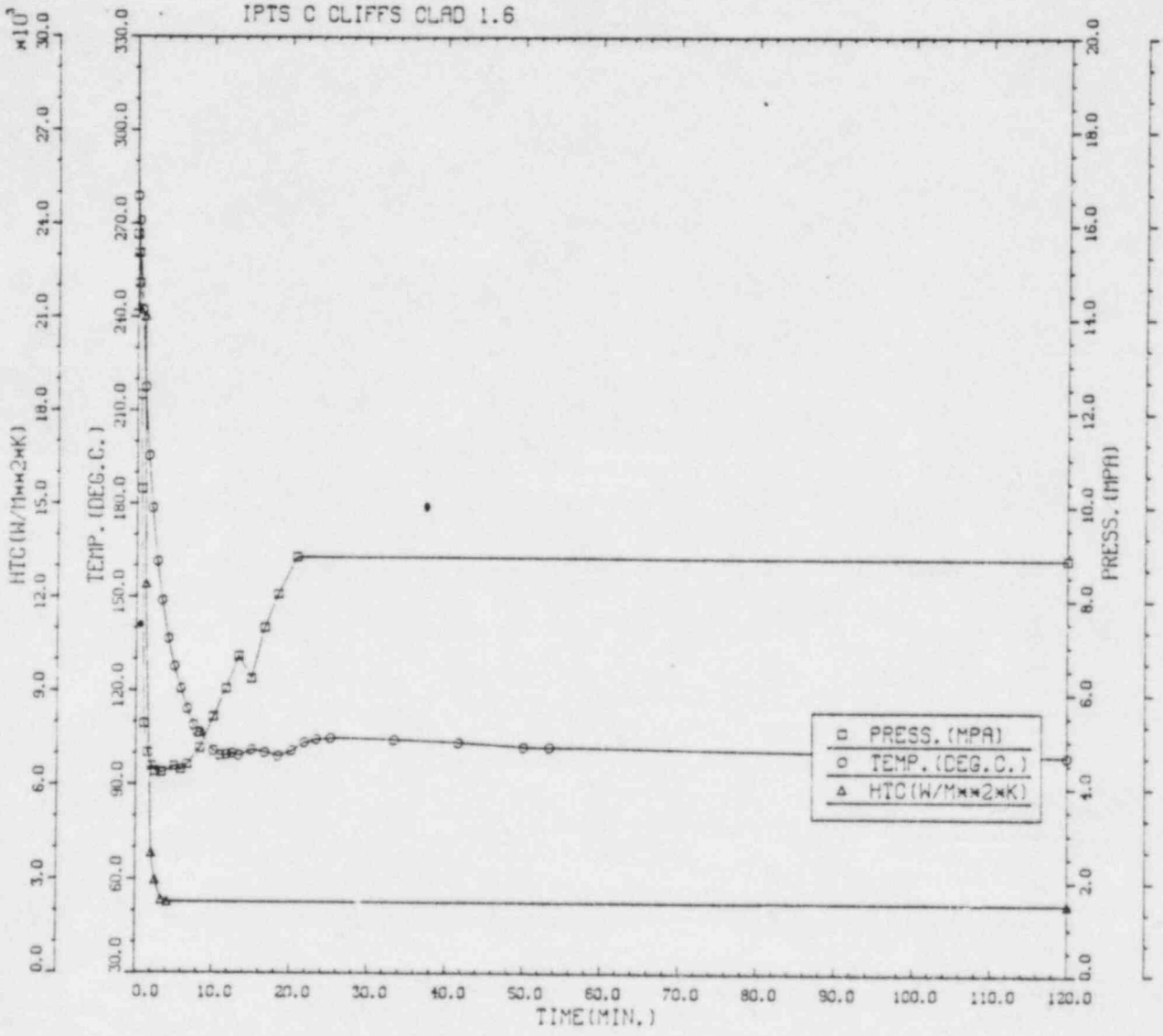
IPTS C CLIFFS CLAD 1.6
HTC(W/M**2*K)
x10³
TEMP.(DEG.C.)
PRESS.(MPA)
TIME(MIN.)
PRESS.(MPA)
TEMP.(DEG.C.)
HTC(W/M**2*K)

IPTS C CLIFFS CLAD 1.6 1. FLAWS/M**3 FO = 6.060D+19

WELD	P(F/E)	UNADJUSTED 95%CI	%ERR	P(INITIA)	N*V	ADJUSTED P(F/E)	%ERR	NTRIALS
1	1.71D-03	1.56D-04	9.69	4.96D-03	0.025	4.28D-05		140000
2	2.70D-05	1.10D-05	40.87	1.16D-04	0.050	1.35D-06		500000
3 *	3.42D-04	3.93D-05	11.49	1.24D-03	0.021	7.18D-06		500000
					VESSEL	5.13D-05	9.31	

DEPTHS FOR INITIAL INITIATION (MM)

	2.16	6.68	11.62	17.03	22.95	29.42	36.51	44.25	52.72
NUMBER	158	1554	464	128	22	7	1	0	0
PERCENT	6.8	66.6	19.9	5.5	0.9	0.3	0.0	0.0	0.0

TIMES OF FAILURE(MINUTES)

	0.0	10.0	20.0	30.0	40.0	50.0	60.0	70.0	80.0	90.0	100.0	110.0	120.0
NUMBER	0	0	0	0	7	60	106	135	125	108	93	87	
PERCENT *	0.0	0.0	0.0	0.0	1.0	8.3	14.7	18.8	17.3	15.0	12.9	12.0	

INITIATION T-RTNDT(DEG.C)

	-55.6	-41.7	-27.8	-13.9	0.0	13.9	27.8	41.7	55.6	69.4	83.3	97.2	111.1
NUMBER	1	10	90	455	1285	1327	708	135	3	0	0	0	
PERCENT	0.0	0.2	2.0	11.4	32.1	33.1	17.7	3.4	0.1	0.0	0.0	0.0	

ARREST T-RTNDT(DEG.C)

	-27.8	-13.9	0.0	13.9	27.8	41.7	55.6	69.4	83.3	97.2	111.1	125.0	138.9
NUMBER	0	0	0	1	1	14	239	1451	1285	251	41	0	
PERCENT	0.0	0.0	0.0	0.0	0.0	0.4	7.3	44.2	39.2	7.6	1.2	0.0	

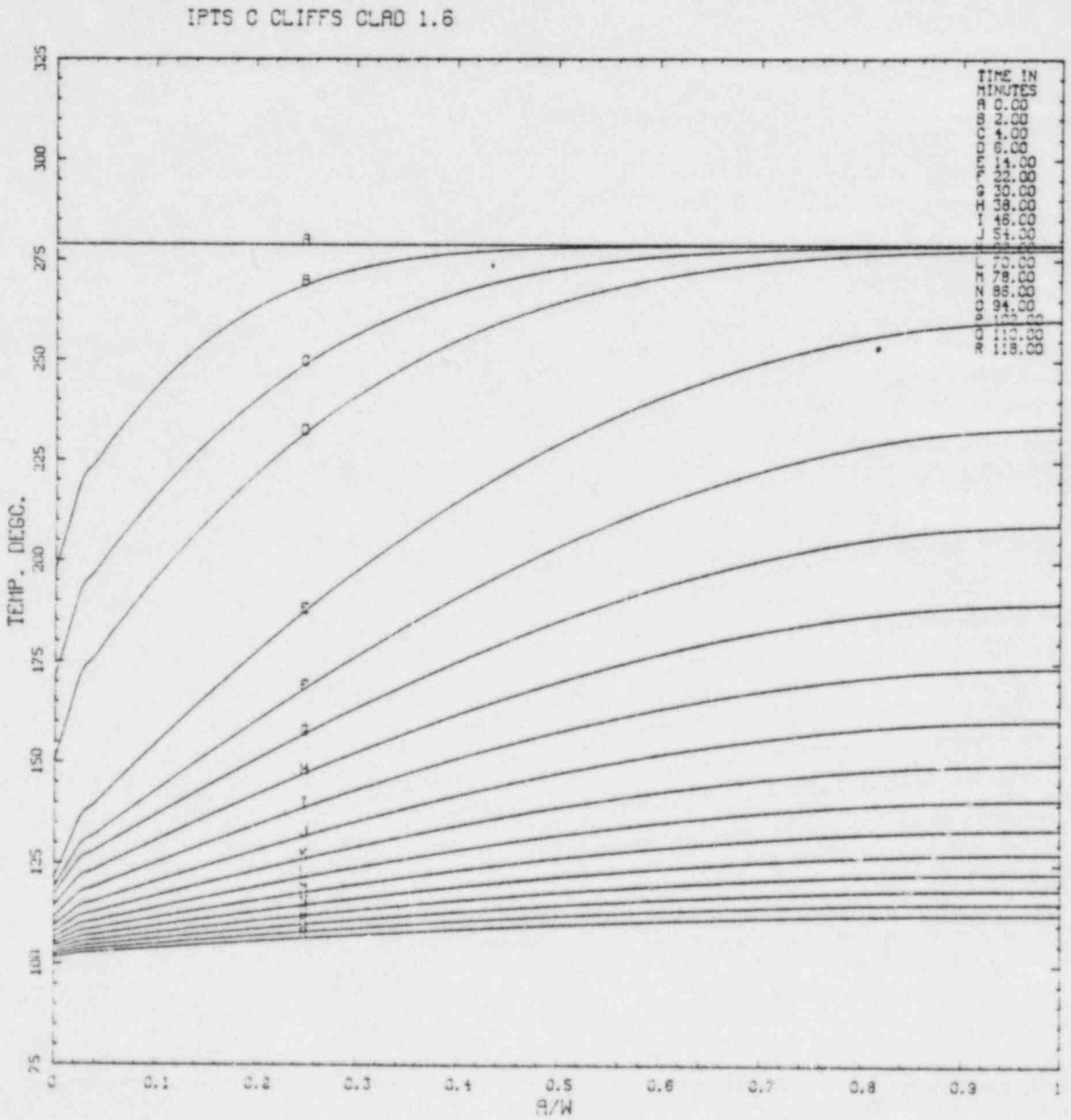
IPTS C CLIFFS CLAD 1.6
TEMP. DEGC.
R/W
TIME IN MINUTES
A 0.00
B 2.00
C 4.00
D 6.00
E 14.00
F 22.00
G 30.00
H 38.00
I 46.00
J 54.00
K 70.00
L 78.00
M 86.00
N 94.00
O 110.00
P 118.00

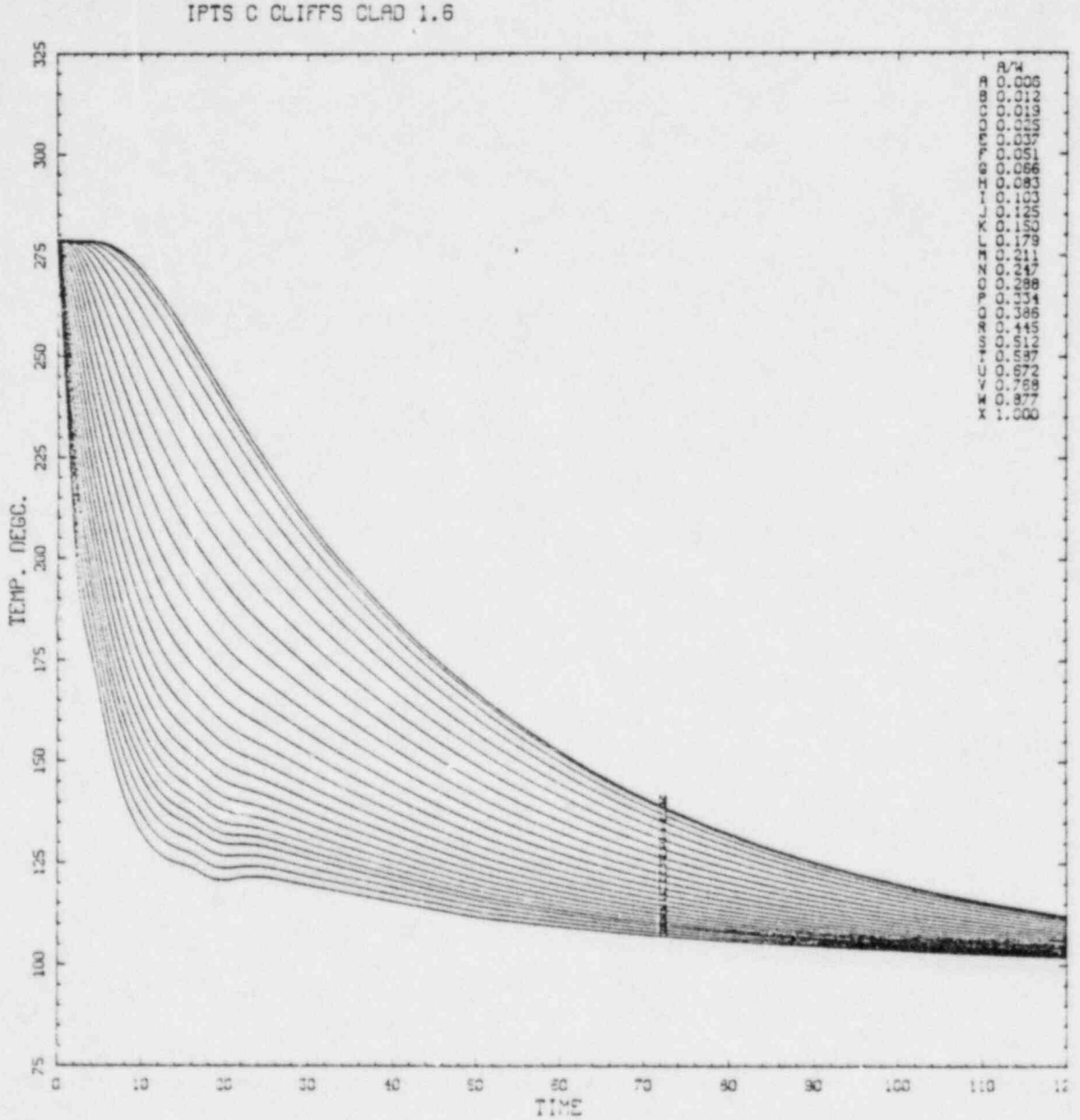
IPTS C CLIFFS CLAD 1.6
TEMP. DEGC.
TIME
A/W
A 0.006
B 0.012
C 0.019
D 0.025
E 0.051
F 0.066
G 0.083
H 0.103
I 0.125
J 0.150
K 0.179
L 0.211
M 0.247
N 0.288
O 0.334
P 0.386
Q 0.445
R 0.512
S 0.587
T 0.672
U 0.768
V 0.877
W 1.000

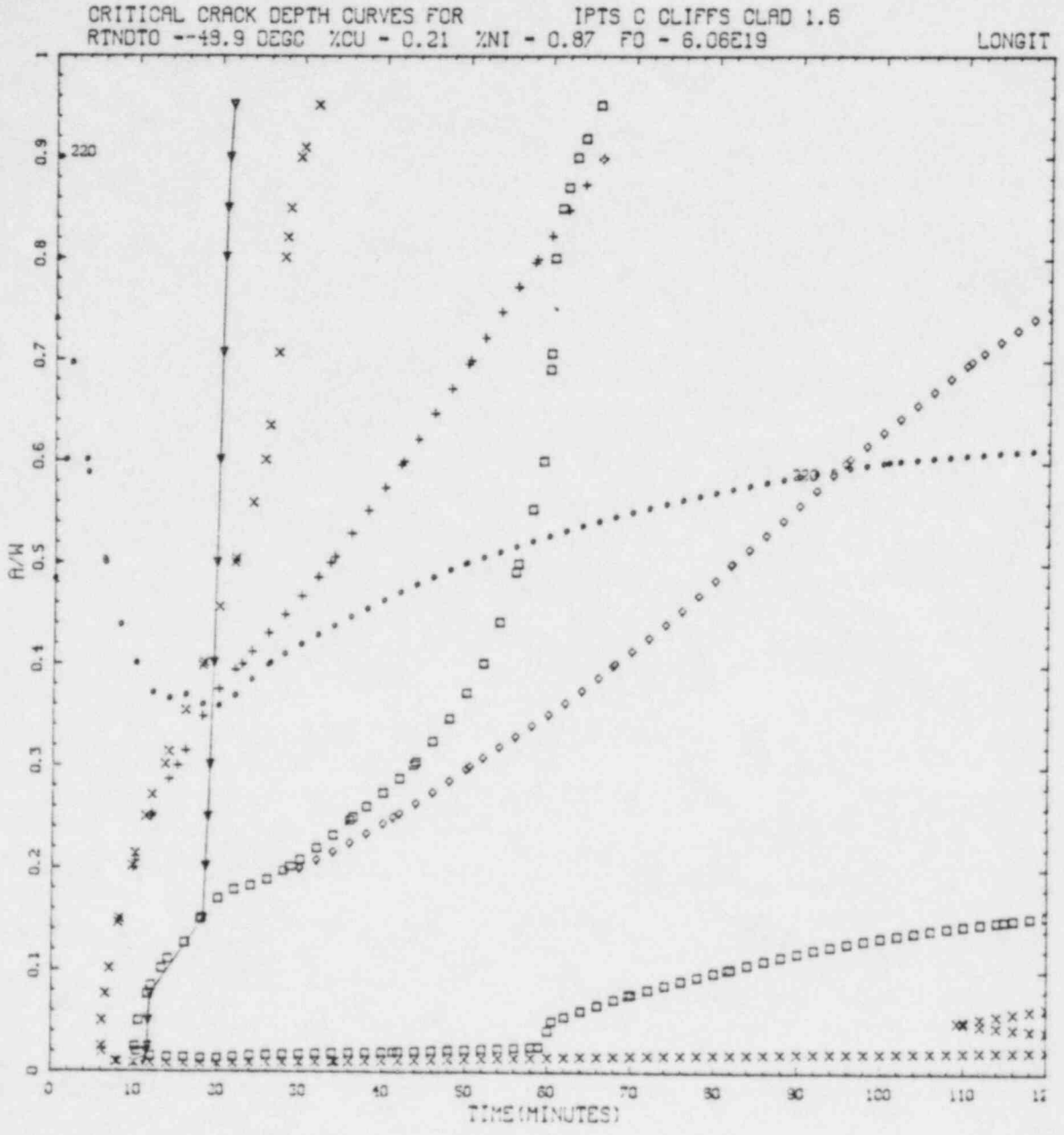
CRITICAL CRACK DEPTH CURVES FOR IPTS C CLIFFS CLAD 1.6
RTNDTO --48.9 DEGC %CU - 0.21 %NI - 0.87 FO - 6.06E19
LONGIT
220
A/W
TIME(MINUTES)

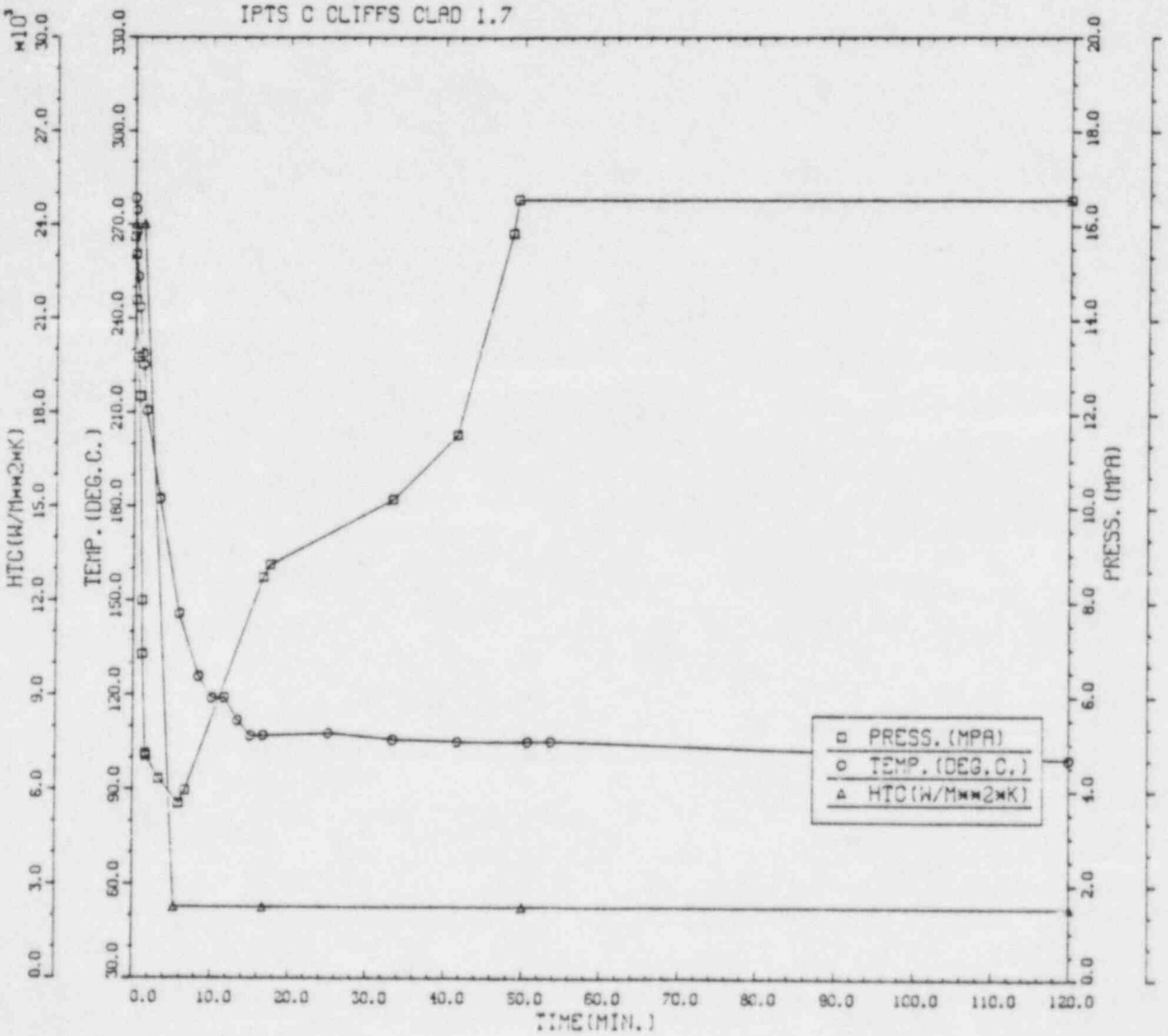
IPTS C CLIFFS CLAD 1.7
HTC(W/M**2*K)
*10**3
TEMP.(DEG.C.)
PRESS.(MPA)
TIME(MIN.)
PRESS.(MPA)
TEMP.(DEG.C.)
HTC(W/M**2*K)

IPTS C CLIFFS CLAD 1.7 1. FLAWS/M**3 FO = 6.060D+19

WELD	P(F/E)	95%CI	%ERR	P(INITIA)	N*V	P(F/E)	%ERR	NTRIALS
	UNADJUSTED					ADJUSTED		
1	5.95D-03	5.76D-04	9.69	6.08D-03	0.025	1.49D-04		40000
2	1.96D-04	2.97D-05	15.16	2.11D-04	0.050	9.81D-06		500000
3	1.67D-03	1.64D-04	9.82	1.72D-03	0.021	3.50D-05		140000
					VESSEL	1.93D-04	7.69	

DEPTHS FOR INITIAL INITIATION (MM)

	2.16	6.58	11.52	17.03	22.95	29.42	36.51	44.25	52.72
NUMBER	18	538	218	91	20	14	3	1	0
PERCENT	1.8	63.6	21.7	9.1	2.0	1.4	0.3	0.1	0.0

TIMES OF FAILURE(MINUTES)

	0.0	10.0	20.0	30.0	40.0	50.0	60.0	70.0	80.0	90.0	100.0	110.0	120.0
NUMBER	0	0	0	0	363	258	112	97	65	34	26	14	
PERCENT	0.0	0.0	0.0	0.0	37.5	26.6	11.6	10.0	6.7	3.5	2.7	1.4	

INITIATION T-RTNDT(DEG.C)

	-55.6	-41.7	-27.8	-13.9	0.0	13.9	27.8	41.7	55.6	69.4	83.3	97.2	111.1
NUMBER	0	6	72	293	450	229	367	239	19	0	0	0	
PERCENT	0.0	0.4	4.3	17.5	26.9	13.7	21.9	14.3	1.1	0.0	0.0	0.0	

ARREST T-RTNDT(DEG.C)

	-27.8	-13.9	0.0	13.9	27.8	41.7	55.6	69.4	83.3	97.2	111.1	125.0	138.9
NUMBER	0	0	3	9	3	1	11	134	415	68	12	0	
PERCENT	0.0	0.0	0.4	1.3	0.4	0.1	1.6	20.1	58.9	9.6	1.7	0.0	

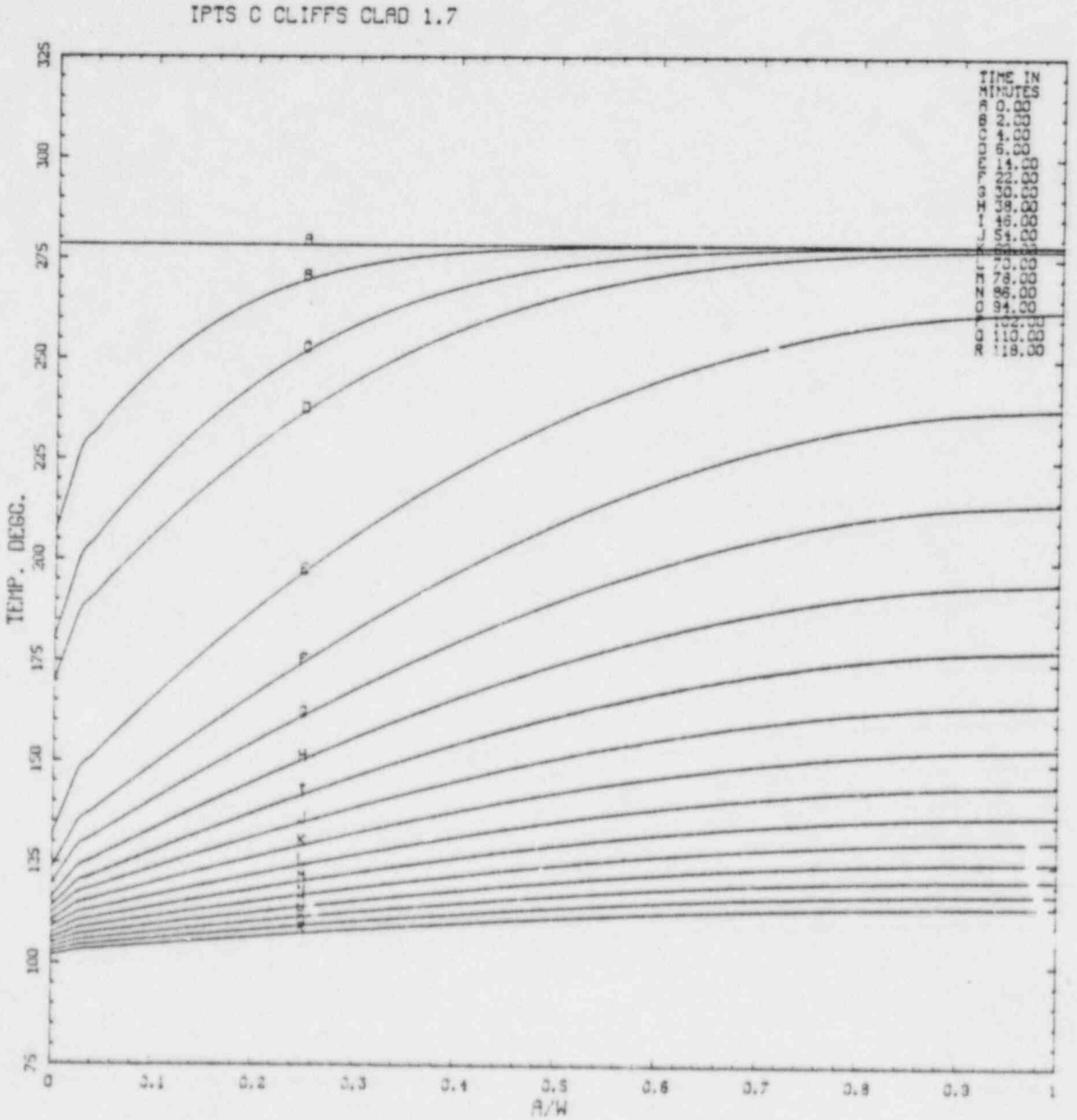
IPTS C CLIFFS CLAD 1.7
TEMP. DEGC.
325
300
275
250
225
200
175
150
125
100
75
0
0.1
0.2
0.3
0.4
0.5
0.6
0.7
0.8
0.9
1
R/W
TIME IN MINUTES
A 0.00
B 2.00
C 4.00
D 6.00
E 14.00
F 22.00
G 30.00
H 38.00
I 46.00
J 54.00
K 62.00
L 70.00
M 78.00
N 86.00
O 94.00
P 102.00
Q 110.00
R 118.00

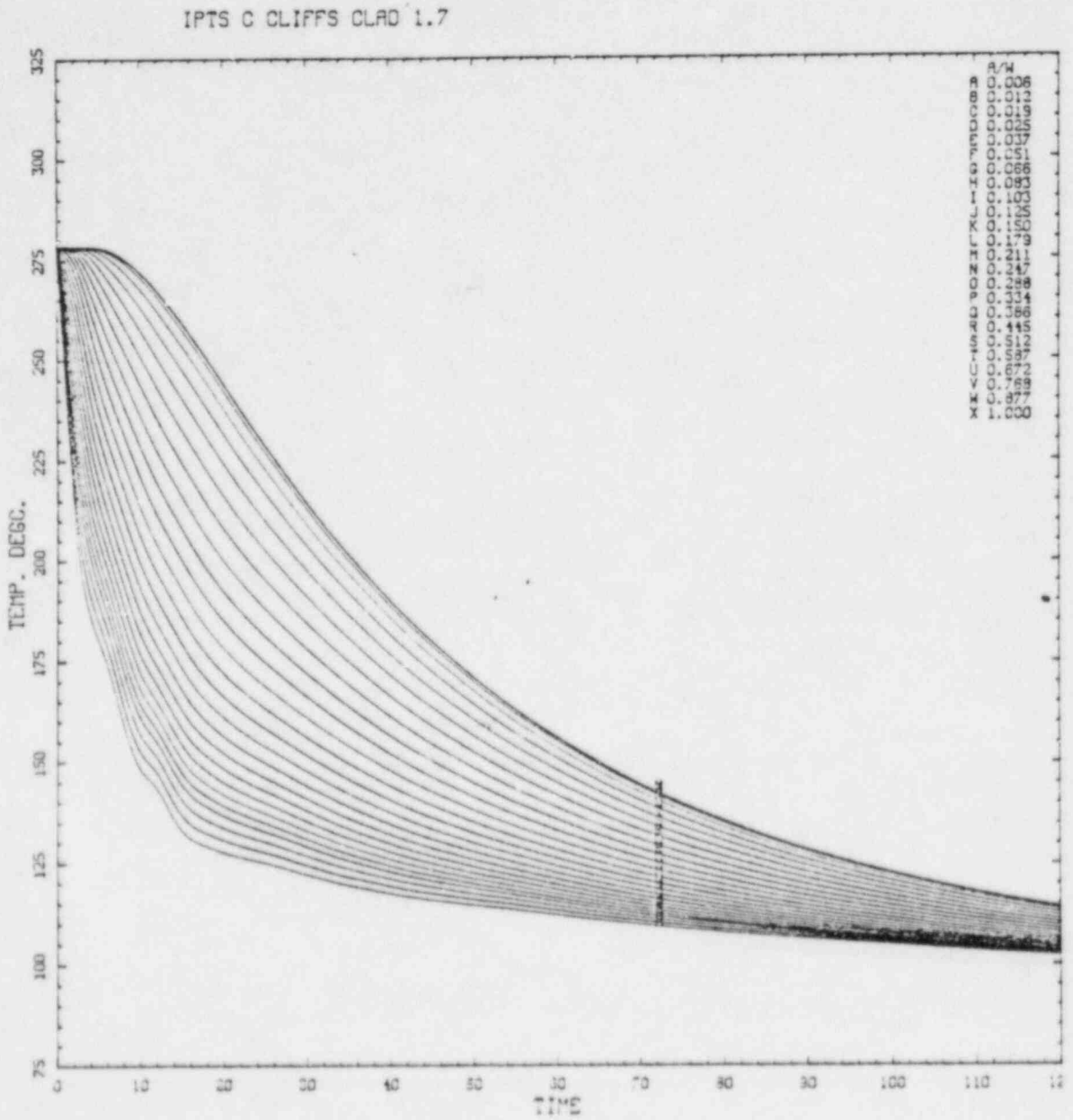
IPTS C CLIFFS CLAD 1.7
TEMP. DEGC.
TIME
A/W
A 0.006
B 0.013
C 0.019
D 0.025
E 0.037
F 0.051
G 0.066
H 0.083
I 0.103
J 0.125
K 0.150
L 0.179
M 0.211
N 0.247
O 0.288
P 0.334
Q 0.386
R 0.445
S 0.512
T 0.587
U 0.672
V 0.769
W 0.877
X 1.000

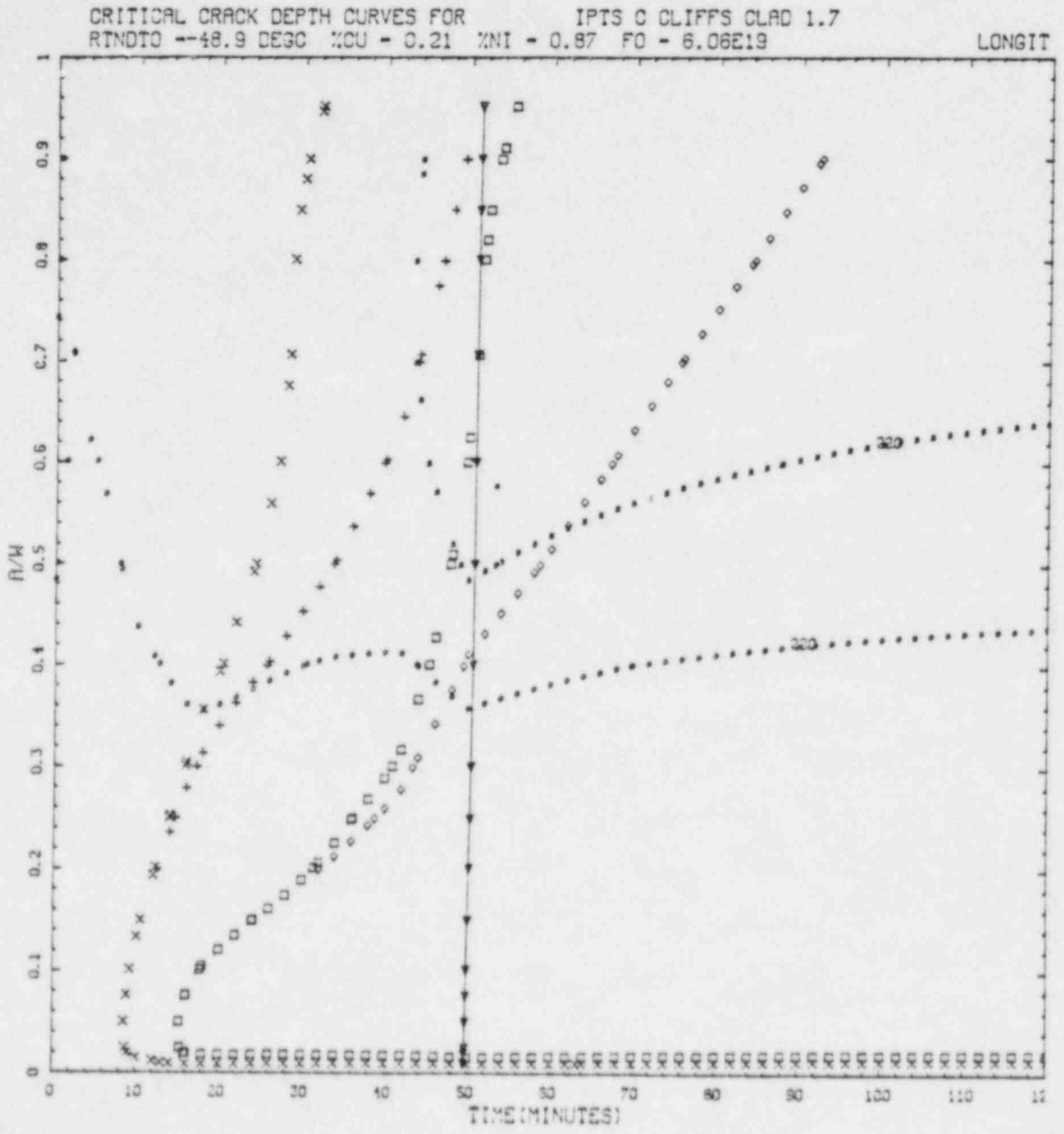
CRITICAL CRACK DEPTH CURVES FOR IPTS C CLIFFS CLAD 1.7
RTNDTO --48.9 DEGC %CU - 0.21 %NI - 0.87 FO - 6.06E19
LONGIT
A/W
TIME(MINUTES)
0
0.1
0.2
0.3
0.4
0.5
0.6
0.7
0.8
0.9
1
10
20
30
40
50
60
70
80
90
100
110
120

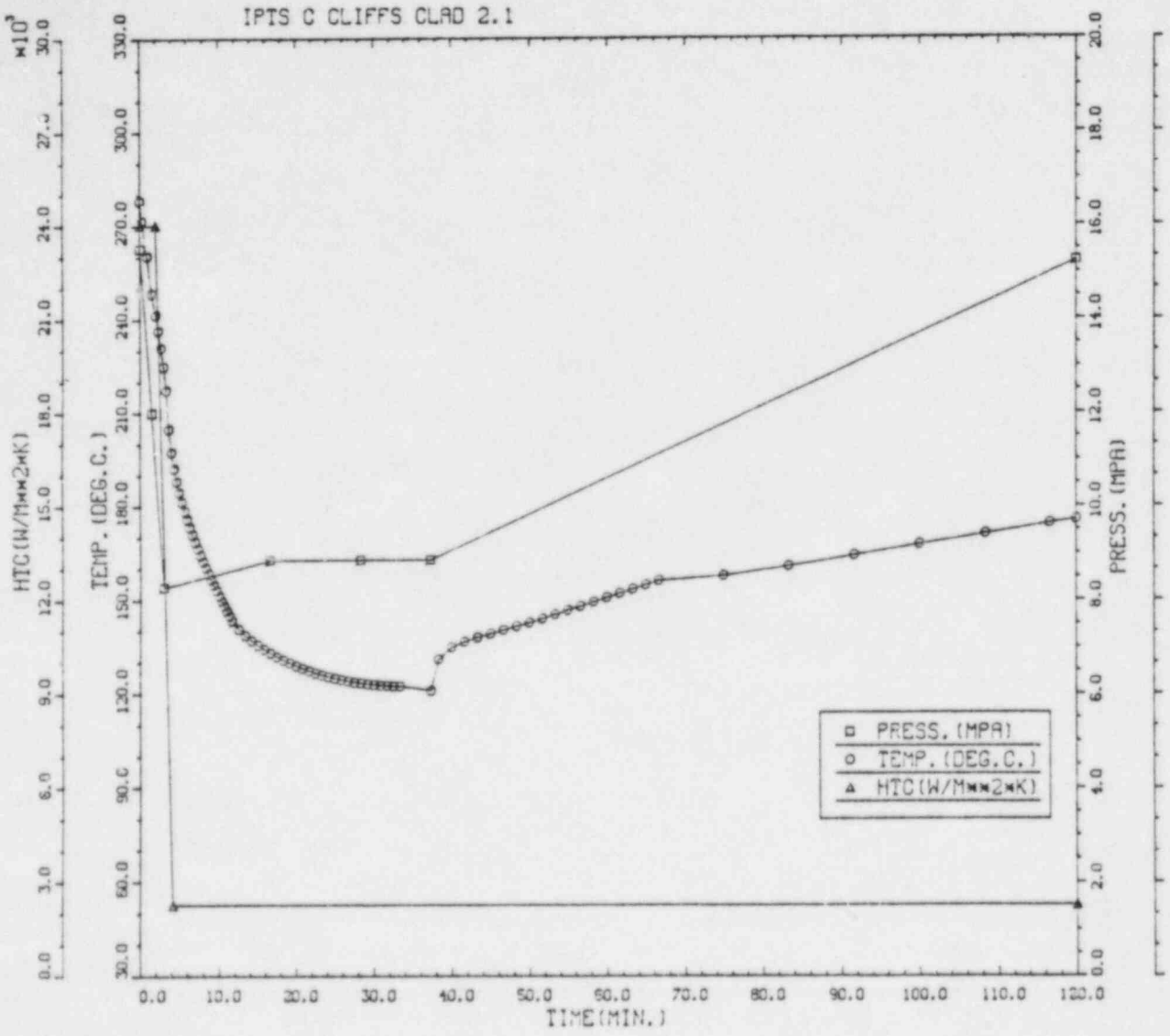
IPTS C CLIFFS CLAD 2.1
HTC(W/M**2*K)
TEMP.(DEG.C.)
PRESS.(MPA)
TIME(MIN.)
PRESS.(MPA)
TEMP.(DEG.C.)
HTC(W/M**2*K)

IPTS C CLIFFS CLAD 2.1 1. FLAWS/M**3 FO = 6.060D+19

WELD	UNADJUSTED P(F/E)	95%CI	%ERR	P(INITIA)	N*V	ADJUSTED P(F/E)	%ERR	NTRIALS
1	3.52D-06	3.99D-06	113.16	2.42D-04	0.025	8.81D-08		500000
2	0.00D+00	0.00D+00	0.00	2.35D-06	0.050	0.00D+00		500000
3	0.00D+00	0.00D+00	0.00	3.64D-05	0.021	0.00D+00		500000
					VESSEL	8.81D-08	113.16	

DEPTHS FOR INITIAL INITIATION (MM)

	2.16	6.68	11.62	17.03	22.95	29.42	36.51	44.25	52.72
NUMBER	1	158	60	15	4	1	0	0	0
PERCENT	0.4	66.1	25.1	6.3	1.7	0.4	0.0	0.0	0.0

TIMES OF FAILURE(MINUTES)

	0.0	10.0	20.0	30.0	40.0	50.0	60.0	70.0	80.0	90.0	100.0	110.0	120.0
NUMBER	0	0	0	0	0	0	1	0	1	1	0	0	
PERCENT	0.0	0.0	0.0	0.0	0.0	0.0	33.3	0.0	33.3	33.3	0.0	0.0	

INITIATION T-RTNDT(DEG.C)

	-55.6	-41.7	-27.8	-13.9	0.0	13.9	27.8	41.7	55.6	69.4	83.3	97.2	111.1
NUMBER	0	0	3	58	122	47	11	3	0	0	0	0	
PERCENT	0.0	0.0	1.2	26.8	48.0	18.5	4.3	1.2	0.0	0.0	0.0	0.0	

ARREST T-RTNDT(DEG.C)

	-27.8	-13.9	0.0	13.9	27.8	41.7	55.6	69.4	83.3	97.2	111.1	125.0	138.9
NUMBER	0	0	0	3	0	1	13	77	129	28	3	0	
PERCENT	0.0	0.0	0.0	1.2	0.0	0.4	5.2	30.7	51.4	11.2	0.0	0.0	

6/25/84

IPTS C CLIFFS CLAD 2.1 — 1. FLAWS/M**3 — F0 = 6.060D+19

WELD	P(F/E) UNADJUSTED	95%CI	%ERR	P(INITIA)	K*V	P(F/E) ADJUSTED	%ERR	TRIALS
1	5.29D-06	3.45D-06	65.33	2.52D-04	0.025	1.32D-07		1000000
					VESSEL	1.32D-07	65.33	

DEPTHS FOR INITIAL INITIATION (MM)

	2.46	6.66	11.62	17.03	22.95	29.42	36.51	44.25	52.72
NUMBER	5	275	99	30	12	4	0	0	0
PERCENT	1.2	65.0	23.1	7.0	2.8	0.9	0.0	0.0	0.0

TIMES OF FAILURE(MINUTES)

	0.0	10.0	20.0	30.0	40.0	50.0	60.0	70.0	80.0	90.0	100.0	110.0	120.0
NUMBER	0	0	0	0	0	1	1	1	5	1	0	0	
PERCENT	0.0	0.0	0.0	0.0	0.0	11.1	11.1	11.1	55.6	11.1	0.0	0.0	

INITIATION T-RTNDT(DEG.C)

	-55.6	-41.7	-27.8	-13.9	0.0	13.9	27.8	41.7	55.6	69.4	83.3	97.2	111.1
NUMBER	0	1	10	112	224	78	27	7	0	0	0	0	
PERCENT	0.0	0.2	2.2	24.4	48.8	17.0	5.9	1.5	0.0	0.0	0.0	0.0	

ARREST T-RTNDT(DEG.C)

	-27.8	-13.9	0.0	13.9	27.8	41.7	55.6	69.4	83.3	97.2	111.1	125.0	138.9
NUMBER	0	0	1	8	1	2	22	157	220	39	0	0	
PERCENT	0.0	0.0	0.2	1.8	0.2	0.4	4.9	34.9	48.9	8.7	0.0	0.0	

CC-L.39

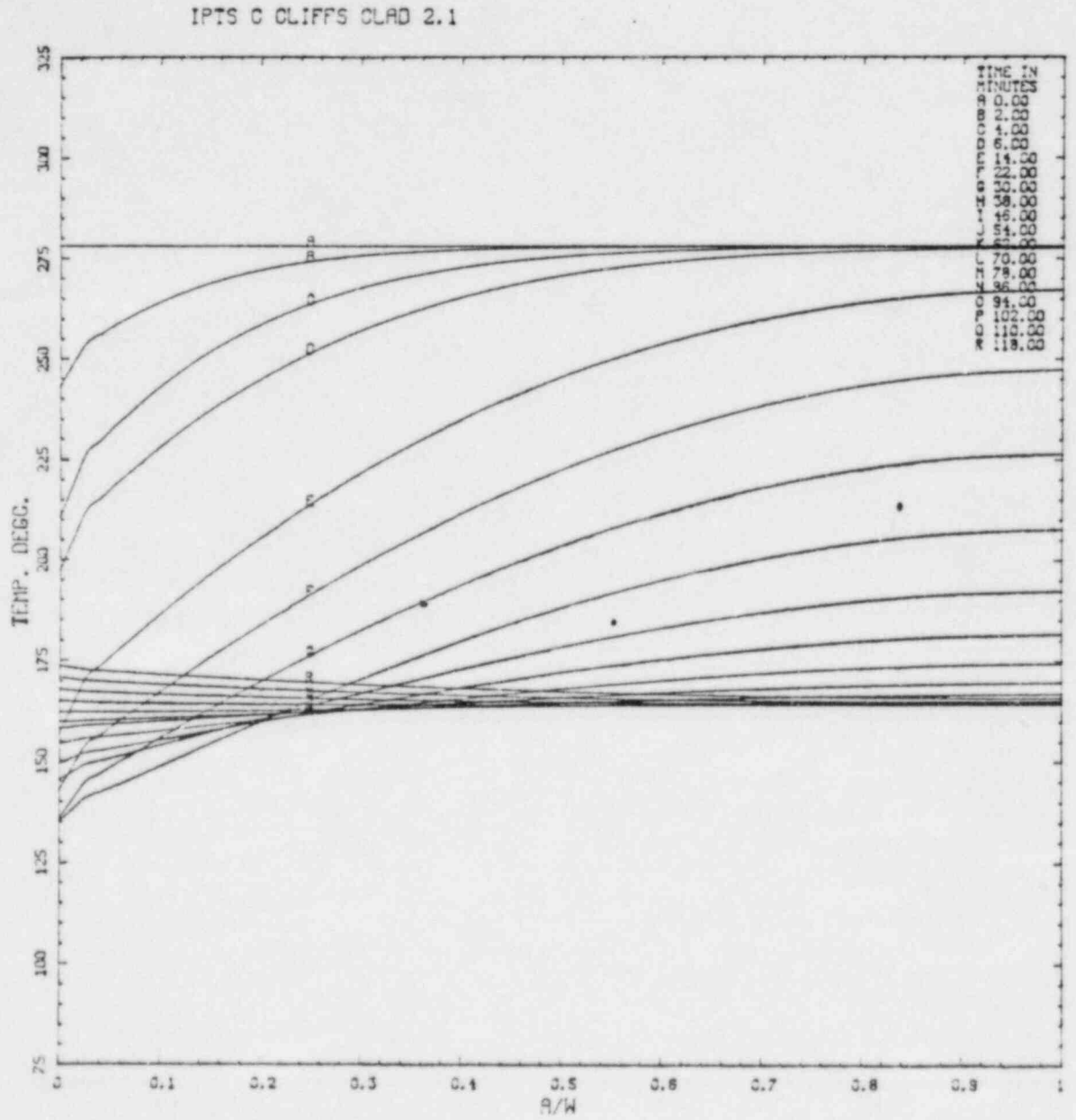
IPTS C CLIFFS CLAD 2.1
TEMP. DEGC.
75
100
125
150
175
200
225
250
275
300
325
0
0.1
0.2
0.3
0.4
0.5
0.6
0.7
0.8
0.9
1
R/W
TIME IN MINUTES
A 0.00
B 2.00
C 4.00
D 6.00
E 14.00
F 22.00
G 30.00
H 38.00
I 46.00
J 54.00
K 62.00
L 70.00
M 78.00
N 86.00
O 94.00
P 102.00
Q 110.00
R 118.00

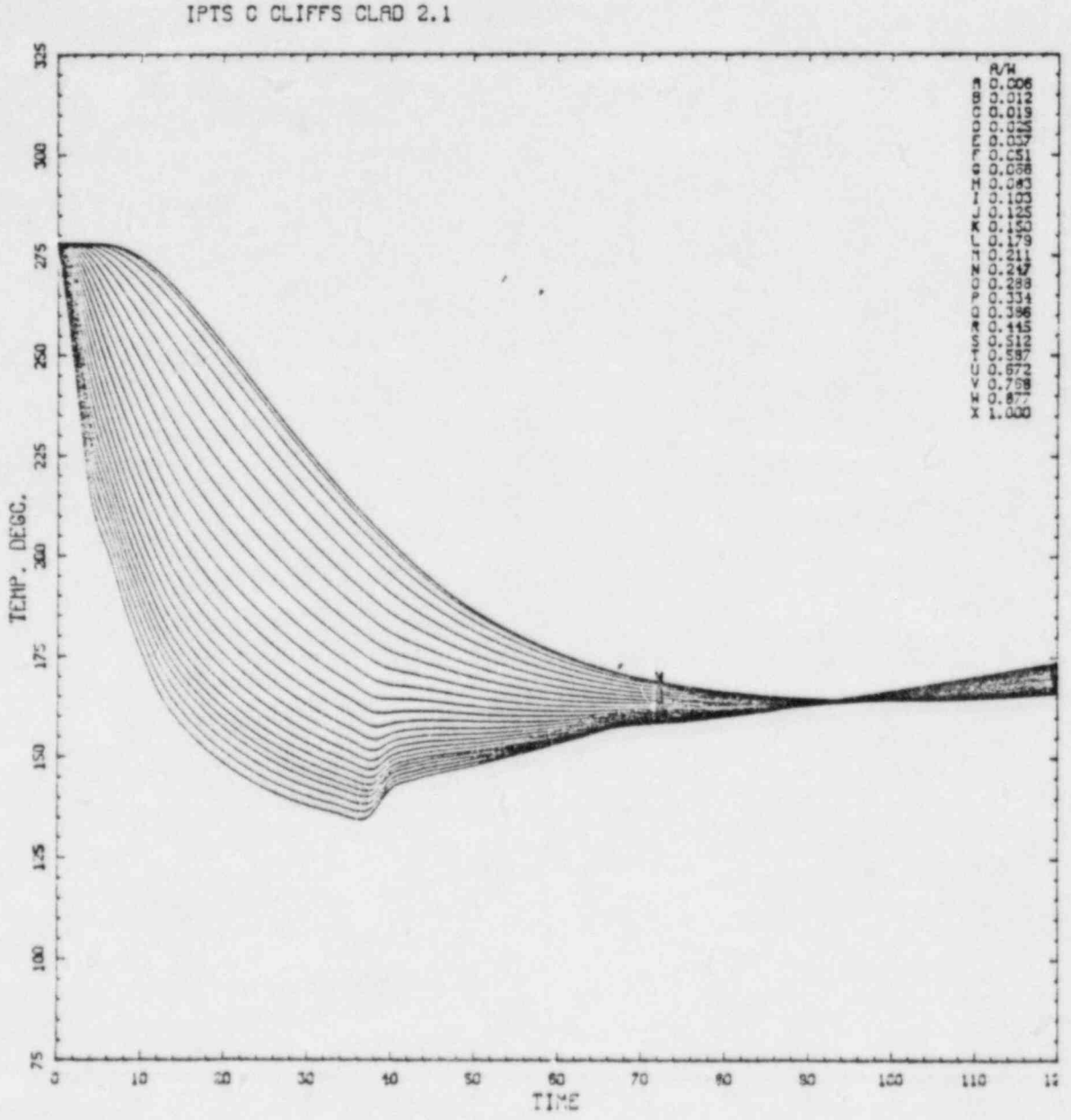
IPTS C CLIFFS CLAD 2.1
TEMP. DEGC.
TIME
R/H
A 0.006
B 0.012
C 0.019
D 0.025
E 0.031
F 0.051
G 0.068
H 0.083
I 0.103
J 0.125
K 0.150
L 0.179
M 0.211
N 0.247
O 0.288
P 0.334
Q 0.386
R 0.445
S 0.512
T 0.587
U 0.672
V 0.768
W 0.877
X 1.000

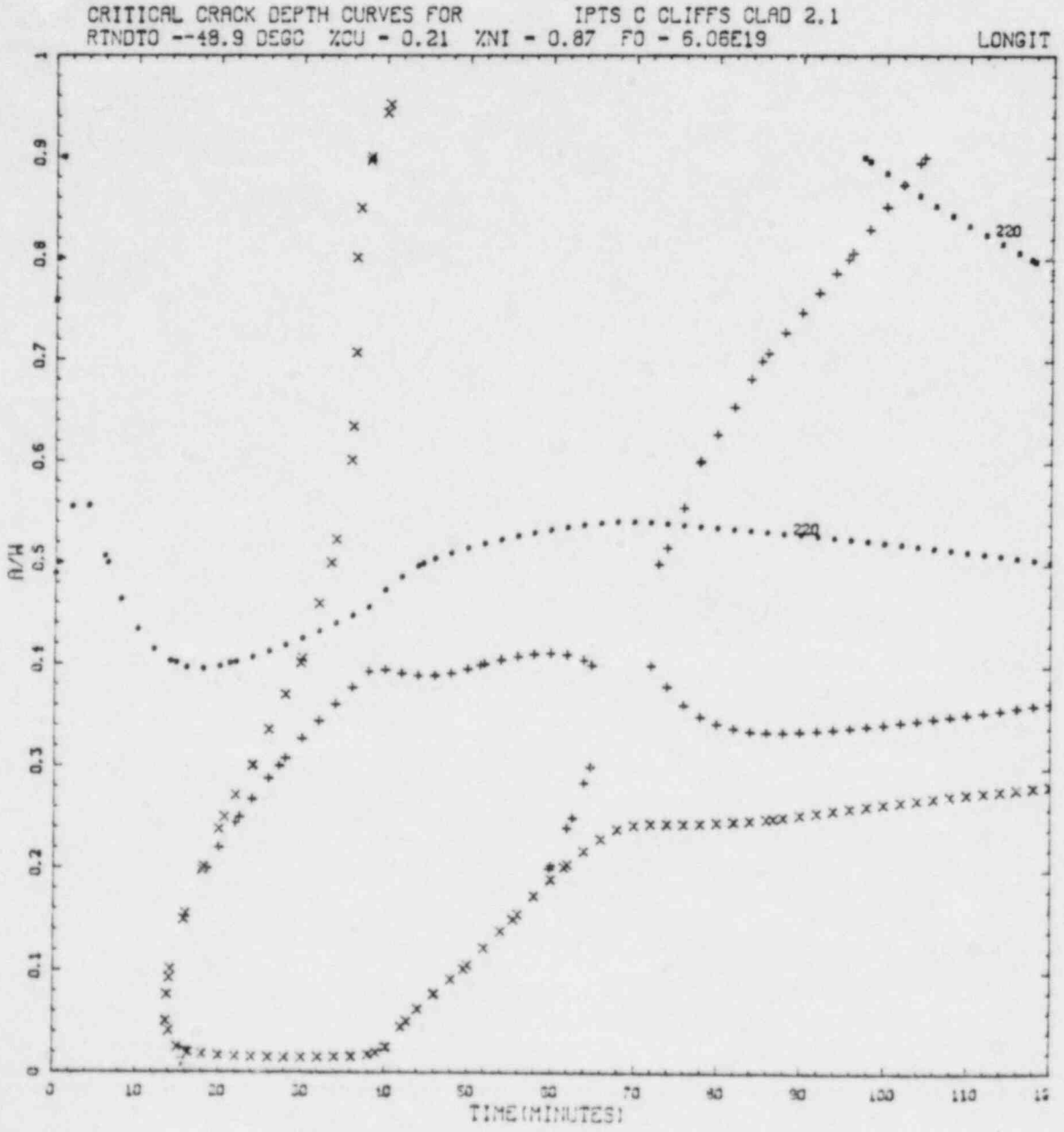
CRITICAL CRACK DEPTH CURVES FOR IPTS C CLIFFS CLAD 2.1
RTNDTO --48.9 DEGC %CU - 0.21 %NI - 0.87 FO - 6.06E19
LONGIT
220
220
A/W
TIME(MINUTES)

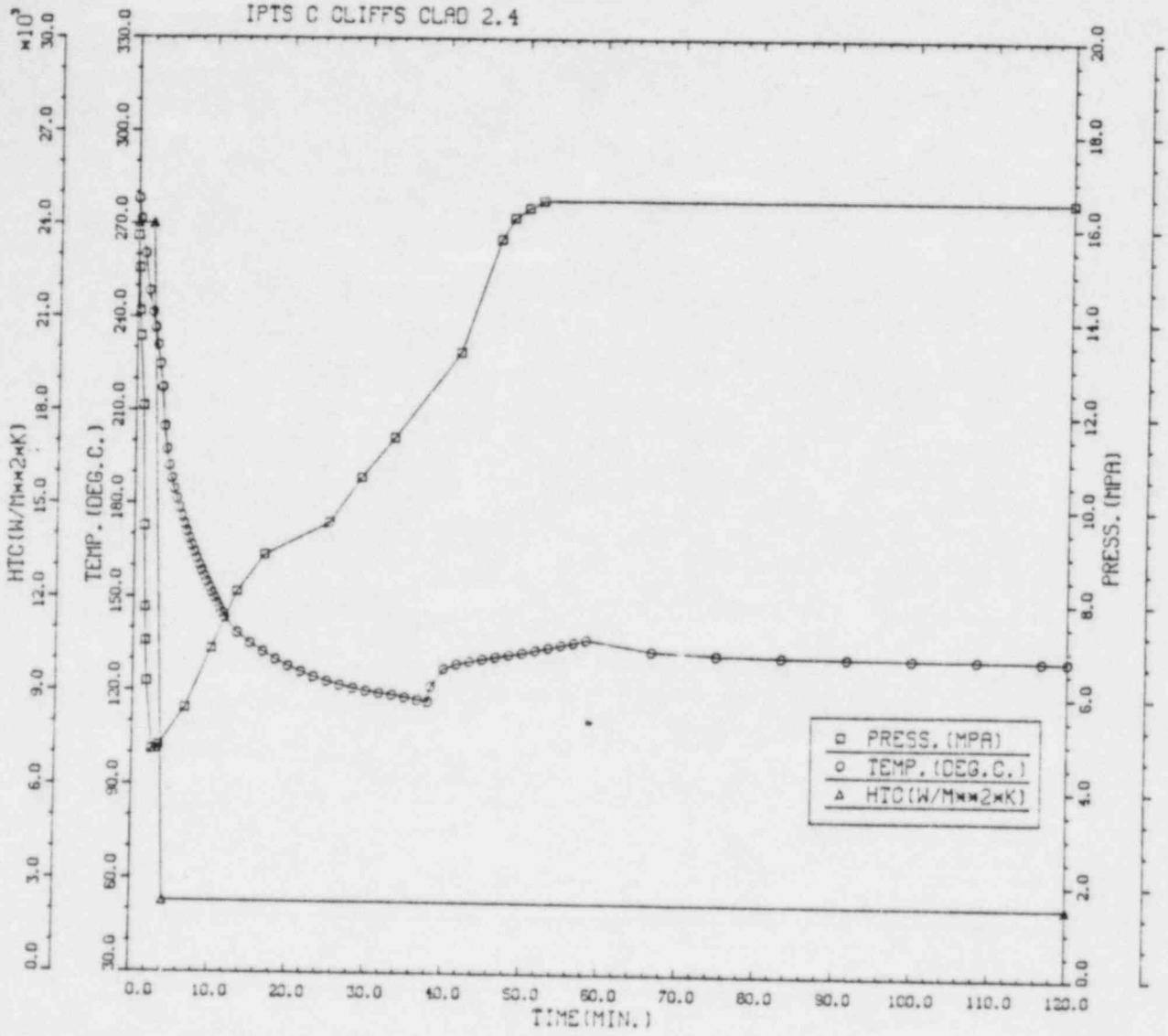
IPTS C CLIFFS CLAD 2.4
HTC(W/M**2*K)
*10**3
TEMP.(DEG.C.)
PRESS.(MPA)
TIME(MIN.)
PRESS.(MPA)
TEMP.(DEG.C.)
HTC(W/M**2*K)

IPTS C CLIFFS CLAD 2.4 1. FLAWS/M**3 FO = 5.060D+19

WELD	UNADJUSTED P(F/E)	95%CI	%ERR	P(INITIA)	N*V	ADJUSTED P(F/E)	%ERR	NTRIALS
1	5.76D-04	5.63D-05	9.77	9.34D-04	0.025	1.44D-05		410000
2	8.22D-06	6.09D-06	74.08	1.29D-05	0.050	4.11D-07		500000
3	8.69D-05	1.98D-05	22.78	1.59D-04	0.021	1.83D-06		500000
					VESSEL	1.66D-05	9.01	

DEPTHS FOR INITIAL INITIATION (MM)

	2.16	6.68	11.62	17.03	22.95	29.42	36.51	44.25	52.72
NUMBER	10	523	190	65	14	4	1	0	0
PERCENT	1.2	64.8	23.5	8.1	1.7	0.5	0.1	0.0	0.0

TIMES OF FAILURE(MINUTES)

	0.0	10.0	20.0	30.0	40.0	50.0	60.0	70.0	80.0	90.0	100.0	110.0	120.0
NUMBER	0	0	0	6	46	42	64	73	73	61	64	49	
PERCENT	0.0	0.0	0.0	1.2	9.5	8.7	13.3	15.1	16.1	12.6	13.3	10.1	

INITIATION T-RTNDT(DEG.C)

	-55.6	-41.7	-27.8	-13.9	0.0	13.9	27.8	41.7	55.6	69.4	83.3	97.2	111.1
NUMBER	0	1	54	230	381	157	262	207	7	0	0	0	
PERCENT	0.0	0.1	4.1	17.6	29.1	12.8	20.0	15.8	0.5	0.0	0.0	0.0	

ARREST T-RTNDT(DEG.C)

	-27.8	-13.9	0.0	13.9	27.8	41.7	55.6	69.4	83.3	97.2	111.1	125.0	138.9
NUMBER	0	0	0	6	3	1	7	132	590	87	0	0	
PERCENT	0.0	0.0	0.0	0.7	0.4	0.1	0.8	16.0	71.4	10.5	0.0	0.0	

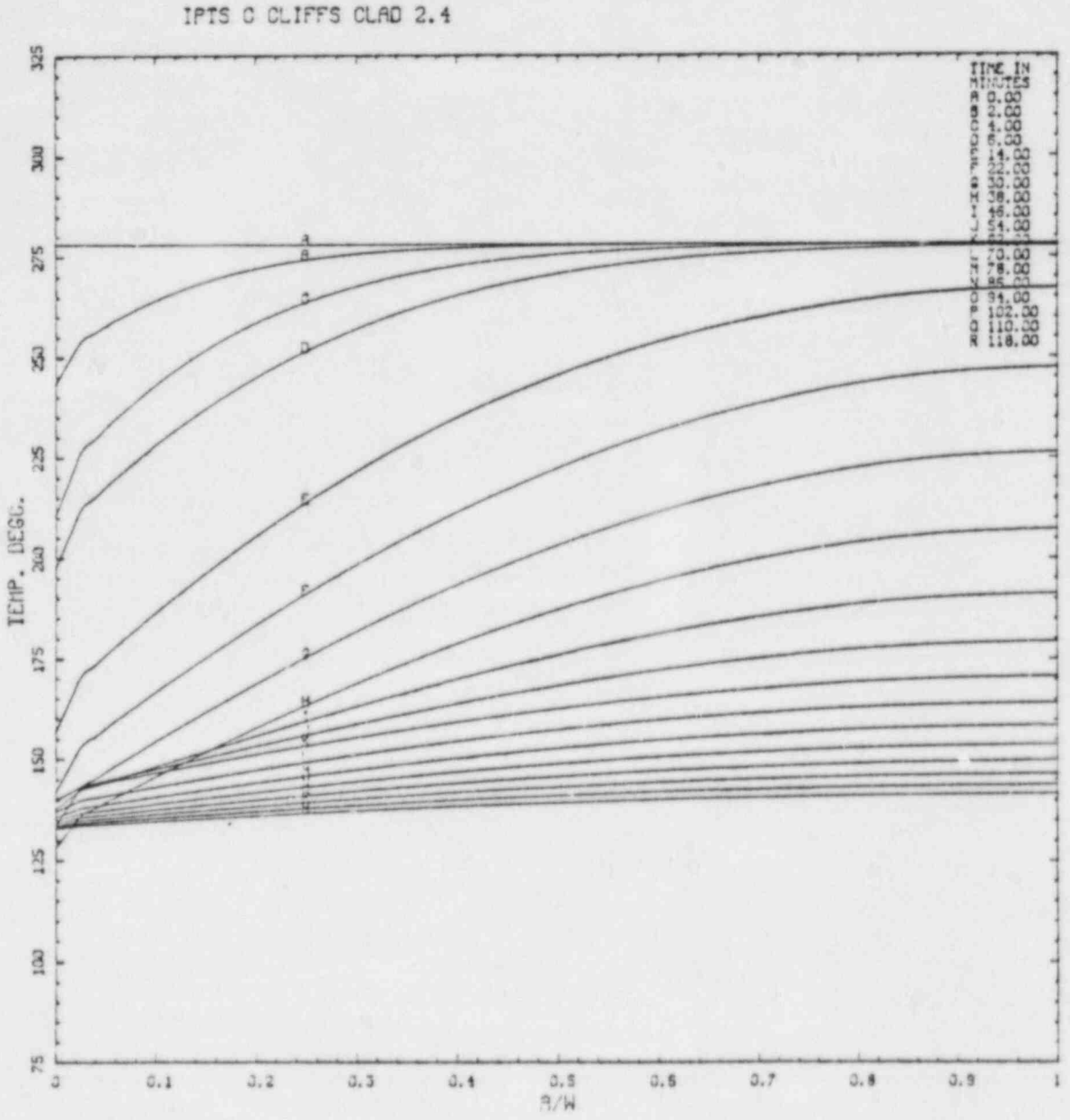
IPTS C CLIFFS CLAD 2.4
TIME IN MINUTES
A 0.00
B 2.00
C 4.00
D 6.00
E 14.00
F 22.00
G 30.00
H 38.00
I 46.00
J 54.00
K 62.00
L 70.00
M 78.00
N 86.00
O 94.00
P 102.00
Q 110.00
R 118.00
TEMP. DEGC.
325
300
275
250
225
200
175
150
125
100
75
0
0.1
0.2
0.3
0.4
0.5
0.6
0.7
0.8
0.9
1
R/W

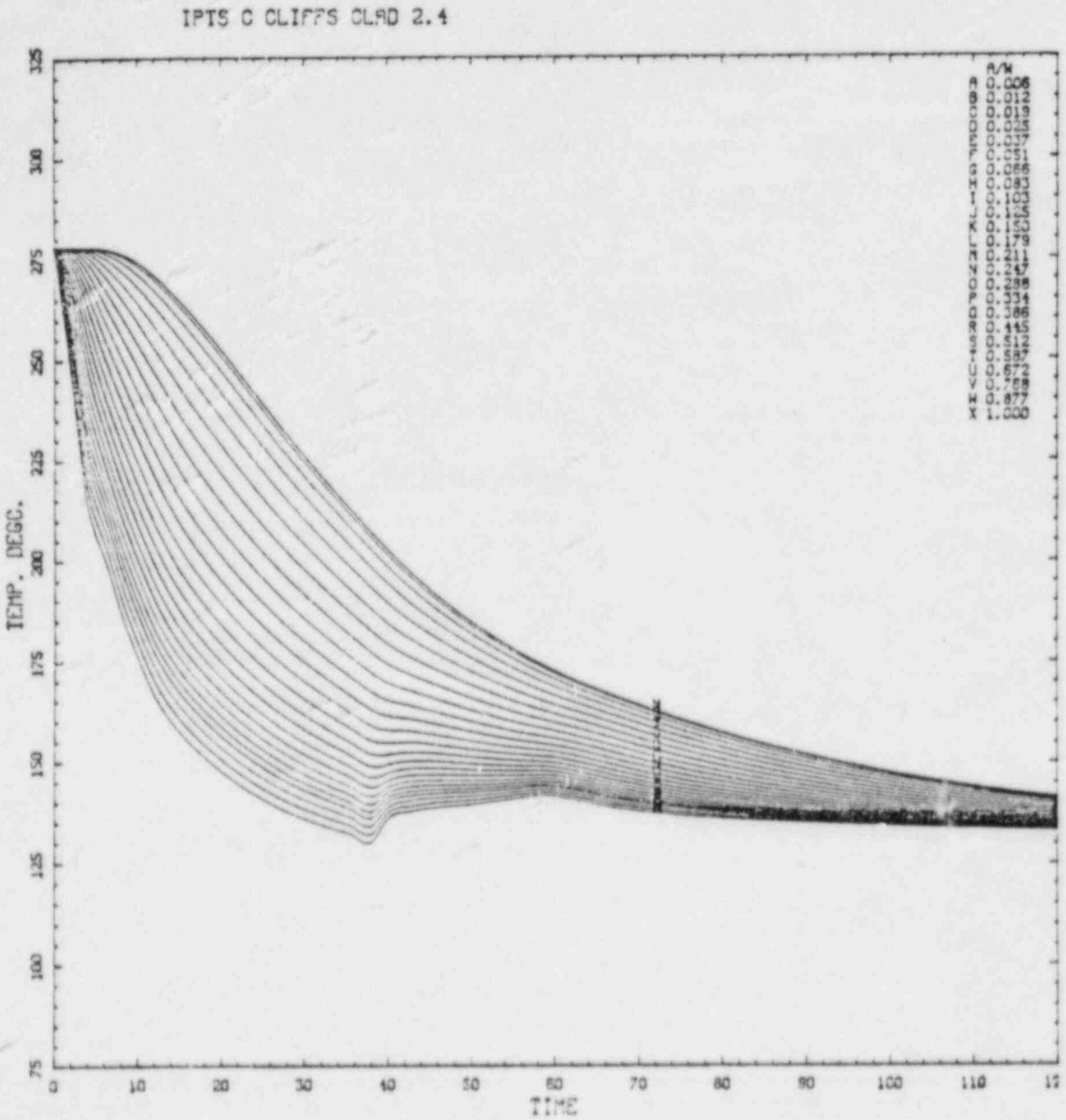
IPTS C CLIFFS CLAD 2.4
TEMP. DEGC.
TIME
75
100
125
150
175
200
225
250
275
300
325
0
10
20
30
40
50
60
70
80
90
100
110
120
R/W
0.006
0.012
0.019
0.877
1.000

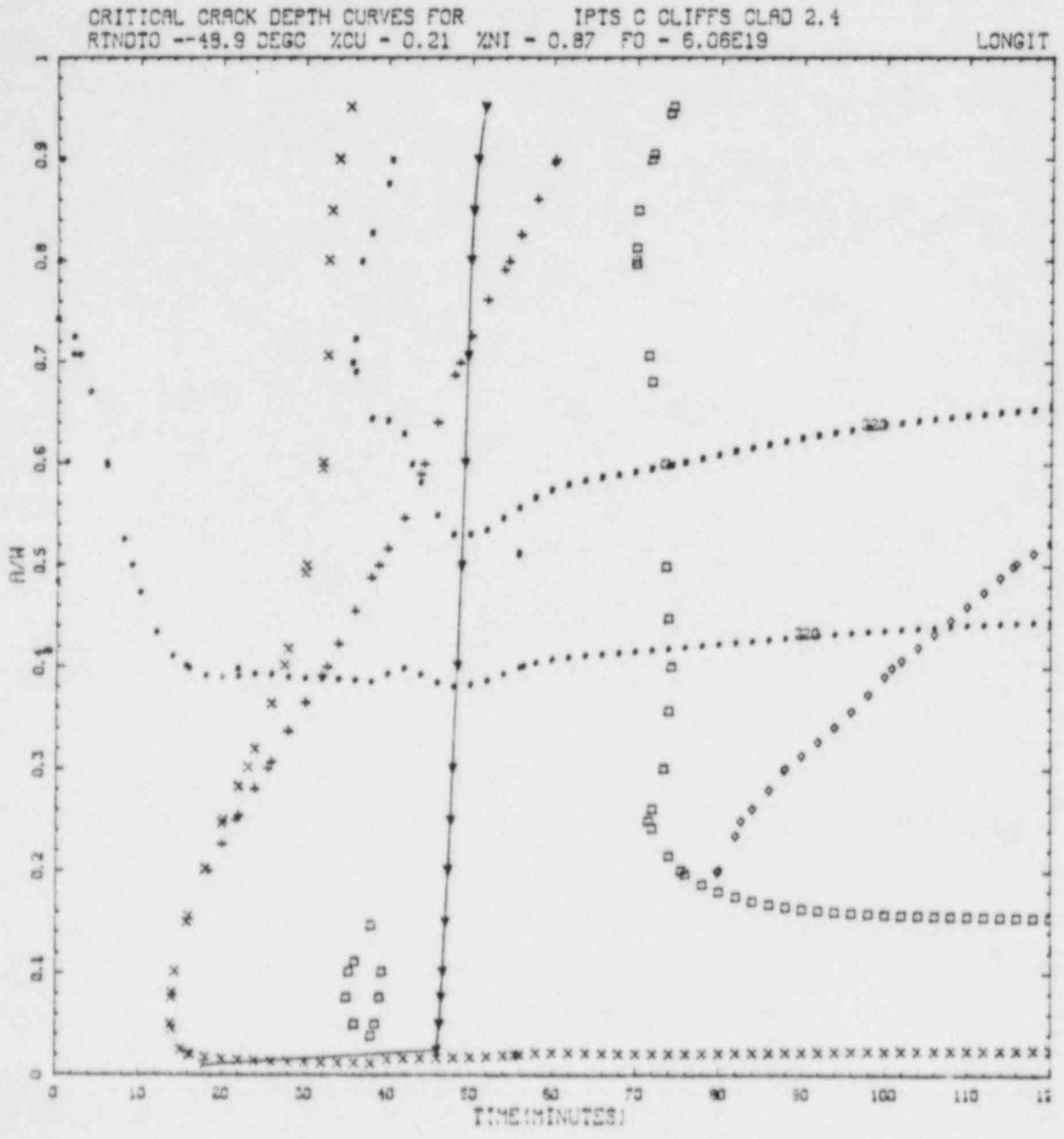
CRITICAL CRACK DEPTH CURVES FOR IPTS C CLIFFS CLAD 2.4
RTNDTO --48.9 DEGC %CU - 0.21 %NI - 0.87 FO - 6.06E19
LONGIT
A/W
TIME(MINUTES)

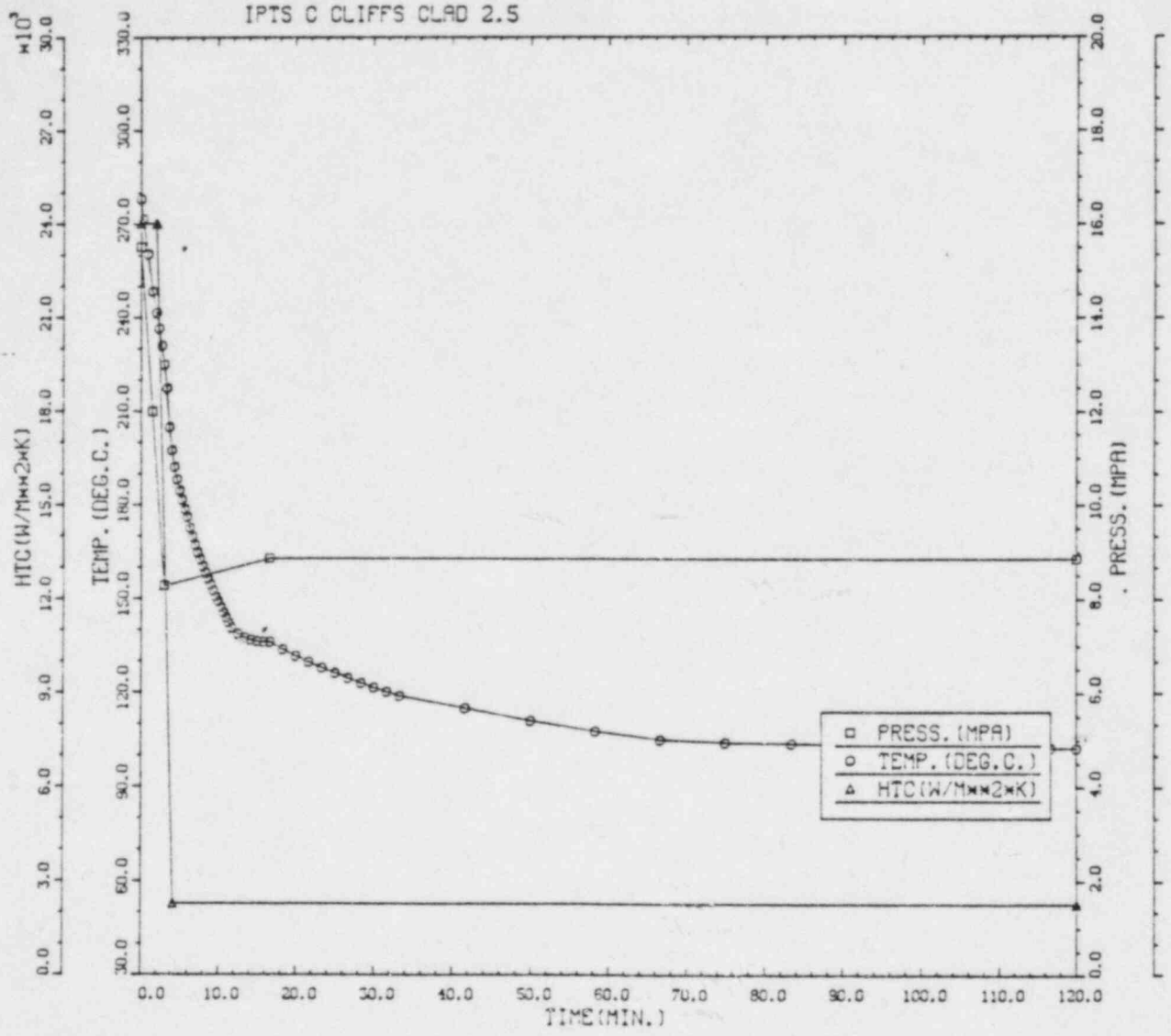
IPTS C CLIFFS CLAD 2.5
HTC(W/M**2*K)
*10**3
TEMP.(DEG.C.)
PRESS.(MPA)
TIME(MIN.)
PRESS.(MPA)
TEMP.(DEG.C.)
HTC(W/M**2*K)

IPTS C CLIFFS CLAD 2.5 1. FLAWS/M**3 FO = 6.060D+19

WELD	P(F/E) UNADJUSTED	95%CI	%ERR	P(INITIA)	N*V	P(F/E) ADJUSTED	%ERR	NTRIALS
1	2.70D-04	3.49D-05	12.92	5.72D-04	0.025	6.75D-06		500000
2	3.52D-06	3.99D-06	113.16	1.17D-05	0.050	1.76D-07		500000
3	3.29D-05	1.22D-05	37.04	1.27D-04	0.021	6.91D-07		500000
					VESSEL	7.52D-06	12.22	

DEPTHS FOR INITIAL INITIATION (MM)

	2.16	6.68	11.62	17.03	22.95	29.42	36.51	44.25	52.72
NUMBER	2	402	126	53	15	5	1	0	0
PERCENT	0.3	66.4	20.8	8.8	2.5	1.0	0.2	0.0	0.0

TIMES OF FAILURE(MINUTES)

	0.0	10.0	20.0	30.0	40.0	50.0	60.0	70.0	80.0	90.0	100.0	110.0	120.0
NUMBER	0	0	0	0	1	9	38	47	51	35	40	40	
PERCENT	0.0	0.0	0.0	0.0	0.4	3.4	14.6	18.0	19.5	13.4	15.3	15.3	

INITIATION T-RTNDT(DEG.C)

	-55.6	-41.7	-27.8	-13.9	0.0	13.9	27.8	41.7	55.6	69.4	83.3	97.2	111.1
NUMBER	0	0	13	228	345	250	146	20	1	0	0	0	
PERCENT	0.0	0.0	1.3	22.7	34.4	24.9	14.6	2.0	0.1	0.0	0.0	0.0	

ARREST T-RTNDT(DEG.C)

	-27.8	-13.9	0.0	13.9	27.8	41.7	55.6	69.4	83.3	97.2	111.1	125.0	138.9
NUMBER	0	7	44	26	3	3	46	372	208	14	0	0	
PERCENT	0.0	0.9	5.9	3.5	0.4	0.4	6.8	50.1	28.0	1.9	0.0	0.0	

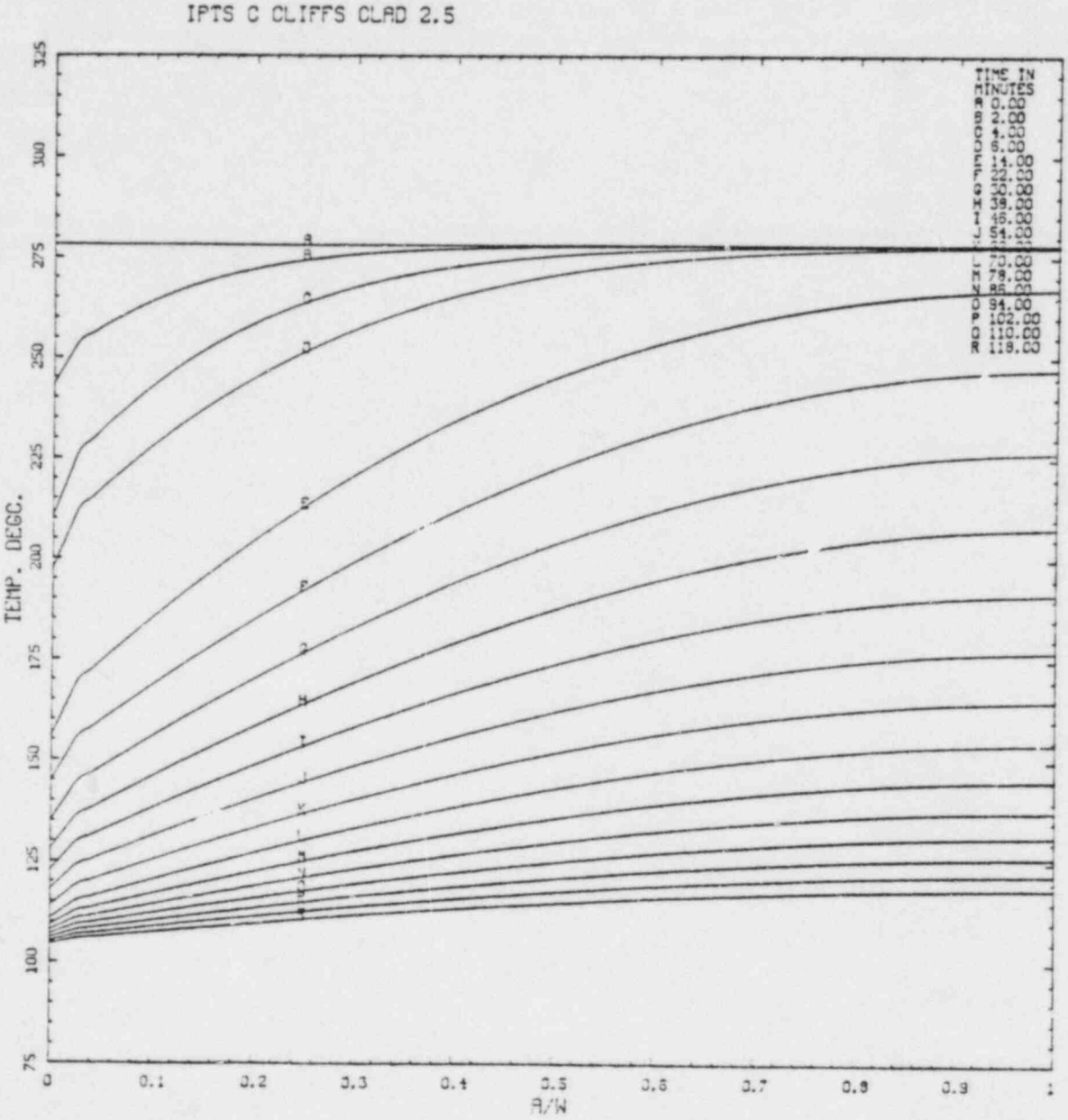
IPTS C CLIFFS CLAD 2.5
TEMP. DEGC.
R/W
TIME IN MINUTES
A 0.00
B 2.00
C 4.00
D 6.00
E 14.00
F 22.00
G 30.00
H 38.00
I 46.00
J 54.00
K 70.00
L 78.00
M 86.00
N 94.00
O 102.00
P 110.00
Q 118.00

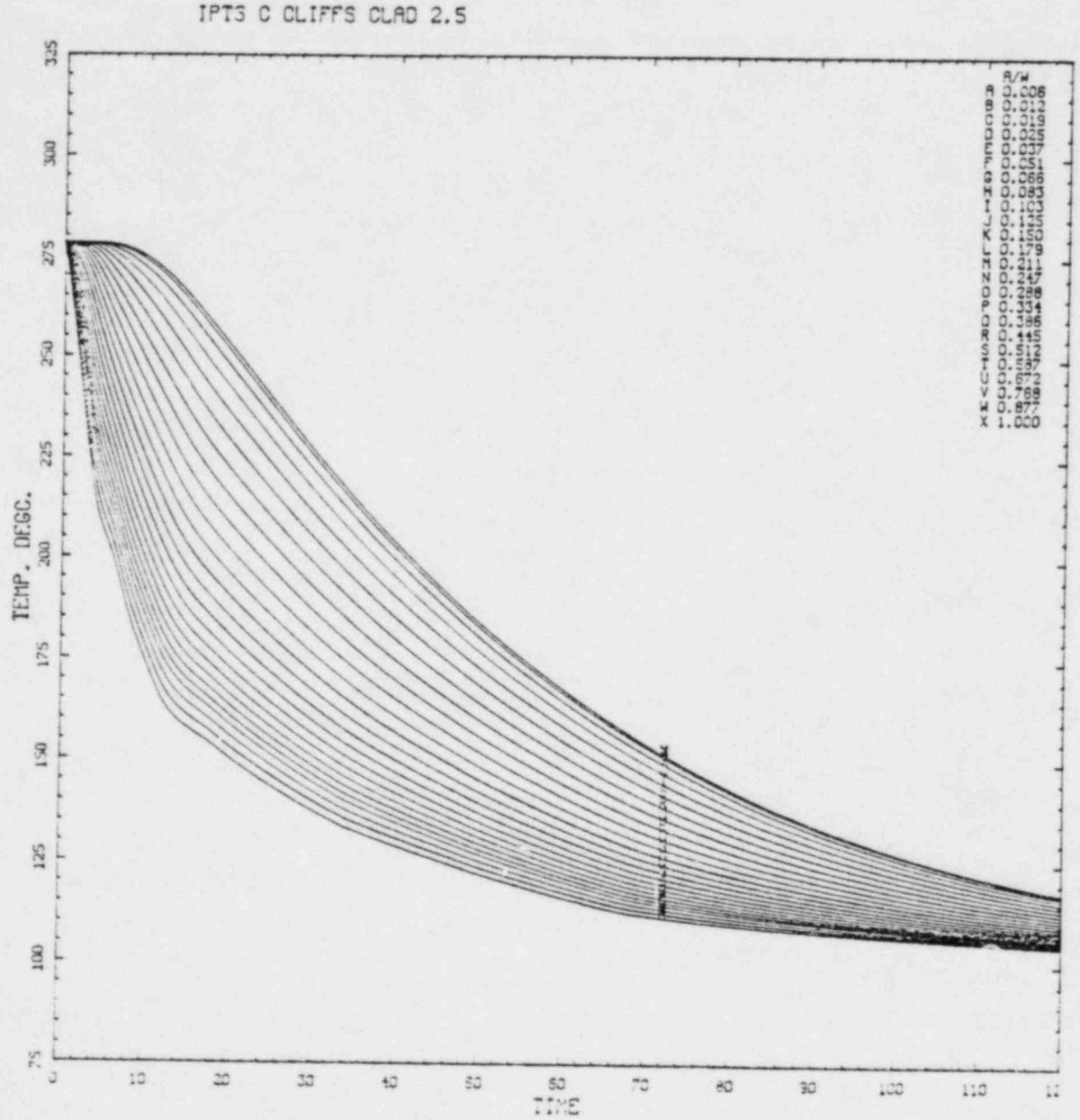
IPTS C CLIFFS CLAD 2.5
TEMP. DEGC.
TIME
R/W
A 0.006
K 1.000

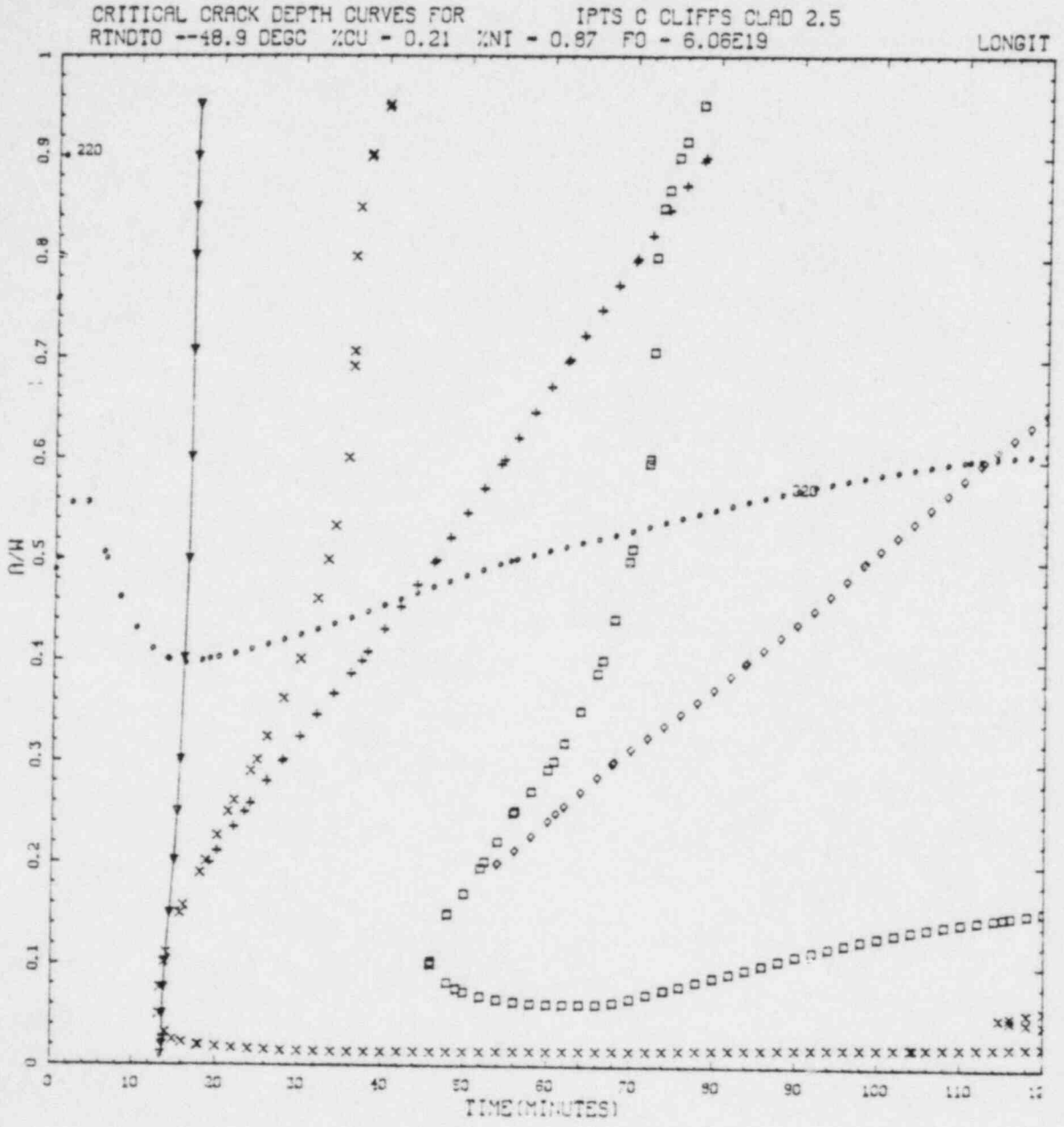
CRITICAL CRACK DEPTH CURVES FOR IPTS C CLIFFS CLAD 2.5
RTNDTO --48.9 DEGC %CU - 0.21 %NI - 0.87 FO - 6.06E19
LONGIT
220
320
A/W
TIME(MINUTES)
0
0.1
0.2
0.3
0.4
0.5
0.6
0.7
0.8
0.9
1
10
20
30
40
50
60
70
80
90
100
110

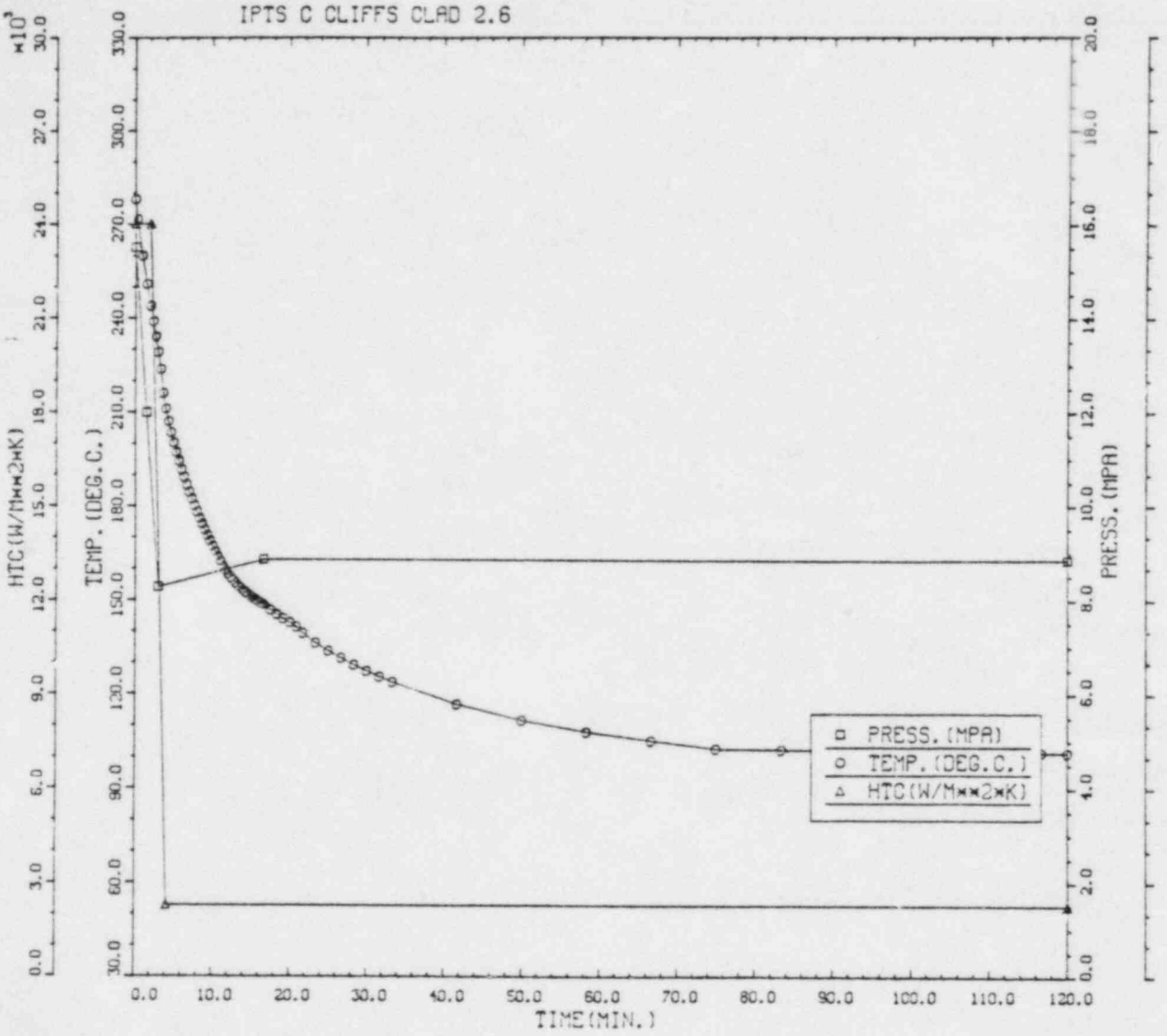
IPTS C CLIFFS CLAD 2.6
HTC(W/M**2*K)
*10³
TEMP. (DEG.C.)
PRESS. (MPA)
TIME(MIN.)
PRESS. (MPA)
TEMP. (DEG.C.)
HTC(W/M**2*K)

IPTS C CLIFFS CLAD 2.6 1. FLAWS/M**3 FO = 6.060D+19

WELD	UNADJUSTED P(F/E)	95%CI	%ERR	P(INITIA)	N*V	ADJUSTED P(F/E)	%ERR	NTRIALS
1	2.88D-04	3.60D-05	12.52	6.32D-04	0.025	7.19D-06		500000
2	4.70D-06	4.60D-06	98.00	1.53D-05	0.050	2.35D-07		500000
3	3.88D-05	1.32D-05	34.12	1.35D-04	0.021	8.14D-07		500000
					VESSEL	8.24D-06	11.77	

DEPTHS FOR INITIAL INITIATION (MM)

	2.16	6.68	11.52	17.03	22.95	29.42	36.51	44.25	52.72
NUMBER	1	450	129	61	15	7	1	1	0
PERCENT	0.2	67.6	19.4	9.2	2.4	1.1	0.2	0.2	0.0

TIMES OF FAILURE(MINUTES)

	0.0	10.0	20.0	30.0	40.0	50.0	60.0	70.0	80.0	90.0	100.0	110.0	120.0
NUMBER	0	0	0	0	0	8	20	56	66	50	47	35	
PERCENT	0.0	0.0	0.0	0.0	0.0	2.8	7.1	19.9	23.4	17.7	16.7	12.4	

INITIATION T-RTNDT(DEG.C)

	-55.6	-41.7	-27.8	-13.9	0.0	13.9	27.8	41.7	55.6	69.4	83.3	97.2	111.1
NUMBER	0	2	41	274	350	229	121	21	0	0	0	0	
PERCENT	0.0	0.2	3.9	26.4	33.7	22.1	11.7	2.0	0.0	0.0	0.0	0.0	

ARREST T-RTNDT(DEG.C)

	-27.8	-13.9	0.0	13.9	27.8	41.7	55.6	69.4	83.3	97.2	111.1	125.0	138.9
NUMBER	0	7	57	34	3	0	52	425	168	0	0	0	
PERCENT	0.0	0.9	7.5	4.5	0.4	0.0	8.2	56.2	22.2	0.0	0.0	0.0	

IPTS C CLIFFS CLAD 2.6

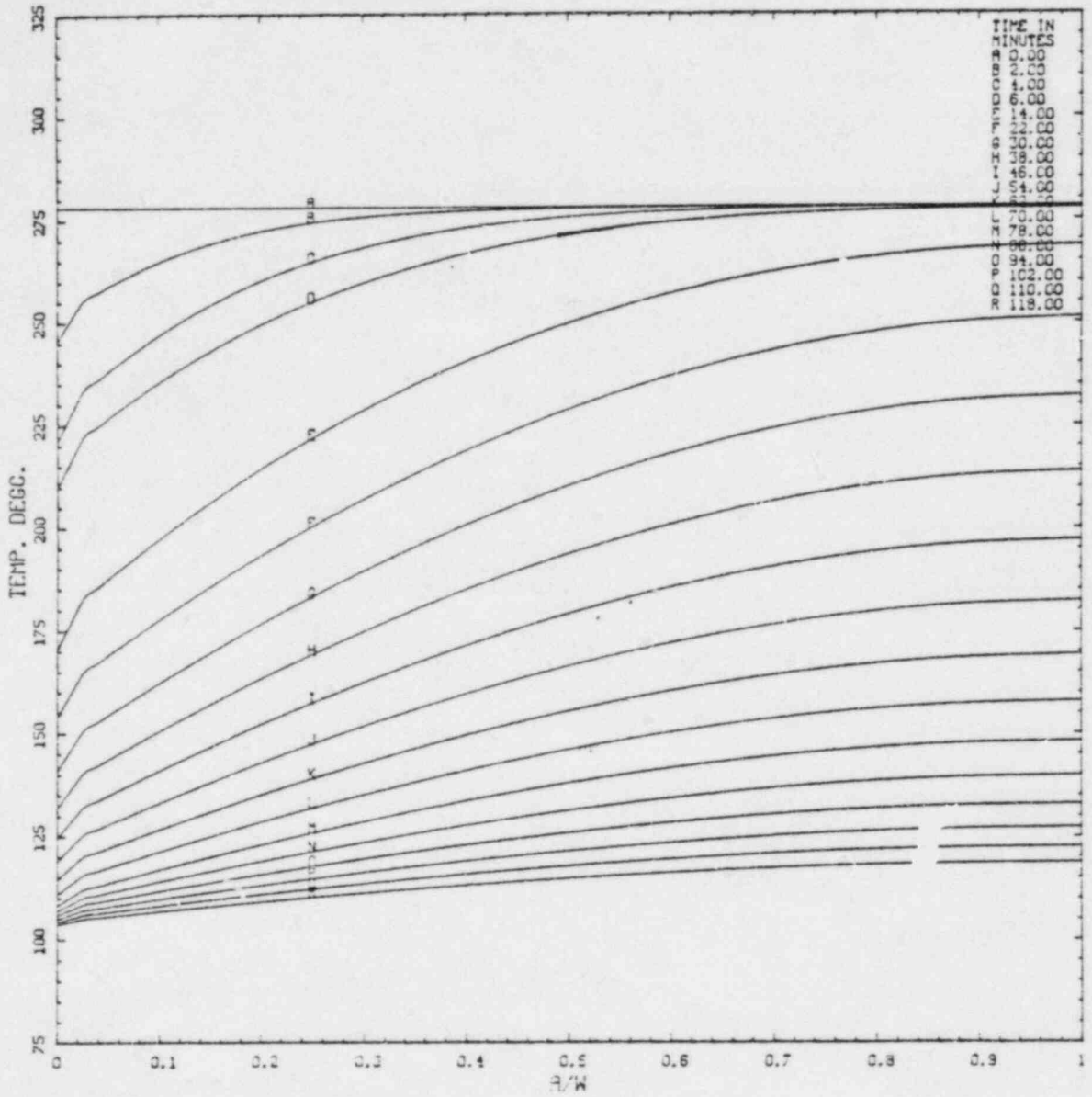

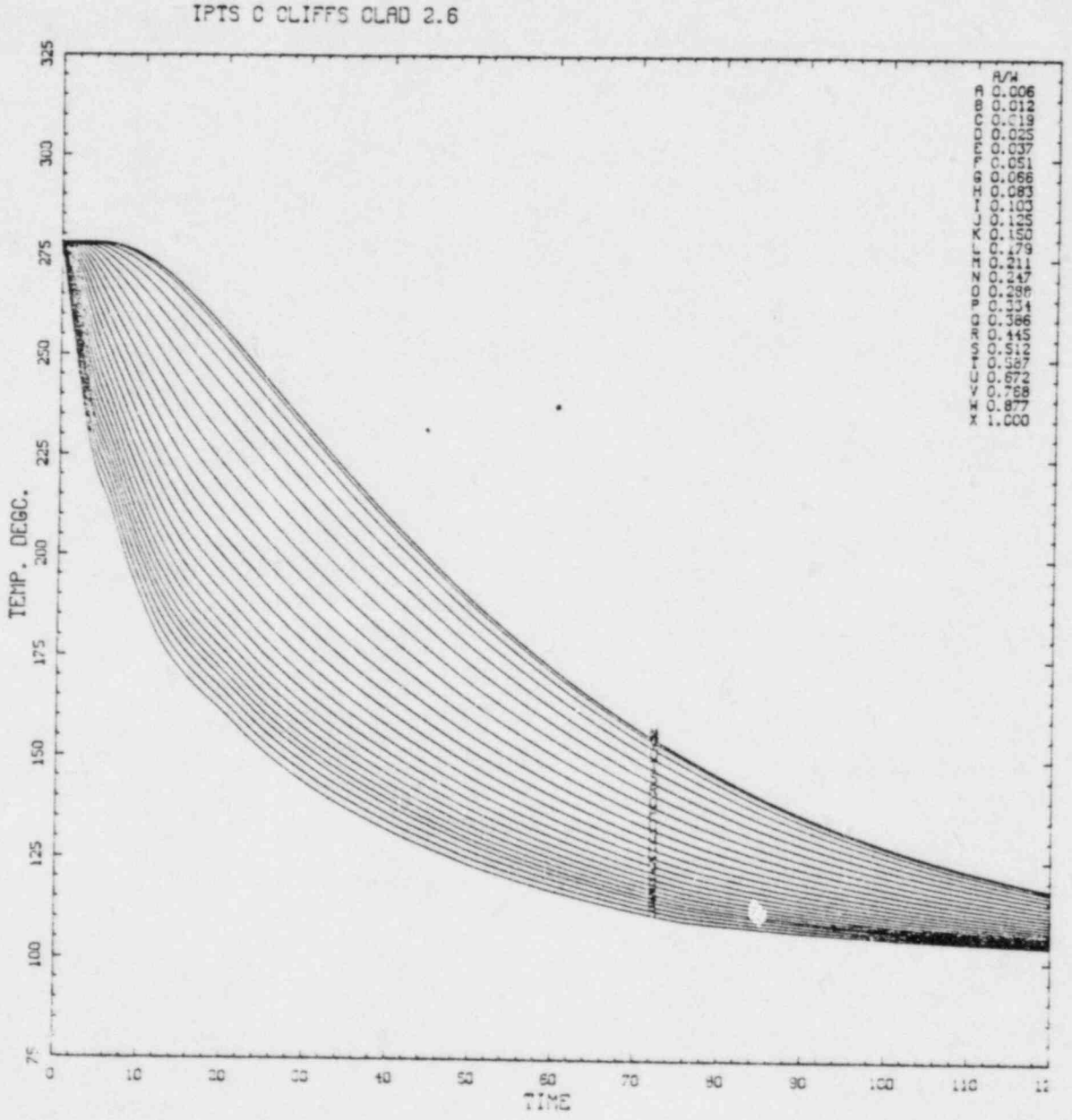
IPTS C CLIFFS CLAD 2.6
TEMP. DEGC.
TIME
R/W
A 0.006
B 0.012
C 0.019
D 0.025
E 0.037
F 0.051
G 0.066
H 0.083
I 0.103
J 0.125
K 0.150
L 0.179
M 0.211
N 0.247
O 0.286
P 0.334
Q 0.386
R 0.445
S 0.512
T 0.587
U 0.672
V 0.768
W 0.877
X 1.000

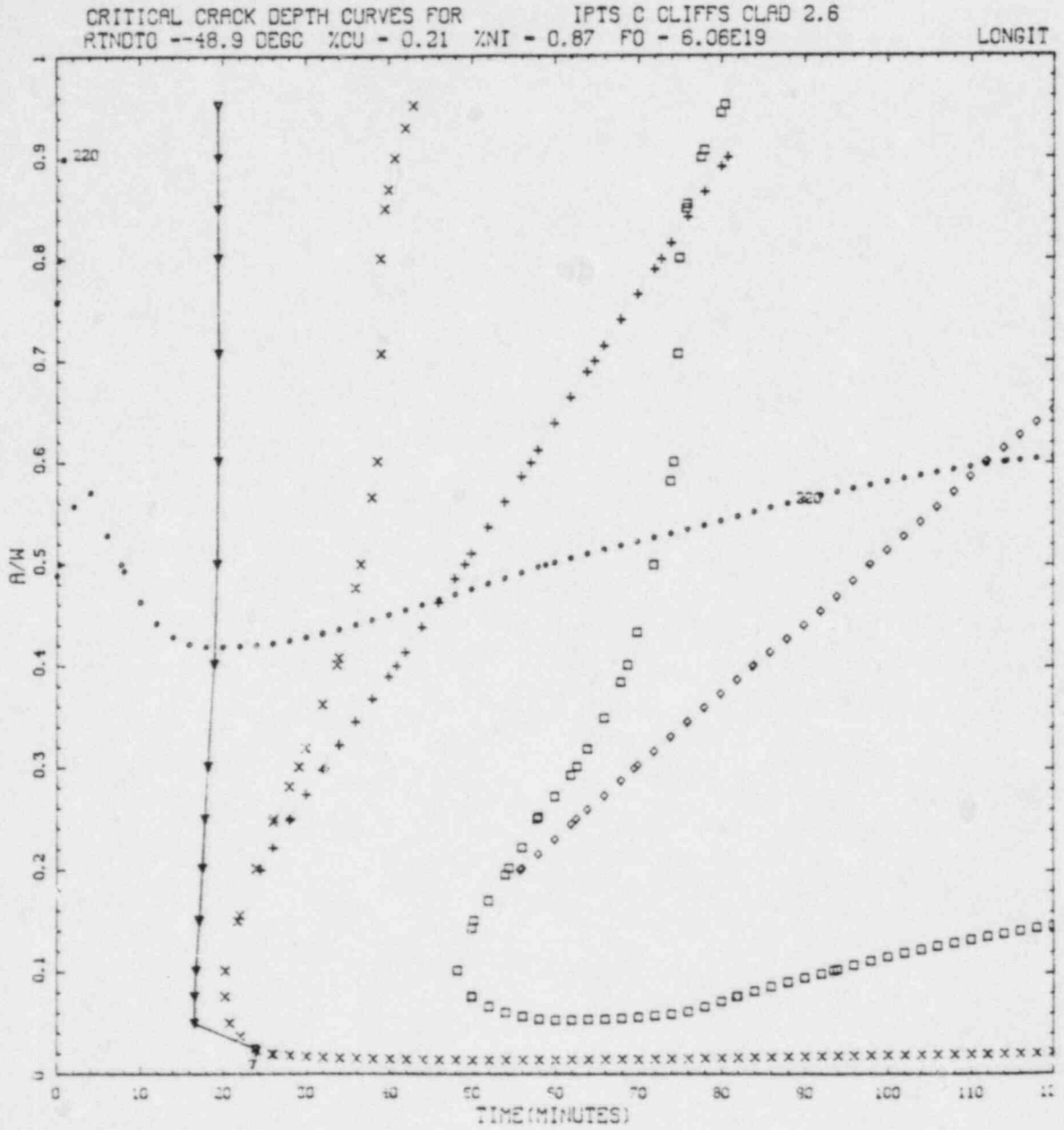
CRITICAL CRACK DEPTH CURVES FOR IPTS C CLIFFS CLAD 2.6
RTNDT0 --48.9 DEGC %CU - 0.21 %NI - 0.87 FO - 6.06E19
LONGIT
220
220
A/W
TIME(MINUTES)

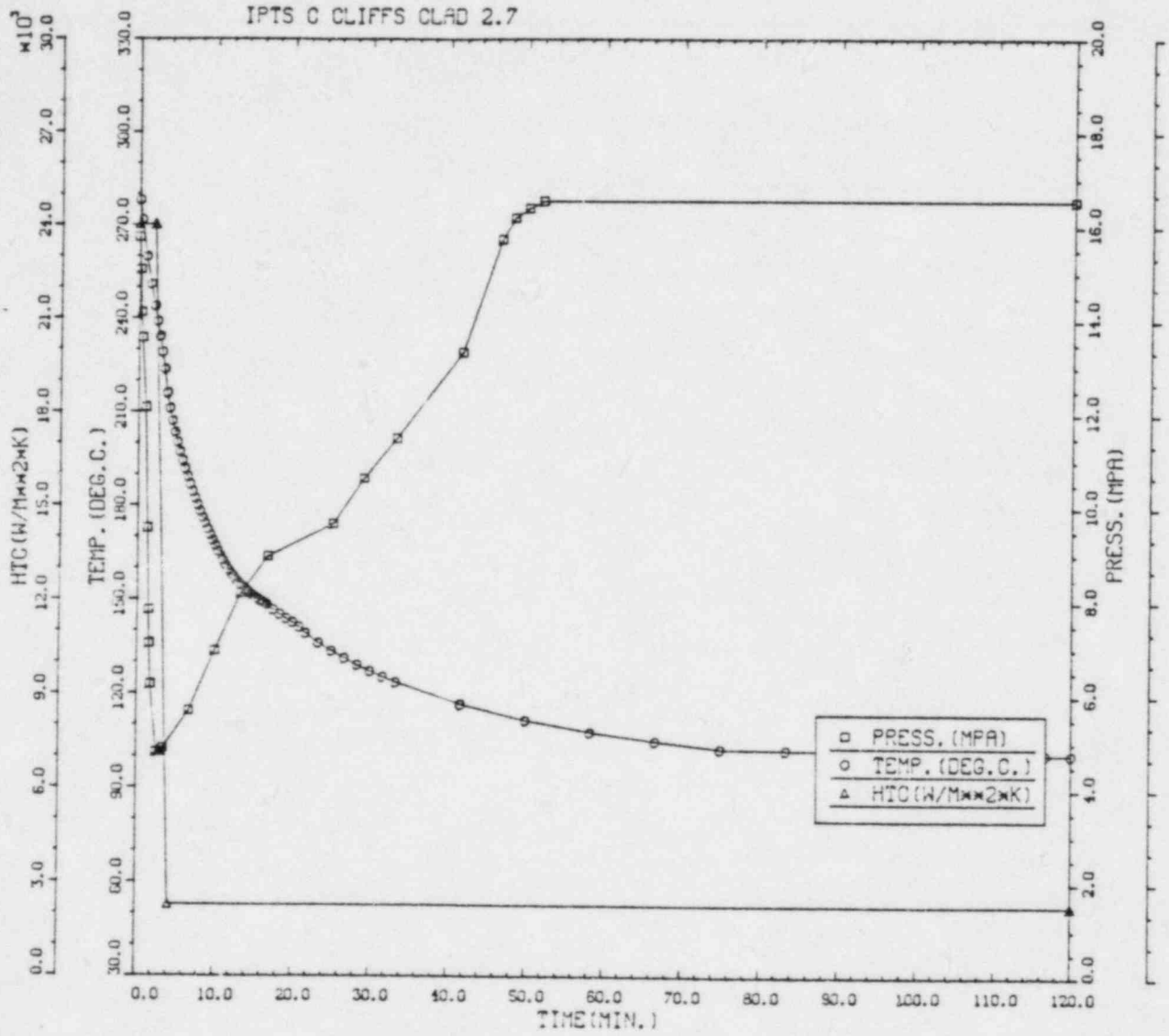
IPTS C CLIFFS CLAD 2.7
HTC(W/M**2*K)
*10**3
TEMP.(DEG.C.)
PRESS.(MPA)
TIME(MIN.)
PRESS.(MPA)
TEMP.(DEG.C.)
HTC(W/M**2*K)

IPTS C CLIFFS CLAD 2.7 1. FLAWS/M**3 FO = 5.060D+19

WELD	UNADJUSTED P(F/E)	95%CI	%ERR	P(INITIA)	N*V	ADJUSTED P(F/E)	%ERR	NTRIALS
1	5.33D-03	4.88D-04	9.16	5.42D-03	0.025	1.33D-04		50000
2	2.21D-04	3.16D-05	14.29	2.28D-04	0.050	1.10D-05		500000
3	1.53D-03	1.52D-04	9.89	1.55D-03	0.021	3.22D-05		150000
					VESSEL	1.77D-04	7.20	

DEPTHS FOR INITIAL INITIATION (MM)

	2.5	6.68	11.52	17.03	22.95	29.42	36.51	44.25	52.72
NUMBER	1	659	229	105	30	13	4	1	0
PERCENT	1.0	62.6	21.8	10.0	2.9	1.2	0.4	0.1	0.0

TIMES OF FAILURE(MINUTES)

	0.0	10.0	20.0	30.0	40.0	50.0	60.0	70.0	80.0	90.0	100.0	110.0	120.0
NUMBER	0	0	0	2	244	330	222	157	37	25	11	6	
PERCENT	0.0	0.0	0.0	0.2	23.6	31.9	21.5	15.2	3.6	2.4	1.1	0.6	

INITIATION T-RTNDT(DEG.C)

	-55.6	-41.7	-27.8	-13.9	0.0	13.9	27.8	41.7	55.6	69.4	83.3	97.2	111.1
NUMBER	1	5	59	308	501	171	116	87	9	0	0	0	
PERCENT	0.1	0.4	4.7	24.5	39.9	13.6	9.2	6.9	0.7	0.0	0.0	0.0	

ARREST T-RTNDT(DEG.C)

	-27.8	-13.9	0.0	13.9	27.8	41.7	55.6	69.4	83.3	97.2	111.1	125.0	138.9
NUMBER	0	0	3	5	1	0	0	23	181	9	0	0	
PERCENT	0.0	0.0	1.3	2.7	0.4	0.0	0.0	10.3	81.2	4.0	0.0	0.0	

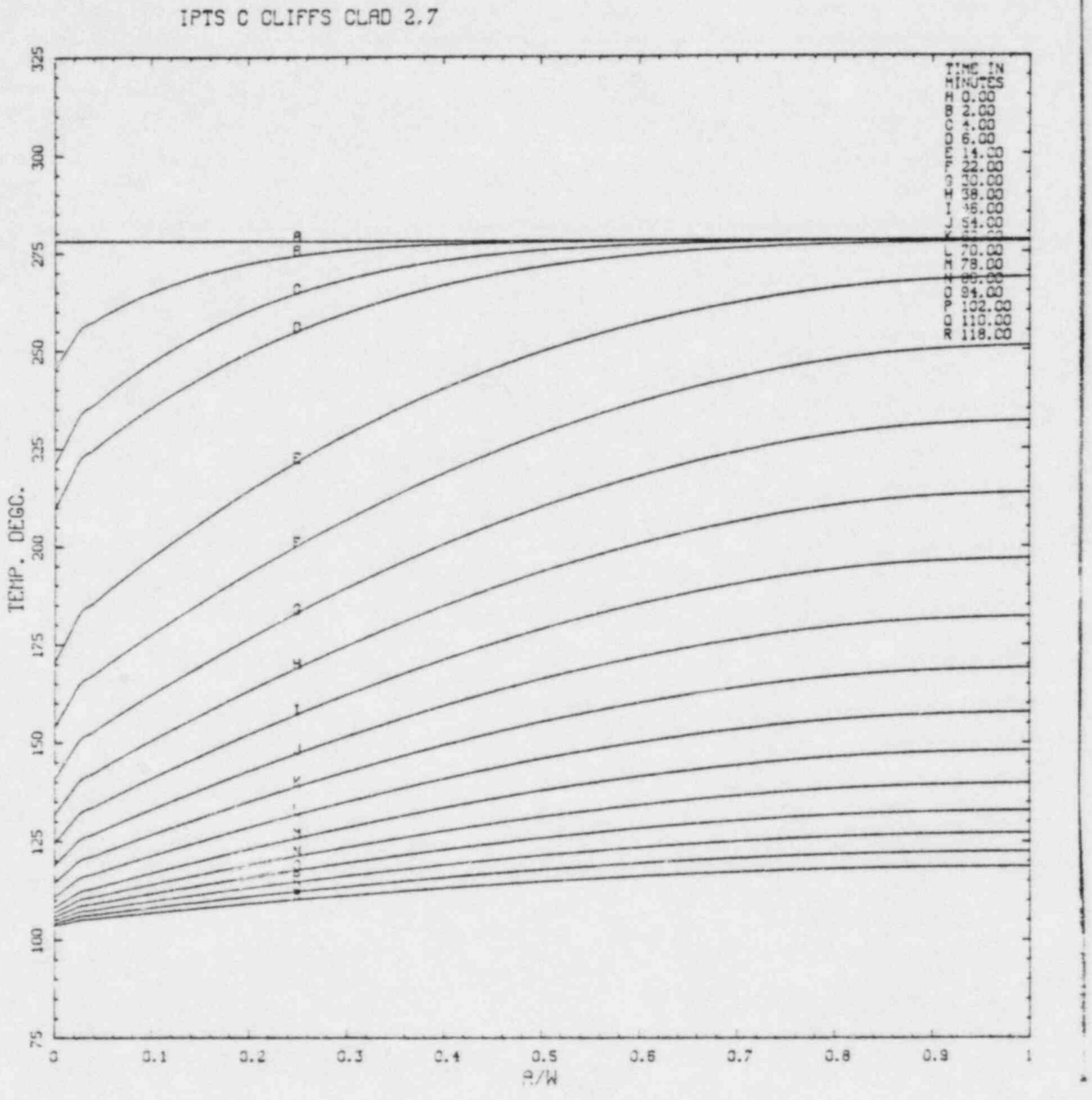
IPTS C CLIFFS CLAD 2.7
TEMP. DEGC.
R/W
TIME IN MINUTES
0.000
2.400
4.800
6.800
14.
22.
30.
38.
46.
54.
62.
70.
78.
86.
94.
102.
110.
118.
A
B
C
D
E
F
G
H
I
J
K
L
M
N
O
P
Q
R

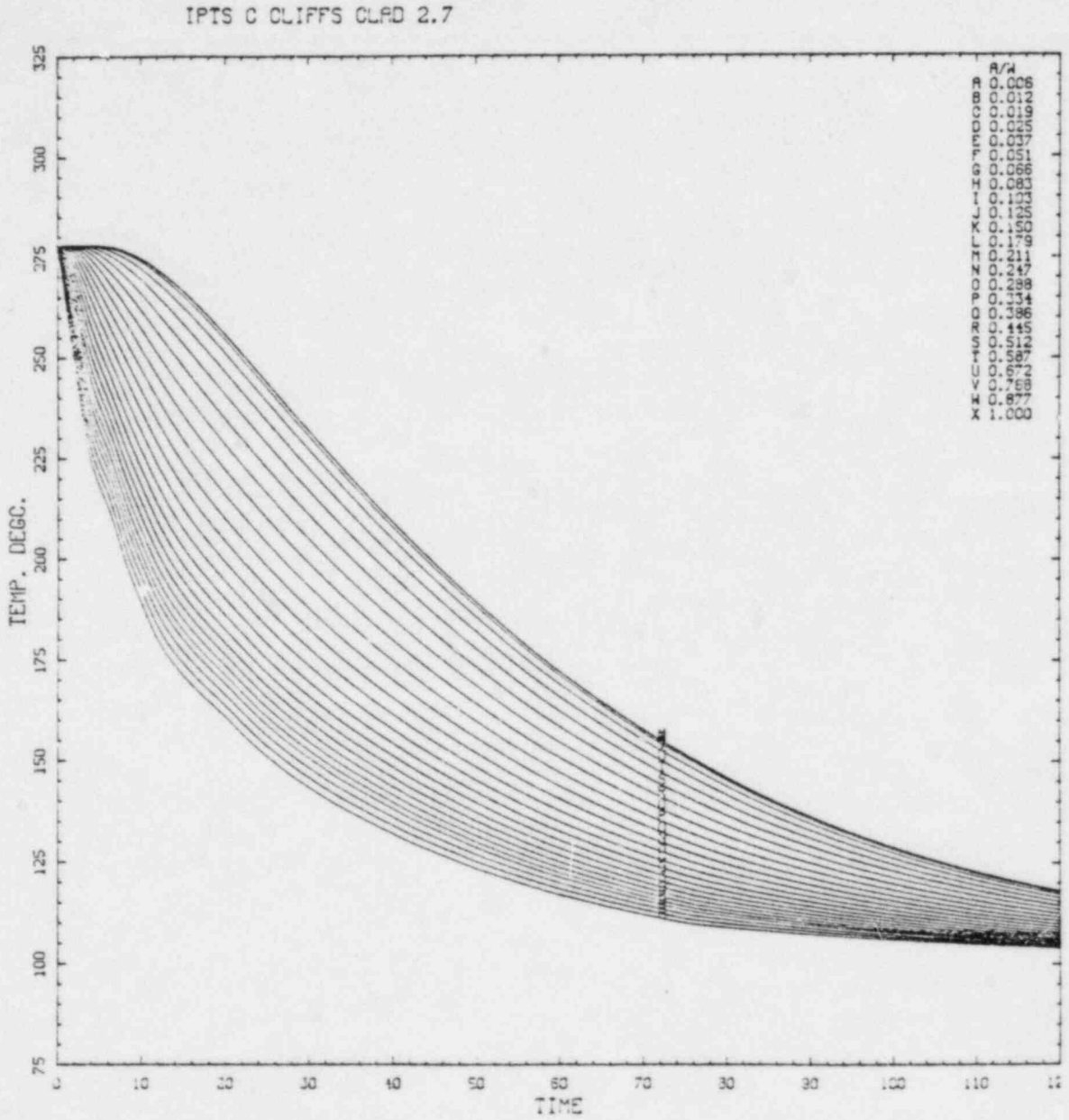
IPTS C CLIFFS CLAD 2.7
TEMP. DEGC.
TIME
A/d
A 0.006
B 0.012
C 0.019
D 0.025
E 0.037
F 0.051
G 0.066
H 0.083
I 0.101
J 0.120
K 0.140
L 0.160
M 0.179
N 0.211
O 0.247
P 0.288
Q 0.334
R 0.386
S 0.445
T 0.512
U 0.587
V 0.672
W 0.768
X 1.000

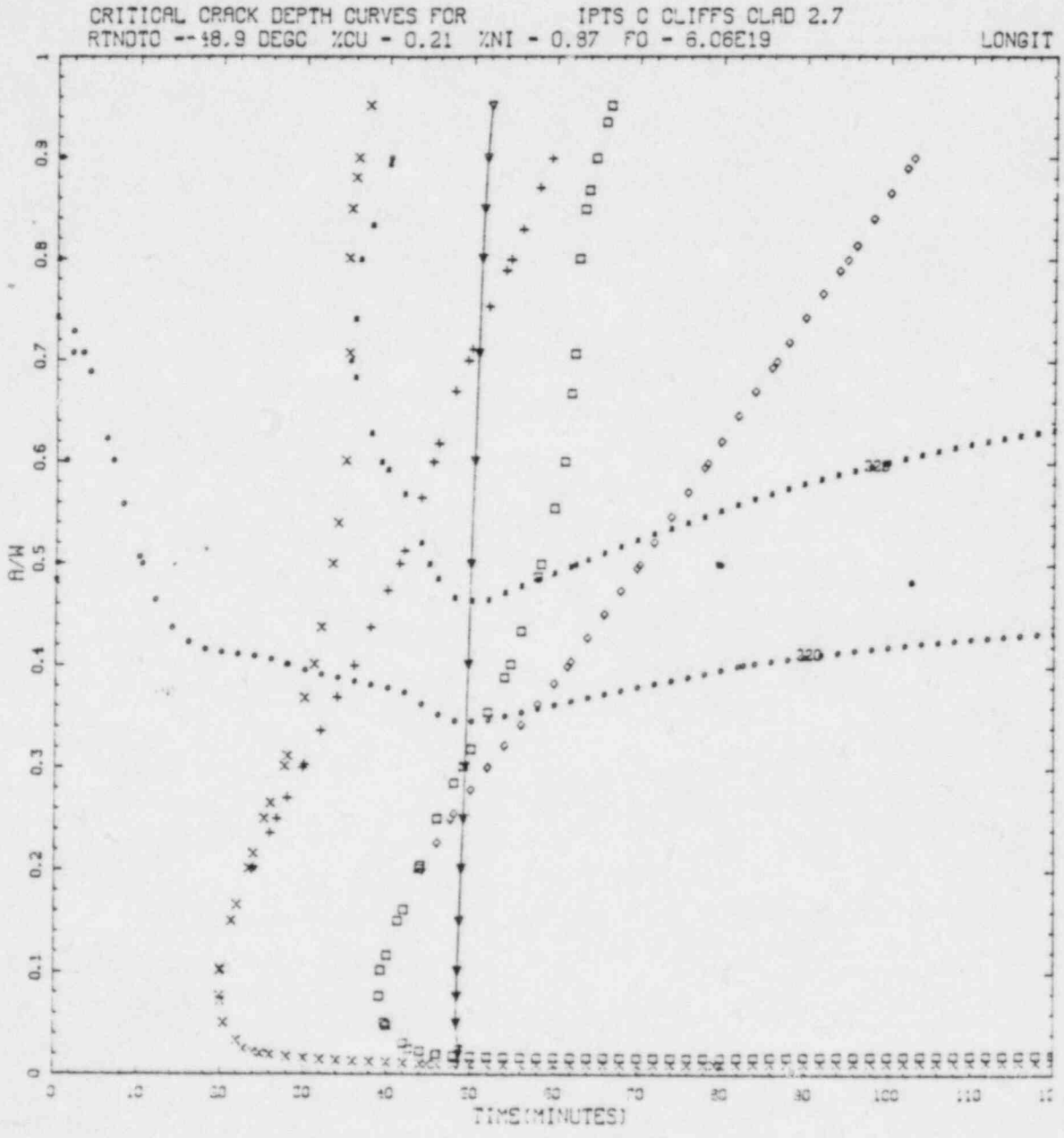
CRITICAL CRACK DEPTH CURVES FOR IPTS C CLIFFS CLAD 2.7
RTNDTO --48.9 DEGC %CU - 0.21 %NI - 0.87 FO - 6.06E19
LONGIT
A/W
TIME(MINUTES)
320
320

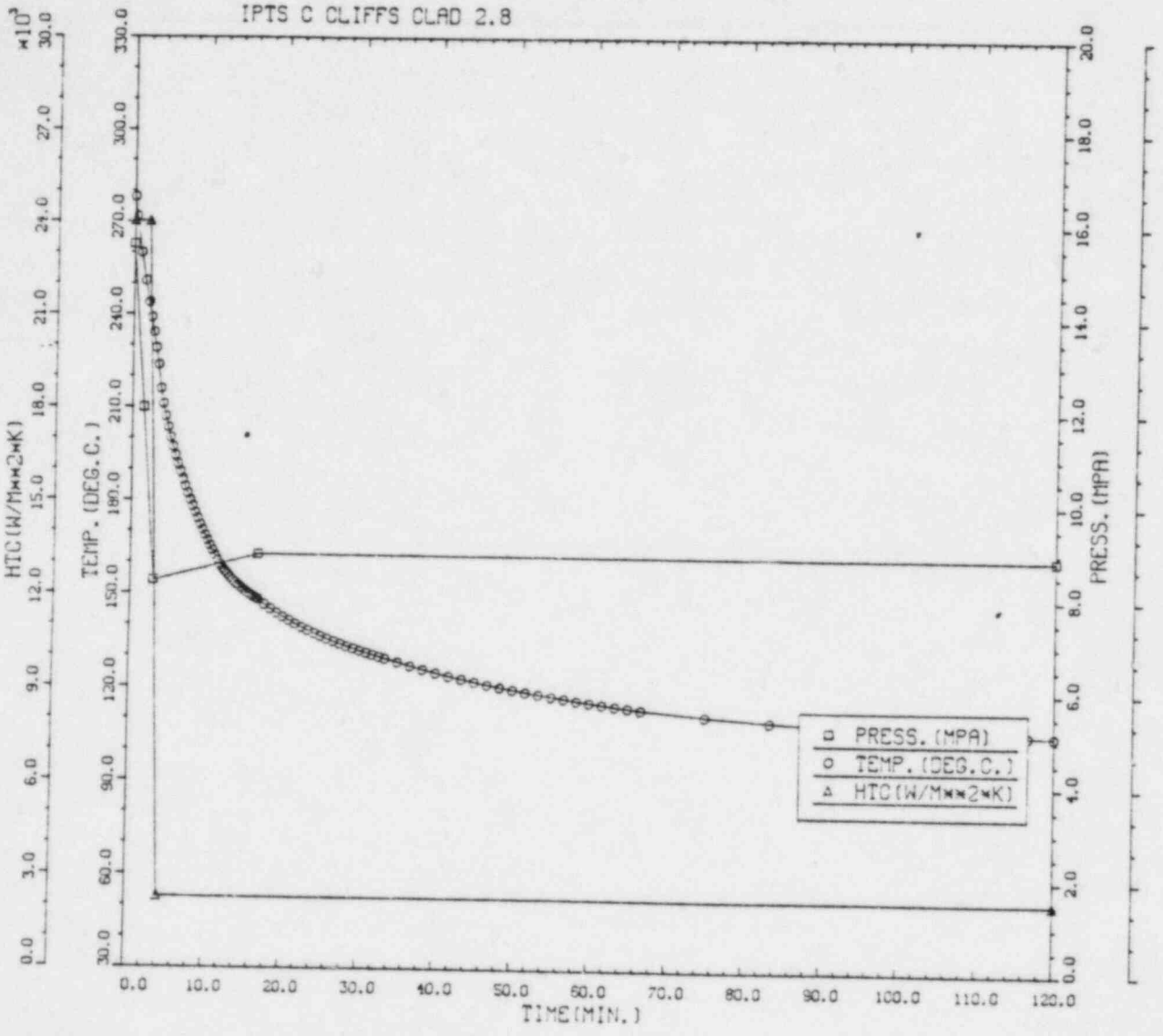
IPTS C CLIFFS CLAD 2.8
HTC(W/M**2*K)
x10³
TEMP.(DEG.C.)
PRESS.(MPA)
TIME(MIN.)
PRESS.(MPA)
TEMP.(DEG.C.)
HTC(W/M**2*K)

IPTS C CLIFFS CLAD 2.8 1. FLAWS/M**3 FO = 6.060D+19

WELD	UNADJUSTED P(F/E)	95%CI	%ERR	P(INITIA)	N*V	ADJUSTED P(F/E)	%ERR	NTRIALS
1	8.11D-05	1.91D-05	23.59	1.71D-04	0.025	2.03D-06		500000
2	0.00D+00	0.00D+00	0.00	1.17D-06	0.050	0.00D+00		500000
3	1.17D-05	7.28D-06	61.98	2.94D-05	0.021	2.47D-07		500000
					VESSEL	2.27D-06	22.08	

DEPTHS FOR INITIAL INITIATION (MM)

	2.16	6.58	11.62	17.03	22.95	29.42	36.51	44.25	52.72
NUMBER	0	119	34	13	5	1	0	0	0
PERCENT	0.0	69.2	19.8	7.6	2.9	0.6	0.0	0.0	0.0

TIMES OF FAILURE(MINUTES)

	0.0	10.0	20.0	30.0	40.0	50.0	60.0	70.0	80.0	90.0	100.0	110.0	120.0
NUMBER	0	0	0	0	0	1	7	12	18	18	15	8	
PERCENT	0.0	0.0	0.0	0.0	0.0	1.3	8.9	15.2	22.8	22.8	19.0	10.1	

INITIATION T-RTNDT(DEG.C)

	-55.6	-41.7	-27.8	-13.9	0.0	13.9	27.8	41.7	55.6	69.4	83.3	97.2	111.1
NUMBER	0	0	11	67	93	72	31	3	0	0	0	0	
PERCENT	0.0	0.0	4.0	24.2	33.6	26.0	11.2	1.1	0.0	0.0	0.0	0.0	

ARREST T-RTNDT(DEG.C)

	-27.8	-13.9	0.0	13.9	27.8	41.7	55.6	69.4	83.3	97.2	111.1	125.0	138.9
NUMBER	0	2	34	10	0	0	17	108	40	0	0	0	
PERCENT	0.0	1.0	12.1	3.5	0.0	0.0	8.6	54.5	20.2	0.0	0.0	0.0	

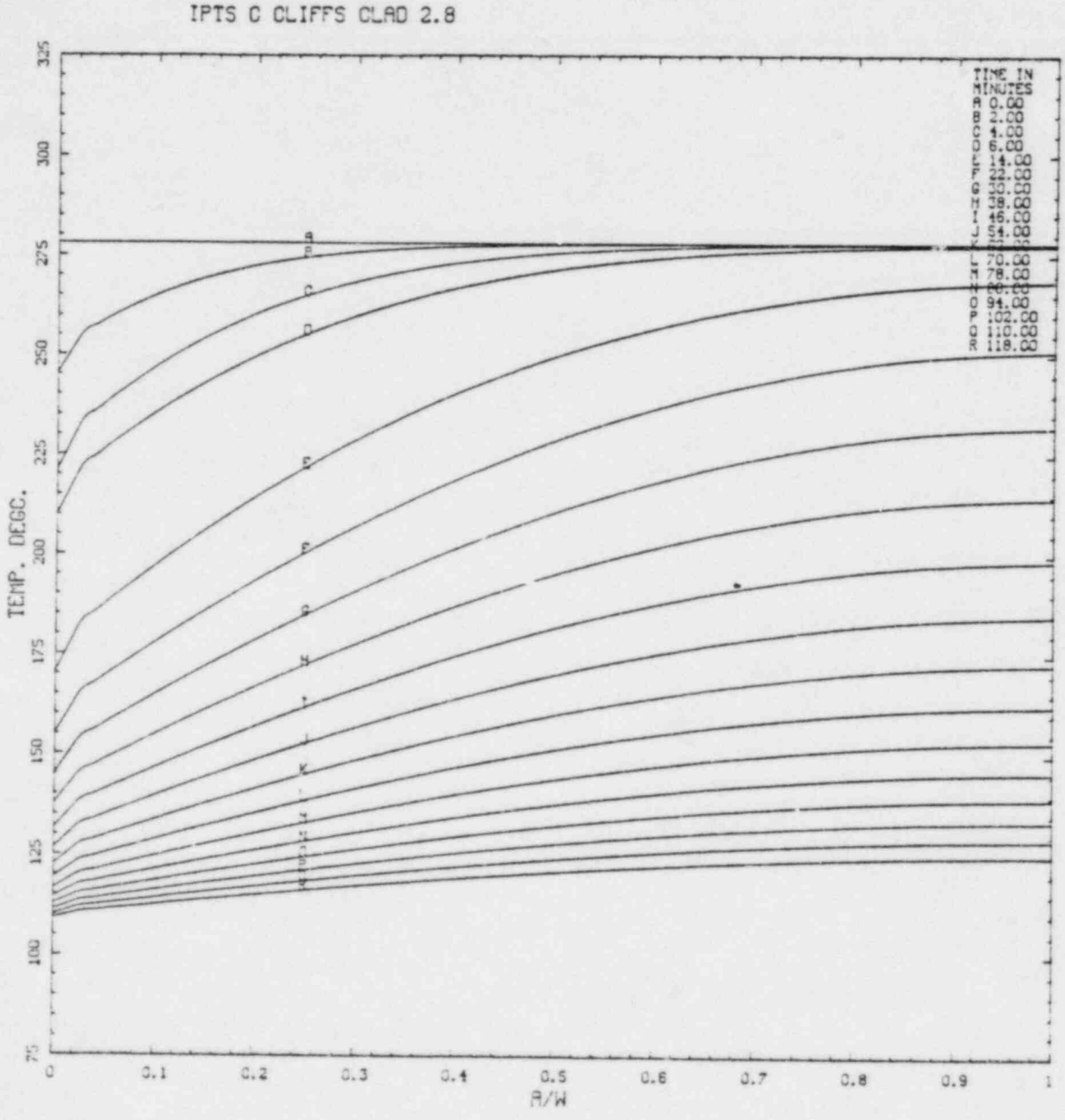
IPTS C CLIFFS CLAD 2.8
TEMP. DEGC.
R/W
TIME IN MINUTES
A 0.00
B 2.00
C 4.00
D 6.00
E 14.00
F 22.00
G 30.00
H 38.00
I 46.00
J 54.00
K 62.00
L 70.00
M 78.00
N 86.00
O 94.00
P 102.00
Q 110.00
R 118.00

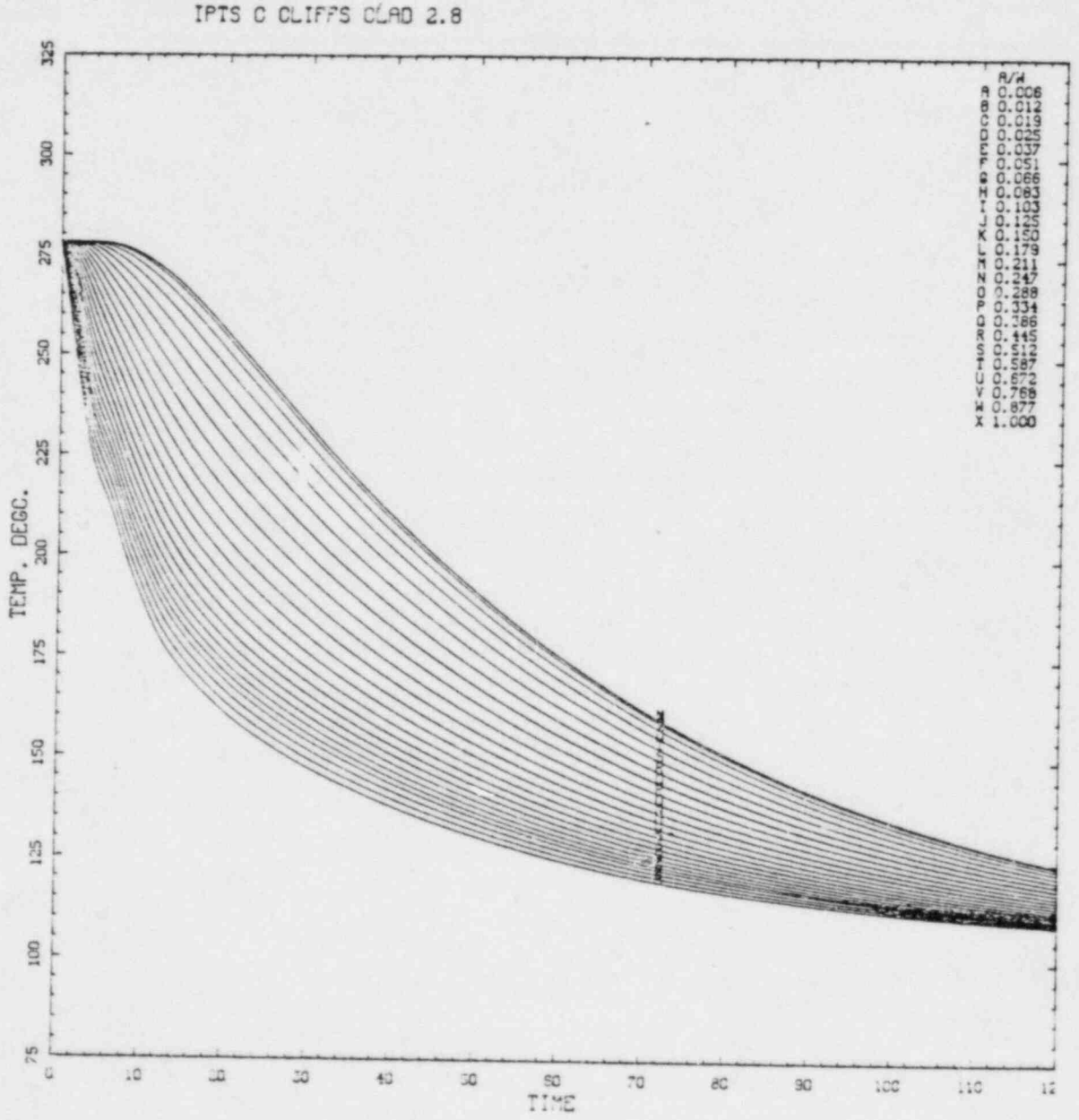
IPTS C CLIFFS CLAD 2.8
TEMP. DEGC.
TIME
R/d
A 0.006
B 0.012
C 0.019
D 0.025
E 0.037
F 0.051
G 0.066
H 0.083
I 0.103
J 0.125
K 0.150
L 0.179
M 0.211
N 0.247
O 0.288
P 0.334
Q 0.386
R 0.445
S 0.512
T 0.587
U 0.672
V 0.768
W 0.877
X 1.000

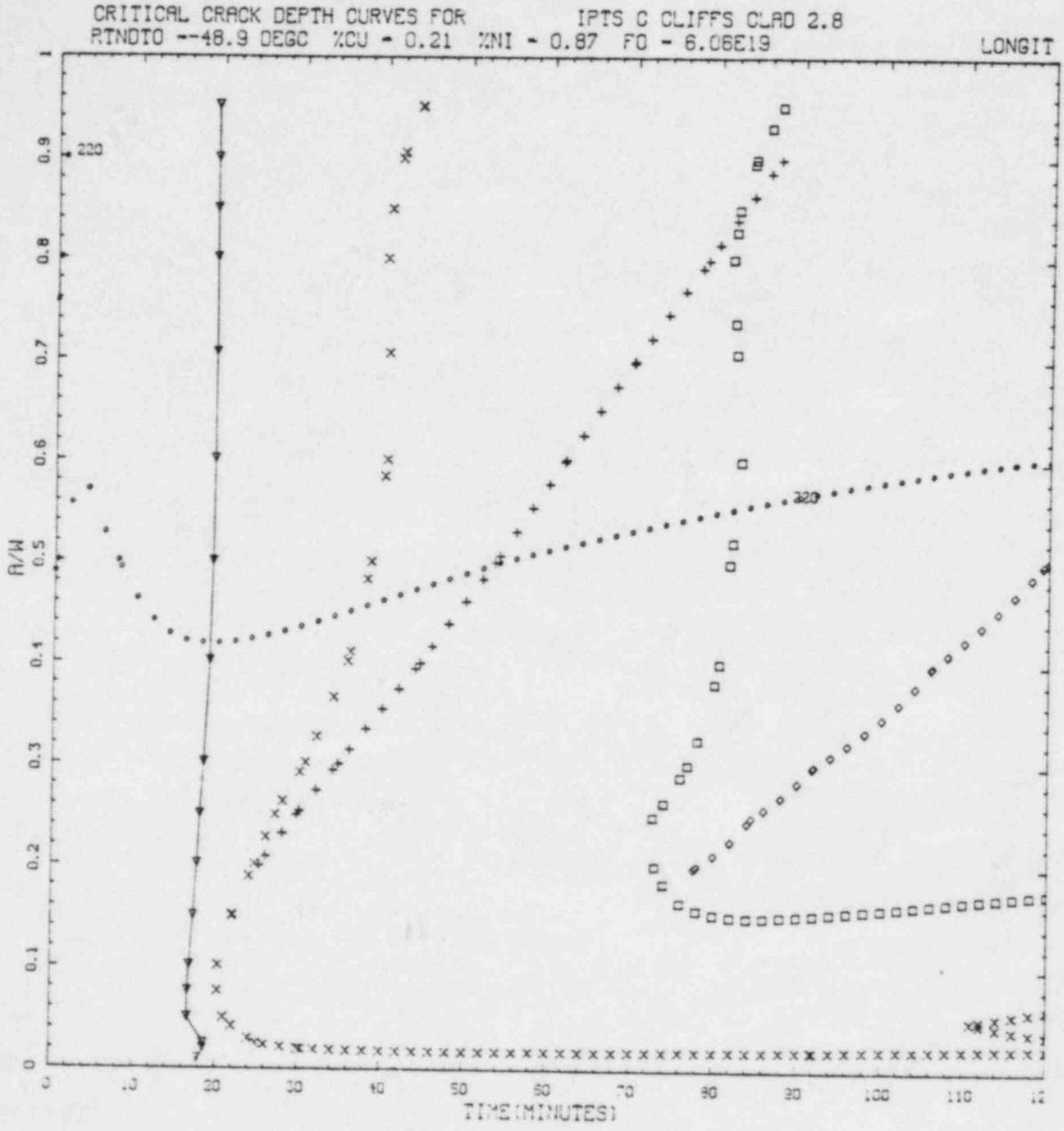
CRITICAL CRACK DEPTH CURVES FOR IPTS C CLIFFS CLAD 2.8
RTNDTO --48.9 DEGC %CU - 0.21 %NI - 0.87 FO - 6.06E19
LONGIT
220
320
A/W
TIME(MINUTES)

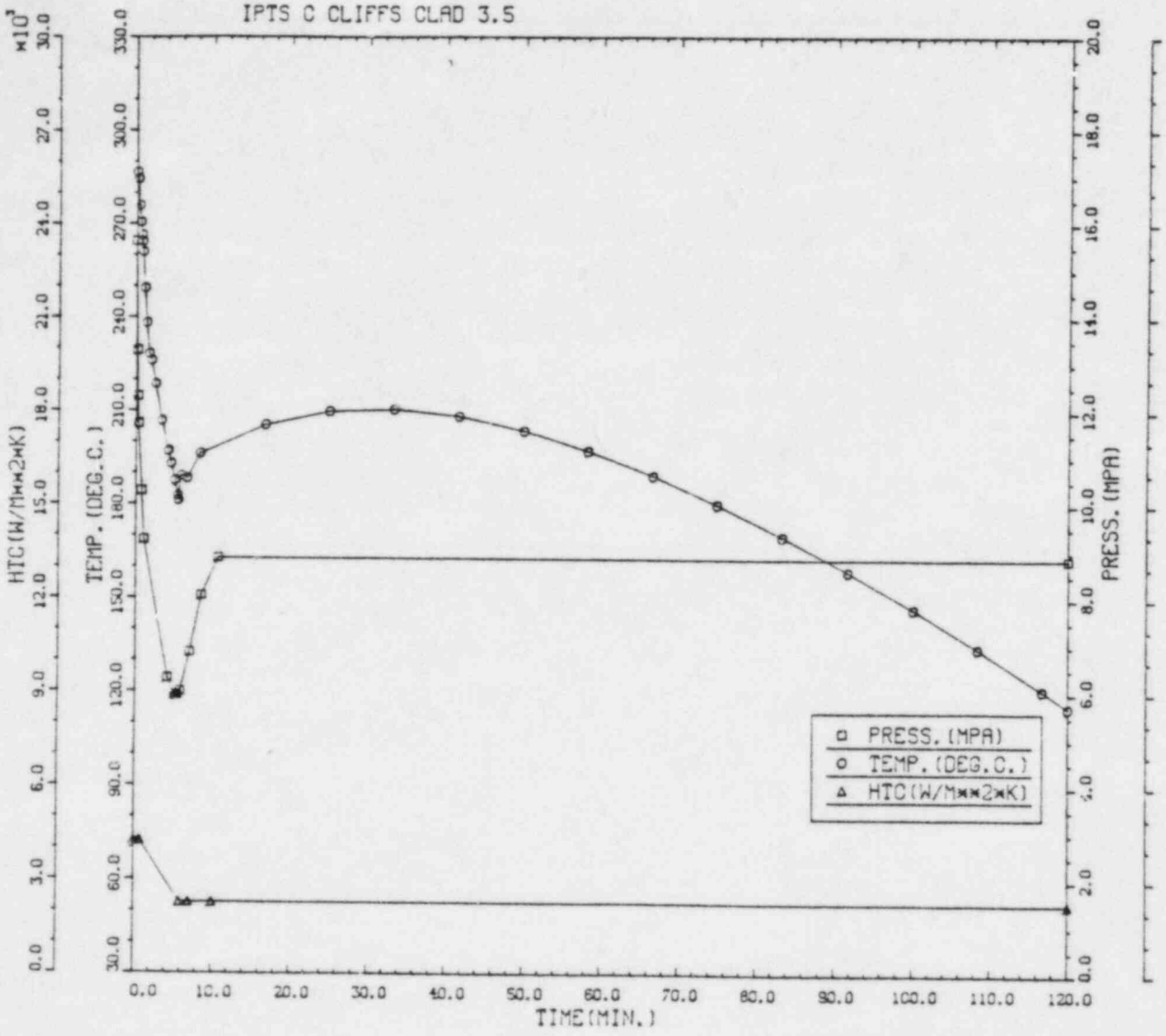
IPTS C CLIFFS CLAD 3.5
HTC(W/M**2*K)
*10³
TEMP.(DEG.C.)
PRESS.(MPA)
TIME(MIN.)
PRESS.(MPA)
TEMP.(DEG.C.)
HTC(W/M**2*K)

IPTS C CLIFFS CLAD 3.5 1. FLAWS/M**3 FO = 6.060D+19

WELD	UNADJUSTED P(F/E)	95%CI	%ERR	P(INITIA)	N*V	ADJUSTED P(F/E)	%ERR	NTRIALS
1	3.52D-06	3.99D-05	113.16	1.35D-04	0.025	8.81D-08		500000
2	0.00D+00	0.00D+00	0.00	1.17D-05	0.050	0.00D+00		500000
3	0.00D+00	0.00D+00	0.00	2.35D-05	0.021	0.00D+00		500000
					VESSEL	8.81D-08	113.16	

DEPTHS FOR INITIAL INITIATION (MM)

	2.16	6.68	11.62	17.03	22.95	29.42	36.51	44.25	52.72
NUMBER	0	101	23	9	2	1	0	0	0
PERCENT	0.0	74.3	16.9	6.6	1.5	0.7	0.0	0.0	0.0

TIMES OF FAILURE(MINUTES)

	0.0	10.0	20.0	30.0	40.0	50.0	60.0	70.0	80.0	90.0	100.0	110.0	120.0
NUMBER	0	0	0	0	0	0	0	0	0	0	0	0	3
PERCENT	0.0	0.0	0.0	0.0	0.0	0.0	0.0	0.0	0.0	0.0	0.0	0.0	100.0

INITIATION T-RTNDT(DEG.C)

	-55.6	-41.7	-27.8	-13.9	0.0	13.9	27.8	41.7	55.6	69.4	83.3	97.2	111.1
NUMBER	0	20	35	52	25	0	0	0	0	0	0	0	0
PERCENT	0.0	14.1	24.6	43.7	17.6	0.0	0.0	0.0	0.0	0.0	0.0	0.0	0.0

ARREST T-RTNDT(DEG.C)

	-27.8	-13.9	0.0	13.9	27.8	41.7	55.6	69.4	83.3	97.2	111.1	125.0	138.9
NUMBER	5	16	28	0	0	1	43	45	0	0	0	0	
PERCENT	3.6	11.6	20.3	0.0	0.0	0.7	31.2	32.6	0.0	0.0	0.0	0.0	

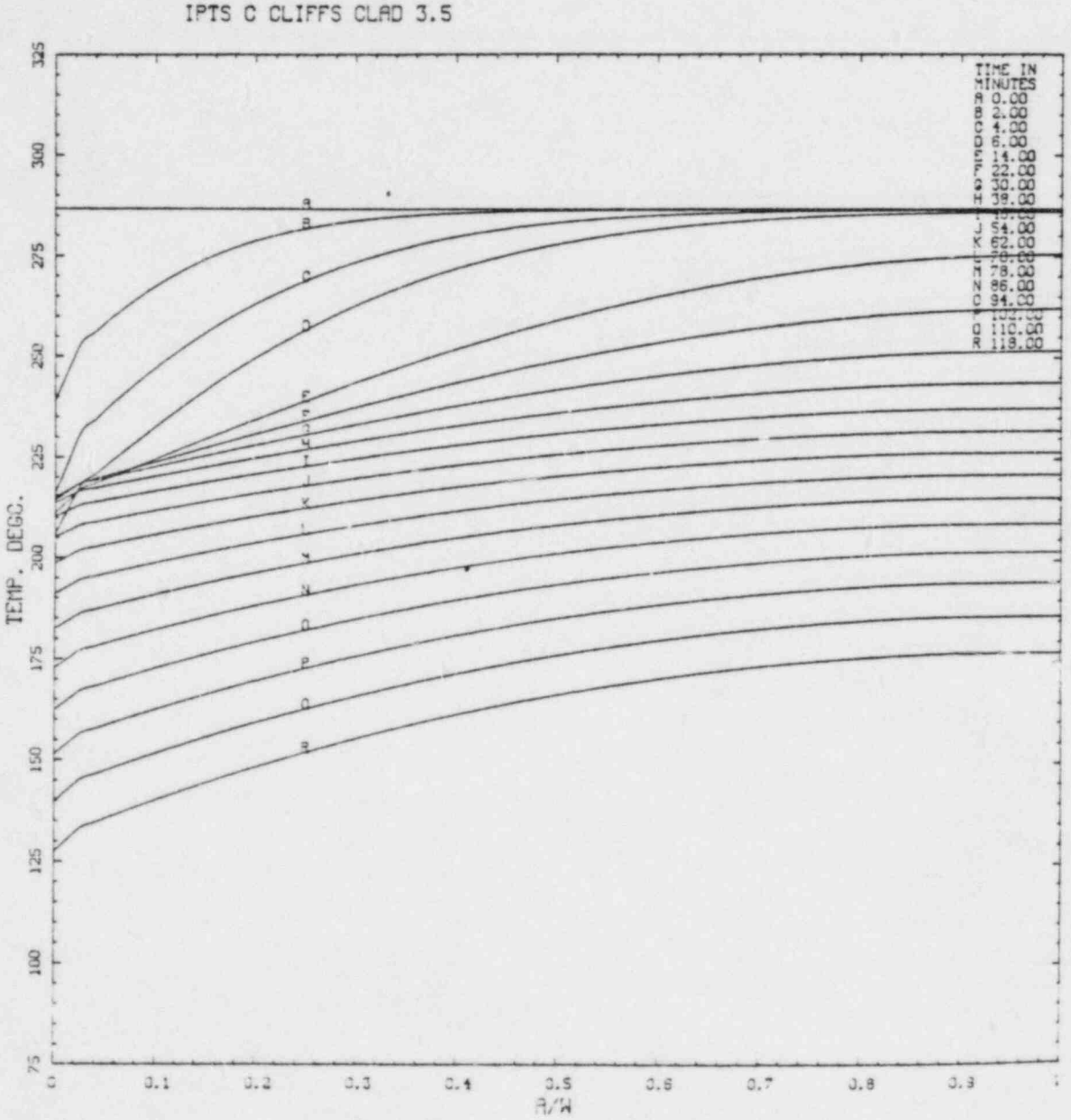
IPTS C CLIFFS CLAD 3.5
TEMP. DEGC.
R/W
TIME IN MINUTES
A 0.00
B 2.00
C 4.00
D 6.00
E 14.00
F 22.00
G 30.00
H 38.00
J 54.00
K 62.00
M 78.00
N 86.00
O 94.00
Q 110.00
R 118.00

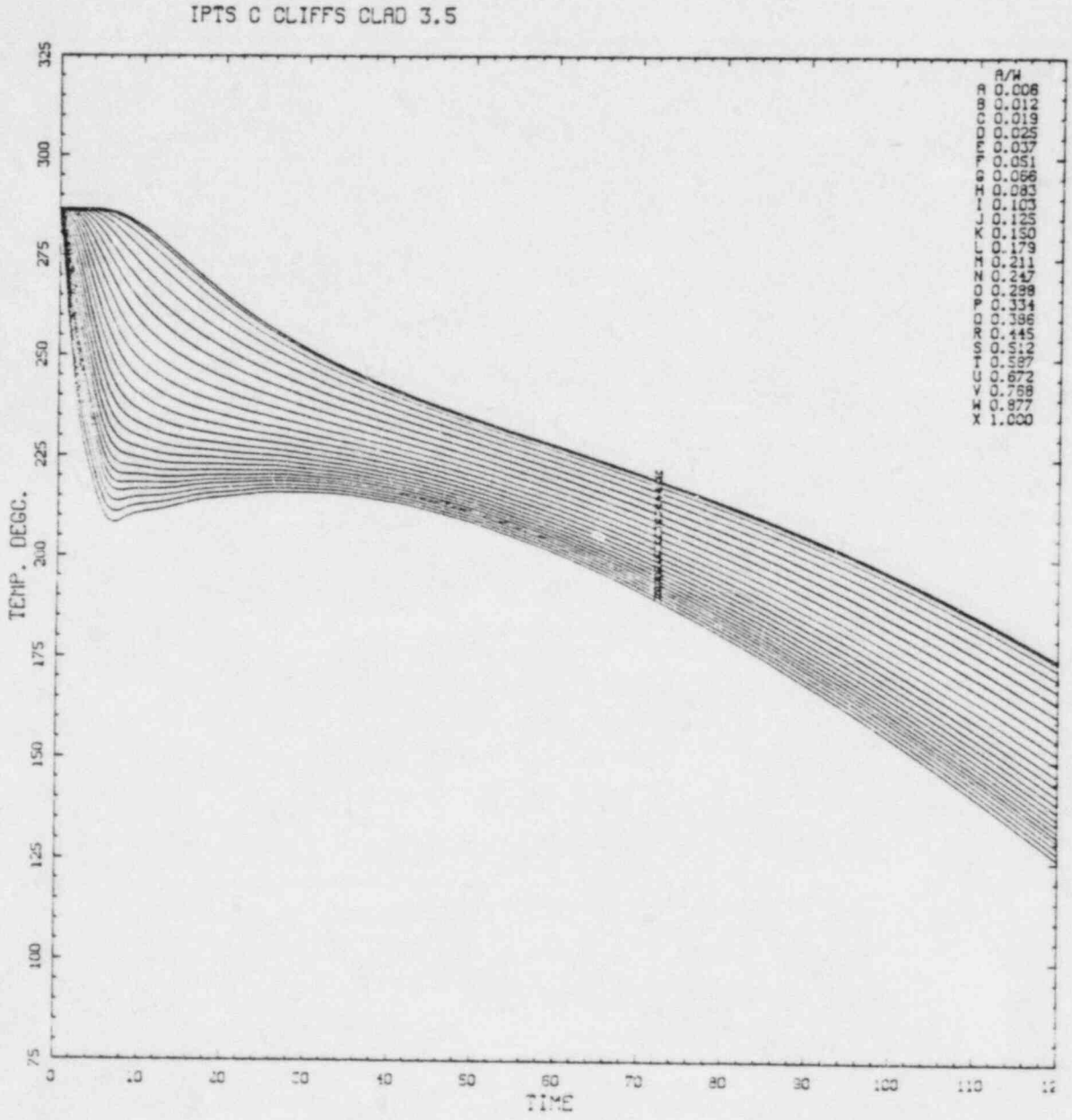
IPTS C CLIFFS CLAD 3.5
TEMP. DEGC.
TIME
A/W
A 0.006
B 0.012
C 0.019
D 0.025
E 0.037
F 0.051
G 0.066
H 0.083
I 0.103
J 0.125
K 0.150
L 0.179
M 0.211
N 0.247
O 0.288
P 0.334
Q 0.386
R 0.445
S 0.512
T 0.587
U 0.672
V 0.768
W 0.877
X 1.000

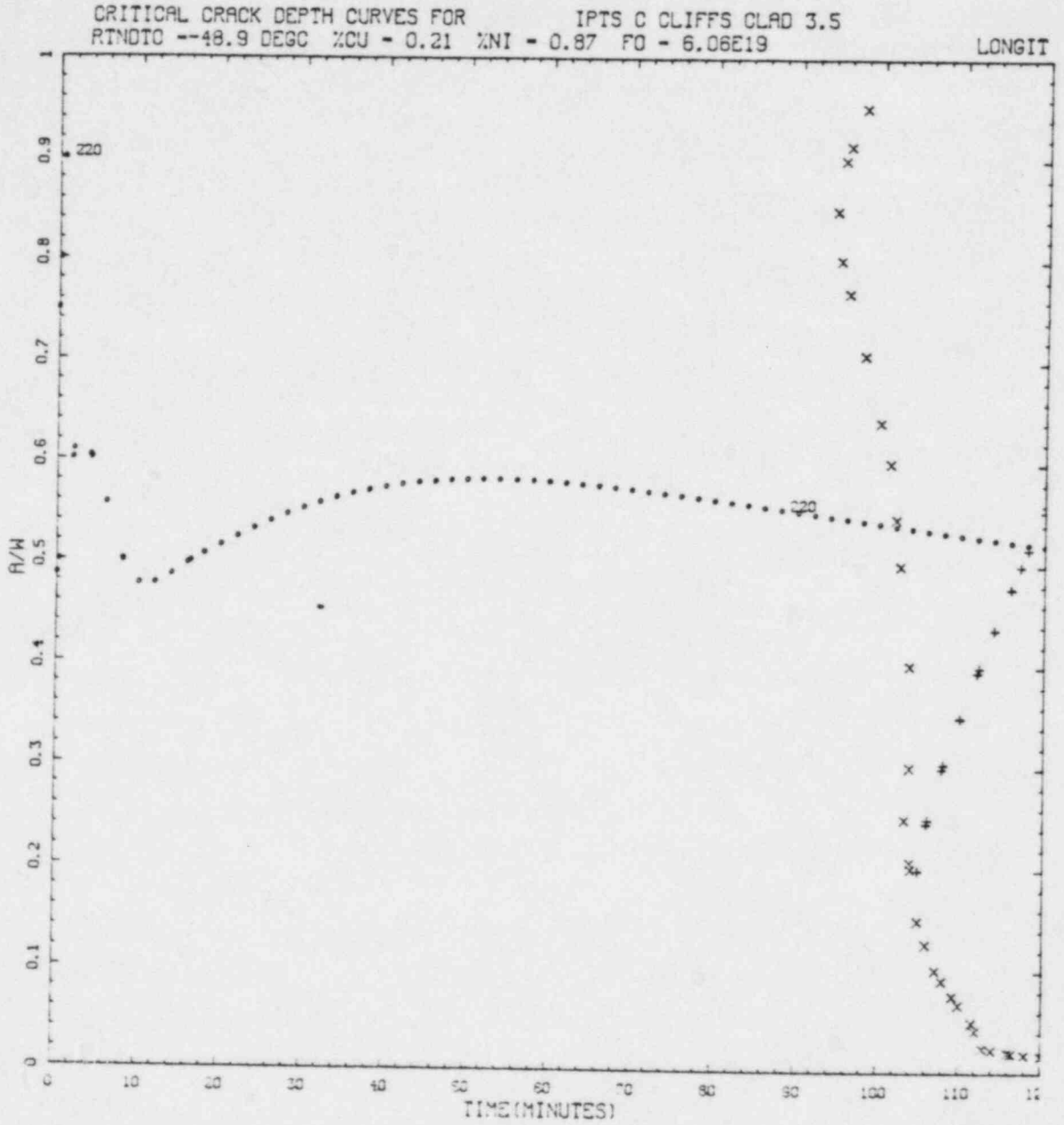
CRITICAL CRACK DEPTH CURVES FOR IPTS C CLIFFS CLAD 3.5
RTNDTC --48.9 DEGC %CU - 0.21 %NI - 0.87 FO - 6.06E19
LONGIT
220
220
A/W
TIME(MINUTES)
0
0.1
0.2
0.3
0.4
0.5
0.6
0.7
0.8
0.9
1
10
20
30
40
50
60
70
80
90
100
110

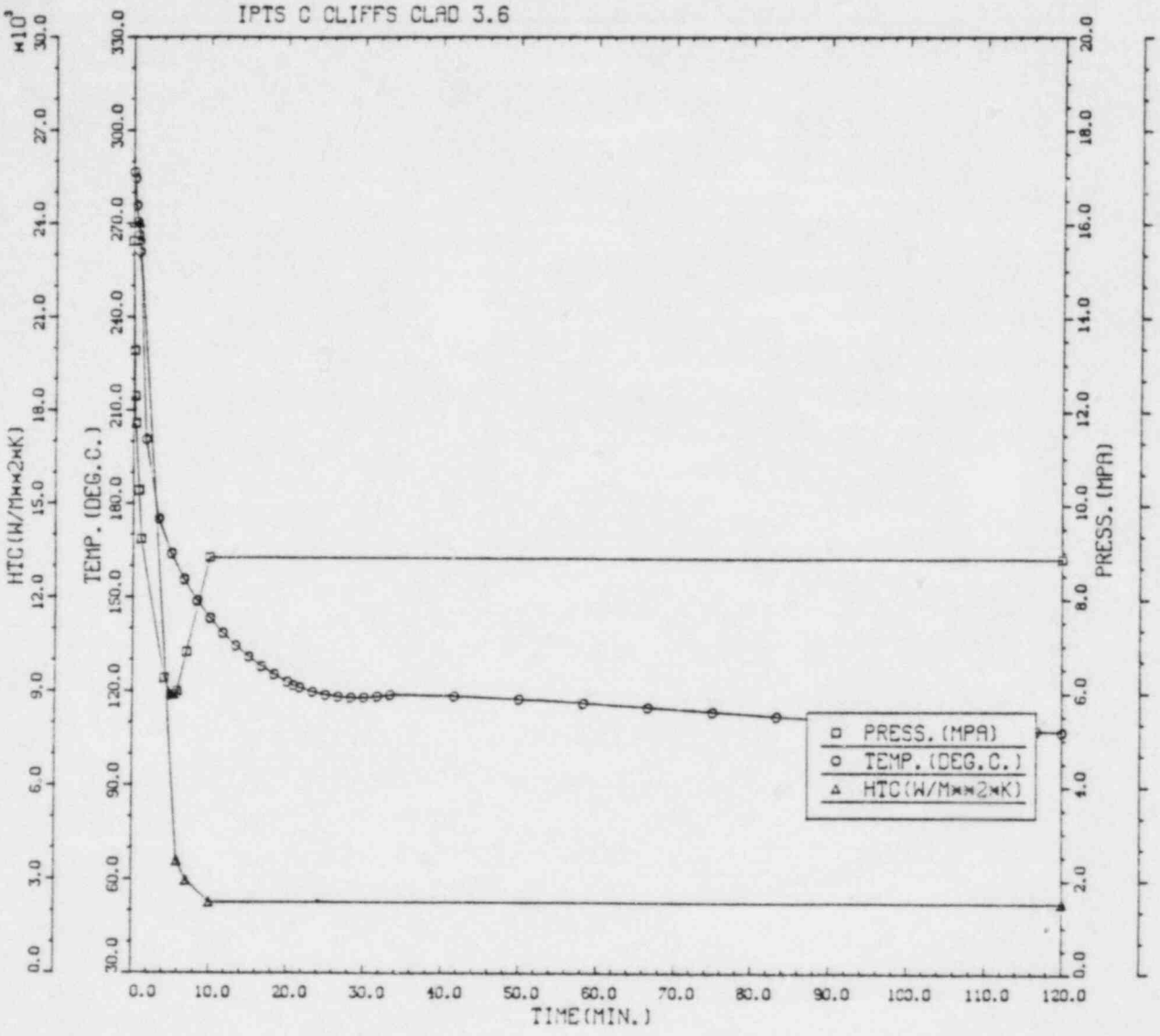
IPTS C CLIFFS CLAD 3.6
HTC(W/M**2*K)
*10³
TEMP.(DEG.C.)
PRESS.(MPA)
TIME(MIN.)
PRESS.(MPA)
TEMP.(DEG.C.)
HTC(W/M**2*K)

IPTS C CLIFFS CLAD 3.6 1. FLAWS/M**3 FO = 6.060D+19

WELD	UNADJUSTED P(F/E)	95%CI	%ERR	P(INITIA)	N*V	ADJUSTED P(F/E)	%ERR	NTRIALS
1	2.53D-04	3.38D-05	13.36	5.50D-04	0.025	6.31D-06		500000
2	1.17D-06	2.30D-06	196.00	3.52D-06	0.050	5.87D-08		500000
3	3.75D-05	1.30D-05	34.65	9.75D-05	0.021	7.89D-07		500000
					VESSEL	7.16D-06	12.49	

DEPTHS FOR INITIAL INITIATION (MM)

	2.16	6.68	11.52	17.03	22.95	29.42	36.51	44.25	52.72
NUMBER	13	374	129	38	7	2	0	0	0
PERCENT	2.3	66.4	22.9	6.7	1.2	0.4	0.0	0.0	0.0

TIMES OF FAILURE(MINUTES)

	0.0	10.0	20.0	30.0	40.0	50.0	60.0	70.0	80.0	90.0	100.0	110.0	120.0
NUMBER	0	0	0	0	1	13	32	39	41	48	33	41	
PERCENT	0.0	0.0	0.0	0.0	0.4	5.2	12.9	15.7	16.5	19.4	13.3	16.5	

INITIATION T-RTNDT(DEG.C)

	-55.6	-41.7	-27.8	-13.9	0.0	13.9	27.8	41.7	55.6	69.4	83.3	97.2	111.1
NUMBER	0	0	12	129	347	346	133	16	0	0	0	0	
PERCENT	0.0	0.0	1.9	13.5	36.2	33.0	13.9	1.7	0.0	0.0	0.0	0.0	

ARREST T-RTNDT(DEG.C)

	-27.8	-13.9	0.0	13.9	27.8	41.7	55.6	69.4	83.3	97.2	111.1	125.0	138.9
NUMBER	0	0	0	2	5	3	59	255	255	112	0	0	
PERCENT	0.0	0.0	0.0	0.3	0.7	0.4	8.3	37.3	37.3	16.8	0.0	0.0	

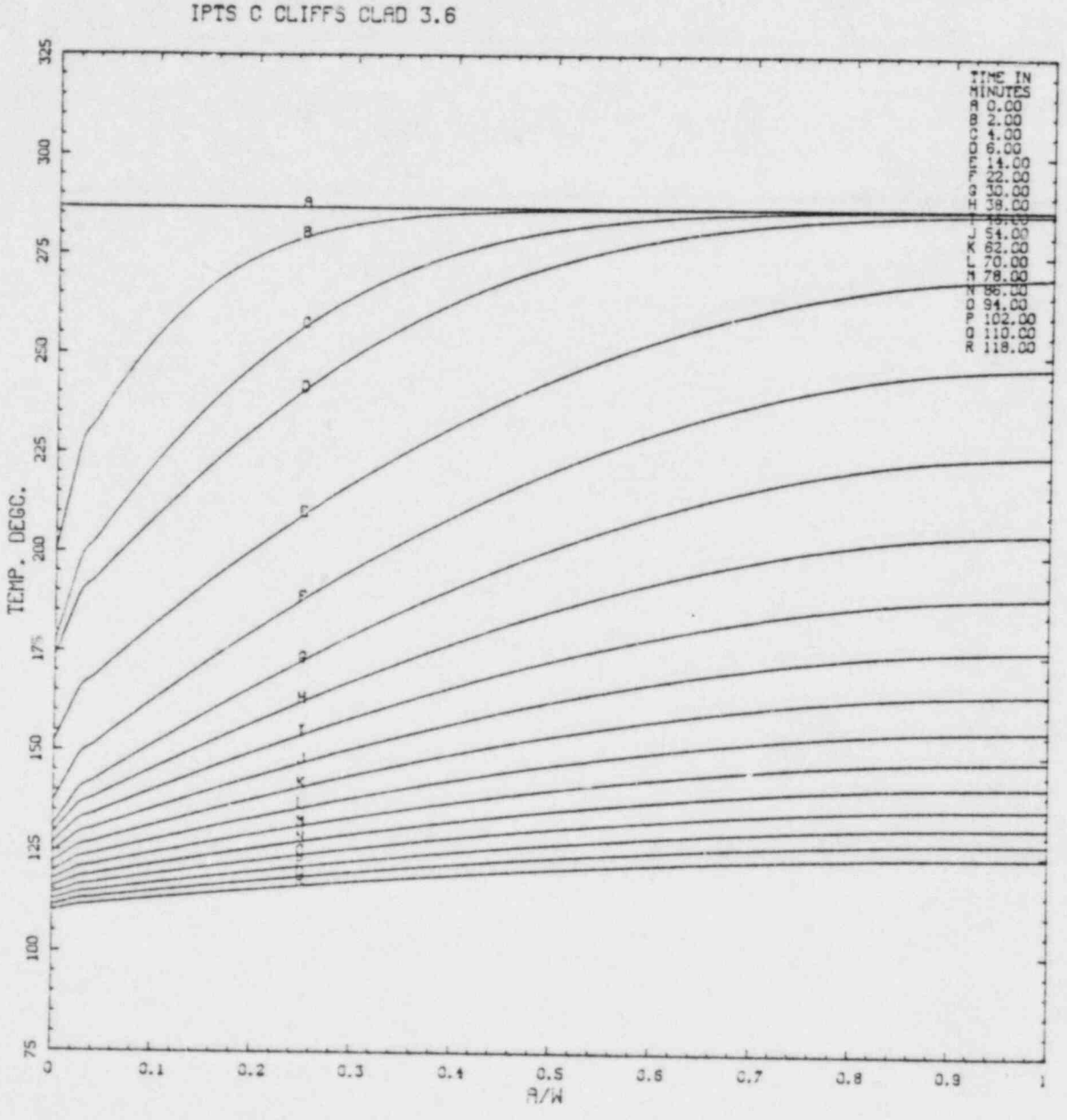
IPTS C CLIFFS CLAD 3.6
TEMP. DEGC.
A/W
TIME IN MINUTES
A 0.00
B 2.00
C 4.00
D 6.00
E 14.00
F 22.00
G 30.00
H 38.00
I 46.00
J 54.00
K 62.00
L 70.00
M 78.00
N 86.00
O 94.00
P 102.00
Q 110.00
R 118.00

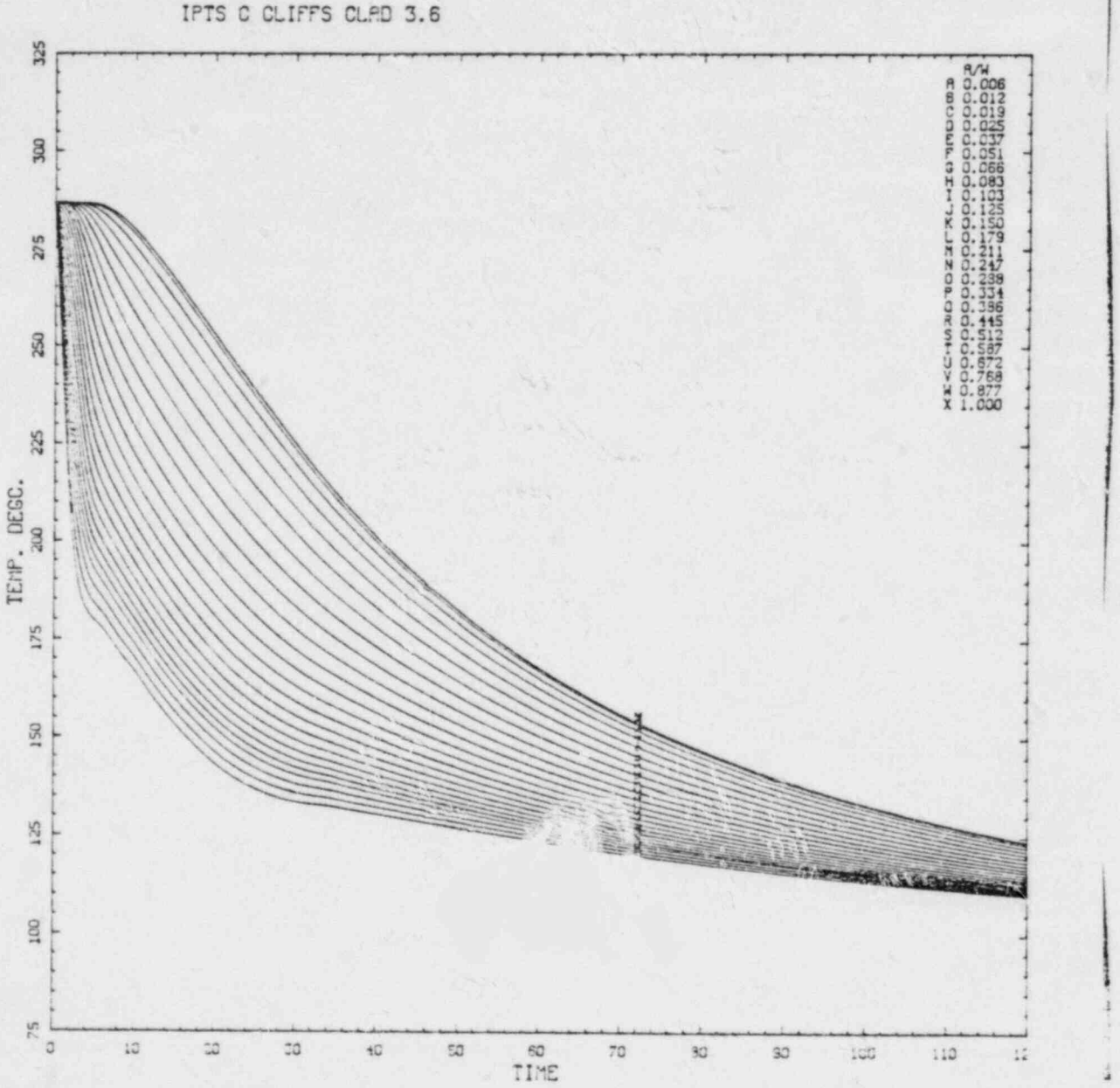
IPTS C CLIFFS CLAD 3.6
TEMP. DEGC.
TIME
R/W
A 0.006
B 0.012
C 0.019
D 0.025
E 0.037
F 0.051
G 0.066
H 0.083
I 0.103
J 0.125
K 0.150
L 0.179
M 0.211
N 0.247
O 0.288
P 0.334
Q 0.386
R 0.445
S 0.513
T 0.587
U 0.672
V 0.768
W 0.877
X 1.000

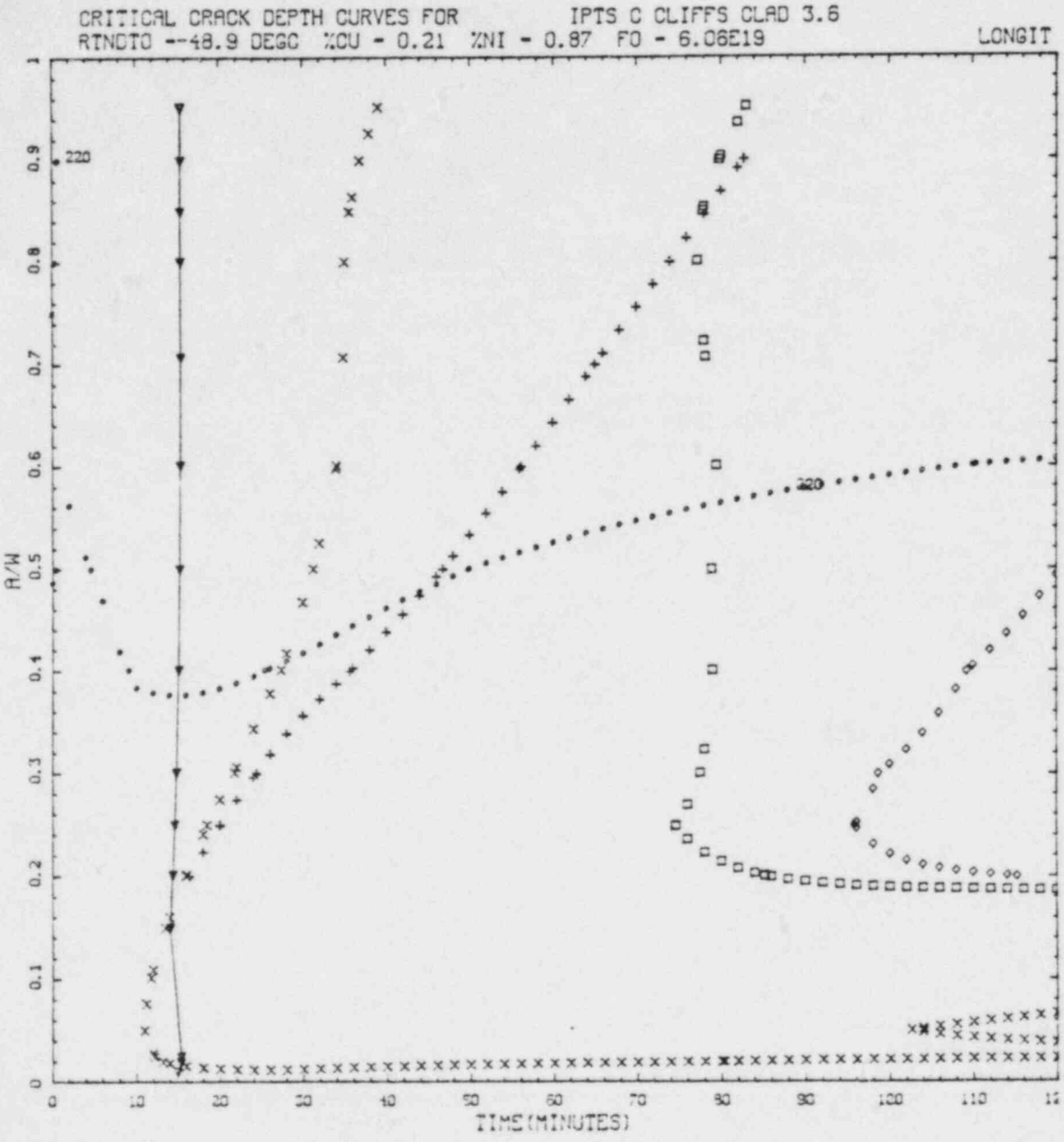
CRITICAL CRACK DEPTH CURVES FOR IPTS C CLIFFS CLAD 3.6
RTNDTO --48.9 DEGC %CU - 0.21 %NI - 0.87 FO - 6.06E19
LONGIT
220
220
A/W
TIME(MINUTES)

IPTS C CLIFFS CLAD 3.10 1. FLAWS/M**3 FO = 6.060D+19

WELD	UNADJUSTED P(F/E)	UNADJUSTED 95%CI	UNADJUSTED %ERR	P(INITIA)	N*V	ADJUSTED P(F/E)	ADJUSTED %ERR	NTRIALS
1	2.18D-03	2.11D-04	9.67	2.27D-03	0.025	5.46D-05		110000
2	4.23D-05	1.38D-05	32.67	4.70D-05	0.050	2.11D-06		500000
3	5.05D-04	5.03D-05	9.96	7.30D-04	0.021	1.06D-05		450000
					VESSEL	6.73D-05	8.07	

DEPTHS FOR INITIAL INITIATION (MM)

	2.16	6.68	11.52	17.03	22.95	29.42	36.51	44.25	52.72
NUMBER	18	539	194	70	32	15	3	0	0
PERCENT	2.1	61.9	22.3	8.0	3.7	1.7	0.3	0.0	0.0

TIMES OF FAILURE(MINUTES)

	0.0	10.0	20.0	30.0	40.0	50.0	60.0	70.0	80.0	90.0	100.0	110.0	120.0
NUMBER	0	0	368	177	49	77	62	26	25	15	16	17	
PERCENT	0.0	0.0	44.2	21.3	5.9	9.3	7.5	3.1	3.0	1.8	1.9	2.0	

INITIATION T-RTNDT(DEG.C)

	-55.6	-41.7	-27.8	-13.9	0.0	13.9	27.8	41.7	55.6	69.4	83.3	97.2	111.1
NUMBER	0	1	9	146	435	270	125	61	2	0	0	0	
PERCENT	0.0	0.1	0.9	13.9	41.5	25.7	11.9	5.8	0.2	0.0	0.0	0.0	

ARREST T-RTNDT(DEG.C)

	-27.8	-13.9	0.0	13.9	27.8	41.7	55.6	69.4	83.3	97.2	111.1	125.0	138.9
NUMBER	0	8	20	7	3	0	1	32	75	47	24	0	
PERCENT	0.0	3.7	9.2	3.2	1.4	0.0	0.5	14.7	34.6	21.7	11.1	0.0	

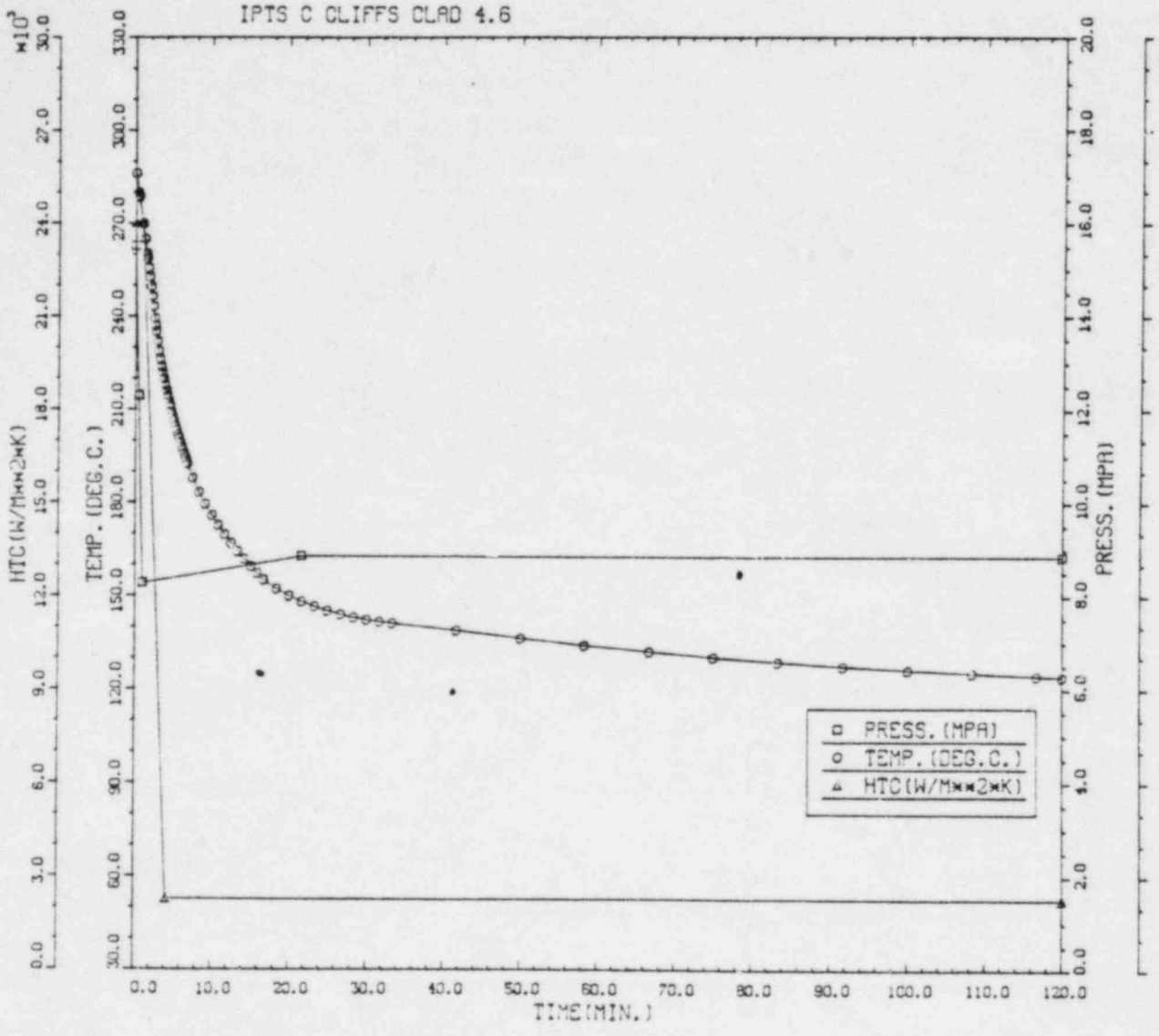
IPTS C CLIFFS CLAD 4.6
HTC(W/M**2*K)
*10**3
TEMP.(DEG.C.)
PRESS.(MPA)
TIME(MIN.)
PRESS.(MPA)
TEMP.(DEG.C.)
HTC(W/M**2*K)

IPTS C CLIFFS CLAD 4.6 1. FLAWS/M**3 FO = 6.060D+19

WELD	UNADJUSTED P(F/E)	95%CI	%ERR	P(INITIA)	N*V	ADJUSTED P(F/E)	%ERR	NTRIALS
1	8.22D-06	6.09D-05	74.08	1.41D-05	0.025	2.06D-07		500000
2	0.00D+00	0.00D+00	0.00	0.00D+00	0.050	0.00D+00		500000
3	0.00D+00	0.00D+00	0.00	1.17D-06	0.021	0.00D+00		500000
					VESSEL	2.06D-07	74.08	

DEPTHS FOR INITIAL INITIATION (MM)

	2.16	5.68	11.52	17.03	22.95	29.42	36.51	44.25	52.72
NUMBER	0	10	2	0	1	0	0	0	0
PERCENT	0.0	76.9	15.4	0.0	7.7	0.0	0.0	0.0	0.0

TIMES OF FAILURE(MINUTES)

	0.0	10.0	20.0	30.0	40.0	50.0	60.0	70.0	80.0	90.0	100.0	110.0	120.0
NUMBER	0	0	0	0	0	0	0	1	3	1	1	1	
PERCENT	0.0	0.0	0.0	0.0	0.0	0.0	0.0	14.3	42.9	14.3	14.3	14.3	

INITIATION T-RTNDT(DEG.C)

	-55.6	-41.7	-27.8	-13.9	0.0	13.9	27.8	41.7	55.6	69.4	83.3	97.2	111.1
NUMBER	0	0	1	3	8	8	4	0	0	0	0	0	
PERCENT	0.0	0.0	4.2	12.5	33.3	33.3	16.7	0.0	0.0	0.0	0.0	0.0	

ARREST T-RTNDT(DEG.C)

	-27.8	-13.9	0.0	13.9	27.8	41.7	55.6	69.4	83.3	97.2	111.1	125.0	138.9
NUMBER	0	0	0	1	0	0	3	8	5	0	0	0	
PERCENT	0.0	0.0	0.0	5.9	0.0	0.0	17.6	47.1	29.4	0.0	0.0	0.0	

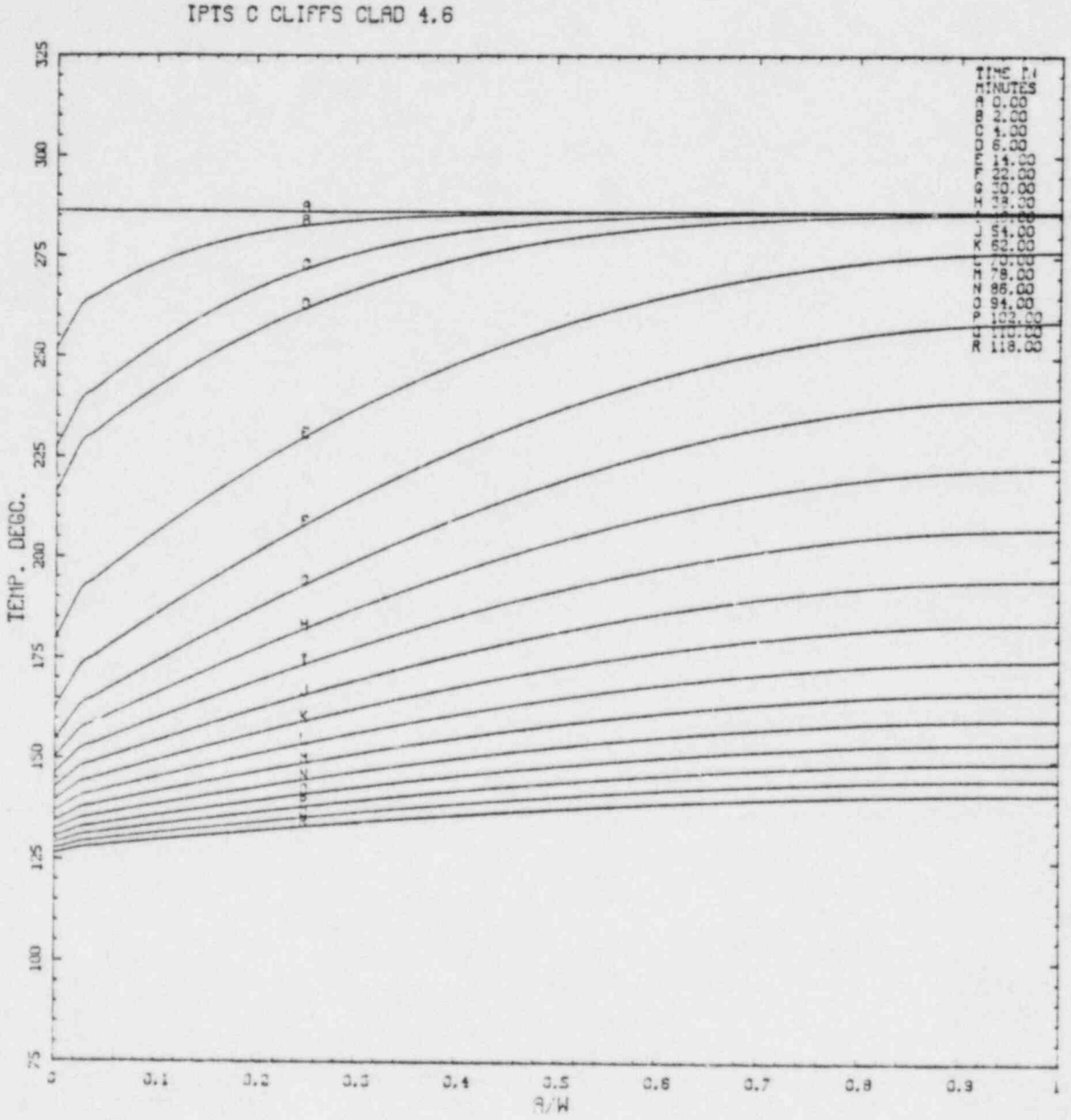
IPTS C CLIFFS CLAD 4.6
TEMP. DEGC.
325
300
275
250
225
200
175
150
125
100
75
0
0.1
0.2
0.3
0.4
0.5
0.6
0.7
0.8
0.9
1
R/W
TIME IN
MINUTES
0.00
2.00
4.00
6.00
14.
22.00
30.00
38.00
46.00
54.00
62.00
70.00
78.00
86.00
94.00
102.00
110.00
118.00

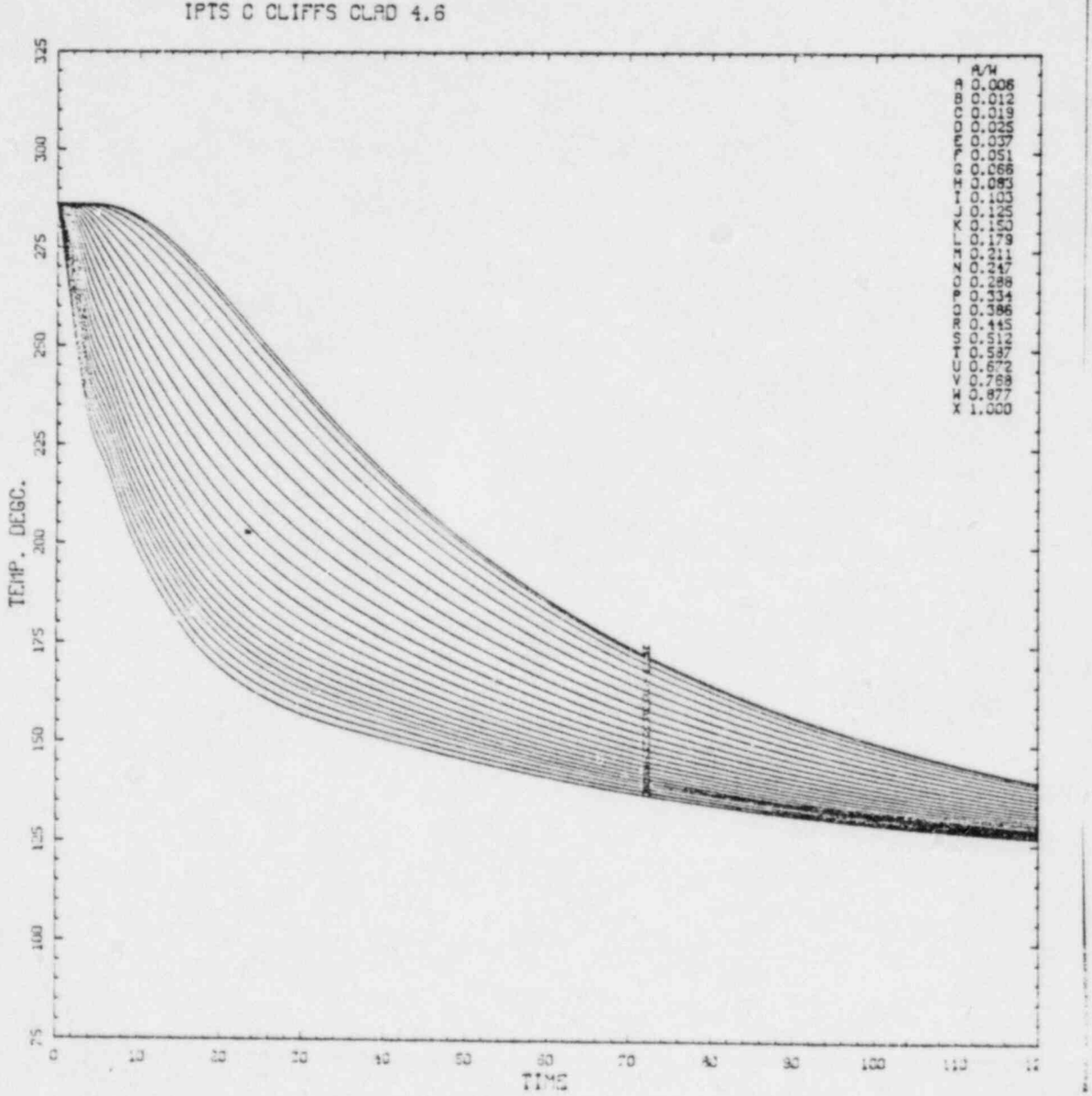
IPTS C CLIFFS CLAD 4.6
TEMP. DEGC.
TIME
A/W
A 0.006
B 0.012
C 0.019
D 0.025
E 0.037
F 0.051
G 0.068
H 0.083
I 0.103
J 0.125
K 0.150
L 0.179
M 0.211
N 0.247
O 0.288
P 0.334
Q 0.386
R 0.445
S 0.512
T 0.587
U 0.672
V 0.768
W 0.877
X 1.000

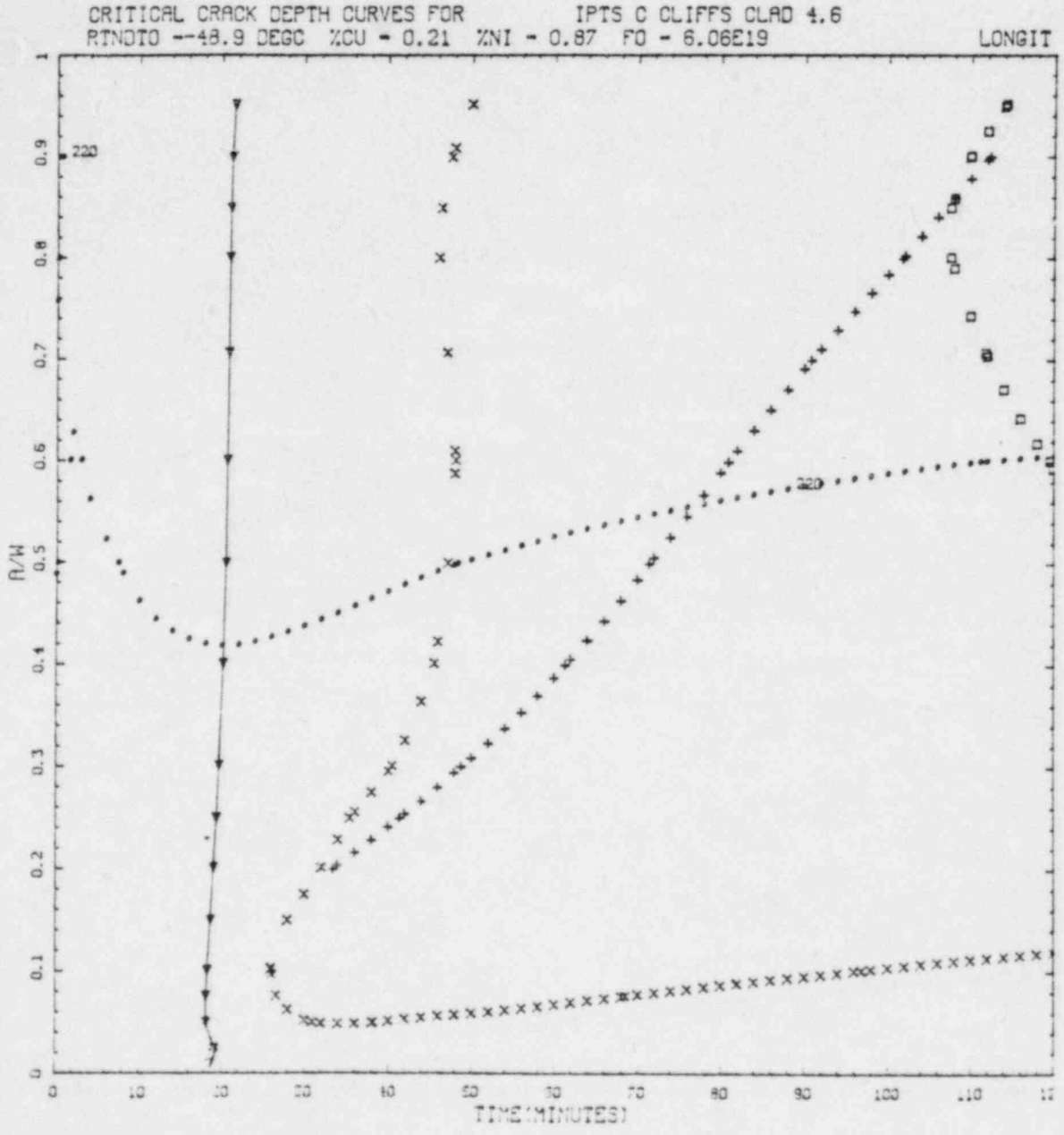
CRITICAL CRACK DEPTH CURVES FOR IPTS C CLIFFS CLAD 4.6
RTNDTO --48.9 DEGC %CU - 0.21 %NI - 0.87 FO - 6.06E19
LONGIT
220
220
A/W
TIME(MINUTES)

IPTS C CLIFFS CLAD 4.13 1. FLAWS/M**3 FO = 6.060D+19

WELD	UNADJUSTED P(F/E)	95%CI	%ERR	P(INITIA)	N*V	ADJUSTED P(F/E)	%ERR	NTRIALS
1	2.03D-04	3.03D-05	14.90	2.27D-04	0.025	5.08D-06		500000
2	3.52D-06	3.99D-06	113.16	3.52D-06	0.050	1.76D-07		500000
3	3.29D-05	1.22D-05	37.04	3.99D-05	0.021	6.91D-07		500000
					VESSEL	5.95D-06	13.85	

DEPTHS FOR INITIAL INITIATION (MM)

	2.16	6.68	11.62	17.03	22.95	29.42	36.51	44.25	52.72
NUMBER	0	136	50	26	10	5	2	1	0
PERCENT	0.0	59.1	21.7	11.3	4.3	2.2	0.9	0.4	0.0

TIMES OF FAILURE(MINUTES)

	0.0	10.0	20.0	30.0	40.0	50.0	60.0	70.0	80.0	90.0	100.0	110.0	120.0
NUMBER	0	0	6	59	26	27	24	27	11	15	5	4	
PERCENT	0.0	0.0	2.9	28.9	12.7	13.2	11.8	13.2	5.4	7.4	2.5	2.0	

INITIATION T-RTNDT(DEG.C)

	-55.6	-41.7	-27.8	-13.9	0.0	13.9	27.8	41.7	55.6	69.4	83.3	97.2	111.1
NUMBER	0	0	1	53	119	56	23	11	1	0	0	0	
PERCENT	0.0	0.0	0.4	20.1	45.1	21.2	8.7	4.2	0.4	0.0	0.0	0.0	

ARREST T-RTNDT(DEG.C)

	-27.8	-13.9	0.0	13.9	27.8	41.7	55.6	69.4	83.3	97.2	111.1	125.0	138.9
NUMBER	0	1	13	2	0	0	0	5	23	16	0	0	
PERCENT	0.0	1.7	21.7	3.3	0.0	0.0	0.0	8.3	38.3	26.7	0.0	0.0	

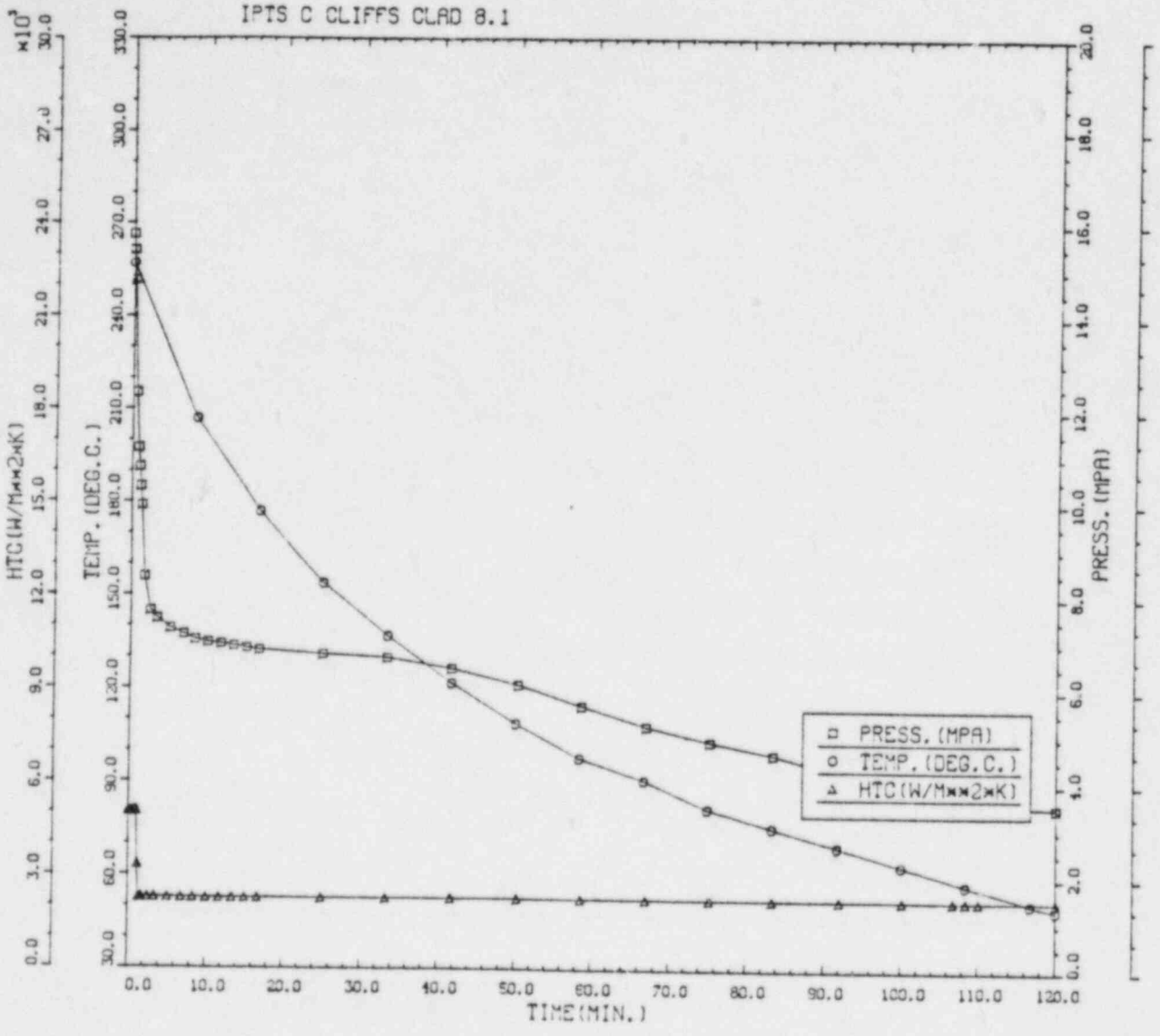
IPTS C CLIFFS CLAD 8.1
HTC(W/M**2*K)
TEMP.(DEG.C.)
PRESS.(MPA)
TIME(MIN.)
PRESS.(MPA)
TEMP.(DEG.C.)
HTC(W/M**2*K)

IPTS C CLIFFS CLAD 8.1 1. FLAWS/M**3 FO = 6.060D+19

WELD	UNADJUSTED P(F/E)	95%CI	%ERR	P(INITIA)	N*V	ADJUSTED P(F/E)	%ERR	NTRIALS
1	1.53D-05	8.30D-06	54.36	3.69D-03	0.025	3.82D-07		500000
2	0.00D+00	0.00D+00	0.00	6.91D-04	0.050	0.00D+00		500000
3	0.00D+00	0.00D+00	0.00	1.89D-03	0.021	0.00D+00		500000
					VESSEL	3.82D-07	54.36	

DEPTHS FOR INITIAL INITIATION (MM)

	2.16	6.68	11.62	17.03	22.95	29.42	36.51	44.25	52.72
NUMBER	0	4705	354	193	68	18	5	2	0
PERCENT	0.0	88.0	6.5	3.6	1.3	0.3	0.1	0.0	0.0

TIMES OF FAILURE(MINUTES)

	0.0	10.0	20.0	30.0	40.0	50.0	60.0	70.0	80.0	90.0	100.0	110.0	120.0
NUMBER		0	0	0	0	0	0	0	2	1	0	10	
PERCENT	0.0	0.0	0.0	0.0	0.0	0.0	0.0	0.0	15.4	7.7	0.0	76.9	

INITIATION T-RTNDT(DEG.C)

	-55.6	-41.7	-27.8	-13.9	0.0	13.9	27.8	41.7	55.6	69.4	83.3	97.2	111.1
NUMBER	377	1095	2042	1779	537	151	35	1	0	0	0	0	
PERCENT	6.3	18.2	33.9	29.6	8.9	2.5	0.6	0.0	0.0	0.0	0.0	0.0	

ARREST T-RTNDT(DEG.C)

	-27.8	-13.9	0.0	13.9	27.8	41.7	55.6	69.4	83.3	97.2	111.1	125.0	138.9
NUMBER	1335	1284	421	202	316	551	838	183	1	0	0	0	
PERCENT	35.0	25.0	8.2	3.9	6.2	10.7	16.3	3.6	0.0	0.0	0.0	0.0	

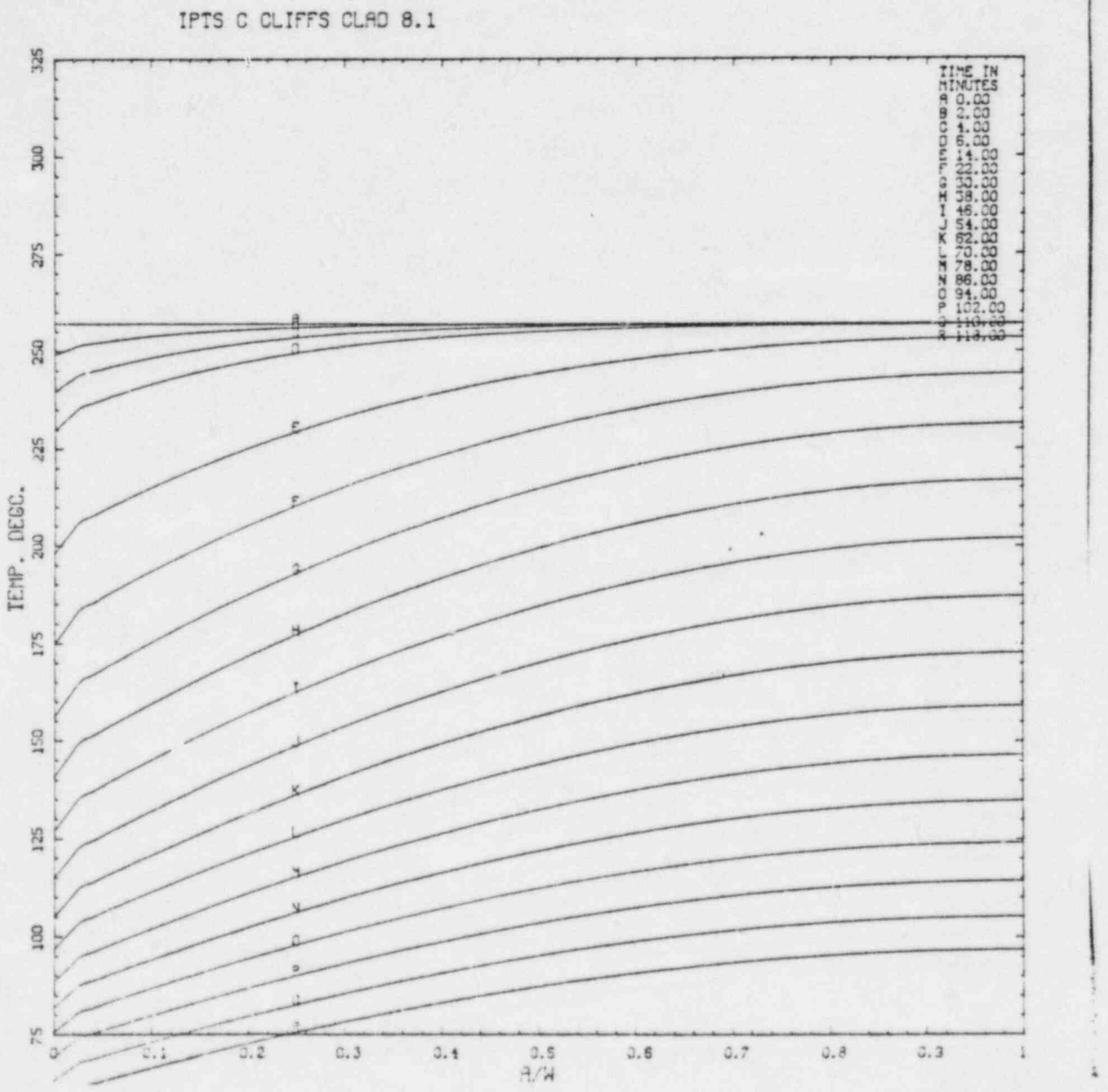
IPTS C CLIFFS CLAD 8.1
TEMP. DEGC.
75
100
125
150
175
200
225
250
275
300
325
0
0.1
0.2
0.3
0.4
0.5
0.6
0.7
0.8
0.9
1
R/W
TIME IN MINUTES
A 0.00
B 2.00
C 6.00
D 14.00
E 22.00
F 30.00
G 38.00
H 46.00
I 54.00
J 62.00
K 70.00
L 78.00
M 86.00
N 94.00
O 102.00
P 110.00
Q 118.00

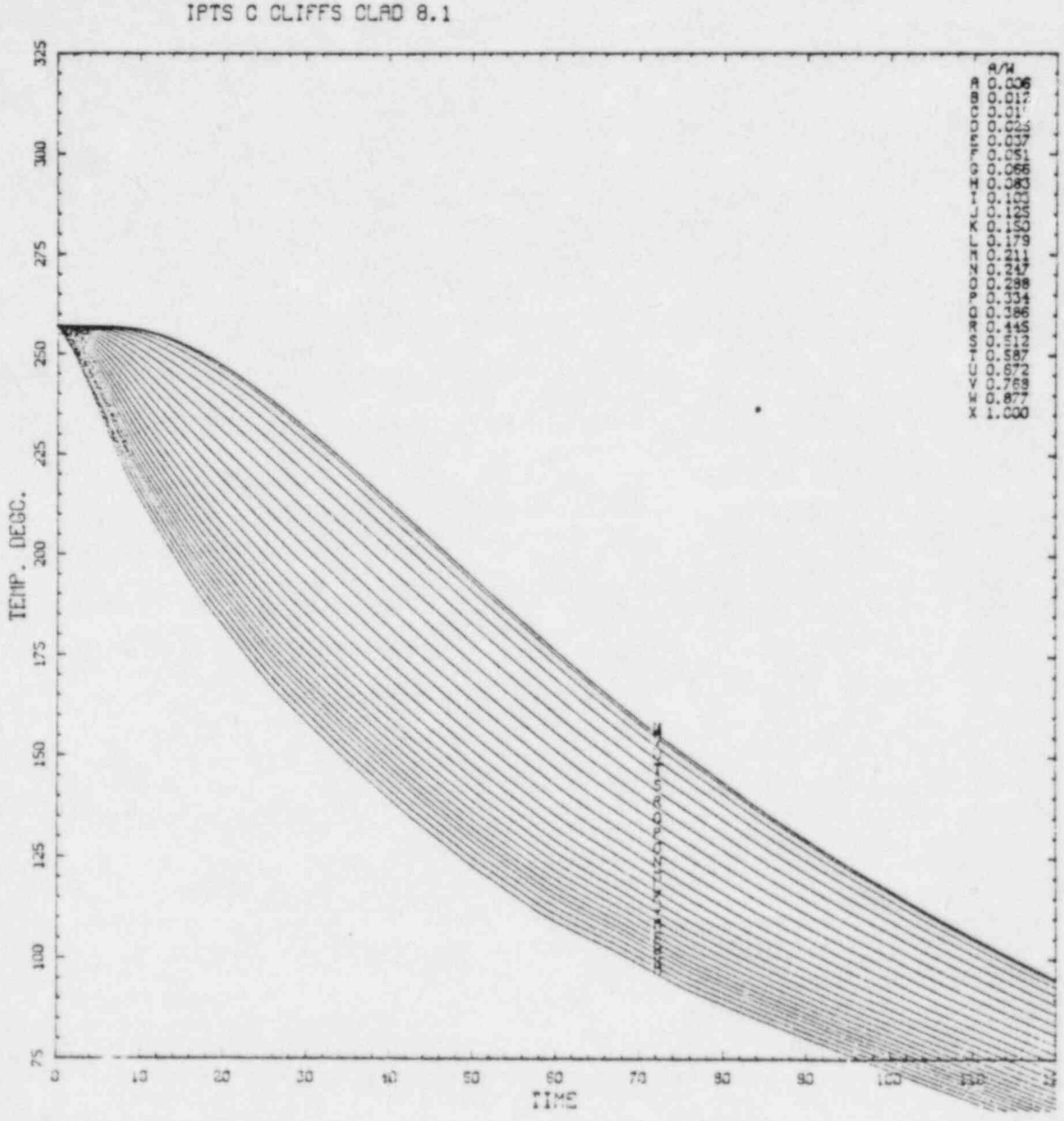
IPTS C CLIFFS CLAD 8.1
TEMP. DEGC.
TIME
75
100
125
150
175
200
225
250
275
300
325
0
10
20
30
40
50
60
70
80
90
100
110
120
A 0.006
B 0.017
X 1.000

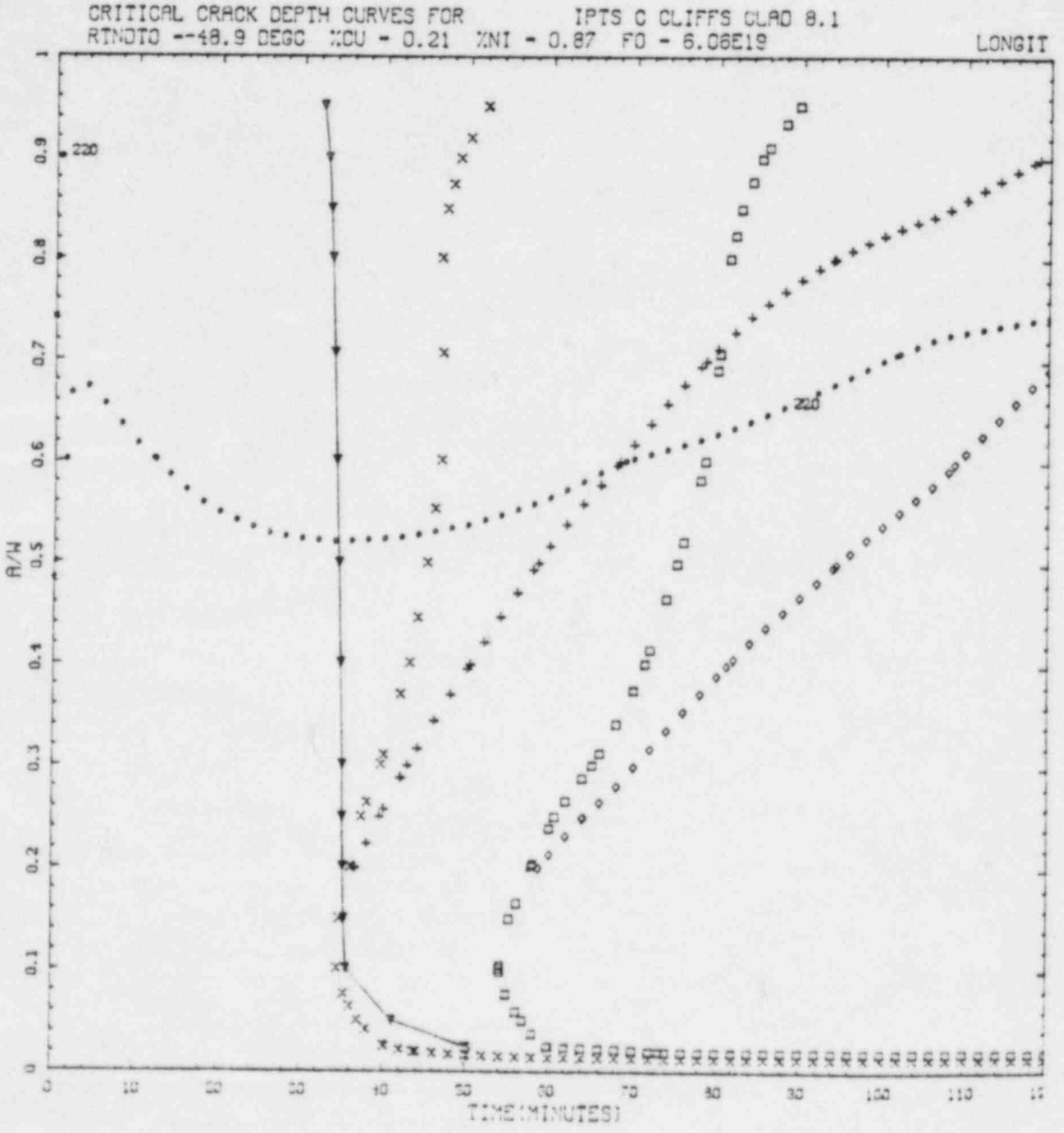
CRITICAL CRACK DEPTH CURVES FOR IPTS C CLIFFS CLAD 8.1
RTNDTO --48.9 DEGC %CU - 0.21 %NI - 0.87 FO - 6.06E19
LONGIT
220
220
A/W
TIME(MINUTES)
0
0.1
0.2
0.3
0.4
0.5
0.6
0.7
0.8
0.9
1
0
10
20
30
40
50
60
70
80
90
100
110

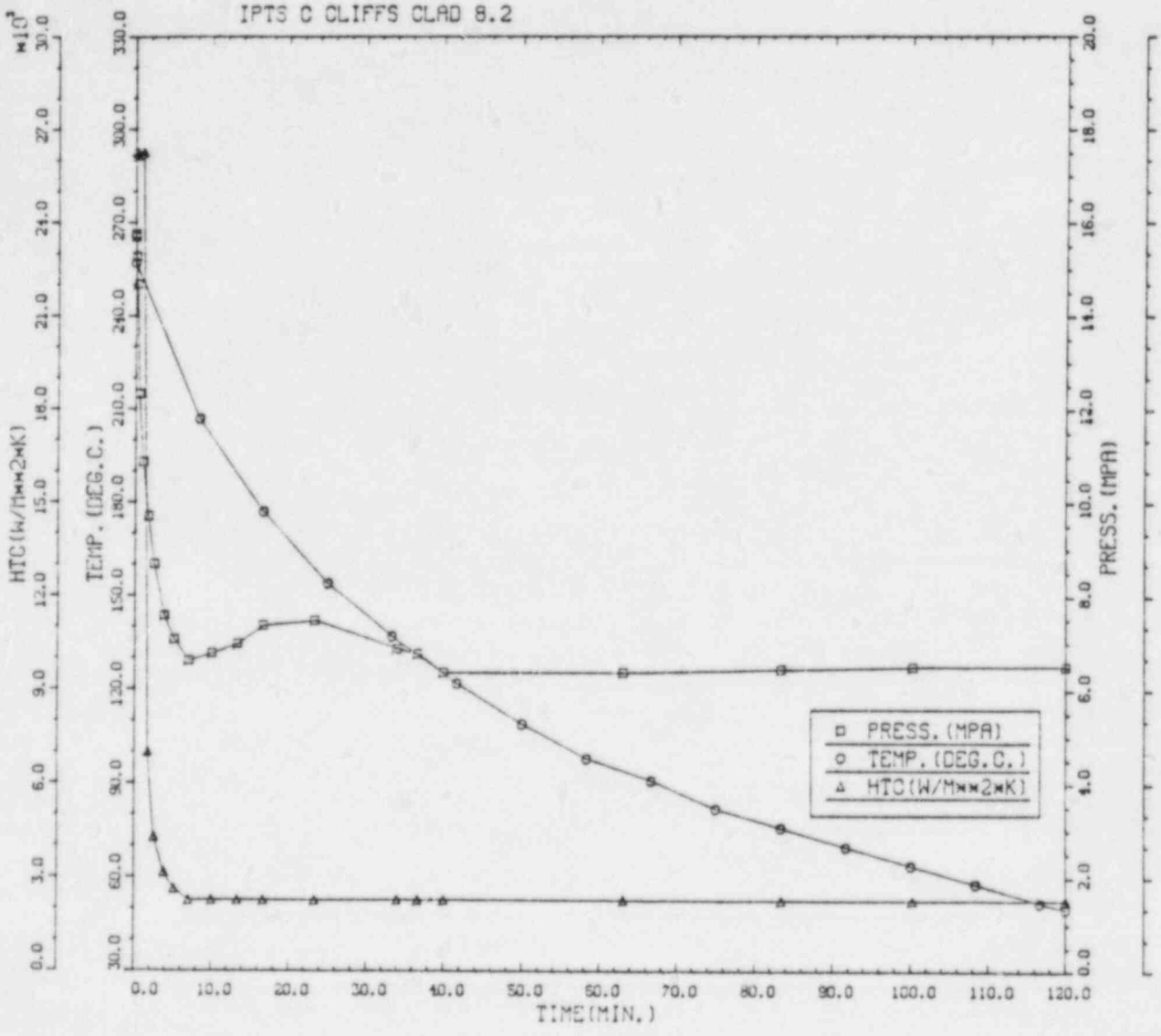
IPTS C CLIFFS CLAD 8.2
HTC(W/M**2*K)
TEMP.(DEG.C.)
PRESS.(MPA)
TIME(MIN.)
PRESS.(MPA)
TEMP.(DEG.C.)
HTC(W/M**2*K)

IPTS C CLIFFS CLAD 8.2 1. FLAWS/M**3 FO = 6.060D+19

	UNADJUSTED					ADJUSTED		
WELD	P(F/E)	95%CI	%ERR	P(INITIA)	N*V	P(F/E)	%ERR	NTRIALS
1	3.98D-03	3.86D-04	9.68	1.15D-02	0.025	9.96D-05		60000
2	3.39D-04	3.91D-05	11.53	2.46D-03	0.050	1.70D-05		500000
3	1.41D-03	1.41D-04	9.99	5.93D-03	0.021	2.96D-05		160000
					VESSEL	1.46D-04	7.03	

DEPTHS FOR INITIAL INITIATION (MM)

	2.16	6.68	11.52	17.03	22.95	29.42	36.51	44.25	52.72
NUMBER	5	4091	431	231	97	29	7	2	0
PERCENT	0.1	83.6	8.8	4.7	2.0	0.6	0.1	0.0	0.0

TIMES OF FAILURE(MINUTES)

	0.0	10.0	20.0	30.0	40.0	50.0	60.0	70.0	80.0	90.0	100.0	110.0	120.0
NUMBER	0	0	0	0	0	0	0	1	22	99	289	669	
PERCENT	0.0	0.0	0.0	0.0	0.0	0.0	0.0	0.1	2.0	9.2	26.8	61.9	

INITIATION T-RTNDT(DEG.C)

	-55.6	-41.7	-27.8	-13.9	0.0	13.9	27.8	41.7	55.6	69.4	83.3	97.2	111.1
NUMBER	330	1011	1931	1470	402	394	122	5	0	0	0	0	
PERCENT	5.8	17.9	34.1	25.9	7.1	7.0	2.2	0.1	0.0	0.0	0.0	0.0	

ARREST T-RTNDT(DEG.C)

	-27.8	-13.9	0.0	13.9	27.8	41.7	55.6	69.4	83.3	97.2	111.1	125.0	138.9
NUMBER	864	1144	407	21	4	402	1398	89	0	0	0	0	
PERCENT	20.0	26.4	9.4	0.5	0.1	9.3	32.3	2.0	0.0	0.0	0.0	0.0	

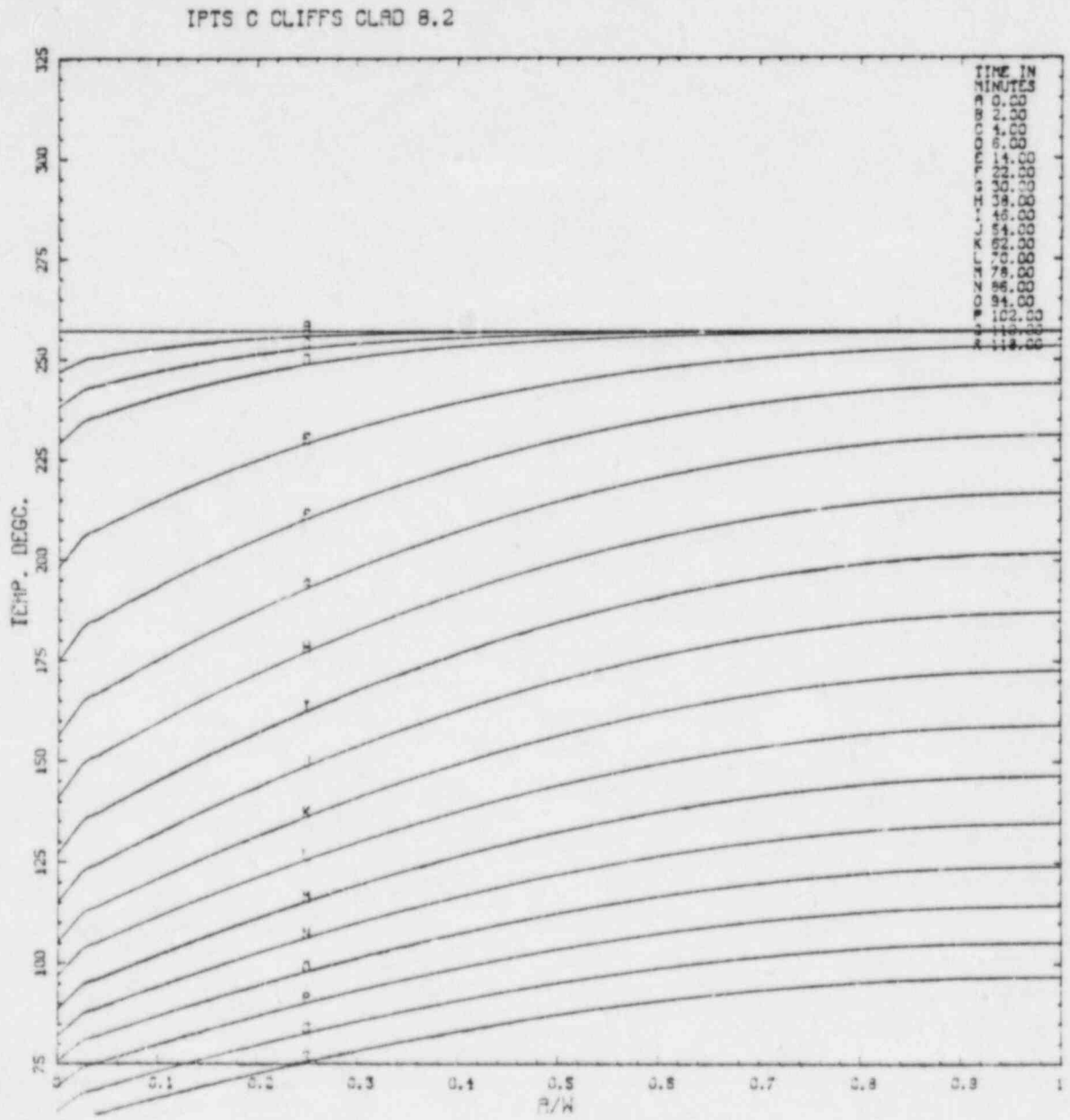
IPTS C CLIFFS CLAD 8.2
TIME IN MINUTES
TEMP. DEGC.
R/W
75
100
125
150
175
200
225
250
275
300
325
0
0.1
0.2
0.3
0.4
0.5
0.6
0.7
0.8
0.9
1

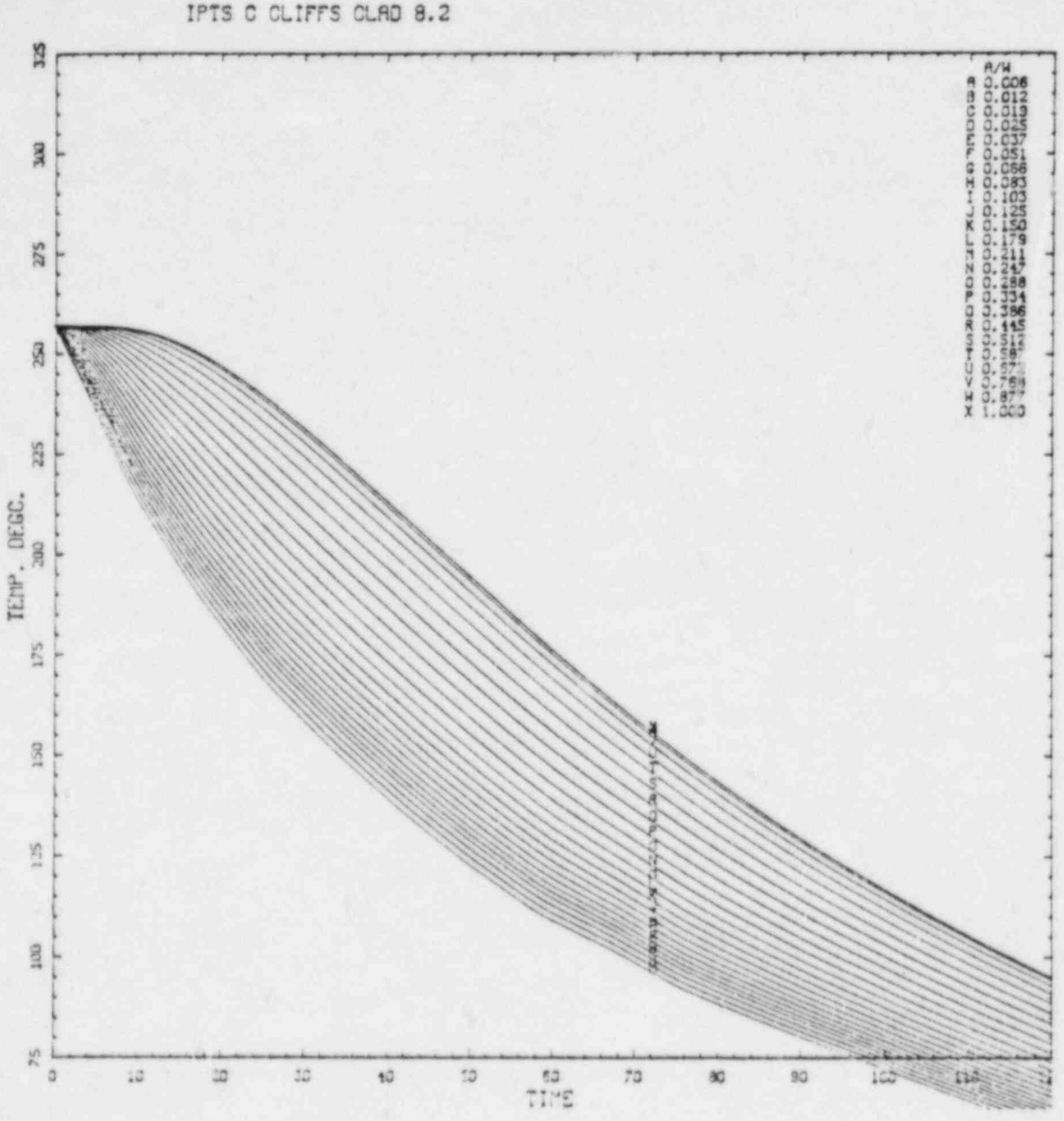
IPTS C CLIFFS CLAD 8.2
TEMP. DEGC.
TIME
A/W
A 0.006
B 0.012
C 0.019
D 0.025
E 0.037
F 0.051
G 0.066
H 0.083
I 0.103
J 0.125
K 0.150
L 0.179
M 0.211
N 0.247
O 0.288
P 0.334
Q 0.386
R 0.445
S 0.513
T 0.587
U 0.677
V 0.788
W 0.877
X 1.000

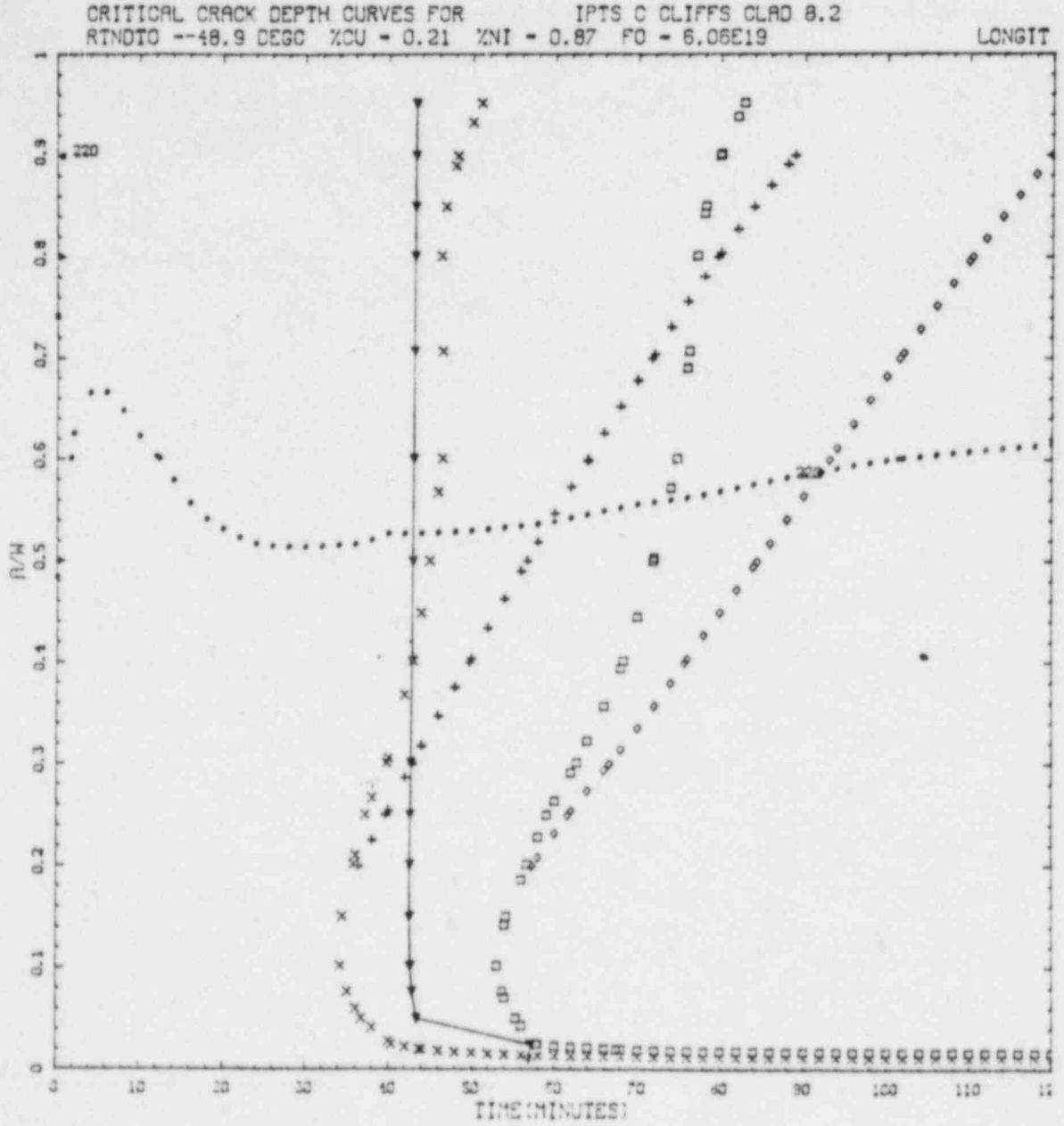
CRITICAL CRACK DEPTH CURVES FOR IPTS C CLIFFS CLAD 8.2
RTNDTO --48.9 DEGC %CU - 0.21 %NI - 0.87 FO - 6.06E19
LONGIT
220
200
A/W
TIME(MINUTES)

IPTS C CLIFFS CLAD 8.3 1. FLAWS/M**3 FO = 6.060D+19

	UNADJUSTED					ADJUSTED		
WELD	P(F/E)	95%CI	%ERR	P(INITIA)	N*V	P(F/E)	%ERR	NTRIALS
1	1.01D-01	4.34D-03	4.31	1.01D-01	0.025	2.52D-03		10000
2	3.81D-02	2.83D-03	7.45	3.84D-02	0.050	1.90D-03		10000
3	7.02D-02	3.73D-03	5.32	7.04D-02	0.021	1.47D-03		10000
					VESSEL	5.90D-03	3.31	

DEPTHS FOR INITIAL INITIATION (MM)

	2.16	6.68	11.62	17.03	22.95	29.42	36.51	44.25	52.72
NUMBER	133	2425	698	236	65	12	5	0	0
PERCENT	3.7	67.8	19.5	6.6	1.8	0.3	0.2	0.0	0.0

TIMES OF FAILURE(MINUTES)

	0.0	10.0	20.0	30.0	40.0	50.0	60.0	70.0	80.0	90.0	100.0	110.0	120.0
NUMBER	0	0	0	0	0	0	0	1	2	1845	707	1004	
PERCENT	0.0	0.0	0.0	0.0	0.0	0.0	0.0	0.0	0.1	51.8	19.9	28.2	

INITIATION T-RTNDT(DEG.C)

	-55.5	-41.7	-27.8	-13.9	0.0	13.9	27.8	41.7	55.6	69.4	83.3	97.2	111.1
NUMBER	226	562	1250	1142	405	46	48	49	6	0	0	0	
PERCENT	6.1	15.1	33.5	30.6	10.8	1.2	1.3	1.3	0.2	0.0	0.0	0.0	

ARREST T-RTNDT(DEG.C)

	-27.8	-13.9	0.0	13.9	27.8	41.7	55.6	69.4	83.3	97.2	111.1	125.0	138.9
NUMBER	3	31	35	1	0	4	78	37	4	0	0	0	
PERCENT	1.7	12.1	14.5	0.6	0.0	2.3	45.1	21.4	2.3	0.0	0.0	0.0	

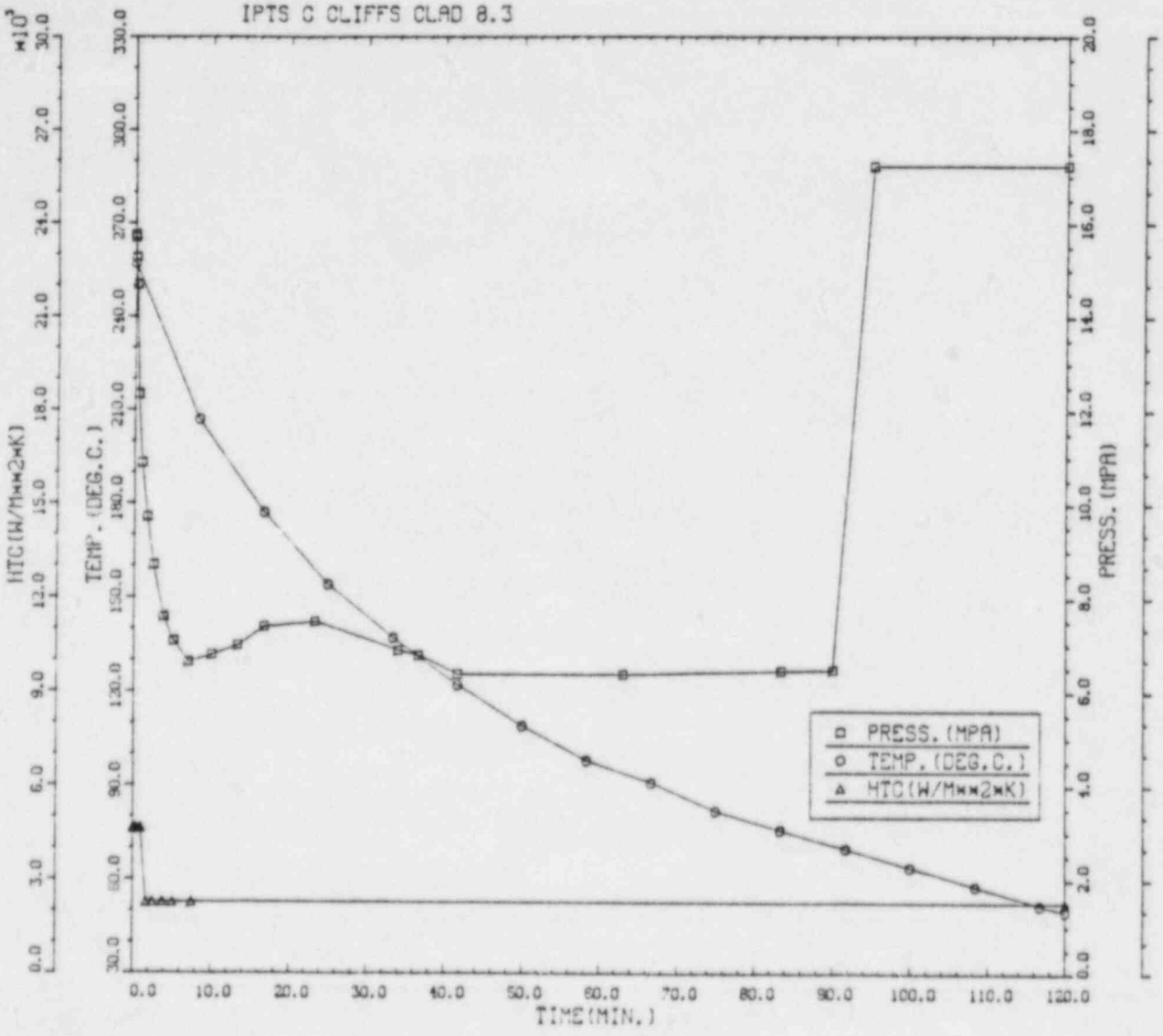
IPTS C CLIFFS CLAD 8.3
HTC(W/M**2*K)
x10³
TEMP.(DEG.C.)
PRESS.(MPA)
TIME(MIN.)
PRESS.(MPA)
TEMP.(DEG.C.)
HTC(W/M**2*K)

IPTS C CLIFFS CLAD 8.3

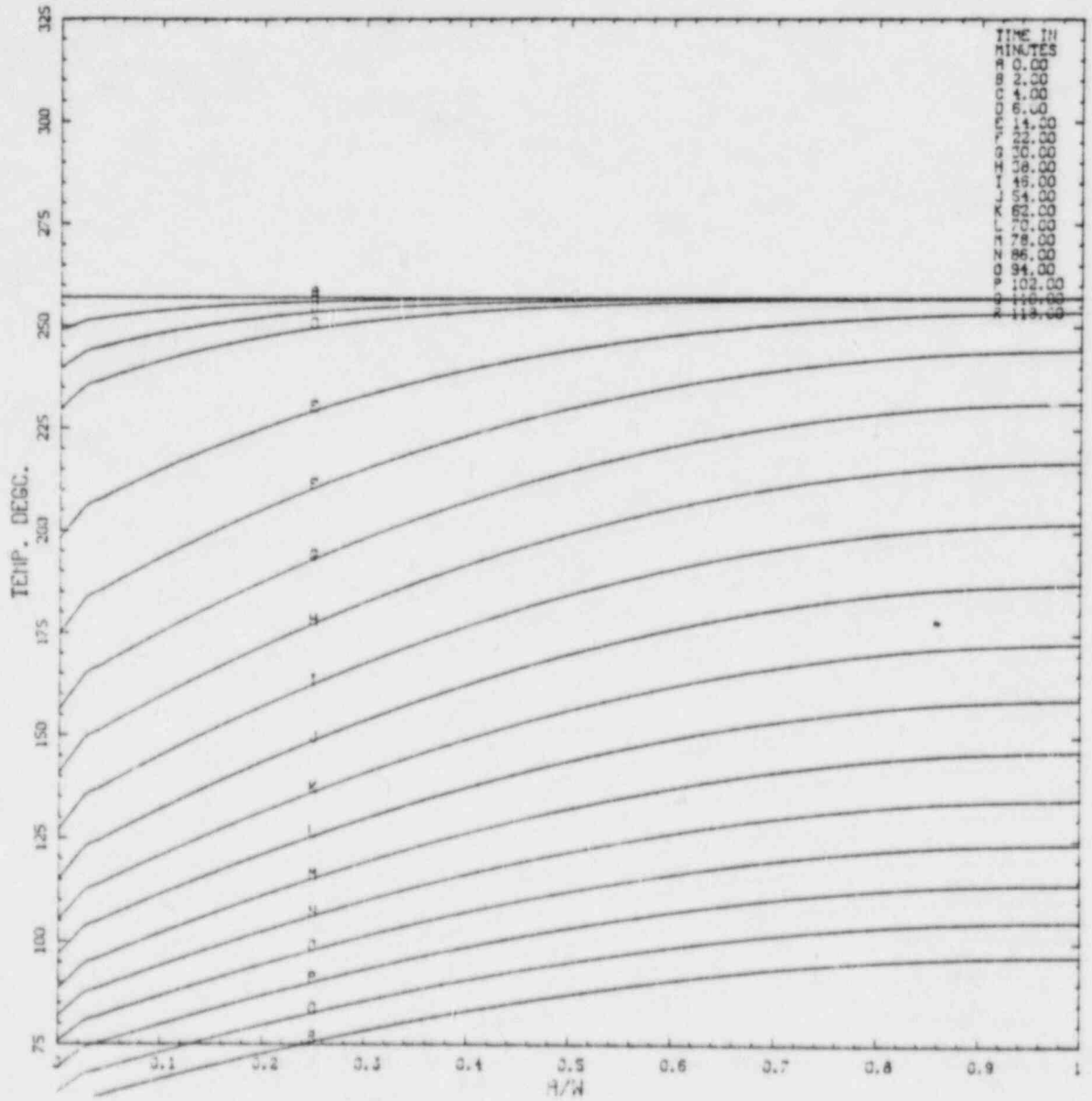

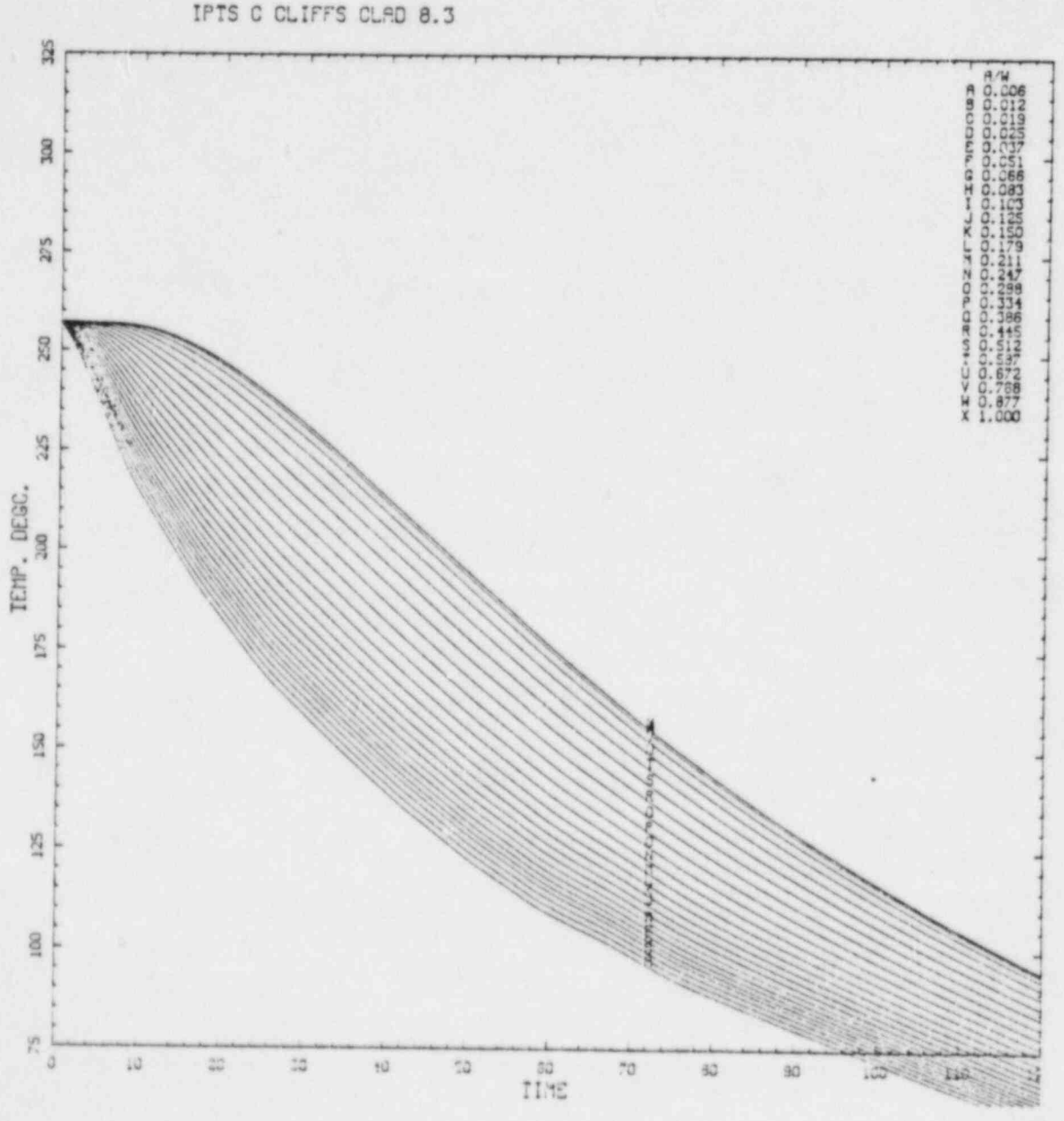
IPTS C CLIFFS CLAD 8.3
TEMP. DEGC.
TIME
325
300
275
250
225
200
175
150
125
100
75
0
10
20
30
40
50
60
70
80
90
100
110
120
X/C
0.000
0.006
0.012
0.019
0.025
0.037
0.051
0.068
0.083
0.103
0.124
0.150
0.177
0.211
0.247
0.288
0.334
0.386
0.445
0.512
0.587
0.677
0.788
0.877
1.000

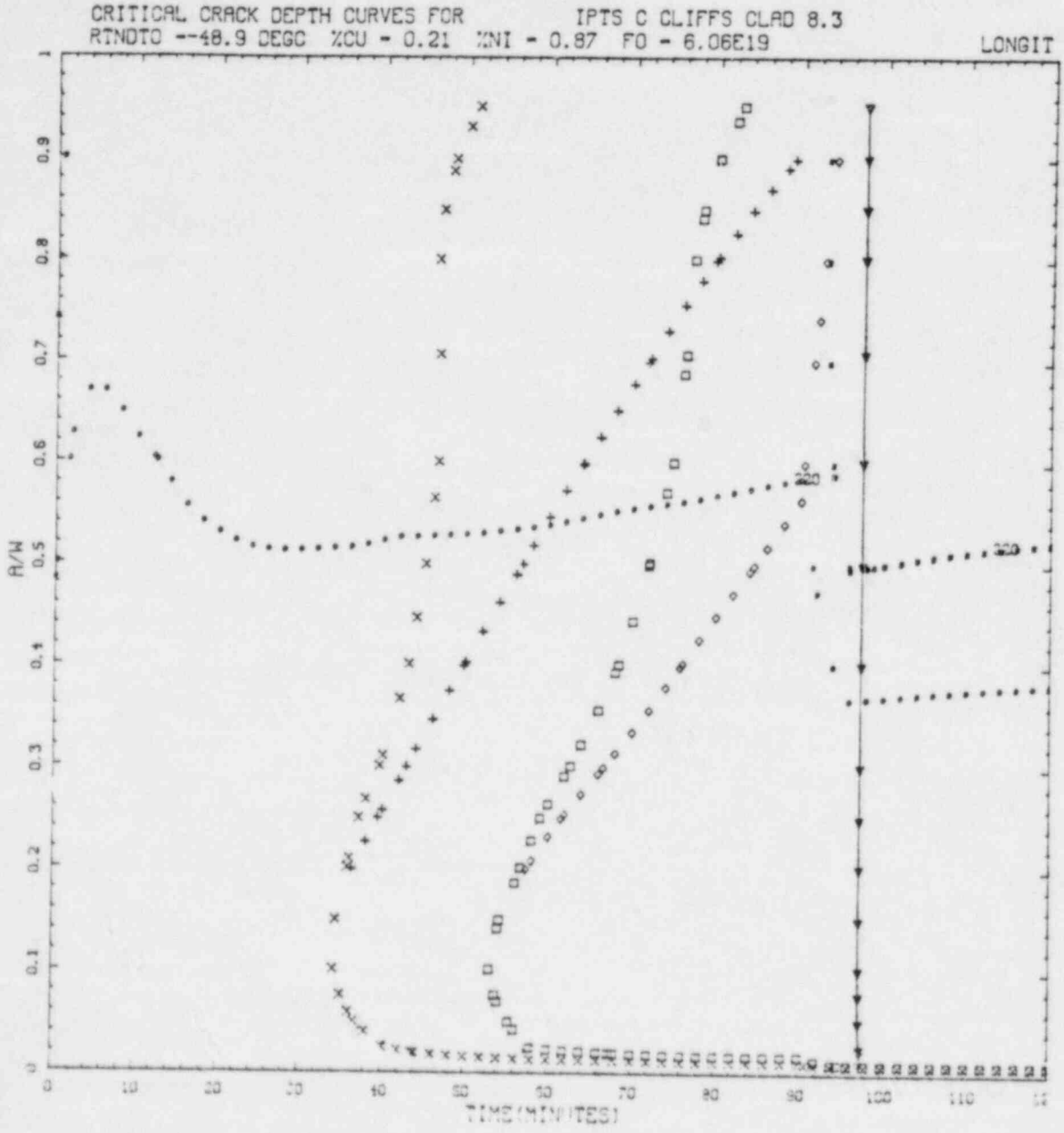
CRITICAL CRACK DEPTH CURVES FOR IPTS C CLIFFS CLAD 8.3
RTNDTC --48.9 DEGC %CU - 0.21 %NI - 0.87 FO - 6.06E19
LONGIT
A/W
TIME(MINUTES)

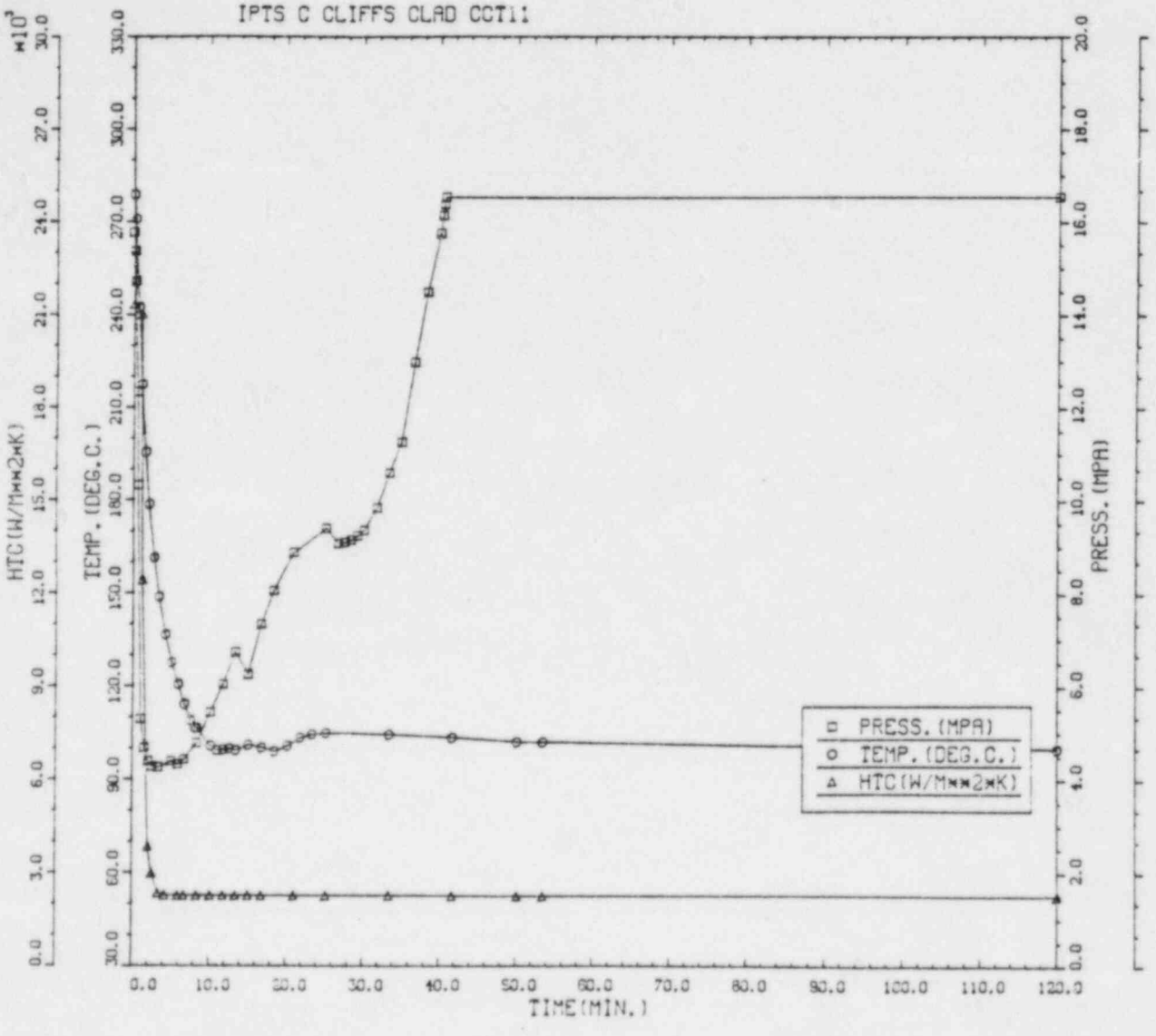
IPTS C CLIFFS CLAD CCT11
HTC(W/M**2*K)
*10**3
TEMP.(DEG.C.)
PRESS.(MPA)
TIME(MIN.)
PRESS.(MPA)
TEMP.(DEG.C.)
HTC(W/M**2*K)

IPTS C CLIFFS CLAD CCT11 1. FLAWS/M**3 FO = 6.060D+19

WELD	UNADJUSTED P(F/E)	95%CI	%ERR	P(INITIA)	N*V	ADJUSTED P(F/E)	%ERR	NTRIALS
1	7.62D-03	7.52D-04	9.87	7.81D-03	0.035	1.90D-04		30000
2	3.10D-04	3.74D-05	12.06	3.30D-04	0.050	1.55D-05		500000
3	2.27D-03	2.26D-04	9.94	2.37D-03	0.021	4.77D-05		100000
					VESSEL	2.54D-04	7.68	

DEPTHS FOR INITIAL INITIATION (MM)

	2.16	6.58	11.52	17.03	22.95	29.42	36.51	44.25	52.72
NUMBER	29	694	226	96	25	9	3	1	0
PERCENT	2.7	64.1	20.9	8.9	2.3	0.8	0.3	0.1	0.0

TIMES OF FAILURE(MINUTES)

	0.0	10.0	20.0	30.0	40.0	50.0	60.0	70.0	80.0	90.0	100.0	110.0	120.0
NUMBER	0	0	0	125	552	144	97	50	19	20	11	12	
PERCENT	0.0	0.0	0.0	12.0	54.0	13.8	9.3	4.8	1.8	1.9	1.1	1.2	

INITIATION T-RTNDT(DEG.C)

	-55.6	-41.7	-27.8	-13.9	0.0	13.9	27.8	41.7	55.6	69.4	83.3	97.2	111.1
NUMBER	1	1	26	215	542	404	423	262	16	0	0	0	
PERCENT	0.1	0.1	1.4	11.4	28.7	21.4	22.4	13.9	0.8	0.0	0.0	0.0	

ARREST T-RTNDT(DEG.C)

	-27.8	-13.9	0.0	13.9	27.8	41.7	55.6	69.4	83.3	97.2	111.1	125.0	138.9
NUMBER	0	0	0	2	0	4	44	244	494	52	10	0	
PERCENT	0.0	0.0	0.0	0.2	0.0	0.5	5.2	28.7	58.1	6.1	1.2	0.0	

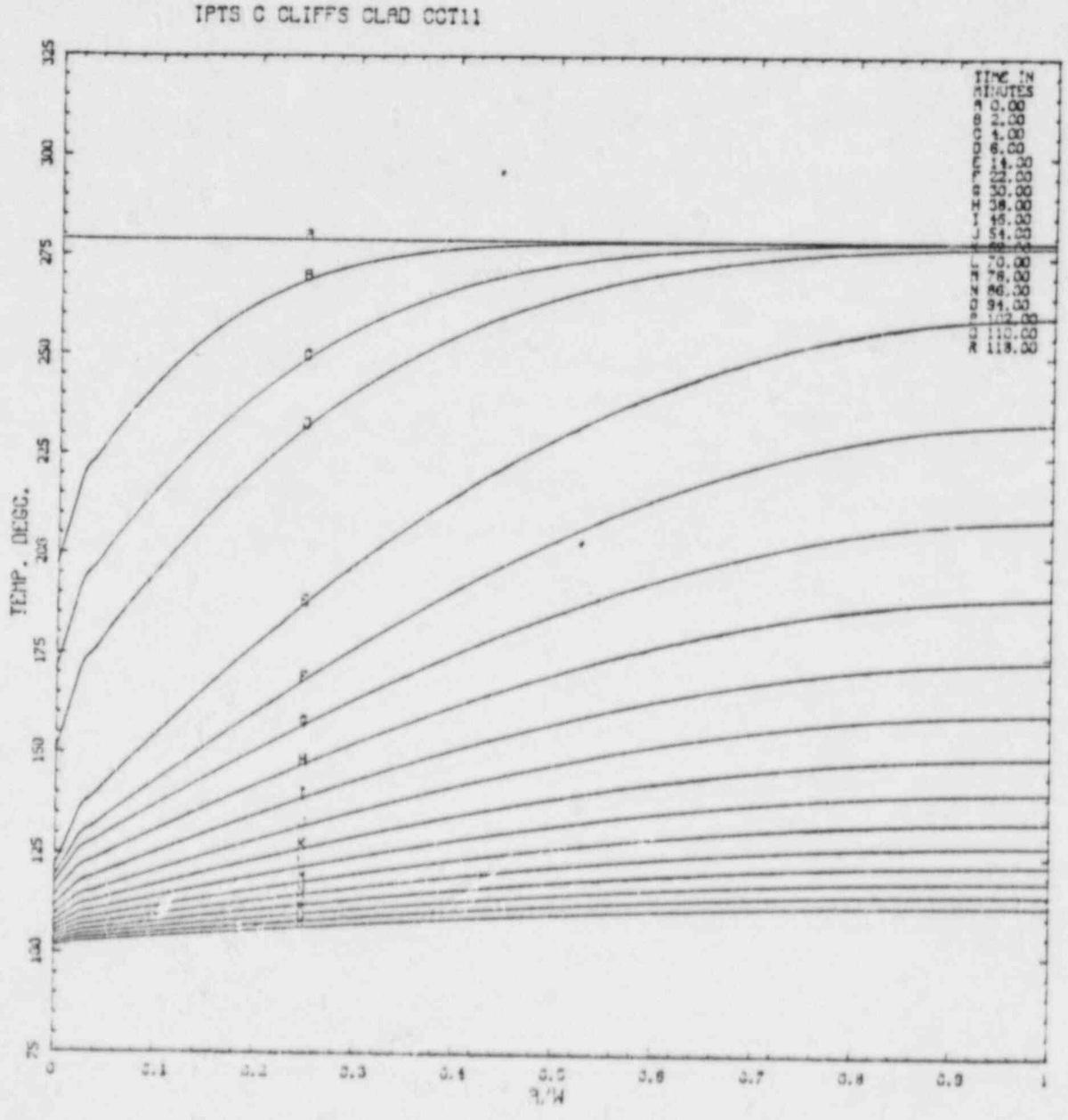
IPTS C CLIFFS CLAD CCT11
TEMP. DEGC.
R/W
TIME IN MINUTES
A 0.00
B 2.00
C 4.00
D 6.00
E 14.00
F 22.00
G 30.00
H 38.00
I 46.00
J 54.00
K 70.00
L 78.00
M 86.00
N 94.00
O 110.00
P 118.00

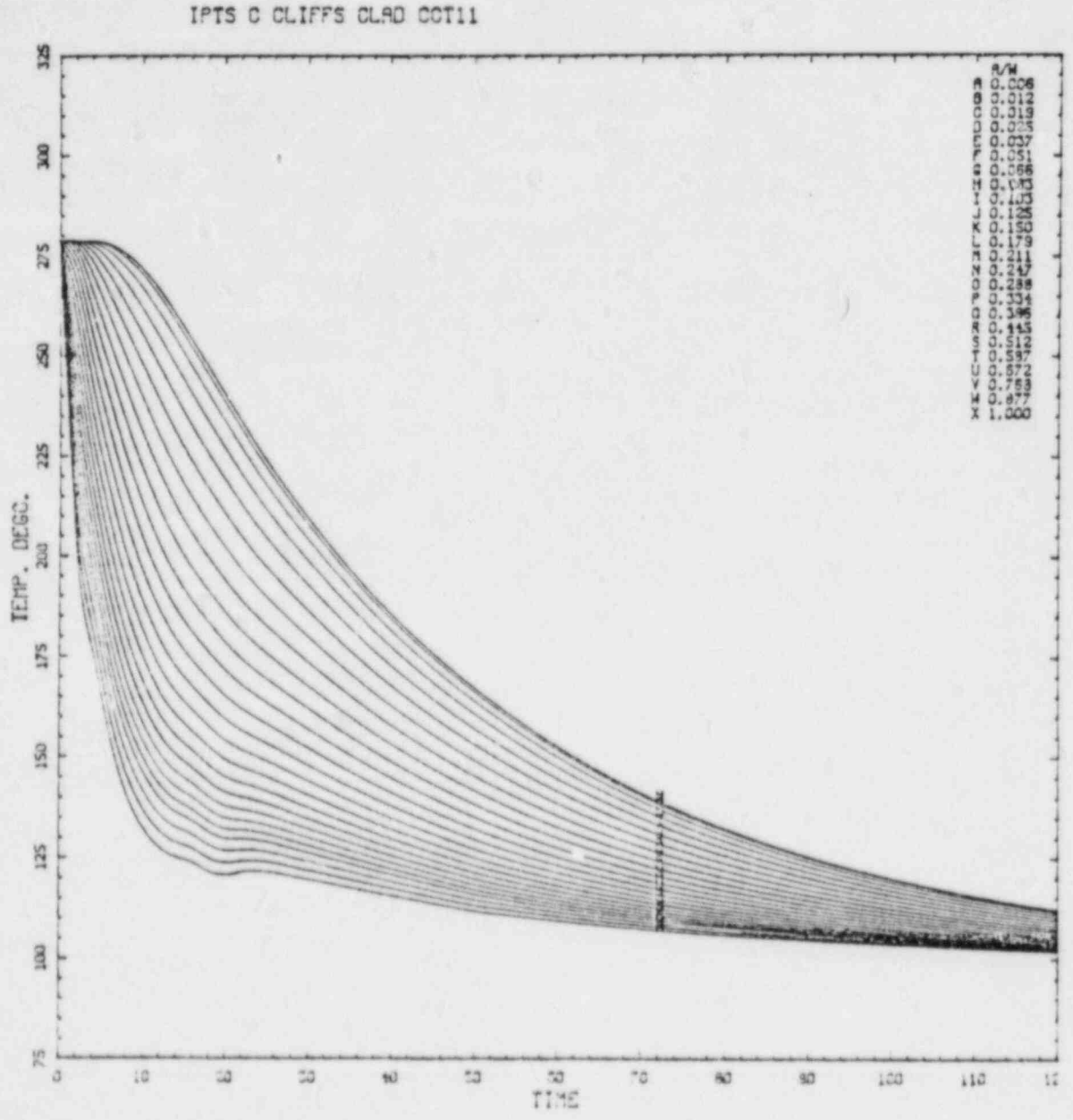
IPTS C CLIFFS CLAD CCT11
TEMP. DEGC.
TIME
R/W
A 0.006
B 0.012
C 0.019
D 0.028
E 0.037
F 0.051
G 0.066
H 0.083
I 0.103
J 0.125
K 0.150
L 0.179
M 0.211
N 0.247
O 0.288
P 0.334
Q 0.386
R 0.443
S 0.512
T 0.597
U 0.672
V 0.769
W 0.877
X 1.000

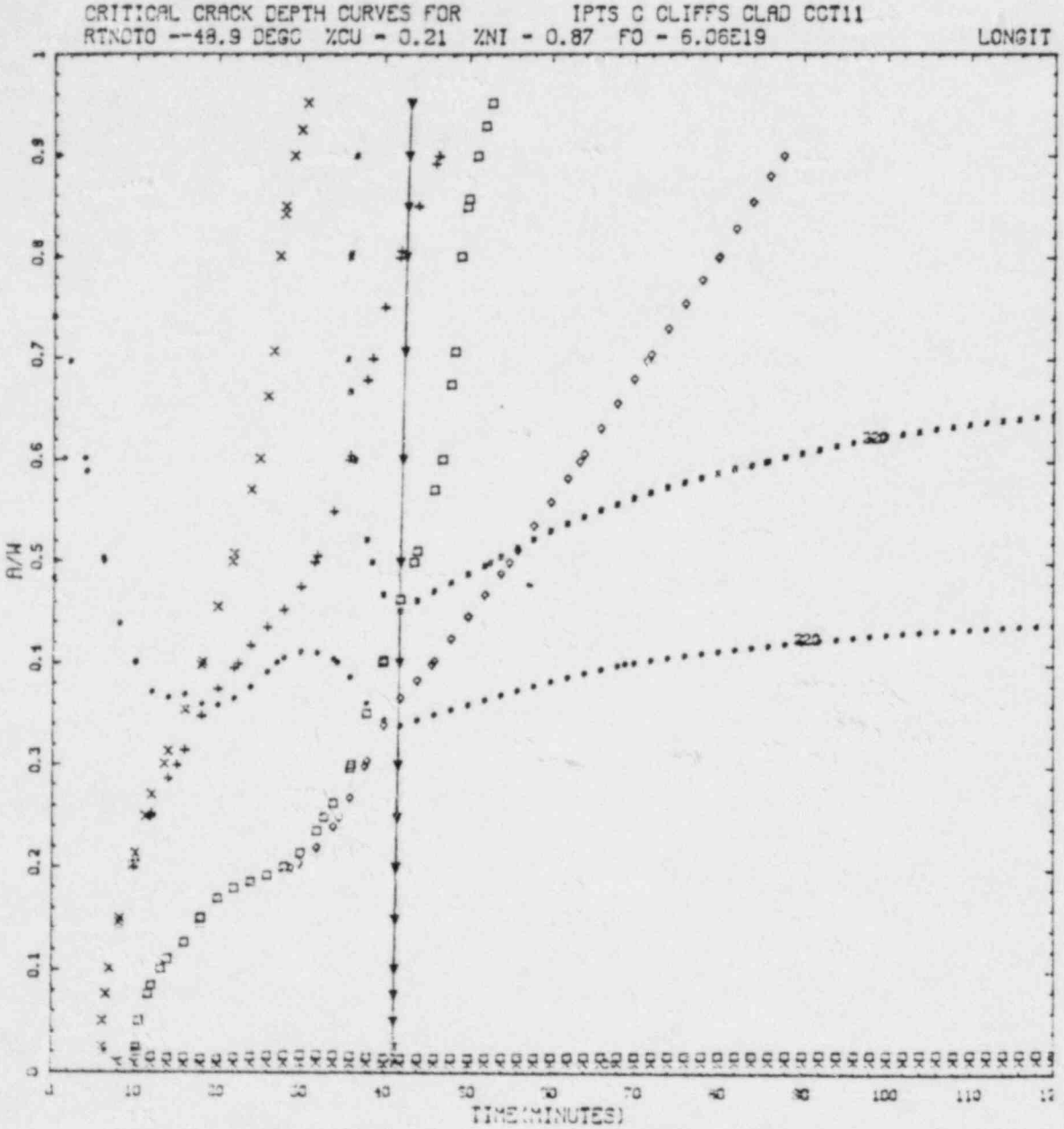
CRITICAL CRACK DEPTH CURVES FOR IPTS C CLIFFS CLAD CCT11
RTNDTO --48.9 DEGC %CU - 0.21 %NI - 0.87 FO - 6.06E19
LONGIT
A/W
TIME(MINUTES)

POR

August 2, 1984

50-317

Roy Woods

Here is the revi[illegible] AUG -8 AM 10 05 of
ORNL's Chapter 5 "TIME REQUESTED" Structure
Mechanics Analysis" for their draft
PTS report based on the Calvert
Cliffs Design. Reviewers
are requested to give me their
comments by August 20.

Carl Johnson

cc: Milt Vagins
Neil Randall
Jack Strosnider
Charles Serpan
Ray Fletcher
Lambros Lois
Don Kirkpatrick
Wayne Lanning
Sandy Israel
David Jatte
Pat Baranowsky
Public Document Room
Jose Reyes